

**Allosteric modulators directed to the PIF pockets of
phosphoinositide-dependent protein kinase 1 (PDK1) and
protein kinase C zeta (PKC ζ)**

Dissertation

zur Erlangung des Grades des Doktors der Naturwissenschaften
der Naturwissenschaftlich-Technischen Fakultät III
Chemie, Pharmazie, Bio- und Werkstoffwissenschaften
der Universität des Saarlandes

vorgelegt von

Dipl. Chem. Adriana Wilhelm geb. Stroba

Saarbrücken
2011

Tag des Kolloquiums: 01. 06. 2012

Dekan: Prof. Dr. Wilhelm F. Maier

Berichterstatter: Prof. Dr. Rolf W. Hartmann

Prof. Dr. Uli Kazmaier

Vorsitz: Prof. Dr. Elmar Heinzle

Akad. Mitarbeiter: Dr. Britta Diesel

Acknowledgements

First of all, I would like to sincerely thank Prof. Dr. R. W. Hartmann for the opportunity to research at the Institute of Pharmaceutical and Medicinal Chemistry, for his understanding and for his scientific support.

I would like to thank my supervisor and mentor, Dr. Matthias Engel, for introducing me in the fascinating field of the AGC kinases, his guidance, his understanding, his support and encouragement throughout my work until the final traces of my thesis.

I want to thank my official referee Prof. Dr. U. Kazmaier for the reviewing of this dissertation.

I am grateful to my co-supervisor Dr. W. Fröhner for his collaboration during my thesis, especially for all the stimulating discussions in the chemistry field.

I wish warmly thank to Nadja Weber for her nice company in the lab, for performing numerous cell assays and for her contribution concerning chemical synthesis and all incidental work.

I would like to thank all past and present members of the Research Group PhosphoSites in Saarbrücken and at the department of Internal Medicine I in Frankfurt, and Dr. R. M. Biondi in particular, for their fruitful collaboration and all contributions to this work. I would like also express my thanks to Laura Lopez und Valerie Hindie for the nice time in Frankfurt and Paris and their friendship.

I would like to thank Dr. Stefan Boettcher for measuring the LC/MS spectra, Dr. Josef Zapp for the NMR measurements and Lothar Jager for his technical assistance.

I would also like to thank all past and present co-workers of the RWH group, especially Cornelia Grombein for her sympathy and friendship, providing welcome distraction during the working hours.

My thesis is dedicated to my family, my parents and in particular to my husband, Frank. Here, I would like to express my sincere and cordial thanks for their unflagging confidence in me, for their support during my Ph.D. and for always being there.

Diese Arbeit entstand unter der Anleitung von Prof. Dr. R.W. Hartmann in der Fachrichtung Pharmazeutische und Medizinische Chemie der Naturwissenschaftlich-Technischen Fakultät III der Universität des Saarlandes von Juli 2005 bis November 2011.

So far the content of this thesis has been published in the following journals:

Engel, M.; Fröhner, W.; Stroba, A., Biondi, R.M. Allosteric protein kinase modulators. *PCT Int. Appl.* **2010**, WO2010043711.

Hindie, V.; Stroba, A.; Zhang, H.; Lopez-Garcia, L. A.; Idrissova, L.; Zeuzem, S.; Hirschberg, D.; Schaeffer, F.; Jorgensen, T. J.; Engel, M.; Alzari, P. M.; Biondi, R. M. High resolution complex structure and allosteric effects of low molecular weight activators on the protein kinase PDK1. *Nat. Chem. Biol.* **2009**, *5*, 758-764.

Stroba, A.; Schaeffer F.; Hindie V.; Lopez-Garcia L.; Adrian I.; Fröhner W.; Hartmann R.W.; Biondi R.M.; Engel M. 3,5-diphenylpent-2-enoic acids as allosteric activators of the protein kinase PDK1: Structure-activity relationships and thermodynamic characterization of binding as paradigms for PIF-binding pocket targeting compounds *J. Med. Chem.* **2009**, *52*, 4683–4693.

Engel, M.; Hindie, V.; Lopez-Garcia, L. A.; Stroba, A.; Schaeffer, F.; Adrian, I.; Imig, J.; Idrissova, L.; Nastainczyk, W.; Zeuzem, S.; Alzari, P. M.; Hartmann, R. W.; Piiper, A.; Biondi, R. M. Allosteric activation of the protein kinase PDK1 with low molecular weight compounds. *EMBO J.* **2006**, *25*, 5469-5480.

ABSTRACT

The phosphoinositide-dependent protein kinase 1 (PDK1), a master kinase in the PI3K signaling pathway, has gained importance as a potential therapeutic target for cancer since several of PDK1's substrates regulate processes for tumor cell growth and survival. As an alternative to the ATP-competitive strategy, we proposed the regulatory PIF pocket on AGC kinases as a drug target site to develop allosteric inhibitors with greater kinase selectivity. A screening identification of a hit compound and its biological evaluation proved that small molecules can allosterically trigger PDK1 activity by modulating the phosphorylation-dependent conformational transition. The optimization approach yielded 3,5-diarylpent-2-enoic acids whose allosteric mechanism was proven using mutants and cocrystallography. In addition to the SAR study, we applied isothermal titration calorimetry to analyze binding energetics of allosteric activators. Structure-based drug design led to a second compound class containing a dicarboxyl-moiety with improved potency and selectivity. Using a prodrug strategy the cell activity and the proof of mechanism was established. Further structure optimization of 3,5-diarylpent-2-enoic acids provided new insights on inhibition efficacy of small molecules toward the atypical protein kinase C, PKC ζ that can occur via binding the PIF pocket. These results demonstrated for the first time, that PIF pocket-directed ligands can be both activators and inhibitors of AGC kinases.

ZUSAMMENFASSUNG

Die Phosphoinositol-abhängige Kinase 1 (PDK1), eine Masterkinase des PI3K Signalweges, stellt ein wichtiges therapeutisches Target für Krebs dar, da viele ihrer Substrate Prozesse der Krebsentstehung regulieren. Mit der Entdeckung der PIF-Tasche wurde ein allosterisches Zentrum der AGC Kinasen für die Entwicklung allosterischer Modulatoren, alternativ zur ATP kompetitiven Strategie, gefunden. Die Identifizierung einer Hitverbindung und deren biologische Evaluierung bestätigten, dass kleine Moleküle die PDK1-Aktivität durch Modulation phosphorylierungs-abhängiger Konformationsübergänge allosterisch triggern können. In einem Optimierungsprozess wurden 3,5-Diarylpent-2-ensäuren synthetisiert und deren allosterischer Mechanismus mit Mutanten und Kokristallen bewiesen. Zusätzlich zu den Struktur-Wirkungs-Beziehungen wurden mittels isothermaler Titrationskalorimetrie die Bindungsenergien der Aktivatoren bestimmt. Strukturbasiertes Wirkstoffdesign führte zu einer zweiten Verbindungsklasse, wobei mit einer zusätzlichen Carboxylgruppe die Steigerung der Potenz und der Selektivität erreicht wurde. Die Zellaktivität und der Proof of Mechanism der Substanzen konnten mittels einer Prodrug-Strategie bestimmt werden. Eine weitere Strukturoptimierung der 3,5-Diarylpent-2-ensäuren lieferte allosterische Inhibitoren der atypischen Proteinkinase C, PKC ζ . Diese Ergebnisse zeigen auf, dass die PIF-Tasche-Liganden sowohl als Aktivatoren als auch als Inhibitoren der AGC Kinasen fungieren können.

ABBREVIATIONS

Å	Ångström
A _{max}	Highest activation efficacy
AC ₅₀	Concentration required for the half maximal activity
Act	Activation
ADME	Acronym for absorption, distribution, metabolism and excretion
AGC	cAMP-dependent, cGMP-dependent and protein kinase C
Akt	Protein kinase B
Ar	Aryl
ATP	Adenosine-5'-triphosphate
Bcr-Abl	Tyrosine kinase (fusion gene)
BIM	Bisindolyl maleimides
BnNEt ₃ Cl	Benzyltriethylammonium chloride
CA	Carbonic anhydrase
CAMK	Calcium/calmodulin-dependent protein kinase
cAMP	Cyclic adenosine monophosphate
CDK	Cyclic-dependent kinase 2
cGMP	Cyclic guanosine monophosphate
CH ₂ Cl ₂	Dichloromethane
Chk1	Cycle checkpoint kinase 1
CK1	Casein kinase 1
CLK	CDC-like kinase
CMGC	Group containing CDK, MAPK, GSK3, CLK families
Conc	concentration
c-Rel	Transcription factor
CML	Chronic myelogenous leukemia
COX	Cyclooxygenase
Cpd	Compound
CS	Catalytic domain
DAG	Diacylglycerol
DME	Dimethoxyethane
DMEM	Dulbecco's Modified Eagles Medium
DMF	Dimethylformamide
DMSO	Dimethylsulfoxid
ELKS	Regulatory subunit of the IKK complex
EGFR	Epidermal-Growth-Factor-Receptor
ErbB	Epidermal-Growth-Factor-Receptor
EtOH	Ethanol
Fas	Fatty acid synthase
FBS	Fetal bovine serum
FLT3	FMS-like tyrosine kinase 3
FXXXF	Hydrophobic sequence motif
G	Gibbs free energy
GLP	Glucagon-like peptide
GLUT4	Glucose transporter type 4
GPCR	G-protein-coupled receptor
GSK3	Glycogen synthase kinase 3
GST	Glutathione-S-transferase
h	Hour

<i>H</i>	Enthalpy
HCl	Hydrogen chloride
HEK293	Human embryonic kidney 293
HM	Hydrophobic motif
HPLC	High performance liquid chromatography
HTS	High throughput screening
HWE	Horner-Wadsworth-Emmons reaction
Hz	Hertz
IC ₅₀	Concentration required for 50 % inhibition
IκB	Inhibitor of Nuclear Faktor-κB
IKK	IκB kinase
IL-6	Interleukin-6
IRS1/2	Insulin receptor substrate 1/2
ITC	Isothermal Titration Calorimetry
<i>K_a</i>	Binding affinity constant
<i>K_d</i>	Equilibrium dissociation constant
kDa	Kilodalton
<i>K_I</i>	Binding constant
<i>K_M</i>	Michaelis constant
Kcal	Kilokalorie
K ₂ CO ₃	Potassium Carbonate
L6	Rat skeletal muscle cell line
LPS	Lipopolysaccharides
MAPK	Mitogen activated protein kinase
MgO	Magnesium oxide
MOM	Methoxymethyl group
mRNA	Messenger ribonucleic acid
MS	Mass Spectrometry
mTOR	Mammalian Target of Rapamycin
mTORC1/2	Mammalian Target of Rapamycin complex 1/2
<i>N</i>	Reaction stoichiometry
nb	no binding
nd	not determined
ne	no effect
NEt ₃	Triethylamine
nM	Nanomolar
NaH	Sodium hydride
NaH ₂ PO ₂ ·H ₂ O	Sodium hypophosphite
NaOH	Sodium hydroxide
NF-κB	Nuclear factor kappa light chain enhancer of activated B cells
NSAIDs	Non steroidal anti inflammatory drugs
p50	Transcription factor
p65	Transcription factor
p85	Regulatory subunit of PI3K
PB1	Phox and Bem 1 domains of a PKCs
PBS	Phosphate-buffered saline
PDK1	3-phosphoinositide dependent kinase 1
Pd/C	Palladium on carbon
PDGFR	Platelet Derived Growth Factor Receptor
PH	Pleckstrin homology
PI3K	Phosphoinositid 3-kinase

PIF	PDK1 interacting fragment
PIFtide	Peptide encompassing the hydrophobic motif sequence of PRK2
PIP ₂	Phosphatidylinositol-(4,5)-biphosphate
PIP ₃	Phosphatidylinositol-(3,4,5)-triphosphate
PKA	cAMP-dependent protein kinase
PKB	Protein kinase B (also known as Akt)
PKC (c, n, a)	Protein kinase C (classical, novel, atypical)
PKG	Protein kinase G
PRK	Protein kinase C related kinase
PS	Pseudosubstrate
PS	Research Group PhosphoSites
PtdIns(3,4,)P ₂	PIP ₂
PtdIns(3,4,5)P ₃	PIP ₃
PTEN	Phosphatase and tensin homologue deleted on chromosome ten
RCC	Renal cell carcinoma
ReIA	Transcription factor
ReIB	Transcription factor
RSK	p90 ribosomal S6 kinase
RT	Room temperature
RTK	Receptor tyrosine kinase
S	Entropy
S6K	p70 ribosomal S6 kinases
SAR	Structure activity relationship
SGK	Serum- and glucocorticoid-induced kinase
STE	Homologs of yeast Sterile 7, Sterile 11, Sterile 20 kinases
T308-tide	A polypeptide substrate that comprises the activation loop residues of PKB
TK	Tyrosine kinase
TKL	Tyrosine kinase-like
TNF	Tumor necrosis factor
TR-FRET	Time-Resolved-Fluorescence Resonance Energy Transfer
TRIS	Trishydroxymethylaminomethan
TROSY	Transverse relaxation optimized spectroscopy
UCN-01	7-Hydroxystaurosporine
μM	Micromolar
VEGFR	Vascular endothelial growth factor receptor
WT	Wild Type

Amino acids

Arg	(R)	Arginine
Glu	(E)	Glutamic acid
Ile	(I)	Isoleucine
Leu	(L)	Leucine
Lys	(K)	Lysine
Phe	(F)	Phenylalanine
Ser	(S)	Serine
Thr	(T)	Threonine
Tys	(Y)	Tyrosine
Val	(V)	Valine

TABLE OF CONTENTS

1	Introduction	1
1.1.	Protein kinases.....	1
1.2.	3-Phosphoinositide-dependent protein kinase-1 (PDK1): a master regulator of AGC kinases	3
1.3.	PDK1 as a drug target	4
1.4.	Structure of AGC kinases.....	5
1.5.	The PIF pocket, a regulatory site in PDK1	7
1.6.	The PIF pocket as a novel allosteric target site	10
1.7.	Specificity of compounds targeting PDK1	11
1.8.	Allosteric Inhibitors.....	16
1.9.	State of the art: low molecular weight compounds targeting the allosteric PIF pocket in PDK1	18
1.9.1.	First compounds designed to bind to the PIF pocket of PDK1: activators of catalytic activity	18
1.9.2.	Further PIF pocket-directed compounds referred in the literature	20
1.10.	Atypical PKCs	22
1.11.	PKC ζ as drug target	24
1.12.	Inhibitors of PKC ζ	27
1.13.	Allosteric approach to inhibit PKC ζ	30
2	Aim and work strategy of the present study	33
2.1.	Scientific objective	33
2.2.	General concept to design allosteric modulators of PDK1 and PKC ζ	34
3	Results.....	39
3.1.	Synthesis, structure-activity relationships and thermodynamic characterization of 3,5-diphenylpent-2-enoic acids as allosteric activators of the protein kinase PDK1	39
3.1.1.	Scientific rationale.....	39
3.1.2.	Synthesis.....	40
3.1.3.	Biological results.....	44

3.1.4.	Cocrystallization of 2Z with PDK1 as further biochemical evidence for binding of the small molecule compound in the PIF pocket.	51
3.1.5.	Validation of allosteric activators binding characteristics to PDK1 via Isothermal Titration Calorimetry (ITC).	53
3.1.6.	Interrelationships between Thermodynamic Binding Signature, Structure, and Activity of selected 3,5-diarylpent-2-enoic acids toward PDK1.	58
3.1.7.	Overall Correlations between Enthalpy and Entropy of Binding and the Biological Activity Parameters of Allosteric PDK1 Activators.....	62
3.1.8.	Implication of the Calorimetric Characterization for Lead Selection and Optimization.....	64
3.1.9.	Conclusion.....	65
3.2.	Prodrug approach of 2-(3-oxo-1,3-diphenylpropyl)malonic acids as potent allosteric activators of PDK1 to enable the bioavailability of the high polar dicarboxylic acids.	67
3.2.1.	Scientific rationale.....	67
3.2.2.	Synthesis.....	68
3.2.3.	Biological results.....	70
3.2.4.	Crystal structure of PDK1 in complex with 2-(3-(4-chlorophenyl)-3-oxo-1-phenylpropyl)malonic acid (4A)	81
3.2.5.	Chromatographic Separation of the Enantiomers of 4H	82
3.2.6.	Discussion and Conclusion	86
3.3.	Evaluation of 3,5-diphenylpent-2-enoic acids' inhibitory effect toward PKC ζ : allosteric kinase inhibition targeting the PIF-binding pocket	89
3.3.1.	Introduction	89
3.3.2.	Synthesis.....	90
3.3.3.	Biological results and Discussion	92
3.3.4.	Conclusion.....	101
4	Discussion	103
5	Summary and Conclusion.....	112
6	Experimental Section	117
6.1.	Chemistry	117
6.1.1.	General descriptions.....	117

6.1.2.	Synthetic procedures	118
6.1.3.	Analytical data.....	121
6.2.	Biological Section	196
6.2.1.	Material and reagents	196
6.2.2.	Protein kinases assays	198
6.2.3.	Isothermal titration calorimetry ^{20, 74}	199
6.2.4.	HPLC-MS/MS detection of hydrolysis of the prodrugs in L6 cells.....	199
6.2.5.	Reporter Gene Assay ¹⁶³	200
7	References.....	202

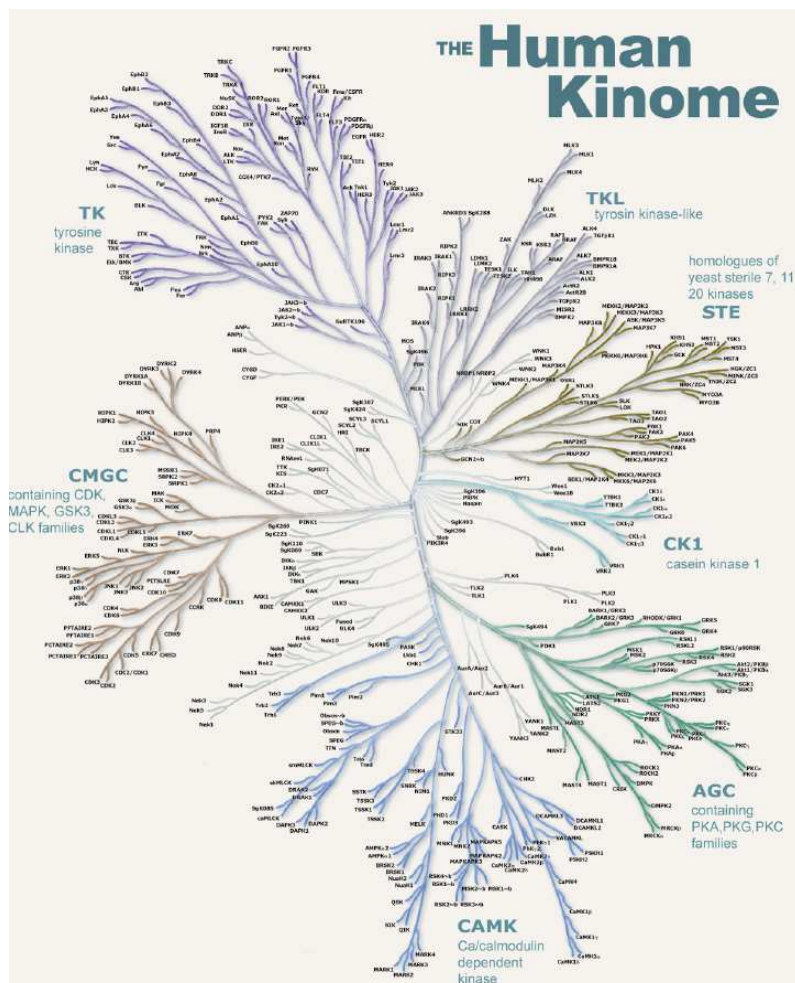
1 Introduction

1.1. Protein kinases

Protein kinases constitute about 2% of human genes and build the second largest and most extensively studied gene families in the human genome.¹

Protein kinases are pivotal regulatory enzymes that change the properties of a substrate by attaching the γ -phosphate group from the cofactor ATP to the hydroxyl group of serine (Ser), threonine (Thr) or tyrosine (Tys) residues and are thus characterized with regard to the substrate specificity in three classes, Ser/Thr, Tys and dual specificity protein kinases.² In addition, based on the similarity between the amino acid sequences of the enzyme catalytic domains, Manning *et al.* classified the kinases into nine major groups, AGC, TK, TKL, STE, CK1, CMGC, CAMK, Other, and Atypical (Figure 1).³

Figure 1: Classification of the protein kinases into nine major groups³



The subgroup AGC family of Ser/Thr protein kinases was already defined in 1995 by Steven Hanks and Tony Hunter. The high analogy to the sequence alignments of the catalytic domain of the members provided a basis.⁴ The term AGC family derives from the appropriate members cAMP-dependent protein kinase 1 (PKA), cGMP-dependent protein kinase (PKG) and protein kinase C (PKC).²

Protein kinases have emerged as an important class of pharmaceutical targets in consequence to the altering the substrate function and triggering a signaling cascade by phosphorylation. Thus, they play a crucial role in signal transduction controlling and regulating cellular processes. In fact, overexpression of protein kinases or loss of kinase regulatory mechanisms are observed in many human diseases, such as cancer, inflammation, neurological (e.g. Alzheimer's disease) and metabolic disorders (e.g. diabetes type-2). Moreover, they are in contrast to protein-protein interaction considered to be more druggable by small molecule weight inhibitors. Not surprisingly, protein kinases are currently among the most important drug target class for the treatment of diverse human diseases.⁵ With several compounds on the market (Table 1) and dozens of inhibitors as drug candidates in clinical trials, small molecule compounds continue to attract attention.⁶ The majority of the protein kinase directed drugs has been used for oncology therapy. But, this development is joined by a particular difficulty, relatively poor target selectivity causing additional site effects. As ATP is the essential cofactor to reach kinase activity, the development of kinase inhibitors focuses on small molecules competing for the ATP binding site. The crucial drawback is the high degree of conservation of the ATP binding site and consequently it is difficult to achieve specific inhibitors. Accordingly, it is a major challenge in this area to develop a drug that selectively suppresses the activity of one kinase to minimize the risk of side effects as the majority of protein kinases inhibitors compete for the ATP binding site.⁷

Table 1: Some examples of launched tyrosine kinases inhibitors⁸

Tyrosinekinase inhibitor	Name	Company	Target	Indication	FDA approval
Imatinib	Gleevec [®]	Novartis	Bcr-Abl, PDGFRA, PDGFRB, KIT	Chronic myelogenous leukemia (CML)	2003
Sorafenib	Nexavar [®]	Bayer	VEGFR2,3	Primary kidney cancer	2005
Erlotinib	Tarceva [®]	Hoffmann-La Roche	EGFR1	Lung cancer, Pancreatic cancer	2005
Sunitinib	Sutent [®]	Pfizer	VEGFR2, PDGFRA, PDGFRB, KIT, FLT3	Renal cell carcinoma (RCC)	2007
Lapatinib	Tykerb [®]	GlaxoSmithKline	ERBB2	Breast cancer, Solid tumors	2007
Pazopanib	Votrient [®]	GlaxoSmithKline	VEGFR, PDGFR, KIT	Renal cell carcinoma	2009

1.2. 3-Phosphoinositide-dependent protein kinase-1 (PDK1): a master regulator of AGC kinases

The phosphoinositide-dependent protein kinase 1 (PDK1), a Ser/Thr protein kinase, is in the centre of growth factor and insulin signaling and is a master kinase which phosphorylates the activation loop of at least 23 protein kinases from the AGC group (Figure 2).²

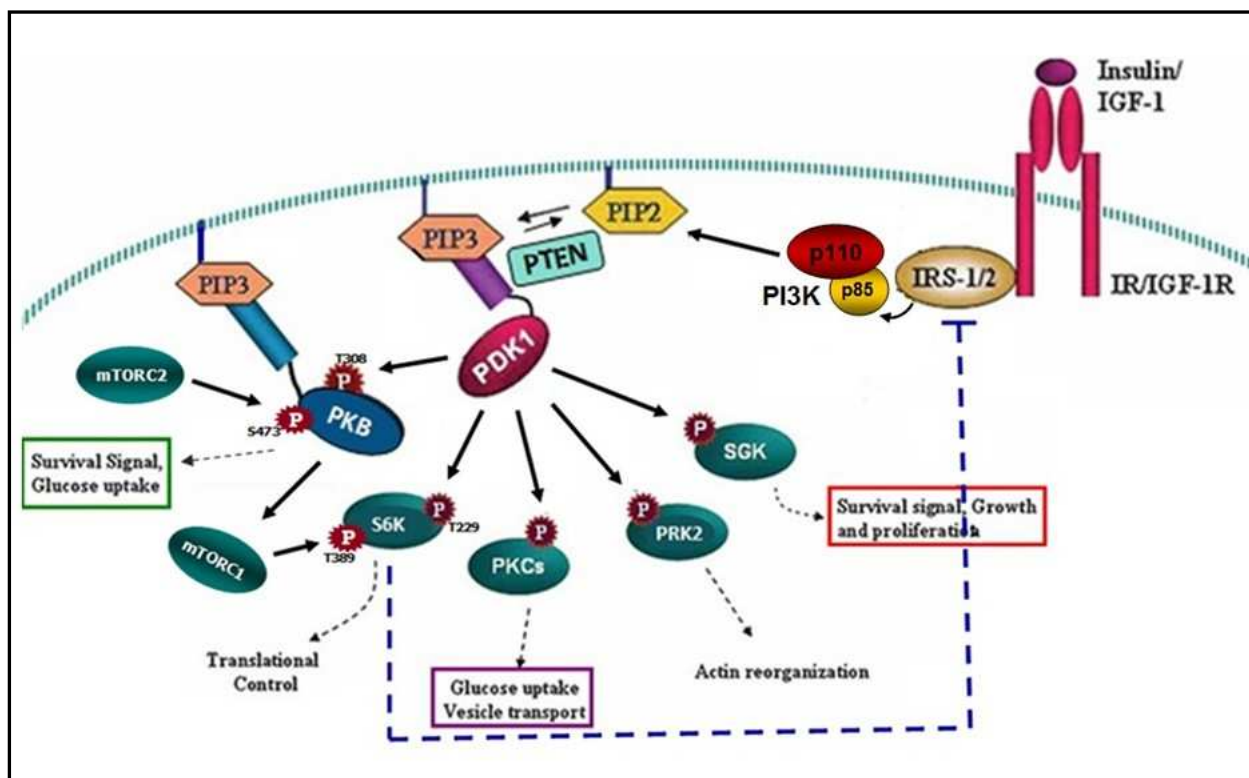
Upon insulin and growth factors binding to the extracellular domain the receptor tyrosine kinase (RTK) becomes dimerized, phosphorylated and activated. Thereby creates RTK a binding site for the p85, a regulatory unit of phosphoinositide 3-kinase (PI3K), (Figure 2). This leads to the full activation of PI3K. Once activated, PI3K converts the phosphatidyl-3,4-biphosphate [PIP₂] into phosphatidylinositol-3,4,5-triphosphate [PIP₃], a potent second messenger, essential for cell growth and survival.⁹ This reaction is reversed by hydrolyzing PIP₃ to PIP₂ by PTEN. PTEN, the phosphatase and tensin homologue deleted on chromosome ten, acts as a tumor suppressor preventing uncontrolled cell growth by keeping cells from growing and dividing in an uncontrolled way and triggering cells to undergo apoptosis.¹⁰ PIP₃ in turn serves as a membrane-bound docking site for proteins with an N-terminal pleckstrin homology (PH) domains, such as PDK1 and PKB, one of its substrate. The PH domains interact with the membrane PIP₃ resulting in the recruitment of PDK1 and PKB (also termed Akt) to the plasma membrane where the two enzymes co-localize. Thus, upon PI3 kinase activation, PDK1 catalyzes the phosphorylation of the Thr308 residue in the activation loop of PKB and leads to a partial activation of PKB.¹¹⁻¹³ The maximal activation of PKB is reached by phosphorylation of the hydrophobic motif (HM) residue Ser473 by mammalian target of rapamycin complex 2 (mTORC2).¹⁴ The mTOR protein kinase is the catalytic component that forms two distinct multiprotein complexes called mTORC1 and mTORC2 and has among PI3K and PDK1 a key role in this signaling pathway.^{15, 16}

PDK1 has received attention, firstly as the kinase that phosphorylates PKB at the activation loop on the residue Thr308 in a PIP₃ dependent manner. Secondly, PDK1 has been shown to phosphorylate and activate other AGC kinases. The remaining PDK1 substrates lack a PH domain and consequently do not interact with PIP₃. By contrast, the substrates SGK, RSK, PKCs and S6K have a homologous region of their activation loops including a consensus substrate recognition site for PDK1.¹⁶ This phosphorylation site is C-terminal to the kinase catalytic domain next to the hydrophobic motif. PDK1 is able to interact with the

substrates by a prior-phosphorylation of this hydrophobic motif.^{12, 17} The detailed molecular mechanism is described in chapter 1.5.

Importantly, PDK1 is constitutively active because of the intrinsic ability to *trans*-phosphorylate its own Ser241 residue and has a wide distribution in cells by binding to soluble inositol phosphates that anchor PDK1 to the cytosol.²

Figure 2: Distinct regulatory mechanism of PDK1



The PI3 kinase signaling pathway is promoted by stimulation of cells with insulin and growth factors. Thereby phosphoinositide 3-kinase (PI3K) activates and generates phosphatidyl-3,4-biphosphate [PtdIns(3,4)P₂] and the second messenger phosphatidylinositol-3,4,5-triphosphate [PtdIns(3,4,5)P₃] which induce the activation of certain members of the AGC subfamily.

1.3. PDK1 as a drug target

Inhibition of PDK1 has been gained high interest due to its crucial role in transducing PI3K signaling pathway. Short treatments with PDK1 inhibitors may affect a decrease of the activation of some substrates of PDK1. A total inhibition of PDK1 activity by compounds is expected to have more effects on broader signaling pathways, besides the effects of PKB. Additionally, PDK1 has been emerged as a potential therapeutic target for cancer since several of the substrate protein kinases, comprising PKB, RSK and S6K, regulate processes which are essential for the tumor cells, such as cell growth and survival.^{18, 19} Their

unphysiological activity leads in the majority of cases to cancer. Loss of regulation arises in mostly cases from an up-regulation or mutation of upstream signal molecules, such as growth factors, or by the loss of the feed-back mechanism decreasing phosphatase activity. Moreover, deregulation of the tight control of such cellular functions also triggers diabetes type-2, autoimmune diseases, inflammation, neurological and metabolic disorders.²⁰ One paramount example is S6K. S6K, as a downstream target of PDK1, plays a crucial role in the metabolic disorder diabetes type-2. PDK1 phosphorylates the activation loop of S6K that require phosphorylation of both HM and activation loop for fully activity. Subsequently, S6K activates a negative feedback loop by inhibiting the insulin receptor substrate-1 (IRS1) regulating the insulin action (Figure 2). In this line, S6K has a key role in insulin resistance. Obesity and diabetes type-2 is associated with increased activity of S6K.^{1, 21} Studies with S6K deficient mice confirmed the mice hypersensitive to insulin and they were protected against diet-induced obesity.²² Identification of PDK1's inhibitors could lead to the development of therapeutic strategies for the treatment of these disorders preventing the activation of S6K and enhancing the insulin sensitivity. In case of cancer PDK1 is a validated target. The indication diabetes type-2 needs to be more investigated.

Hence, proper regulation of the PDK1 is critical for prevention of the overexpression of its substrates. The suppression of the activity of the PDK1 substrates provides an attractive approach and qualifies PDK1 as a potential target for development of novel therapeutics for the treatment of cancer, diabetes type-2 and other diseases.

1.4. Structure of AGC kinases

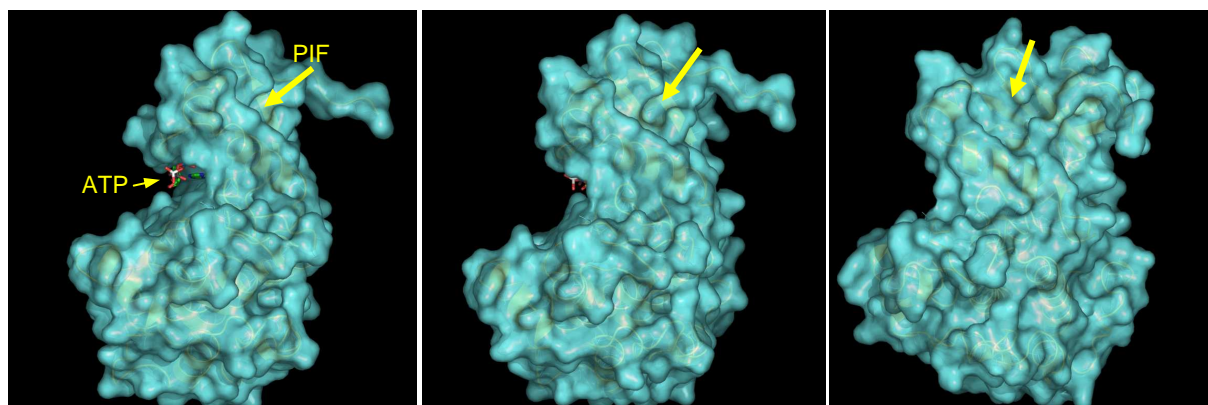
PDK1 and other AGC kinases display a characteristic bilobal structure that is shared by all protein kinases (Figure 3A).^{17, 23} This bilobal fold was firstly presented by X-Ray crystals for cAMP-dependent protein kinase (PKA, Figure 3B) in 1991 and defined the structural features of the catalytic domain of kinases. The aminoterminal small lobe consists of five stranded β -sheets and the carboxy-terminal lobe is larger and heavily α -helical. The ATP binding site is located in a deep cleft between the N-lobe and the C-lobe. Hence, the bound ATP sits below the highly conserved phosphate pocket that links the β -1 and β -2 strands and directs the γ -phosphate outwards while the adenine ring lies deep in the groove between the two lobes. PDK1 and its substrates contain also a central located phosphorylation site at the activation loop. Usually, when the AGC members are active, they are phosphorylated on a

of PDK1.²⁷⁻²⁹ A further structural domain of PDK1 is a hydrophobic groove, termed PDK1 interacting fragment pocket (PIF pocket) that is located on the small lobe. Interestingly, other members of the AGC family possess an equivalent hydrophobic pocket. The following chapter describes the discovery of the PIF pocket and highlights its functions which mediate phosphorylation dependent conformational transitions and its importance as regulatory feature. Phosphorylation of the activation loop and of the PIF pocket is essential for maximal activation of AGC kinases.

1.5. The PIF pocket, a regulatory site in PDK1

The discovery of the PIF pocket and its regulatory functions were first described by our collaborator R.M. Biondi in 2000.²⁶ The PIF-binding pocket of PDK1 is a hydrophobic surface pocket located on the small lobe of the catalytic domain and separated from the ATP binding site (Figure 4). It is formed by the surrounded amino acids Lys115, Ile118 and Ile119 on the α B-helix, Val124, Val127 on the α C-helix, Leu155 on the β 5-sheet and α G-helix. All these residues are arranged to a 5 Å-deep cleft (Figure 5). An equivalent hydrophobic motif (HM) binding pocket regulatory site exists also on other AGC kinases.

Figure 4: Surface representation of the PDK1 kinase domain. Location of the PIF pocket separated from the ATP binding site is highlighted. ATP is shown in stick format.

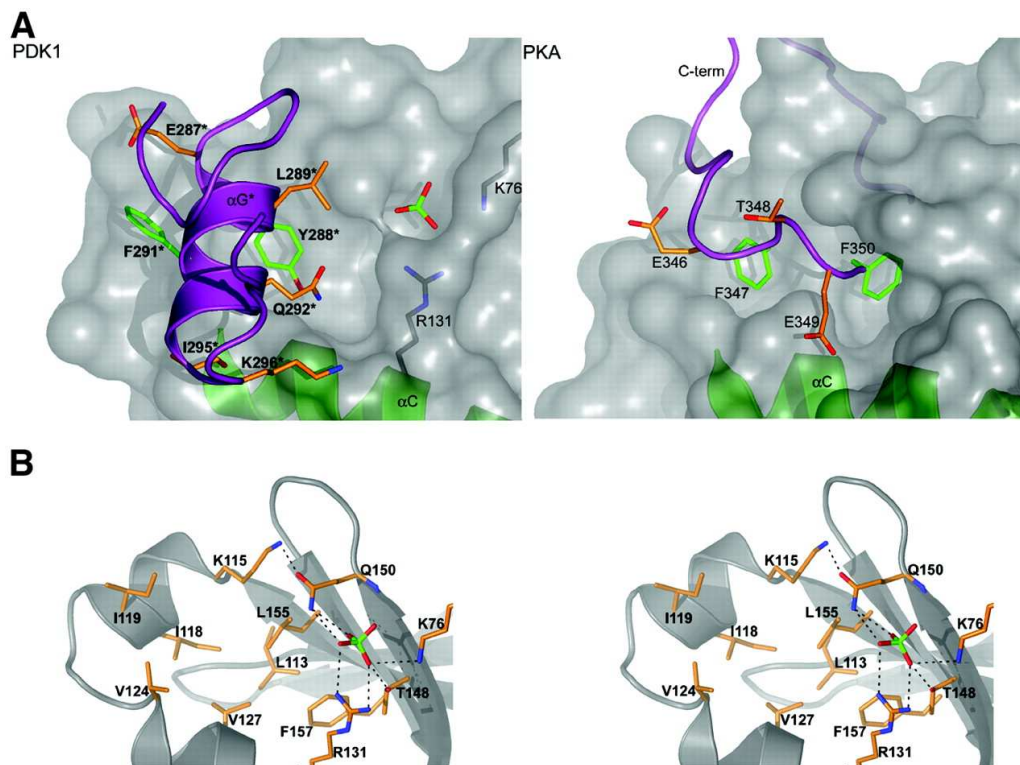


As exemplified with the PKA structure (Figure 5), the C-terminal hydrophobic motif of almost all AGC kinases except PDK1 comprising the sequence FXXF acts as physiological ligand of the own PIF pocket. This intramolecular peptide motif utilizes a considerably larger area for interaction than just the hydrophobic pocket. In contrast to other AGC kinases PDK1

does not possess an intramolecular ligand, the C-terminal extension to the catalytic core, and lacks the hydrophobic motif. Thus, in PDK1 the PIF pocket remains unoccupied and is accessible for transient docking of the HM of its substrates.

Consequently, PDK1 makes use of the PIF pocket both, for the allosteric regulation of the catalytic activity and as docking site for transient interactions with the substrate proteins via their C-terminal peptide motif (HM). Thereby, PDK1 phosphorylates different substrates in different ways. Some substrates are phosphorylated constitutively by PDK1 whereas others, such PKB can be phosphorylated by PDK1 in response to the same cellular agonist but with different temporal regulation. The differential phosphorylation of its substrates relies on the specific ability of PDK1 to recognize and to interact with its substrates.

Figure 5: PIF pocket comparison of PDK1 and PKA



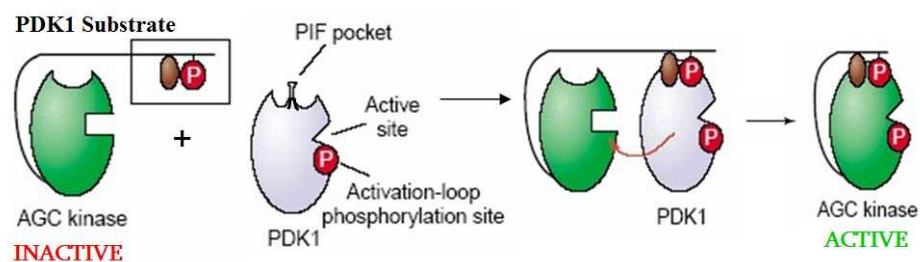
A: Schematic representation of the surface. **B:** Stereo image of the residues linking the PIF pocket and the phosphate pocket.¹⁷

PDK1 detects selective inactive conformations of AGC substrates because they have disrupted PIF pockets and their hydrophobic motifs are available for interactions with the PIF-pocket of PDK1. Binding of the peptides increases the intrinsic catalytic activity of PDK1 and enables PDK1 to phosphorylate almost all substrates, including S6K, SGK, RSK and the

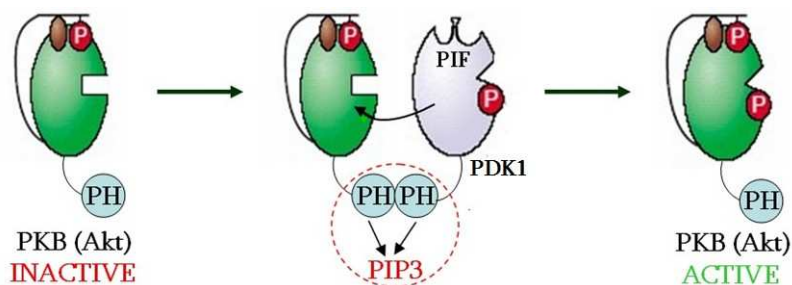
atypical PKCs. This docking interaction with the PDK1 PIF-binding pocket results in full activation of the substrate kinases (Figure 6A).^{11, 30, 31} Through the occurred phosphorylation the binding of the phosphorylated HM to the own PIF pocket (active kinase) is prompted and helps stabilize the active conformation (Figure 6A). Subsequently, the affinity of the substrates to their phosphorylated hydrophobic motif increases. In contrast to the inactive conformations, the active conformations of AGC substrates are not detectable by PDK1 because their PIF pockets are occupied by their own HM and the docking site is not accessible for interaction anymore. As the only known exception, the phosphorylation of PKB does not require the interaction with the PIF pocket of PDK1. As already described in chapter 1.2 and as shown in Figure 6B, both PDK1 and PKB bind their PH domain to the PIP₃ bound on the membrane enabling the phosphate transfer.

Figure 6: Mode of action of PIF pocket discriminates between two pathways **A** and **B**. PDK1's phosphorylation of all substrates except PKB depends on transient docking interactions with the PIF pocket.

A: PDK1 dependent phosphorylation and activation of S6K, SGK, RSK, aPKC.



B: PKB phosphorylation and activation by PDK1.



1.6. The PIF pocket as a novel allosteric target site

Many studies have been reported with the focus on PIF pocket showing PDK1's PIF pocket is essential for the phosphorylation and the following activation of a set of AGC kinases. To investigate whether the ability to phosphorylate and activate the AGC substrates remains Biondi *et al.* generated Leu155Glu mutants of PDK1's PIF pocket. The *in vitro* results suggested the docking site is blocked for the substrates PRK2, S6K1, SGK, PKC and PRK but not for PKB.¹¹ The substrates were phosphorylated and activated very weakly compared to the wild-type PDK1. To further confirm the requirement of an intact PIF pocket for binding and phosphorylation of S6K by PDK1, Collins *et al.* examined the *in vivo* influence of the PIF pocket as substrate interacting site using embryonic stem cells harbouring the Leu155Glu knock-in mutation.^{32, 33} Thus PDK1 exhibited its catalytic activity but received also a functionally inactive PIF pocket. Interestingly, the embryonic stem cells were viable and the PDK1 mutants induced the expected activation of PKB, whereas S6K1, RSK and SGK remained inactive. These *in vivo* mutagenesis results provided further evidence that the PIF pocket is crucial for binding and phosphorylation of S6K1, RSK and SGK by PDK1, except PKB. In addition, investigations with phospho- and dephospho-HM peptides of different AGC kinases indicated a direct influence on the catalytic activity binding on PDK1's PIF pocket.

Based on these results, the PIF pocket has emerged as a possible site for drug development. Small compounds as potential drugs directed to the PIF pocket are predicted to have two effects.

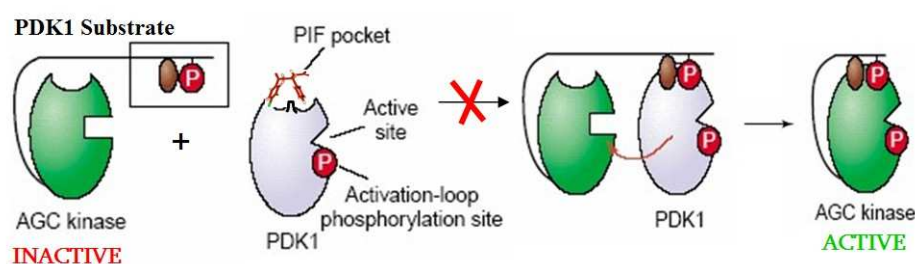
Firstly, occupying the PIF pocket as docking site for the substrates the compounds inhibit the substrates' activation which require the interaction with the PIF pocket (Figure 7). An inhibitor avoids the activation of the PIF substrates, such as SGK1, SGK, PKC, PRK, but not PKB. Binding of a drug molecule to the regulatory PIF pocket site may also increase the catalytic activity despite the blockade of the targeting site for the substrates. This effect is similar to the effects of the Leu155Glu mutant, which renders an active protein but blocks the docking interaction site.

Secondly, the catalytic activity can be modulated by an allosteric mechanism. Compounds binding to the PIF pocket in AGC kinases will probably induce a conformational transition on the ATP binding site, similar to the effect of the phosphorylated HM peptide that also influences the conformation of the ATP binding site binding the PIF pocket. In case the ligand stabilizes a specific conformation of the PIF pocket the catalytic activity of PDK1 will

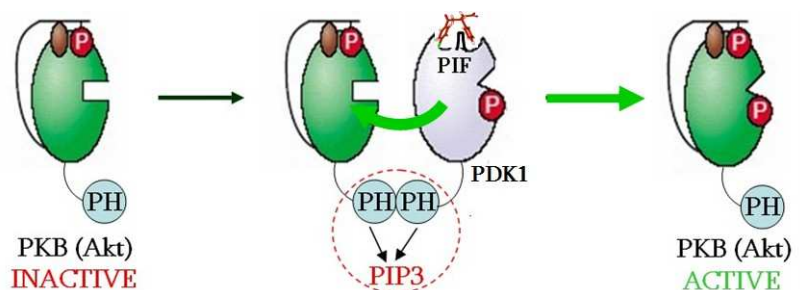
increase. Thereby the ligand acts as a kinase activator. Any aberrant ligand stabilizing conformation of the PIF pocket causes a decrease of the PDK1's activity to the point of an inhibition. An allosteric inhibitor of this type would inhibit not only the substrates that depend on the PIF pocket interaction but also PKB.

Figure 7: Novel mode of action of PIF pocket targeting compounds discriminates between two pathways.

A: S6K, SGK, RSK, aPKC: PIF pocket binding compounds prevent docking
→ no activation.



B: PKB: Activation not affected by PIF pocket-target compounds.
→ PIF pocket binding compound does not affect catalytic activity.



1.7. Specificity of compounds targeting PDK1

PDK1 was discovered in late 90s and is still relatively new drug target.³⁴ Biochemical and genetic studies have shown that PDK1 is a critical activator of other downstream kinases that are important promoters of cancer progression and affected a rise in drug development based on PI3K/PDK1/PKB signaling pathway. Upregulation of PDK1 pathway due to overexpressed growth factor receptor proteins and PTEN mutation notably triggers the downstream signaling. Moreover, a wide range of all human cancers possess significant

overstimulation of the PDK1 signaling pathway^{17, 35, 36} whereby PDK1 represents a most promising target. Directly inhibition of this protein kinase by small molecules is predicted to result in effective control of cancer cell proliferation, particularly because *in vivo* results suggest an incomplete inhibition of PDK1 in cancers where PTEN is mutated. Mice with 10-20 % of PDK1 protein are healthy although they are smaller. However, when they are crossed with knockout mice in a PTEN deficient background, that have spontaneous tumors, the mice with less PDK1 activity have less tumors and extended lifespan.¹⁷ As binding of ATP is essential for kinase activity, the discovery of small molecule ligands that compete for the ATP binding site has been the main source for new kinase inhibitors. Hence, many studies have been reported with the focus on the development of ATP-competitive inhibitors targeting the ATP binding site of PDK1.^{16, 35, 37-42}

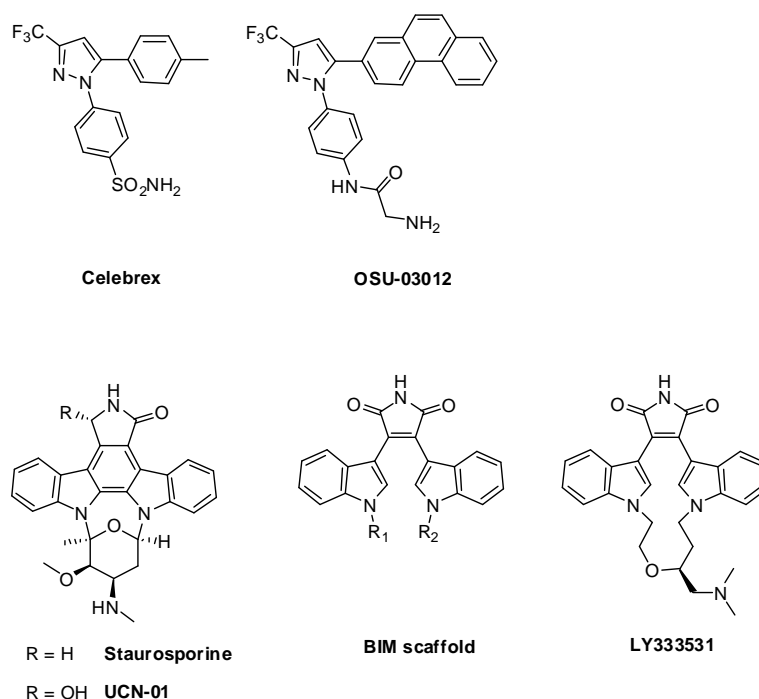
In the course of an evaluation of ATP-competitive PDK1 inhibitors various classes of small-molecules have been published in patents and papers. The inhibitors differ in their chemical scaffold but they share common characteristics corresponding to the hydrophobic nature of the ATP binding site. In addition they include fragments that occupy residues responsible for coordination of the ATP cofactor.

Several of the published PDK1 directed inhibitors are based on two drug classes, firstly staurosporine analogues and secondly sulindac and celecoxib as actual non steroidal anti inflammatory drugs (NSAIDs), that inhibit cyclooxygenase (COX) activities. Few staurosporine derivatives have been identified as PDK1 inhibitors, CGP39360, CGP41251 and UCN-01. Staurosporine, CGP39360 (Figure 8), a very potent broad-range kinase inhibitor significantly reduced the PDK1 activity *in vitro* with an IC_{50} of about 220 nM but it exhibited the most potency toward PKC α ($IC_{50} < 3$ nM). CGP41251 inhibited PDK1 moderately ($IC_{50} < 1.72$ μ M). However, it showed more selectivity toward PKC α with an IC_{50} of 0.04 μ M.⁴³ The most potent staurosporine derivative, UCN-01 (7-hydroxy-staurosporine, Figure 8), exhibited an IC_{50} value of 5 nM and is in clinical trials for treatment of cancer.⁴⁴⁻⁴⁷ Unfortunately this inhibitor turned out to be non specifically targeting many other kinases such as PKC and Chk1.⁴⁸⁻⁵⁰ Several additional reports of PDK1 inhibitors have also appeared in the literature. Different bisindolyl maleimides (BIM) and LY333531 are known to suppress the PDK1 activity as well. These inhibitors are cognates of staurosporine differing slightly in the chemical structure. BIMs possess a maleimide moiety instead of lactam as head group and there is no second covalent bond between the indole rings compared to the indolecarbazole from staurosporine (Figure 8).^{27, 51} This compound class was originally reported as selective

inhibitors of PKC which when tested against a small set of other kinases showed less specificity than thought.⁵¹

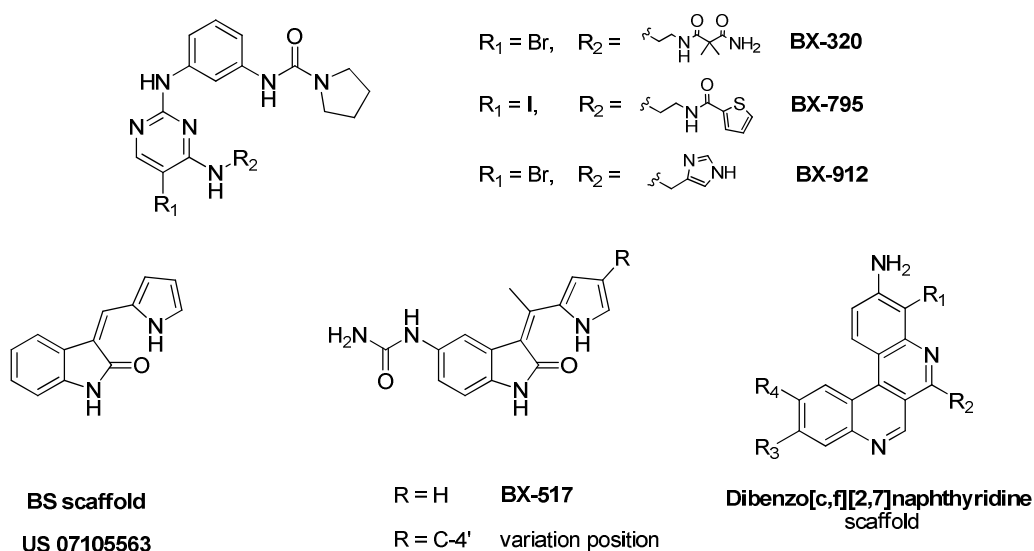
One inhibitor derived from the NSAIDs was Sulindac. Sulindac was found to have an ability to induce apoptosis in colon cancer cells through inhibition of PDK1.^{52, 53} Another example of an effective PDK1 inhibitor from the NSAID class is Celecoxib (Celebrex[®], Figure 8), a cyclooxygenase-2 (COX-2) inhibitor with an analgesic activity. Arico *et al.* reported in 2002 the inhibition of PDK1's enzymatic activity by celecoxib in colon cancer HT29 cells ($IC_{50} = 3.5 \mu\text{M}$).⁵⁴ Kulp *et al.* (2004) examine also the effect of celecoxib toward PDK1 and confirmed its inhibitory influence ($IC_{50} = 48 \mu\text{M}$).⁵⁵ In conclusion, both NSAIDs were neither very potent nor specific inhibitors. Actually, Celecoxib was developed as a selective inhibitor of cyclooxygenase-2 (COX-2) and additionally it was found besides its analgesic effect to inhibit various isoforms of carbonic anhydrase (CA). This is further difficult because higher concentrations are required toward PDK1.⁵⁵ OSU-03012 (Figure 8) was developed as an anticancer agent by blocking PDK1 activity without COX-2 activity in an effort to optimize Celecoxib. OSU-03012 mediated cell death in different cancer cells through inhibition of the PDK1/PKB pathway. Anyway, Zhang *et al.* denied the mechanism of action of this agent suggesting OSU-03012 acts through multiple mechanisms.^{35, 56, 57}

Figure 8: Chemical structures of selected PDK1 kinase inhibitors



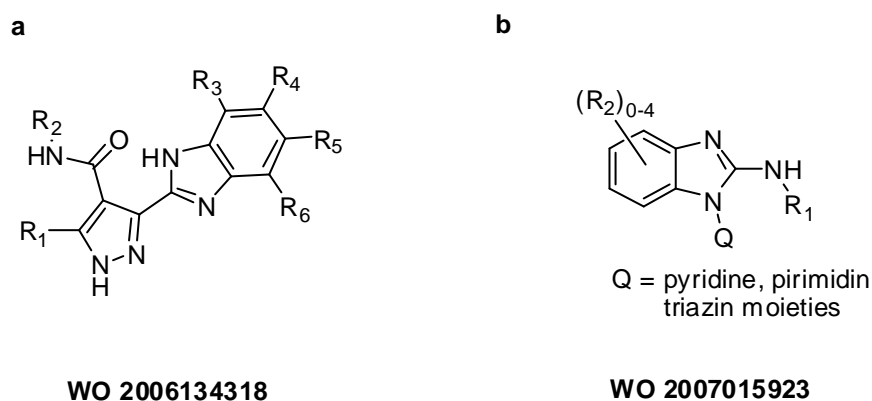
Feldman *et al.* described in 2005 the identification of three ATP-competitive PDK1 inhibitors BX-795, BX-912 and BX-320 (Figure 9) consisting of an aminopyrimidine backbone. The inhibitors were identified in a screening of compound libraries measuring PDK1- and PIP₂-mediated PKB activation.¹⁶ Among the class of aminopyrimidines there are more recent publications with a set of indolinone based PDK1 inhibitors. In a patent application of Bayer Schering Pharma AG in 2006 the (3Z)-3-(1H-pyrrol-2-ylmethylene)-1,3-dihydro-2H-indol-2-one was used as starting point for medicinal chemistry lead optimization, since the unsubstituted compound BS (Figure 9) displayed an inhibition of PKB in lowmicromolar range in a biochemical screening using a PDK1 mediated PKB2 activation assay.^{35, 40} In 2007, Islam *et al.* disclosed the synthesis and SAR of inhibitors derived from the above mentioned high-throughput screening lead BS. A potent (inhibition in nanomolar range) and selective inhibitor, BX-517, was discovered and optimized by exploring substitution at the C-4' position of the pyrrole (Figure 9). Due to the close homology between PKA and PDK1 the selectivity assay was restricted to PKA what should provoke critical thinking. The optimization study was focused on improvement of ADME and solubility properties and resulted in a moderately success. Only few compounds could be found with better pharmacokinetic properties accompanied by loosing cellular potency.^{38, 39, 51} Another recent study presented a novel series of dibenzo[*c,f*][2,7]naphthyridines (Figure 9) as potent and selective PDK1 inhibitors. A crystal structure of PDK1 with the inhibitor was explored to provide insights into structure-based design.⁵⁸

Figure 9: Chemical structures of further selected PDK1 kinase inhibitors.



Further fused heterocycles have been described as PDK1 inhibitors and it becomes apparent that most of the compounds are subsequent optimizations of celebrex and staurosporine scaffolds to mimic the plain adenine moiety to be adaptable for the ATP binding site. In two recently patents, filed by *Vernalis & D Limited*⁵⁹ and *Vertex Pharma*⁶⁰, benzimidazole based scaffolds were developed to target the ATP binding site of PDK1. Researches at Vernalis have discovered pyrazole substituted benzimidazole derivatives with up to a nanomolar inhibition potency (Figure 10) using a fragment based design within literary search. Subsequent optimization led to higher affinity compounds.^{59, 61} Binch *et al.* from the Vertex Pharma filed a patent with benzimidazoles combined with a pyridine, pyrimidine or triazin moieties.⁶⁰

Figure 10: General structures of PDK1 inhibitors: Patents of *Vernalis & D Limited* (a) and *Vertex Pharma* (b)



Numerous additional PDK1 inhibitors directed to the ATP binding site are published and reviewed.³⁵ Herein a short overview with representative structure classes is given in order to present the course of action in drug discovery focused on PDK1. Nevertheless, due to the relative structural conservation of ATP binding sites for several protein kinases and resulting cross reactions with many different kinases, the risk of dose limiting off-target effects increases and it is a challenge to find a new candidate for clinical trials. In fact, not only in case of PDK1 the most ATP-competitive inhibitors show limited selectivity,^{62, 63} implying that certain protein kinases have not been considered as suitable for drug development, in particular protein kinases for which closely related isoforms exist. This raises the question in drug discovery programs, which promising concept could lead in enhancing selectivity.

Currently, the trend toward multi-kinase target strategy is increased in an attempt to become enhanced antitumor efficacy and safety profiles compared to single target drugs. Now that the structures of many kinases have been determined, this may reveal the distinct features and design rules enabling to find an appropriate drug.⁶⁴ Moreover, several programs directed to non-ATP-competitive kinase inhibitors have been launched.

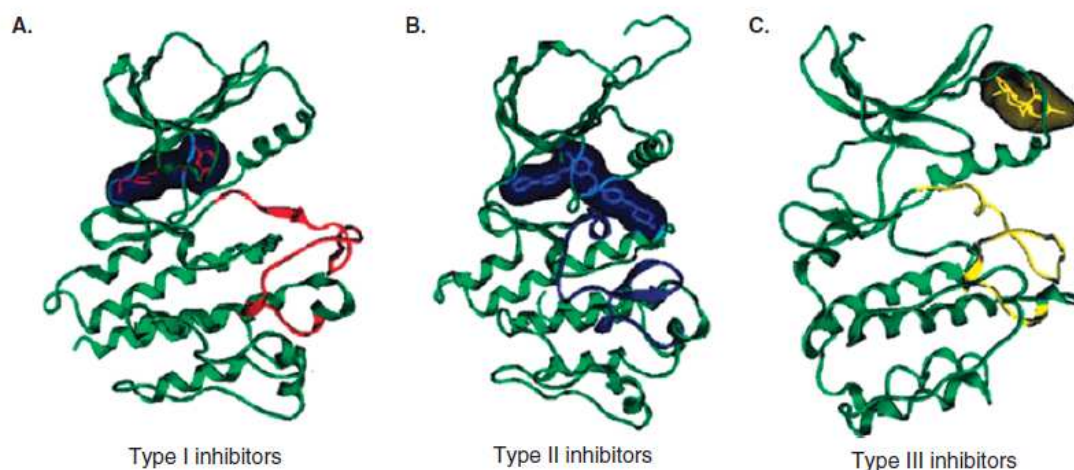
1.8. Allosteric Inhibitors

As an alternative and as a complement to ATP binding site-directed compounds, that are referred also as Type I inhibitors (Figure 11A), there is increasing interest in the development of non-ATP-competitive strategies for protein kinase drug developments. Non-ATP-competitive drug strategy could avoid the poor target selectivity and could extend the therapeutically indications.^{7, 65} The interest in allosteric drugs arose together with the success in the development of G-protein-coupled receptors (GPCR) drugs that bind at sites topographically distinct from the orthosteric site. Allosteric modulators of GPCR provided high selectivity and led to a greater diversity in the repertoire of pharmacological effects.⁶⁶⁻⁶⁸

During the last few years, a series of protein kinase inhibitors have been referred as non-ATP-competitive inhibitors although most of them target at least partially the ATP binding site. They are also termed as Type II inhibitors and occupy in addition to a part of the ATP binding site a neighbouring area (Figure 11B). They act in this manner in some extent in a different, non-competitive mechanism of inhibition. These inhibitors induce a conformational shift in the target enzyme and the kinase is no longer able to function. Well known representatives of Type II inhibitors are imatinib and sorafenib (Table 1). However, although Type II inhibitors are more selective than Type I inhibitors, they are not completely specific due to similar hydrophobic regions adjacent to the ATP binding site among the protein kinases. Furthermore, there is also a strategy to inhibit the kinase activity utilizing an allosteric inhibitor, Type III inhibitors. Allosteric inhibitors act by binding to a part of the enzyme, which is distinctly separated from the active site (Figure 11C) and by inducing a conformational shift (similar to inhibitors Type II) in the target enzyme such that the kinase is no longer able to function properly. Type III inhibitors have been developed for instance for mitogen-activated protein kinase (MAPK).^{69, 70} These Type III inhibitors bind to allosteric sites within the kinase domain, but there are also allosteric inhibitors directed to regulatory regions. Akt inhibitors that target the PH domain and the hinge region have been identified

and investigated showing selective behavior between the three AKT isoforms.^{71,72} Thus, Type III inhibitors are the most selective compounds so far.

Figure 11: The three classes of small molecule kinase inhibitors⁷³



Interestingly, the characterization of novel allosteric sites as druggable sites might enable the development of drugs with more subtle modulation of the protein kinase activity as compared to the complete inhibition of the enzymatic activity. In addition the targeting of allosteric-regulatory sites could potentially generate inhibitors, but also protein kinase activating drugs.

Discovering the PIF pocket of PDK1 as an allosteric site that is situated distant to the ATP binding site and that serves as a regulatory site for interaction with the substrates we were able to identify and suggest this allosteric fragment as a possible target for drugs. Furthermore, we have provided recently first evidence that a small molecule can trigger activation of PDK1.²³

1.9. State of the art: low molecular weight compounds targeting the allosteric PIF pocket in PDK1

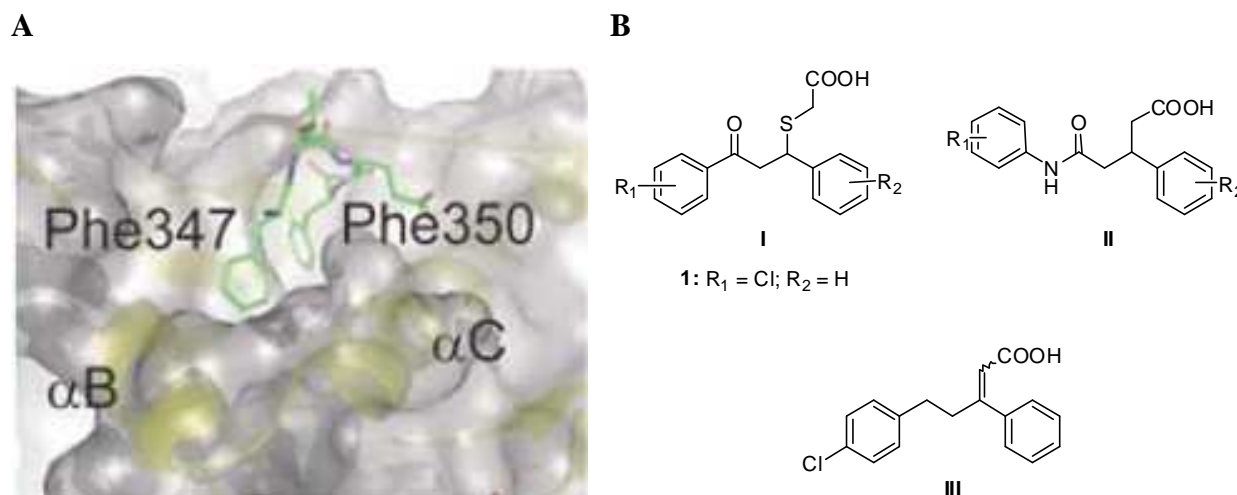
1.9.1. First compounds designed to bind to the PIF pocket of PDK1: activators of catalytic activity

The preliminary work was carried out by Dr. M. Engel and Dr. R.M. Biondi (Research group Phosphosites (PS)). It concerns the discovery of the PIF pocket in PDK1 and its key role in the molecular mechanism for the conformational transitions that take place upon activation of AGC kinases.^{11, 26, 31} Thereby, biochemical and molecular studies shed light on the fact that this binding site is required for intermolecular interactions of PDK1 with its substrates. To identify first small molecules which bind to the PIF pocket a virtual screening approach was employed.⁷⁴ The entry point was provided by the comparison of the crystallized PDK1 PIF pocket with that of the closed, active conformation of PKA within the C-terminal HM. The HM contains two subpockets where the phenyl residues of the terminated sequence FXXF dock (Phe347, Phe350, Figure 12A). Then the definition of a pharmacophore model followed. In the effort to identify compounds with an affinity to the PIF pocket a 3D *in silico* screening of a commercial compound database was performed using the Unity 3DTM-software (Tripos Software) and compounds possess feature similar to the phenyls (Figure 12A) were selected. Finally, the effect of a subset of selected compounds on the activity of different AGC protein kinases was tested *in vitro*. This search resulted in two hit classes, **I** and **II** as illustrated in Figure 12B. The small weight compounds allosterically activate PDK1 mimicking the phosphorylation dependent conformational transition.⁷⁴ Both compounds scaffolds turned out to be particular interest due to their influence on the activity of PDK1 toward a polypeptide substrate that comprises the activation loop residues of PKB, known as T308tide. The molecules with the scaffold of **I** and **II** increased the PDK1 activity. Further characterizations indicated that these compounds competed with the PIF pocket for the binding to PDK1. The first consequent publication restricts to the compound series **I** because of their low AC₅₀ and their relatively specificity toward PDK1, characterizing additionally the mechanism of action of these compounds by mutagenesis experiments of PDK1, interaction-displacement studies and isothermal calorimetry.^{12, 74}

Based on the first hit compounds **I** and **II**, I was able to synthesize the first improved allosteric modulators of PDK1 (**III**, Figure 12B).⁷⁵ As part of the present thesis, I optimized

this new compound series further and carried out a part of the biological evaluation, which will be described in detail in the results chapters 3.1, 3.2 & 3.3.

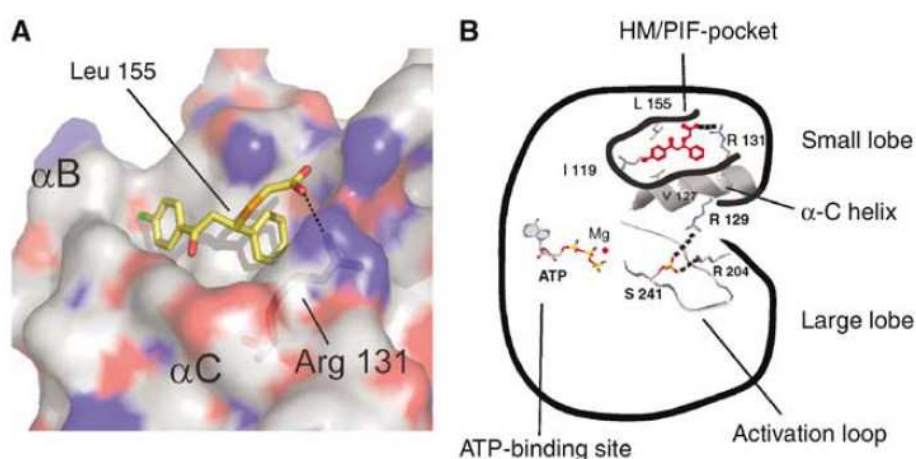
Figure 12: A: Close up of the PIF pocket⁷⁴ **B:** Hit compounds



The active compounds, identified in the screening, display several common structural features, two aromatic rings connected by a three or four atom chain with a side chain carrying a carboxyl function. The requirement of the carboxyl group in compound **1** was investigated comparing to the requirement of the phosphate on the phosphorylated HM (P-HM) polypeptides and comparing on the methyl ester derivative of **1**. PDK1 was activated by polypeptides P-HM but not by non P-HM. Moreover, the ester derivative was inactive. The physiologically achieved negative charge of the carboxyl group in **I** seems to mimic the phosphate moiety contacts. Mutation studies provided evidence that **I** binds to the PIF pocket abolishing the activation of PDK1. Mutants of the PIF pocket did not show PDK1's activity decrease. Further biochemical studies of PDK1 mutants identified Gln150 and Arg131 as the most important residues in a sulphate binding site next to the PIF pocket that was found out analyzing the crystal structure of PDK1 within the comprising residues Arg131, Thr148, Lys76 and Gln150. In the following a series of related compounds containing chlorine substituents at different positions on the left phenyl moiety was synthesized and tested against a panel of AGC kinases. Substituents on *meta* and *para* positions are favored and increase the activity toward PDK1. Substituents on the *ortho* position and on the right phenyl moiety greatly decrease the compounds' ability to activate PDK1. The intrinsic activity of the related AGC kinases was not affected by compound **1**.

A docking model was built on the basis of the mode of interaction of the C-terminal Phe347 und Phe350 to PKA, whereas the carboxylate was positioned to achieve the interaction with the positive charge of Arg131 (Figure 13A). Figure 13B displays the mechanism of PDK1 activation caused by compound **I** highlighting the most important residues.

Figure 13: **A:** Model for compound **I** docking to the PIF pocket on PDK1. **B:** Scheme for the activation of PDK1. ⁷⁴



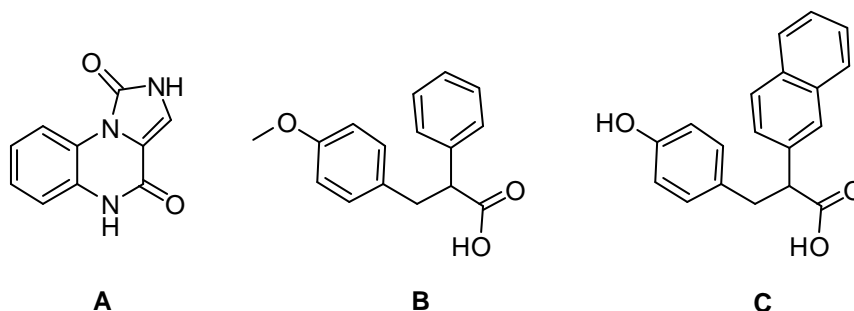
In conclusion, the results provide the evidence that low molecular weight compounds can modulate the conformational inactive-active transition of PDK1 by targeting the PIF pocket (Figure 13A & B).⁷⁴

1.9.2. Further PIF pocket-directed compounds referred in the literature

The published results of the PS group concerning the discovery of the PDK1 interacting fragment pocket, its regulatory properties and in particular the evidence that the PIF pocket is amenable to low molecular weight molecules binding, has caused interest and initiated new approaches to identify new allosteric modulators of PDK1. Nevertheless, our approach is a relatively new one from a drug discovery point of view. Only two reports including new strategies to identify PIF pocket-directed compounds have been published so far. Firstly, NMR-based fragment screening and ¹H-¹⁵N TROSY experiments have been performed by researcher at Pfizer Global Research and Development in order to identify selective small molecule modulators of PDK1.⁷⁶ Stockman *et al.* analyzed a library of chemically diverse compounds in a NMR screening for fragments as an alternative to high throughput screening

(HTS). Thereby, the goal was to identify allosteric and ATP-competitive scaffolds exploiting the PIF pocket site and the ATP binding site. Three activators of PDK1 were identified (Figure 14) whereas these fragments activated PDK1 weakly at high concentrations. In a saturation transfer difference NMR experiment compound **A** turned out to compete ATP and **B** and **C** to bind at the ATP site and PIF pocket, respectively. **B** and **C** are structurally similar compared to compound class **I**. They contain also a negative charged carboxyl group but they differ in its position. Due to this fact they could have a distinct binding mode and need more characterization to be proven as PIF pocket-directed compounds. The data was generated through a Caliper assay and ^{19}F NMR assay to provide evidence for the binding sites of the molecules **A**, **B** and **C**. In summary, since it is known that hits from this NMR spectroscopic method are weaker potent than hits from HTS, this NMR spectroscopic approach offers an option to identify new fragments as starting points for drug development but it does not provide an advance in finding high potent and specific target compounds.

Figure 14: NMR-based fragment screening hits as ATP-competitive and allosteric PIF pocket modulators, respectively

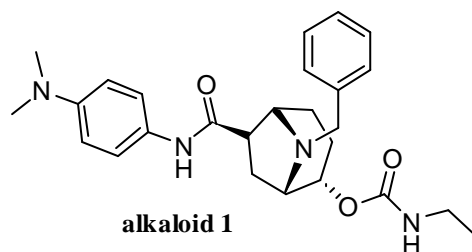


More recently, Merck Research Laboratories presented the discovery of alkaloids as PIF pocket specific ligands using ultrahigh throughput screenings (uHTS) TR-FRET and Alphascreen for lead identification.⁷⁷ Therefore, a biotinylated peptide substrate (PDK1tide) was developed. It engages both the ATP and the PIF pocket of PDK1 pursuing a bisubstrate analogues strategy that is considered to identify highly selective and potent inhibitors. This strategy was selected with the goal to indentify both ATP-competitive inhibitors and allosteric ligands, since PDK1 possesses at least three ligand-binding pockets. In this screening campaign, alkaloid 1 was identified as a hit (Figure 15). However, the authors did not provide experimental evidence that the compound really targeted the PIF-binding pocket. Interestingly, alkaloid 1 lacks the carboxyl function. For this reason alkaloid compounds are

supposed to inhibit PDK1 activity in contrast to compounds including a carboxyl group achieving different mechanism of action.

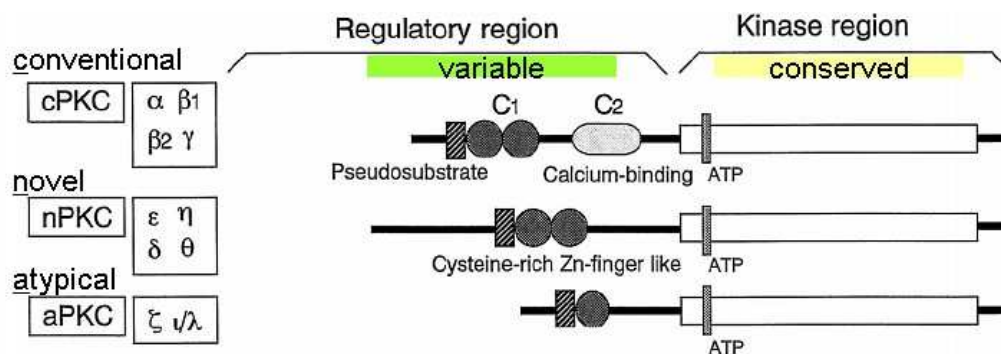
Thus, these results confirmed our findings that different types of small molecules and less diversity in structure can induce different mechanism of action of kinases, activation or inhibition. Testing a series of compounds against a panel of AGC kinases we were able to find activators and inhibitors of AGC kinases. Compounds with the scaffold of **I** (Figure 12B) proved to be potent activators of PDK1. Compound **1** (Figure 12B) served as lead structure for this study to design and synthesize new modulators of PDK1's activity binding the PIF pocket.

Figure 15: Chemical structure of **alkaloid 1**



1.10. Atypical PKCs

Protein kinase C family as a member of AGC superfamily consists of at least eleven related isoforms that form three subfamilies based upon the structure of their regulatory domains: the conventional/classical (cPKCs), the novel (nPKCs) and the atypical (aPKCs) PKCs (Figure 16).⁷⁸ All isoforms of PKC have conserved and variable (C1, C2) domains that are connected by a hinge region and all of them possess a pseudosubstrate (PS) binding site. The C1 domain contains cysteine-rich motifs that serve as sites for diacylglycerol (DAG) and phorbol esters binding.⁷⁹ The C2 domain serves for phospholipids binding that occur in a calcium-dependent manner.⁸⁰ The conserved domain is composed of the ATP binding site and the substrate binding site and defines PKC members within the AGC kinase superfamily.¹⁰ The activation mechanism differs between the three PKC subfamilies.

Figure 16: Structure of Protein Kinase C Isoforms⁸¹

To the conventional PKCs belong PKC α , - β 1, - β 2 and - γ . These enzymes require phosphatidylserine, diacylglycerol (DAG), phorbol esters and calcium (Ca^{2+}) to become optimal activated.⁸²

The novel PKCs consist of the isoenzymes PKC δ , - ϵ , - η and - θ . They are not regulated by Ca^{2+} but can be activated by phorbol esters and DAG in the presence of phosphatidylserine.⁸²

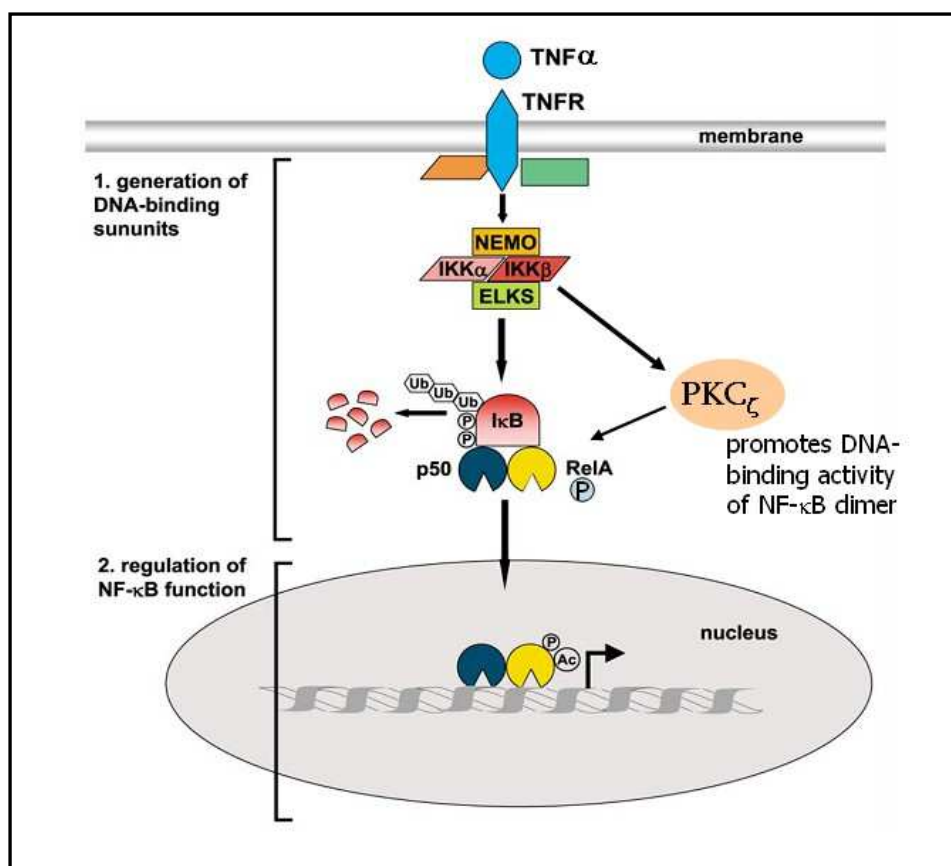
Finally, the atypical PKCs are regulated neither by Ca^{2+} , nor by phorbol esters and by DAG. The aPKCs possess in their regulatory region an atypical C1 domain, thought to participate in lipid binding. Therefore, the aPKCs are activated by lipid components such as phosphatidyl inositol, phosphatidic acids, ceramide and arachidonic acid.⁸² Besides the atypical C1 domain aPKCs possess a PB1 (Phox and Bem 1) domain, which is involved in protein-protein interactions, the regulation of catalytic activity and a pseudosubstrate domain.⁷⁸ The isoforms PKC ζ (PKC ζ), PKC ι (PKC ι) and PKC λ (PKC λ), whereas PKC λ is the mouse orthologue of the human ι , belong to the atypical subfamily and display a strong homology among each other. In spite of a 72 % sequence homology at the amino acid level of PKC ζ and PKC ι , the recent data suggested that both kinases are not functionally redundant.⁸³ Expression profiling studies have revealed that both kinases have distinct patterns of expression in various biological systems. PKC ι/λ showed a ubiquitous expression, whereas PKC ζ exhibited a more restricted pattern of expression. Additionally, investigations of the effect of genetic disruption demonstrated different effects on embryonic development in the mouse. Knockouts of PKC ι/λ are embryonically lethal,⁸⁴ whereas knockouts of PKC ζ resulted in viable mice that exhibit immunological deficiencies in the NF- κ B (nuclear factor kappa B) pathway.^{83, 85} Moreover, PKC ζ and PKC ι/λ are integrated in distinct downstream

signaling pathways. With further experiments it has been shown that PKC ζ rather than PKC ι/λ is involved in the NF- κ B pathway by phosphorylation of Ser311 of the RelA subunit.^{86, 87} Using PKC ζ - or PKC ι -deficient mouse embryo fibroblasts from knockouts of PKC ζ and PKC ι/λ , the PKC ζ deficient fibroblasts exhibited defects in the NF- κ B signaling and PKC ι deficient fibroblasts did not.⁸⁵⁻⁸⁷ Besides, recently Levy *et al.* succeeded in providing evidence on a previously uncharacterized mechanism of the NF- κ B regulation. The study revealed a contrariwise role of the phosphorylated Ser311 residue in the NF- κ B pathway. The phosphorylation of Ser311 by PKC ζ abolished the binding of histone methyltransferase GLP to the RelA subunit and disrupted the following GLP-mediated methylation of histone H3 enabling NF- κ B to become transcriptionally active. Consequently, PKC ζ acquires a critical role as mediator of the chromatin changes necessary for effective NF- κ B target gene expression.^{88, 89}

1.11. PKC ζ as drug target

The knockout study, described above, gives evidence that PKC ζ plays a critical role in the activation of the eukaryotic transcription factor NF- κ B. Several more studies demonstrated additionally PKC ζ 's involvement in the activation of NF- κ B in cell types and organs such as B-cells, T helper cells, T lymphocytes, lung and liver but not in muscles.⁹⁰⁻⁹⁴

NF- κ B is composed of several related transcription factors: p50, p52, RelA (p65), c-Rel and RelB and plays an important role in the immune system. NF- κ B regulates genes controlling of the immune system, apoptosis, cell growth and tissue differentiation.^{17, 95, 96} The essential function of NF- κ B is to prevent the TNF α -induced cell death. There are two signaling pathways leading to the activation of NF- κ B dimers, the canonical pathway and the non-canonical pathway.⁹⁷⁻¹⁰⁰ In both cascades TNF α or other pro-inflammatory cytokines stimulate the activation of the IKK complex. In this thesis the focus is directed to the canonical pathway as it includes PKC ζ in its transductional regulation. In the canonical pathway the activation of NF- κ B dimers, a complex of p50 and RelA (Figure 17), occurs due to IKK-mediated and due to PKC ζ -mediated phosphorylation of I κ B.^{101, 102} Phosphorylated I κ B proteins lead to their subsequent proteasomal degradation enabling the active NF- κ B dimer to translocate into the nucleus and induce the anti-apoptotic target gene expression.

Figure 17: NF- κ B activation: the canonical pathway

The binding of TNF α to the receptor TNFR leads to the recruitment and activation of the IKK complex comprising IKK α , IKK β , NEMO and ELKS. The IKK complex then phosphorylates I κ B, and PKC ζ phosphorylates the subunit RelA leading to degradation by the proteasome. Finally NF- κ B translocates to the nucleus to activate target genes.

Considered together the transcription factor NF- κ B and consequently PKC ζ play fundamental role in immune and inflammatory responses. Not surprisingly, constitutive activation of NF- κ B is implicated in several disease conditions including inflammatory disorders and autoimmune diseases as well as in some forms of cancer, such as leukemia, lymphoma, colon cancer and ovarian cancer.¹⁰³ Since PKC ζ is a molecular switch in this signal transduction, it represents an interesting and important target for the development of novel therapeutics to treat the corresponding diseases. In particular, PKC ζ may provide a specific therapeutic target for the prevention of these diseases because direct inhibition of NF- κ B will cause toxicity due to the protective role of NF- κ B in all cells and tissues.^{104, 105} Moreover, further studies suggested that atypical PKC ζ is required for chemotaxis in various cancer cell lines, such as breast, lung and leukemia cell lines. These results indicate that targeting PKC ζ may emerge as an effective method for blocking both, cancer cell chemotaxis

and tumor associated immune responses. Although in oncology the target validation studies have mainly been focused on the other atypical PKC isoforms PKC ι so far, the literature generated an oncogenic role of PKC ζ . Immunoblotting experiments with the human lymphoma cell line U937 demonstrated that PKC ζ takes a central position in the TNF α -induced pathway. The TNF α mediated activation of NF- κ B in U937 cells resulted in enhanced PKC ζ phosphorylation and activation and in the following transcription of anti-apoptotic genes by NF- κ B.¹⁰⁶ The tumor cell response to chemotherapeutics and cytokines was examined by Filomeno *et al.* in 2002 expressing stably kinase-dead and dominant negative PKC ζ mutant in U937 cells. The results revealed that PKC ζ inhibition by etoposide, an anti-cancer chemotherapy drug, led to acceleration of apoptosis in leukemic cells. Moreover, the etoposide-influenced inhibition of PKC ζ led to a sensitization of cells growth in nude mice.¹⁰⁷

Some more studies demonstrated that PKC ζ phosphorylates further substrates that are involved in the regulation of apoptosis. De Thonel *et al.* investigated the role of PKC ζ in immature myeloid KG1a leukemic cells. The study revealed PKC ζ as a regulator of Fas cell death signaling showing a resistant effect on Fas-induced apoptosis.¹⁰⁸ The role of PKC ζ regulating apoptosis is also supported by the study of Bezombes *et al.* demonstrating that overexpression of PKC ζ in U937 confers resistance daunorubicin and 1- β -D-arabinofuranosylcytosine. These drugs are used for the therapy of acute myeloblastic leukemia.¹⁰⁹

Summing up, the literature data shed light on PKC ζ as a clear target for the development of potent drugs with antileukemic effect and for treatment of inflammatory diseases. However, PKC ζ regulates additionally the insulin-stimulated glucose transport in muscle and adipose tissues.^{110, 111} Skeletal muscle and adipocytes express the major transporter GLUT4 and require insulin for glucose uptake. Binding of insulin to receptors leads to translocation of glucose transporters from the cytoplasm into plasma membrane, allowing glucose to enter the cell. Defects of the insulin action lead to insulin resistance that is manifested by decreased glucose uptake and subsequently to diabetes type-2.^{110, 111} PKC ζ acts as a transducer protein of glucose transport in response to activated PI3K via interaction with insulin receptor substrates (IRS). Activation of PKC ζ could trigger the signal transduction leading to GLUT4 translocation and glucose transport into the cell. Thus, the inactivation of this enzyme might lead to hyperglycaemia and to insulin resistance.¹¹¹ Indeed, Lee *et al.* presented in a recent study *in vivo* experiments using PKC ζ /IL-6 double-knockout mice that indicate PKC ζ

ablation in non-hematopoietic cells but not in the hematopoietic system was sufficient to drive inflammation and IL-6 synthesis in the adipose tissue, as well as insulin resistance.¹¹²

However, it should be taken into account that knockout studies cannot be compared well with the situation where an enzyme is inhibited by a small molecule drug. It can be expected that inhibition by a drug, which happens part-time and too less than 100 %, will not have the same detrimental side effect than a complete knockout of PKC ζ . Therefore, the final validation of PKC ζ as a target can best be done with a suitable small molecule inhibitor.

1.12. Inhibitors of PKC ζ

PKC kinases as a pleiotropic family regulate various cellular processes in multiple cell signaling pathways including proliferation, glucose metabolism, differentiation, cell survival and apoptosis. Elevated level of the particular isoforms were found in various cancer forms, such as breast, lung, liver, colon and prostate cancer as well as hematopoietic lymphomas and leukemias.^{113, 114} However, the biological functions of each PKC isoforms differ in their action of the tumor progression. For this reason investigations on selective PKC inhibitors have attracted great attention during the last years in order to develop potential anti PKC agents. Several inhibitory compounds with large structural variety and with different mechanisms of inhibition have been proposed.^{115, 116} Promising examples entered already clinical trials for several human cancers. Among others, Enzastaurin (LY317615), Midostaurin, Bryostatin, Safingol and ISIS 3521 (Figure 18) have been conducted in clinical studies.

Enzastaurin and Midostaurin derived from optimization approaches of Staurosporine to achieve more selective analogues for clinical trials. Staurosporine was discovered in a screening for PKC inhibitors¹¹⁷ and showed good inhibition of PKC in *in vitro* models.¹¹⁸ Staurosporine's poor selectivity has not been hampered further clinical developments to find analogues with more specificity for PKC isoforms and other kinases as it shows nanomolar activity against many protein kinases. Enzastaurin was described first as a selective inhibitor of PKC β but afterwards it showed also an inhibitory effect toward PKC ϵ . Enzastaurin entered the Phase III clinical trials and turned out to be applicable for different type of cancer. Midostaurin was originally proposed as an inhibitor of multiple isoforms of PKC but it turned out as a multi kinase inhibitor. Midostaurin showed also inhibition effects toward Kit, FLT3, VEGFR and PDGFR.¹¹⁶ In clinical studies Midostaurin entered Phase II and has been tested in

combination with other chemotherapeutics. Enzastaurin and Midostaurin are competitive inhibitors binding the ATP binding site (Table 2).¹¹⁶

Figure 18: Structures of the PKC inhibitors Enzastaurin, Midostaurin, Bryostatin and Safingol

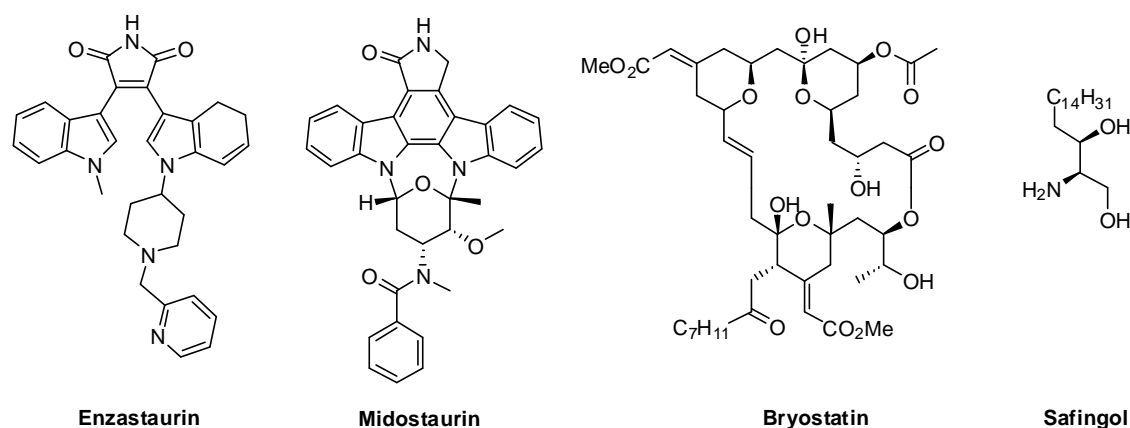


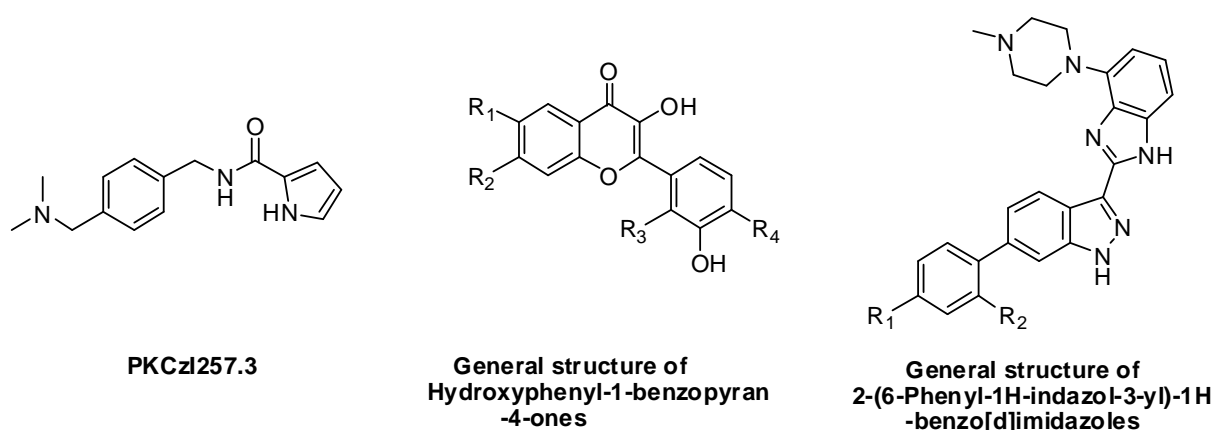
Table 2: Some examples of PKC inhibitors in clinical trials.¹¹⁶

PKC inhibitor	Target	Binding site	Status
Enzastaurin	PKC β	ATP binding site competitive	Phase III
Midostaurin	PKC, FLT3, VEGFR2, Kit PDGFR	ATP binding site competitive	Phase II
Bryostatin	PKC	Regulatory domain DAG	Phase II; discontinued
Safingol	PKC	Regulatory domain DAG	Phase I; discontinued
ISIS 5321	PKC α	mRNA	Phase III; discontinued

The naturally occurring macrocyclic lactone Bryostatin targets the regulatory phorbol ester receptor which means the DAG binding pocket of cPKCs and nPKCs and induces the inhibition of the corresponding PKCs.¹¹⁹ Furthermore, it inhibits phorbol ester induced tumorigenesis and differentiation of leukaemia cells.^{120, 121} Clinical studies were conducted with Bryostatin with disappointing results due to dose-limiting toxicity and were discontinued

(Table 2).¹¹⁶ Safingol, a synthetic drug displayed low efficacy and was discontinued already in Phase I of the clinical trials (Table 2).

To summarize, these examples discussed here reached clinical trials but they display relatively poor target selectivity related to one isoforms of the PKC family. This is attributed to structural conservation of ATP binding sites of the PKC isoenzymes. Therefore, most of the PKC targeting compounds cross-react with other kinases. However, it has been challenging to find specific kinase inhibitors due to the high degree of homology in the ATP binding site pocket between the 11 PKC isoforms. An additional challenge in finding a selective inhibitor of PKC ζ constitutes the closest homologue PKC ι form. Although several attempts were made to develop compounds able to inhibit selectively PKC ζ and several inhibitors were referred to as selective, the approaches failed in finding a truly selective and effective target molecule. The so-called PKC ζ selective inhibitors have been identified by screening libraries and natural compound resources. We will focus the attention on three recently published compound classes. These include PKC ζ I257.3 (*N*-(4-((dimethylamino)methyl)benzyl)-1*H*-pyrrole-2-carboxamide)¹²², Hydroxyphenyl-benzopyran-4-ones¹²³ and 2-(6-Phenyl-1*H*-indazol-3-yl)-1*H*-benzo[*d*]imidazoles (Figure 19).¹²⁴ PKC ζ I257.3 was screened out from a compound library including two hundred compounds in a substrate-specific strategy with an IC₅₀ of 28 μ M. *N*-(4-((dimethylamino)methyl)benzyl)-1*H*-pyrrole-2-carboxamide exhibits a small molecule nature contrary to the widely employed peptide pseudo-substrates. This inhibitor prevents the EGF induced breast cancer cell chemotaxis and migration. The specificity of the compound was evaluated only against PKC α whereby there are no data available about the selectivity toward the most closely related PKC ι .¹²² Yuan *et al.* identified in a screening including a library with structurally diverse heterocyclic compounds hydroxyphenyl-1-benzopyran-4-ones as inhibitors of PKC ζ enzymatic activity. The isoforms selectivity was investigated with a panel of kinases using a Millipore kinase profiler.¹²³ This class of compounds was proved as selective only compared with classical or novel PKCs without details about the specificity toward PKC ι . In an optimization effort Trujillo *et al.* identified a potent and PKC isoform selective compound class of 2-(6-Phenyl-1*H*-indazol-3-yl)-1*H*-benzo[*d*]imidazoles (Figure 19) starting with 6-phenyl-3-benzimidazole. The most active analogue showed a good activity against PKC ζ and CDK-2, but it turned out to be a moderately potent across the range of other kinases which is another hardly manageable feature of compounds targeting the ATP-binding site.¹²⁴ Thus, there are no truly PKC ζ -selective inhibitors described in the literature so far.

Figure 19: Structures of PKC ζ inhibitors.¹²²⁻¹²⁴

1.13. Allosteric approach to inhibit PKC ζ

Despite a lot of efforts have been directed at finding selective ATP-competitive PKC ζ inhibitors, a marginal success was achieved. In recent years the trend is toward non-ATP site-directed approaches as they provide an alternative strategy to find highly specific kinase inhibitors.^{7, 125} An alternative mechanism for the non ATP-competitive inhibition exhibits allosteric one. This is indicated not least by the fact that the allosteric site is less conserved as the ATP binding site. Additionally, the inhibition of allosteric sites stabilizes the inactive conformation of the kinase. Moreover, the development of resistance to kinase inhibitor therapy due to mutation in the ATP binding site that is known with ATP-competitive inhibitors can be prevented by an allosteric inhibitor.

As already precisely described in chapter 1.7 we suggested the PIF pocket that is situated on the catalytic domain of the AGC protein kinase family as an allosteric targeting site for the development of allosteric inhibitors. Based on the example of PDK1 it is shown, the binding of the C-terminal peptide motif of substrate proteins provokes an allosteric activation of the catalytic activity of PDK1. In case of PKCs and other substrate kinases the hydrophobic motif on the C-terminus binds intramolecular in the PIF pocket of the appropriate kinase (Figure 6) stabilizing the active structure. In our previous work we were able to show that by binding to this site, small weight molecules could prompt allosteric conformational changes affecting the activity of PDK1. Thus the small weight molecules mimic the activatory effects of the natural peptide ligands, the phosphorylated hydrophobic motif (HM) peptides, in the catalytic

domain. The PIF pocket is limited to about 60 AGC kinases and is less conserved with amino acids than the ATP binding site. In comparison to other PKC isoenzymes PKC ζ exhibits six different PIF pocket residues (Figure 20). This fact suggests that the development of PIF pocket-directed compounds could result in a specific compound toward PKC ζ without influencing the activity of any other PKC isoenzyme and other AGC members. Thus, the variability of the PIF pocket within the AGC family may enable selectivity.

Figure 20: Alignment of the amino acid sequences of representatives from all PKC subfamilies (cPKCs: alpha, beta, nPKCs: delta, theta, epsilon and aPKCs: iota and zeta) and PDK1.

	430	440	450	460	470	480
PDK1	MDGTAAEPRPG	-----	-----	-----	AGSLQHAQPPPQPR	KKR
PKCalpha	NQEEGEYINVPI	PEGDEEGNMLRQK	FEKAKLGPAGN	---	KVISPSEDRKQPSN	NLDRVK
PKCbeta	SQEEGEYFNVVP	PPEGSEANEELRQ	KFERAKISQGTKV	PPEEKT	TNTVSKFDNNGNR	DRMK
PKCdelta	-DNSGTYGK	-----	-----	-----	IWEGSS	-----KCN
PKCtheta	-DEVDMCH	-----	-----	-----	LPEPELNKERPSL	QIKLK
PKCepsilon	-DNRGEEHRAAS	PDG-----	-----	-----	QLMSPGENGEVR	QQAQLRG
PKCiota	-DQVGEE-K	-----	-----	-----	EAMNTRESGKASS	SLG
PKCzeta	-KDDSEDLK	-----	-----	-----	PVIDGMDGKIKIS	QQLG
	490	500	510	520	530	540
PDK1	PEDFKFGKLL	GEGSFSTVVLARE	LATSREYAIKILE	KRHIKENKVPYVT	REDRVMSRL	-
PKCalpha	LTDFNFLMVL	GKGSFGKVMLADR	KGTEELYAIKIL	KDVIQDDDV	ECTMVEKRV	LALLD
PKCbeta	LTDFNFLMVL	GKGSFGKVMLSER	KGTDDELYAVK	ILKDDVIQDD	VECTMVEKRV	LALPG
PKCdelta	INNFIFHKVL	GKGSFGKVLGEL	KGRGEYFAIKAL	KDVLIDDD	VECTMVEKRV	TLAA
PKCtheta	IEDFILHKML	GKGSFGKVFLAE	FKKTNQFFAIK	ALKDDVLMDD	DVECTMVEKRV	LSLAW
PKCepsilon	LDEFNFIVL	GKGSFGKVMLAE	LKGVAVKVLK	DVILQDDDV	DCTMTEKRI	LALAR
PKCiota	LQDFDLRVI	GRGSYAKVLLV	RLLKKTDRYAM	KVVKELV	DEDED	LDWVQTEKIVFEQAS
PKCzeta	LQDFDLIRVI	GRGSYAKVLLV	RLLKKNQIYAM	KVVKELV	DEDED	LDWVQTEKIVFEQAS
	550	560	570	580	590	600
PDK1	DHPFFVKLYF	TFQDDEKLYF	GLSYAKNGELL	KYIRKIGSFDE	TCTRFYTAIEI	VSALEYLH
PKCalpha	KPPFLTQLHS	CFQTVDRLYF	VMEYVNGGDL	MYHIQOVGK	FKEPQAVFYAA	EISIGLFFLH
PKCbeta	KPPFLTQLHS	CFQTMDRLYF	VMEYVNGGDL	MYHIQOVGR	FKEPHAVFYAA	EIAIGLFFLQ
PKCdelta	ENPFLTHLIC	TFQTKDHLF	VMEFLNGGDL	MYHIQDKGR	FELYRATFYAA	EIMCGLQFLH
PKCtheta	EHPFLTHMFC	TFQTKENLFF	VMEYVNGGDL	MYHIQSCHK	FDLRATFYAA	EIIIGLQFLH
PKCepsilon	KHPYLTQLY	CFQTKDRLFF	VMEYVNGGDL	MFQIQRSR	KFDEPRSRFYA	AEVTSALMFLH
PKCiota	NHPFLVGLHS	CFQTESRLLF	VIEYVNGGDL	MFHMQRQR	KLPEEHARFYA	EISLALNYLH
PKCzeta	SNPFLVGLHS	CFQTTSRLLF	VIEYVNGGDL	MFHMQRQR	KLPEEHARFYA	EICIALNFLH
	610	620	630	640	650	660
PDK1	GKGI IHRDL	KPENILLNEDMH	IQTDFGTAKVLS	PESKQARANSF	VGTAQYVSP	PELLTEK
PKCalpha	KRGIIYRDL	KLDNVMLDSEGH	IKIADFGMCK	--EHMMDGVT	TRTFCGTPDY	IAPETIAYQ
PKCbeta	SKGIIYRDL	KLDNVMLDSEGH	IKIADFGMCK	--ENIWDGVT	TKTFCGTPDY	IAPETIAYQ
PKCdelta	SKGIIYRDL	KLDNVLLDRDGH	IKIADFGMCK	--ENIFGESRA	STFCGTPDY	IAPETILQGL
PKCtheta	SKGIVYRDL	KLDNILLDKDGH	IKIADFGMCK	--ENMLGDAK	TNTFCGTPDY	IAPETILGQ
PKCepsilon	QHGVIIYRDL	KLDNILLDAEGH	CKLADFGMCK	--EGILNGVT	TTTTFCGTPDY	IAPETILQEL
PKCiota	ERGIIYRDL	KLDNVLLDSEGH	IKLTDYGMCK	--EGLRPGDT	TSTFCGTPNY	IAPETILRGE
PKCzeta	ERGIIYRDL	KLDNVLLDADGH	IKLTDYGMCK	--EGLGPGDT	TSTFCGTPNY	IAPETILRGE
	670	680	690	700	710	720
PDK1	SACKSSDLWAL	GCI IYQLVAGL	PPFR-----	AGNEYLIFQKI	IKLEYDFPEK	FFPK
PKCalpha	PYGKSVDDW	WAVGVLLYEML	AGQPPFD-----	GEDEDEL	FQSIMEHNV	SPKSLSKE
PKCbeta	PYGKSVDDW	WAVGVLLYEML	AGQAPFE-----	GEDEDEL	FQSIMEHNV	AVPKSMSKE

PKCdelta	KYTFSDVWWSFGVLLYEMLIGQSPFH-----GDEDELFEFESIRVDTPHYPRWITKE
PKCtheta	KYNHSVDWWSFGVLLYEMLIGQSPFH-----GQDEEELFHSIRMDNPFYPRWLEKE
PKCepsilon	EYGPSVDWWALGVLMYEMMAGQPPFE-----ADNEDDLFEFESILHDDVLYPVWLSKE
PKCiota	DYGFSDVWALGVLMFEMMAGRSPFDIVGSSDNPDQNTEDYLFQVILEKQIRIPRSLSVK
PKCzeta	EYGFSDVWALGVLMFEMMAGRSPFDII--TDNPDMDNTEDYLFQVILEKPIRIPRFLSVK
	730 740 750 760 770 780
PDK1	ARDLVEKLLVLDATKRLGCEEM-EGYGPLKAHPFFESVTWENLHQQTTPKLTAYLPAMSE
PKCalpha	AVSICKGLMTKHPAKRLGCGPE--GERDVREHAFFRRIDWEKLENR---EIQPPFKPKVC
PKCbeta	AVAICKGLMTKHPKRLGCGPE--GERDIKEHAFFRYIDWEKLERK---EIQPPYKPKAR
PKCdelta	SKDILEKLFEREPTKRLGVTGN-----IKIHPFFKTINWTLLEKR---RLEPPFRPKVK
PKCtheta	AKDLLVKLVFREPEKRLGVRGD-----IRQHPLFREINWEELEK---EIDPPFRPKVK
PKCepsilon	AVSILKAFMTKNPHKRLGCVASQNGEDAIAKQHPFFKEIDWVLEQK---KIKPPFKPRIK
PKCiota	AASVLKSFNLKDPKERLGCHPQ-TGFADIQGHFFFRNVDWDMMEQK---QVPPFKPNIS
PKCzeta	ASHVLKGFNLKDPKERLGCRPQ-TGFSDIKSHAFFRSIDWDLLEKK---QALPPFQPQIT
	790 800 810 820 830 840
PDK1	DDEDCYGNYNLLSQFGCMQVSSSSSSSHLSASDTGLPQRSGSNIQYIHDLDNSNFELD
PKCalpha	GK-GAENFDKFFTRGQPVLTTPDQLVIANIDQSDFEFQSYVNPQFVHPILQSAV-----
PKCbeta	DKRDTSNFDKEFTRQPVELTPDKLFI MNLDQNEFAGFSYTNPEFVINV-----
PKCdelta	SPRDYSNFDQEFLENEKARLSYSDKNLIDSMDQSAFAGFSFVNPKFEHLLD-----
PKCtheta	SPFDCSNFDKEFLNEKPRLSFADRALINSMDQNMFRNFSFMNPGMERLIS-----
PKCepsilon	TKRDVNNFDQDFTRREPVLTLVDEAIVKQINQEEFKGFSYFGEDLMP-----
PKCiota	GEFGLDNFDSQFTNEPVQLTPDDDDIVRKIDQSEFEGFEYINPLLSAEECV-----
PKCzeta	DDYGLDNFDTQFTSEPVQLTPDDEDAIKRIDQSEFEGFEYINPLLLSTEEVS-----

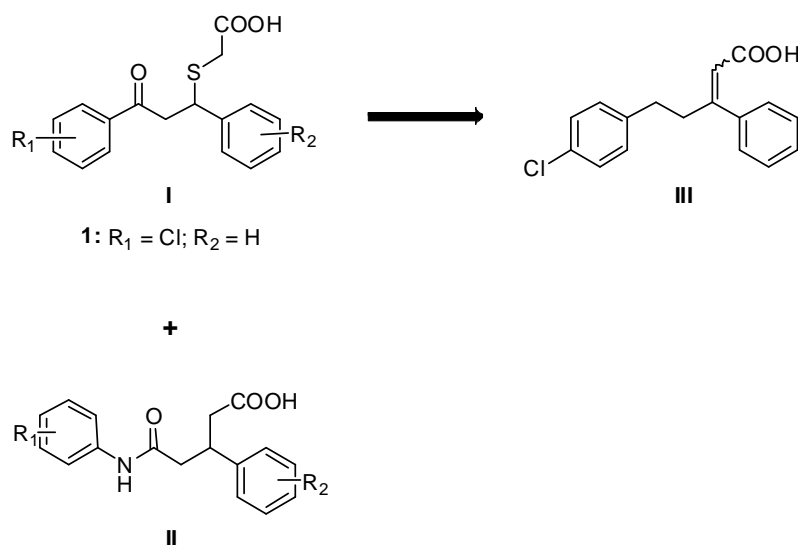
The PIF pocket residues of the individual protein kinases are displayed in yellow. The residues labelled in red are specific for PKC_{iota} and PKC_{zeta}. The blue labelled residues represent the highly conserved ATP binding site and the grey residues belong to the hydrophobic motif including the phosphorylatable rest (= intramolecular ligand of the PIF pocket). The numbering is based upon the PKC_{epsilon}.

2 Aim and work strategy of the present study

2.1. Scientific objective

The first kinase drug imatinib mesylate (“Gleevec[®]”) was introduced in US in 2001 and set the stage for protein kinases as drug targets. It was followed by several other small molecule kinase inhibitors that were launched, primarily for oncology application. However, protein kinase drug developments are still hampered by severe problems in the development of specific compounds. The reason for the lack of specificity is that most compounds target the ATP binding site, which is a relatively conserved site in the over 500 protein kinases encoded by the human genome. As an alternative to the ATP binding site-directed approach the interest has been increased in non ATP-competitive strategy to yield highly potent and specific drugs for protein kinases and to prevent side effects. Most interestingly, the characterization of novel allosteric sites as drugable sites might enable the development of drugs with more subtle modulation of the protein kinase activity as compared to the complete inhibition of the enzymatic activity. Since aberrant activation of the PI3K/PDK1 signaling pathway is associated with diseases such as cancer and diabetes, compounds that modulate the PDK1 activity gained interest to be useful as therapeutic agents.

With the discovery of the PIF pocket as an allosteric regulatory site between PDK1 and its substrates, we have provided a specific and selective control in the PI3K signaling transduction. Consequently, we suggested a novel pharmacological approach using the PIF pocket in PDK1 as a target site for small compounds in order to inhibit the phosphorylation of these substrates that require interaction with the PIF pocket. Hence, compounds directed to the PIF pocket are predicted to have more specificity. Actually, we were able to provide evidence that small drug like molecules can trigger activation of PDK1 binding the PIF pocket. In our initial work we identified hit compound classes (**I** and **II**, Figure 21) that modulate the PDK1 activity. These compounds display several common structural features: non polar bicyclic scaffold with non polar substituents and a polar side chain carrying a carboxyl function. Based on these results our group synthesized a series of compounds, comprising variations of substituents, extensions of the structure and ring variations to investigate the structure activity relationships (SAR).

Figure 21: Hit compounds identified in a virtual screening

The final goals of this thesis were:

- 1) to develop small molecule compounds which act via an allosteric mode by binding to the PIF pocket,
- 2) to optimize selectivity for PDK1 but potentially also for the atypical Protein kinase C isoform PKC ζ , which belongs to the same subfamily of AGC protein kinases, and
- 3) to increase potency of allosteric modulators directed to the PIF pocket of PDK1 to the nanomolar range. This goal was important to demonstrate druggability of the PIF pocket.

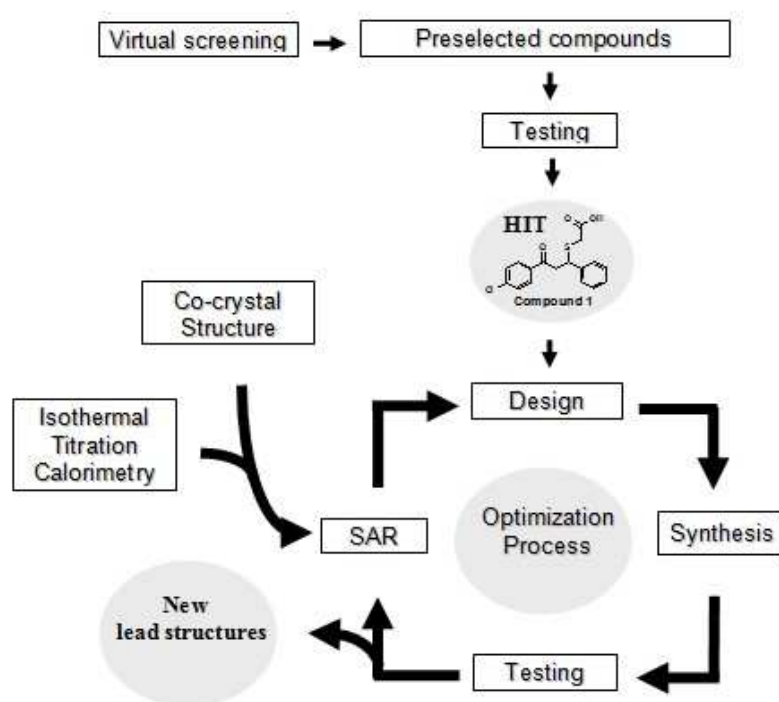
2.2. General concept to design allosteric modulators of PDK1 and PKC ζ

One of the present thesis aims was to optimize the hit compound **1**⁷⁴ (Figure 21) by targeted structural modifications in order to enhance the potency and selectivity and to evaluate the binding mechanism of the compounds with the enzyme. The focus was directed to overcome the structural drawbacks of **1**, especially the existence of the chiral centre yielding a racemic mixture that needs more effort to isolate the active enantiomer and the sulfanyl moiety that can undergo oxidations and retro Michael reactions. Moreover, due to the

low affinity this compound class rendered further studies difficult. The docking model presented in Figure 13 served as starting point for the development of further small compounds targeting the PIF pocket of the AGC kinases. Already during my diploma thesis I was able to synthesize a new potent allosteric modulator **III**⁷⁵ (Figure 21).

The working strategy used in this thesis is depicted in the following scheme (Scheme 1). Starting point is the molecular design of potential modulators of PDK1 and PKC ζ , based on the hit compound **1**, followed by the synthesis considering the minimal structural requirements for compounds to bind to the PIF-binding pocket and the evaluation of the biological activity and selectivity of the compounds.

Scheme 1: Design concept of allosteric modulators of PDK1 and PKC ζ ,1



As long as there was no cocrystal structure available, the rational design was performed based on molecular modelling supported by biochemical analysis of the effect of the compounds on protein kinases which are mutated in residues within the PIF pocket. In order to measure the effect of the synthesized compounds on the PDK1 catalytic activity we performed a radioactive kinase activity assay employing T308tide, a peptide derived from the activation loop of PKB, as a substrate. In order to characterize biochemically the binding site we compared the ability of the compounds to activate wildtype PDK1 versus PDK1 proteins

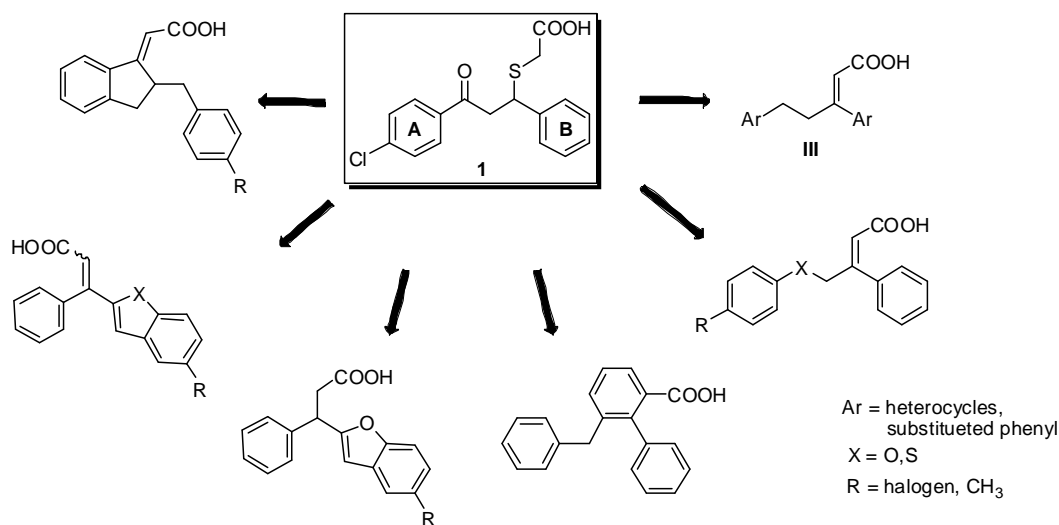
mutated within the PIF-binding pocket. Moreover, we studied the specificity of the compounds toward a panel of AGC kinase. To elucidate relationships between structural properties, binding affinity and allosteric activation we performed isothermal titration calorimetry experiments with selected compounds. Obtaining first novel PIF-binding pocket-directed compounds with higher potency, we were also able in collaboration with the Institute Pasteur (Paris) to cocrystallize PDK1 with the compound and we could use the X-Ray analysis results for further improvement of the affinity of the compounds to the PIF pocket. Having these results we were able to gain insight into binding mode of the compounds and the molecular mechanism underlying the allosteric activation.

The following traditional medicinal chemistry strategies were employed to optimize the new hit compound **III**:

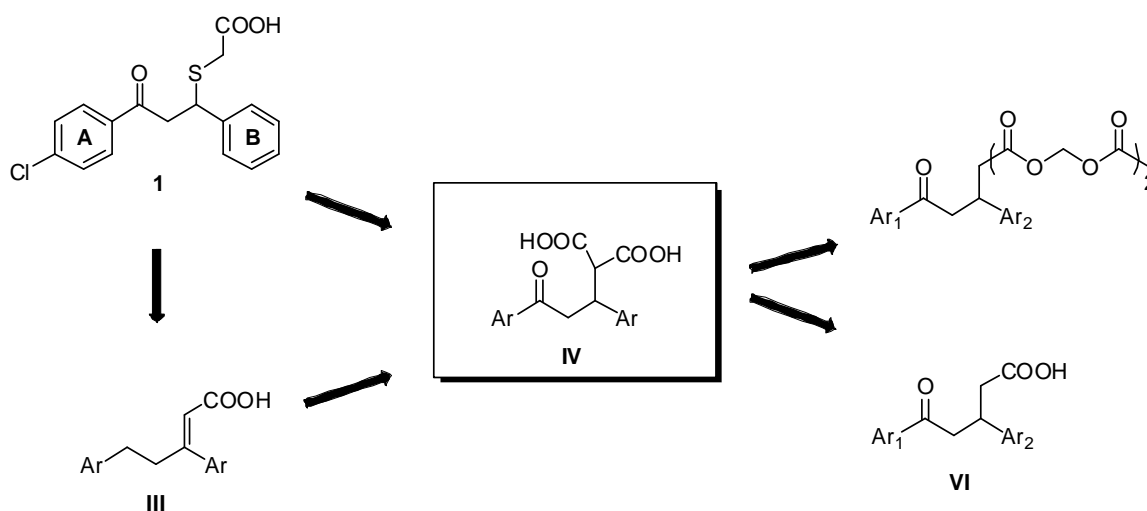
- Variation of the ring substituents
- Extension of the structure
- Rigidification

Verifying the ring substituents and their position at the phenyl moiety we wanted to evaluate the most favourable derivatization model for further search of more active compounds. Moreover, the focus was on additional H-bonding interactions of the mostly hydrophobic PIF pocket. Furthermore, the extension of the allosteric modulator structures aimed with a special interest to find out when the maximum of the PIF pocket is filled out keeping good potency of the compounds. The rigidification strategy also served to investigate the structural features of the target site with regard to optimization of the target molecules.

First we designed 3,5-diphenylpent-2-enoic acids (Scheme 2) as new structural analogues containing a double bond as replacement of the chiral centre of the lead compound **I** where the combination of two sp^3 and one sp^2 hybridized C-atoms in the chain connecting the benzene rings is retained. Additionally, by introducing a shorter olefinic carboxyl side chain we wanted to reduce the total number of rotatable bonds. Moreover, we replaced the A-phenyl moiety with other aromatic systems and we introduced polar ether groups in the backbone chain. Furthermore, we planned to prepare cyclized chalcones and we inserted fused heterocycles to the carbon chain to create more scaffold rigidity. Isothermal titration calorimetry experiments were performed to evaluate the affinity of the compounds to the PIF pocket of PDK1.

Scheme 2: General structures

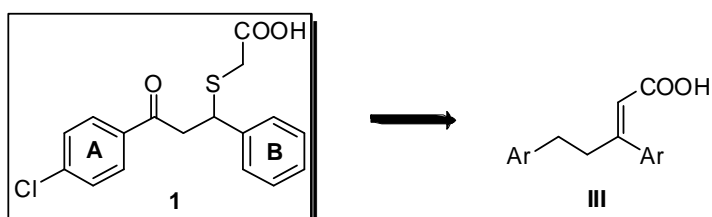
On the basis of the biological and the SAR results of the 3,5-diphenylpent-2-enoic acids and exploiting the cocrystal structure we designed a chimeric compound for further improvement of the potency toward PDK1. We combined the carbonyl function from the lead compound 1 with the short side chain from compound III (Scheme 3). In addition, we planned to introduce a second carboxyl function, to vary the substituents on the phenyl moieties and to replace the phenyl residues by different aromatic systems. Moreover, we changed the dicarboxylic functionality into the corresponding bisacetoxymethyl ester derivatives to convert the 2-(3-oxo-1,3-diphenylpropyl)malonic acids into prodrugs to enhance their bioavailability.

Scheme 3: General structures

The malonic moiety of the 2-(3-oxo-1,3-diphenylpropyl)malonic acids provided additionally a synthetic access to another substance class, the corresponding monoacid derivatives. A comparison with the corresponding 2-(3-oxo-1,3-diphenylpropyl)malonic acids can shed light on the significance of the polar moiety.

Additionally, in order to extend the first approach that is outlined above we evaluated the role of the phenyl moiety B of compound **III** (Scheme 4) because we found that those bigger residues on this position lead to an inhibitory effect on the PKC ζ activity. Thereby we introduced different aromatic residues and investigated their influence on PKC ζ activity.

Scheme 4: General structures



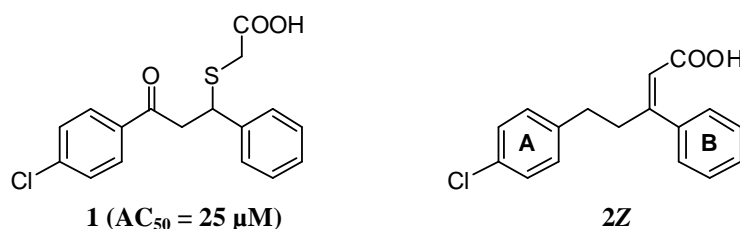
3 Results

3.1. Synthesis, structure-activity relationships and thermodynamic characterization of 3,5-diphenylpent-2-enoic acids as allosteric activators of the protein kinase PDK1

3.1.1. Scientific rationale

As explained in the introduction (chapter 1.8), allosteric inhibitors might represent a superior alternative to the traditional ATP-competitive drugs, also because they might allow a more subtle modulation of the protein kinase activity provides the allosteric inhibition.⁷ In this regard, by characterizing the molecular mechanism of regulation of PDK1 and discovering of the PIF pocket we provided a novel allosteric drugable site. Actually, we were able to develop first small molecule compounds that can trigger the PDK1 activity *in vitro* by interaction with the PIF pocket. Thereby the PIF pocket-directed compounds could potentially generate inhibitors but also protein kinase activating drugs.

Figure 22: Structures of the hit compound **1** and the new lead compound **2Z**



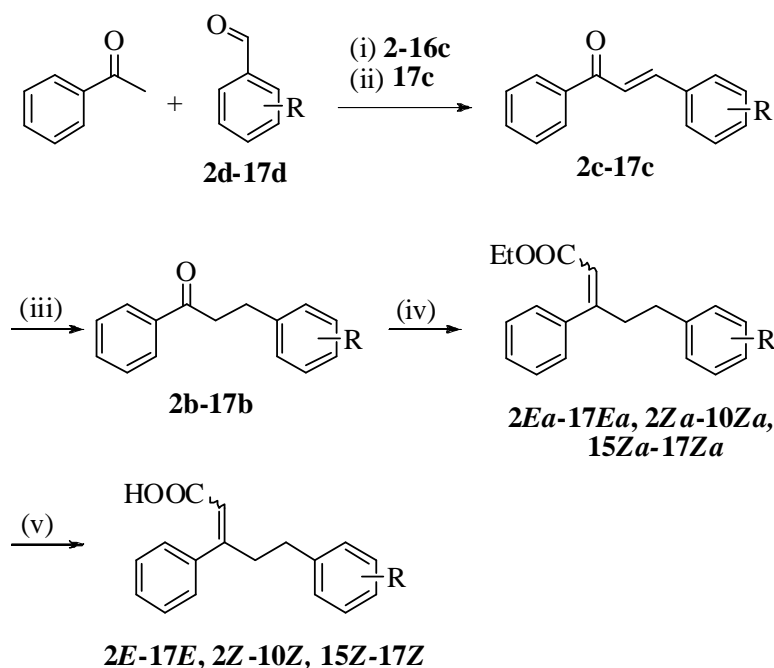
Compound **1** (Figure 22) was identified as an activator of PDK1 with an AC_{50} of $25 \mu\text{M}$.⁷⁴ We used the structure as starting point in an effort to synthesize more potent and selective compounds using structure based drug design. In the following we describe the structure refinements of **1** that led to a novel series of 3,5-diarylpent-2-enoic acids as PIF-binding pocket-directed compounds, their SAR data on their allosteric activation potency and as well as the binding energetics of allosteric activators. Using isothermal titration calorimetry (ITC) we shed light on relationships between structural properties, binding affinity and allosteric activation. Moreover, presenting the cocrystal structure of compound **2Z** with PDK1 we discuss the general requirements for HM/PIF-binding pocket compounds. With the obtained

cocrystal structure we were also able to elucidate the allosteric mechanism changes of PDK1 induced by the 3,5-diarylpent-2-enoic acids that are normally triggered by binding of phosphorylated HM motifs.¹²⁶

3.1.2. Synthesis

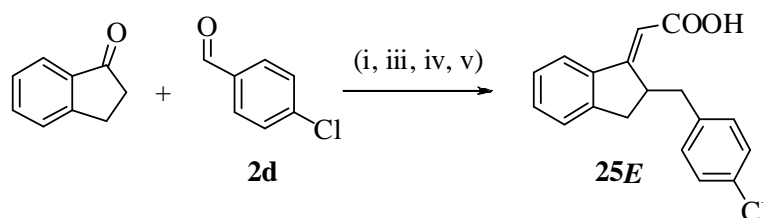
The optimization approach was focused on two general changes of compound **1** to gain the target molecules more drug-like. Firstly, the chiral centre should be replaced to circumvent a racemic mixture with unknown contribution of each enantiomer to the total activity. Secondly, analogues should lack the sulfanyl moiety, which is prone to oxidations and potentially retro-Michael reactions. The design of the new structural analogues, 3,5-diarylpent-2-enoic acids, resulted at replacement of the chiral centre by a double bond while retaining the combination of two sp^3 and one sp^2 hybridized C-atoms in the chain connecting the benzene rings, thus leading to compound **2Z** (Figure 22).

Syntheses of **2** and analogues **3-17** started with a Claisen-Schmitt condensation (Method A) between acetophenone and a series of benzaldehydes **2d-17d** to obtain the chalcones **2c-17c** (Scheme 5). To selectively reduce the conjugated double bond of the chalcones we utilized a convenient hydride transfer reaction (Method B) from 3,5-bis(ethoxycarbonyl)-1,4-dihydro-2,6-dimethylpyridine (HEH) catalyzed by silica gel,¹²⁷ which quantitatively afforded the saturated ketones **2b-17b**. In order to perform the reaction we had first to synthesize the reducing agent.¹²⁸ The synthesis of Hantzsch-1,4-dihydropyridines we performed under microwave irradiation, whereas ethylacetate, formaldehyde and ammonium acetate reacted at a rate of 2:1:1. Olefination of the carbonyl group in **2b-17b** was achieved by Horner-Wadsworth-Emmons reaction (HWE) (Method C) with triethyl phosphonoacetate, yielding *E/Z*-mixtures of ethyl 3,5-diphenylpent-2-enoates (**2a-17a**, Scheme 5) which could be efficiently separated by flash column chromatography in all cases. We intentionally chose the reaction conditions to favour formation of both stereoisomers in order to isolate both compounds and test them separately. In the last step the ethyl ester was hydrolyzed (Method D) under basic conditions to yield the free 3,5-diphenylpent-2-enoic acids (**2E -17E**, **2Z -17Z**). All these synthesis steps containing the corresponding reaction mechanisms are already described in the diploma thesis for compound **2Z**.^{20, 75}

Scheme 5^a: Synthesis of compounds **2E-17E**, **2Z-17Z**

^a: (i) Method A: NaOH, EtOH, 1 h, rt; (ii) piperidine, EtOH, reflux, 16 h; (iii) Method B: 3,5-bis(ethoxycarbonyl)-1,4-dihydro-2,6-dimethylpyridine, toluene, silica gel, 70 °C, 16 h; (iv) Method C: triethyl phosphonoacetate, NaH, DME, 80 °C, 4 h; (v) Method D: NaOH, EtOH, rt, 3 h. For substituents R see Table 3, Table 4 and Table 5.

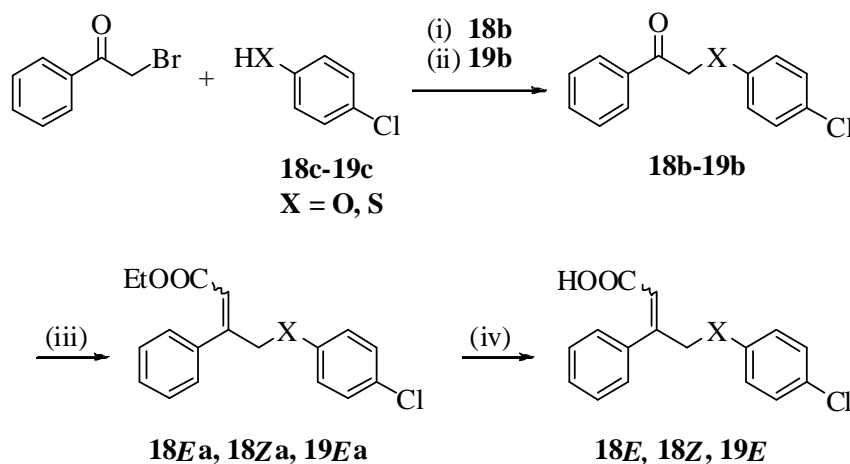
An even more rigid, cyclized analogue **25E** was prepared by condensation of 4-chlorobenzaldehyde **2d** with 1-indanone, reduction of the resulting cyclized chalcone, HWE reaction, and subsequent ester hydrolysis (Scheme 6). **25E** was isolated as diastereomeric mixture exclusively in the (*E*)-form.

Scheme 6^a: Synthesis of **25E**

^a: (i) Method A: NaOH, EtOH, 1 h, rt; (iii) Method B: 3,5-bis(ethoxycarbonyl)-1,4-dihydro-2,6-dimethylpyridine, toluene, silica gel, 70 °C, 16 h; (iv) Method C: triethyl phosphonoacetate, NaH, DME, 80 °C, 4 h; (v) Method D: NaOH, EtOH, rt, 3 h.

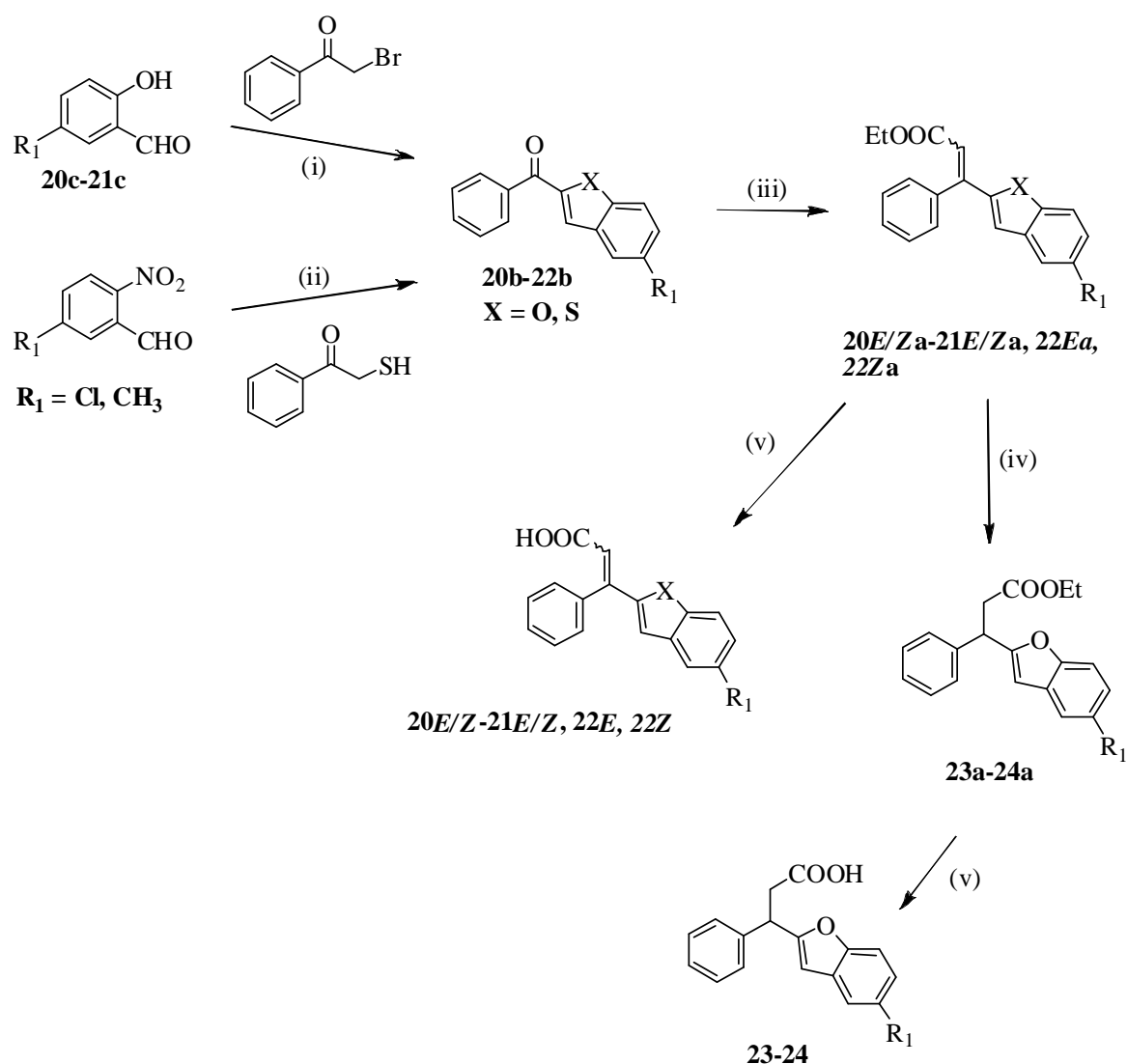
In another subset of compounds we replaced the ring **A** benzylic methylene by oxygen or sulphur. The strategy for the synthesis of these hetero analogues of **2Z** is illustrated in Scheme 7. Bromoacetophenone was subjected to an S_N reaction with 4-chlorophenol **18c** and 4-chlorophenyl mercaptane **19c**, respectively, to yield 2-(4-chlorophenoxy)acetophenone **18b** and 2-(4-chlorophenylthio)acetophenone **19b**. The final compounds, (*E*)- and (*Z*)-4-(4-chlorophenoxy)-(**18E**, **18Z**) and (*E*)-4-(4-chlorophenylthio)-3-phenylbut-2-enoic acid (**19E**), were obtained via HWE reaction (Method C) and hydrolysis (Method D) analogously to the 3,5-diphenylpentenoic acids.

Scheme 7^a: Synthesis of compounds **18E**, **18Z** and **19E**



^a: reagents and conditions: (i) K_2CO_3 , EtOH, 80 °C, 1 h; (ii) 5 % BnNEt_3Cl , 30 % NaOH, CH_2Cl_2 , rt, 16 h; (iii) Method C: triethyl phosphonoacetate, NaH, DME, 80 °C, 4 h; (iv) Method D: NaOH, EtOH, rt, 3 h. For substituents X see Table 6.

In addition, we prepared heterocyclic analogues via two different synthetic pathways (Scheme 8). Rap-Stoermer reaction of salicylaldehydes **20c** and **21c** with phenacyl bromide (Method E) provided the substituted 2-benzoylbenzofurans **20b** and **21b**¹²⁹ while synthesis of 2-(4-chlorobenzoyl)benzothiophene **22b** was accomplished by a one-step nucleophilic aromatic displacement of an activated nitro function by mercaptoacetophenone followed by an intramolecular aldol condensation.¹³⁰ The heterocyclic precursors were further processed to the corresponding acrylic acids (**20-21**, **22E**, **22Z**) analogously to compounds **2b-17b**. Finally, we also reduced the acrylic acids (**20E/Za** -**21E/Za**) to the corresponding propionic acids (**23a-24a**) by means of a catalytic transfer hydrogenation (Method F) using sodium hypophosphite in combination with Pd/C.

Scheme 8^a: Synthesis of compounds **20-21**, **22E**, **22Z**, **23** and **24**


^a: reagents and conditions: (i) Method E: K₂CO₃, EtOH, reflux, 2 h; (ii) K₂CO₃, DMF, 0 °C to rt, 3 h; (iii) Method C: triethyl phosphonoacetate, NaH, DME, 80 °C, 4 h; (iv) Method F: NaH₂PO₂·H₂O, 10 % Pd/C, EtOH/H₂O, 60 °C, 2.5 h; (v) Method D: NaOH, EtOH, rt, 3 h. For substituents R see Table 7 and Table 8.

For **2E** and **2Z**, we determined the *E/Z* configuration exemplarily using 2D-NOESY-¹H-NMR (see experimental chapter).⁷⁵ The *E/Z* assignment of the other compound pairs was done by comparison of the corresponding NMR spectra with those of **2E** and **2Z**. Thus, by introducing a shorter olefinic carboxyl side chain we reduced the total number of rotatable bonds from seven (**1**) to five (**2Z**).

3.1.3. Biological results

3.1.3.1. Biological Activity of the 3,5-diarylpent-2-enoic acid analogues

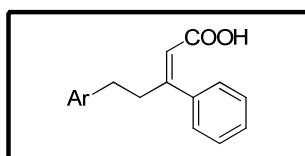
The biological *in vitro* activity of the compounds toward PDK1 was studied in a radioactive kinase activity assay in the Department of Medicine I (Universitätsklinikum Frankfurt/Main) by our collaborator group under the supervision of Dr. Ricardo M. Biondi.²⁶ Additionally, the specificity of the compounds against a panel of other AGC protein kinases was tested. All reactions were performed in a 96 well format in the presence of [γ -³²P]ATP using T308tide, a peptide derived from the activation loop of PKB, as a substrate. The incorporation of ³²P was quantified using Phosphorimager and the corresponding Software Image-QuantTM. All kinase assays were done in duplicates. The intensity of the obtained spots directly correlates with the activity of the enzyme compared to the control values with DMSO alone were normalized to 100 %.

The effects of substituents on the ability of the compounds to activate PDK1 and selected AGC kinases and the corresponding structure activity relationship (SAR) conclusions are listed in Table 3, Table 5, Table 6, Table 7, Table 8, Table 9. We tested different concentrations of the compounds. Using Kaleidagraph software we calculated subsequently the half maximal activity (AC₅₀) and maximal activities of the compounds, compared to the basal activity (set to 100 %). As presented in the individual tables (Table 3-Table 9) the results of this study revealed that the obtained geometric isomers of the 3,5-diarylpent-2-enoic acid analogues possessed different intrinsic potency toward PDK1. Thereby, the isomers carrying the carboxyl group *cis* relatively to the phenyl ring **B** (**2-16Z**, **18-24Z**, Figure 22) exhibited an increase on the activation potency of PDK1. In contrast, the isomers with the opposite conformation were mostly inactive. The only exception displayed compound **17**. Both geometric isomers of **17** disclosed a relatively similar AC₅₀ (*Z* = 7.6 μ M; *E* = 8.8 μ M). However, both isomers activated PDK1 with only low efficacy.

Initially, our chemical strategy regarding the innovative PDK1 activators was focused on the substitution of 3,5-diarylpent-2-enoic acid analogues with hydrophobic substituents, mostly halogens, on different positions at the 5-phenyl moiety. We can conclude that the halogen substitution on the *para* position improved relatively selective the PDK1 activation potency in case of the *cis* 3,5-diarylpent-2-enoic acid analogues (**2Z**, **4Z**, **5Z**) (Table 3). The activity of the compounds increased in the following order F < Br < Cl. The compounds carrying additionally to the halogen group on the *para* position a second halogen either on the *meta* position (**7Z**) or on the *ortho* position (**8,9**) are characterized by AC₅₀ values in low

micromolar range. The introduction of a *para*-trifluoromethyl group at the 5-phenyl moiety in **6Z** resulted in a 4.4-fold activation potency but a moderate AC_{50} (7.1 μ M). An ethyl substitution into the phenyl ring **A** at the *para* position abolished the activating effect on PDK1 considerably. The results in table below also indicate that several of the 3,5-diarylpent-2-enoic acid analogues triggered additionally an inhibition effect on some related AGC kinases. Compounds **2E,Z**, **3E,Z** and **8Z** exhibited stronger inhibition potency toward PKC ζ whereas compounds **5E**, **6E**, **7E** and **10Z** showed only a slight inhibition. Some compound showed also a weak inhibition of S6K and SGK.

Table 3: Activity of 3,5-diarylpent-2-enoic acids analogues substituted at the 5-phenyl moiety with hydrophobic substituents toward PDK1 and a panel of AGC kinases



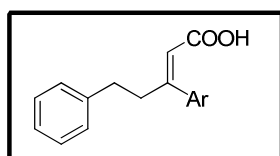
Compound	Ar	PDK1		PKC ζ	PKB β	PKA	SGK	S6K
		A_{max} fold	AC_{50} μ M	50 μ M	50 μ M	50 μ M	50 μ M	50 μ M
2Z		4.0	8.0	40	ne	ne	ne	ne
2E		ne	ne	50	ne	ne	ne	ne
3Z		2.2	9.5	45	80	ne	ne	90
3E		ne	ne	50	80	ne	75	85
4Z		3.3	41.0	ne	ne	ne	ne	ne
4E		ne	ne	ne	ne	ne	ne	ne
5Z		3.9	9.8	nd	ne	ne	ne	ne
5E		ne	ne	70	ne	ne	ne	ne
6Z		4.4	7.1	ne	ne	ne	ne	ne
6E		ne	ne	60	ne	ne	ne	ne
7Z		2.4	2.8	nd	70	nd	ne	ne
7E		ne	ne	70	ne	ne	ne	85
8Z		2.1	4.7	50	ne	nd	80	75
8E		ne	ne	nd	ne	nd	ne	75
9Z		3.9	4.0	nd	ne	nd	ne	ne
9E		ne	ne	ne	ne	nd	ne	ne
10Z		1.4	> 30	70	ne	ne	80	ne
10E		ne	ne	ne	ne	ne	ne	ne

Values in % catalytic activity (DMSO-treated control = 100%)

nd: not determined; ne: no effect

Furthermore, we synthesized also derivatives including fluorine atoms on the phenyl moiety **B** at varied positions (**11-13**) and we substituted the phenyl ring by pyridine moiety (**14**). Thereby, we have succeeded to isolate only the corresponding *E* isomers. The PIF-binding pocket of PDK1 appeared to be not accommodating for the substituents on the phenyl moiety **B** since the *E* analogues afforded a decrease of the kinase activity. But besides activation of PDK1 these compounds promoted selective inhibition of other AGC kinases, in particular PKC ζ and S6K. This emerging effect on PKC ζ was exploited in another part of my thesis for the development of PKC ζ selective inhibitors. With respect to PDK1 activators, we decided to omit the derivatization of the phenyl moiety **B**.

Table 4: Activity of 3,5-diarylpent-2-enoic acids analogues substituted at the 1-phenyl moiety toward PDK1 and a panel of AGC kinases



Compound	Ar	PDK1		PKC ζ	PKB β	PKA	SGK	S6K
		A _{max} fold	AC ₅₀ μ M	50 μ M	50 μ M	50 μ M	50 μ M	50 μ M
11Z		-	-	-	-	-	-	-
11E		ne	ne	50	ne	nd	80	85
12Z		-	-	-	-	-	-	-
12E		80	ne	55	ne	nd	ne	ne
13Z		-	-	-	-	-	-	-
13E		ne	ne	50	ne	nd	80	85
14Z		-	-	-	-	-	-	-
14E		75	ne	ne	ne	nd	ne	ne

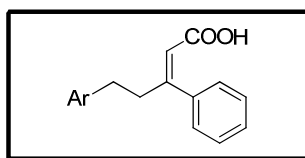
Values in % catalytic activity (DMSO-treated control = 100%)

nd: not determined; ne: no effect

To explore the requirements to increase the potency binding to PDK1, we prepared compounds substituting the phenyl moiety **A** with different aromatic systems (Table 5). We determined that the aromatic analogues improved moderately the potency. The naphthyl analogue showed the highest increase of potency (3.6 fold). Despite the aromatic derivatives exhibited an elevated activation of the enzyme this substitution was less beneficial relating to the poor AC₅₀ values. As already described above, compound **17** constituted an exception. In opposite to **15** and **16** whose *E* isomers did not show any activity effect, there is hardly any difference in activity between the geometric isomers of **17**. Interestingly, the aromatic derivatives

showed a slight inhibition effect toward PKA and S6K and compounds **15Z** and **16Z** showed even a stronger inhibition of PKC ζ .

Table 5: Activity of 3,5-diarylpent-2-enoic acid analogues substituted with different aromatic systems at the 5-phenyl moiety toward PDK1 and a panel of AGC kinases



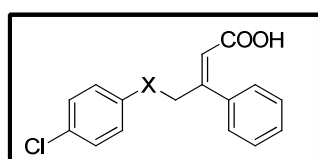
Compound	Ar	PDK1		PKC ζ	PKB β	PKA	SGK	S6K
		A _{max} fold	AC ₅₀ μ M	50 μ M	50 μ M	50 μ M	50 μ M	50 μ M
15Z		3.2	6.0	10	ne	60	ne	ne
15E		ne	ne	ne	ne	nd	ne	80
16Z		3.6	6.0	15	ne	30	ne	ne
16E		ne	ne	30	ne	nd	70	70
17Z		3.1	7.6	ne	ne	60	ne	ne
17E		2.2	8.8	ne	ne	ne	ne	80

Values in % catalytic activity (DMSO-treated control = 100%)

nd: not determined; ne: no effect

Derivatization of the backbone chain by insertion of ether and thioether groups served to increase the polarity of the scaffold. This modification resulted in a significantly decrease of potency (AC₅₀ = 22.8 μ M, Table 6). For the phenyloxy- and phenylthio-substituted series, both a slight reduction of the maximum activation of PDK1 and an increase of the AC₅₀ values was noted compared with **2Z** (**18E** and **19E**). The *trans*-4-chloro-phenoxy compound **18Z** was completely inactive. However, the inhibitory profile of the ether and thioether analogues regarding the related AGC kinases is comparable to the corresponding 3-carbon chain analogues (3,5-diarylpent-2-enoic acids) with a slightly increased inhibitory potency toward PKC ζ and S6K. Particular the derivative including the thioether function (**19E**) exhibited enhanced potency toward PKC ζ .

Table 6: Activity of 3,5-diarylpent-2-enoic acids analogues substituted at the backbone chain with ether and thioether groups toward PDK1 and a panel of AGC kinases



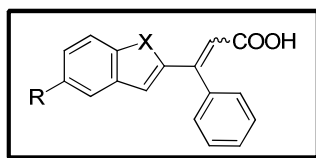
Compound	X	PDK1		PKC ζ	PKB β	PKA	SGK	S6K
		A _{max} fold	AC ₅₀ μ M	50 μ M	50 μ M	50 μ M	50 μ M	50 μ M
18E	O	3.0	22.8	72	ne	nd	ne	82
18Z		ne	ne	72	ne	nd	ne	85
19E	S	2.6	22.8	22	ne	nd	ne	80

Values in % catalytic activity (DMSO-treated control = 100%)

nd: not determined; ne: no effect

The same trend was observed for the biological *in vitro* data of compounds that were synthesized incorporating two carbons of the backbone chain into heterocycles (Table 7) to increase binding affinity but also to probe the potential overall conformation required for a compound to bind to the PIF-binding pocket. The scaffold rigidification of the afforded 3-benzofuran-2-yl-3-phenylacrylic acid derivatives (**20E**, **21E**) and (*E*)-3-(5-chlorobenzo[b]thiophen-2-yl)-3-phenylacrylic acid did not improve notably the activity toward PDK1 and led to AC₅₀ values that are extraordinary high. However, enhanced inhibition potency on PKC ζ is also observed in case of compounds **22E** and **22Z**.

Table 7: Activity of rigid analogues substituted with ether and thioether groups toward PDK1 and a panel of AGC kinases



Compound	X	R	PDK1		PKC ζ	PKB β	PKA	SGK	S6K
			A _{max} fold	AC ₅₀ μ M	50 μ M	50 μ M	50 μ M	50 μ M	50 μ M
20E	O	Cl	3.2	31.6	60	85	nd	ne	ne
21E	O	Me	3.6	41.3	85	ne	nd	ne	ne
22E	S	Cl	3.1	13.2	20	ne	40	ne	75
22Z			ne	ne	20	ne	ne	50	85

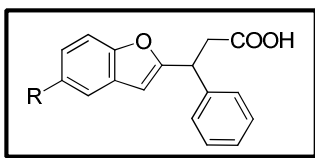
Values in % catalytic activity (DMSO-treated control = 100%)

nd: not determined; ne: no effect

In a further effort we reduced the double bond to a single bond (Table 8) what did not induce any changes in the activatory potency. Both the maximal activity and the half maximal

activity of compounds **23** and **24** (AC_{50}) are approximately within the same range and comparable to compounds **20-22**.

Table 8: Activity of rigid analogues substituted with ether group toward PDK1 and a panel of AGC kinases



Compound	R	PDK1		PKC ζ	PKB β	PKA	SGK	S6K
		A_{max} fold	AC_{50} μ M	50 μ M	50 μ M	50 μ M	50 μ M	50 μ M
23	Cl	2.9	19.0	ne	ne	ne	ne	ne
24	Me	2.7	29.1	75	ne	70	ne	ne

Values in % catalytic activity (DMSO-treated control = 100%)

nd: not determined; ne: no effect

Rigidification of the compound incorporating two carbons of the backbone chain into 2,3-dihydroindene, whereas the acrylic acid residue is situated on the 1-position of the 2,3-dihydroindene moiety, resulted in a decrease of activity toward PDK1 (Table 9). (*E*)-2-(2-(4-Chlorobenzyl)-2,3-dihydro-1H-inden-1-ylidene)acetic acid did not exhibit any additional effect on the related AGC kinases except a weak inhibition of PKC ζ , suggesting that the benzene ring of the 2,3-dihydroindene was not fixed with the right dihedral angle relative to the double bond..

Table 9: Activity of rigid analogues without additional polar groups toward PDK1 and a panel of AGC kinases

Compound	PDK1	PKC ζ	PKB β	PKA	SGK	S6K		
							A_{max} fold	AC_{50} μ M
25		1.8	30.0	45	85	ne	ne	ne

Values in % catalytic activity (DMSO-treated control = 100%)

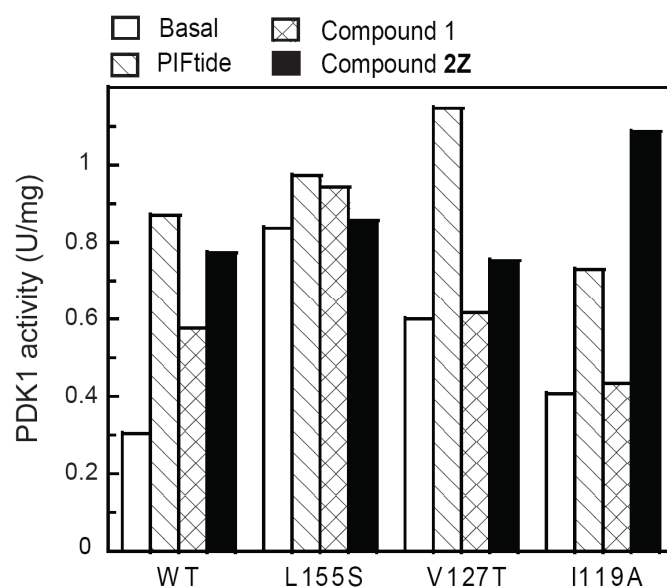
ne: no effect

3.1.3.2. PIF pocket Mutant Assay to confirm that compound **2Z** activates PDK1 by targeting the PIF-binding pocket.

The *in vitro* data of the series of 3,5-diarylpent-2-enoic acids revealed that most of corresponding *cis* isomers are good activators of PDK1. However, among the compounds we tested, several showed also inhibition potency mainly toward PKC ζ . To corroborate that these effects were mediated by binding of the compounds to the PIF-binding pocket, the kinase activity assay was supplemented by further biochemical assays. In one effort we performed mutation assays whereas the experiments were done in our collaborator laboratory of Dr. Ricardo M. Biondi. We constructed first mutants of the PIF-binding pocket of PDK1 by conversion of leucine to serine at amino acid 155 (L155S), valine to threonine at amino acid 127 (V127T) and by conversion of isoleucine to alanine at amino acid 119 (I119A). The mutated amino acids were situated within or surrounding the HM/PIF pocket. Subsequently, we choose compound **2Z**, since it was the first new lead structure we synthesized in the optimization study of compound **1**. Similarly to the 24 amino acid polypeptide PIFtide, characterized to bind to the PIF-binding pocket and activate PDK1,²⁶ compound **2Z** increased the activity of wild type (wt) PDK1 with the same activation efficacy (data for PIFtide not shown) and it displayed a 4-fold lower AC₅₀ than the hit compound **1**. Having **2Z** we evaluated biochemically the ability of **2Z** to activate the recombinant wt PDK1 versus PDK1 proteins mutated. For comparison, we performed the mutant assays also with compound **1**. As shown in Figure 23 incubation of wt PDK1 both with PIFtide and with the compounds has led to activity increase. But with the replacement of serine into lysine all three effectors (PIFtide, **2Z** and **1**) did not affect the kinase activity. This can be attributed to the fact that the character of the PIF-binding pocket is completely changed in the mutant PDK1^{L155S}. This result suggested that the PIF-binding pocket site was required by all three effectors. In contrast, the mutant PDK1^{V127T} discriminated between the natural ligand and the small molecule compounds **2Z** and **1**. On the one hand the ability of **2Z** to activate PDK1 was lost toward the PDK1^{V127T} mutant. On the other hand, the assay of the same mutant and PIFtide resulted in an increase of the enzyme activity. This was not surprising since previous experiments revealed that PDK1 mutants of V127 with larger hydrophobic residue (Leu) led to retained ability to bind and be activated by PIFtide. The subsequent downregulation of the enzyme to interact and phosphorylate the substrate SGK, that relies on the binding of its hydrophobic motif to the PIF-binding pocket on PDK1⁷⁴, was triggered by this PDK1^{V127T} mutant. Thus, we can conclude that the residue at position 127 is not essential for HM polypeptides while a valine

residue at position 127 within the hydrophobic PIF-binding pocket is necessary for the binding of the small molecule compound **2Z**. Interestingly, we found out that the PDK1^{I119A} mutant was well activated by **2Z**, whereas both compound **1** and PIFtide caused a decrease of the PDK1^{I119A} activity. Taken together, the mutagenesis results strongly indicate that the compounds mediated their effects via the PIF pocket. However, there were significant differences on the requirements between **2Z**, **1** and PIFtide, which had also been suggested to bind to the same site.

Figure 23: PIF pocket mutant assay



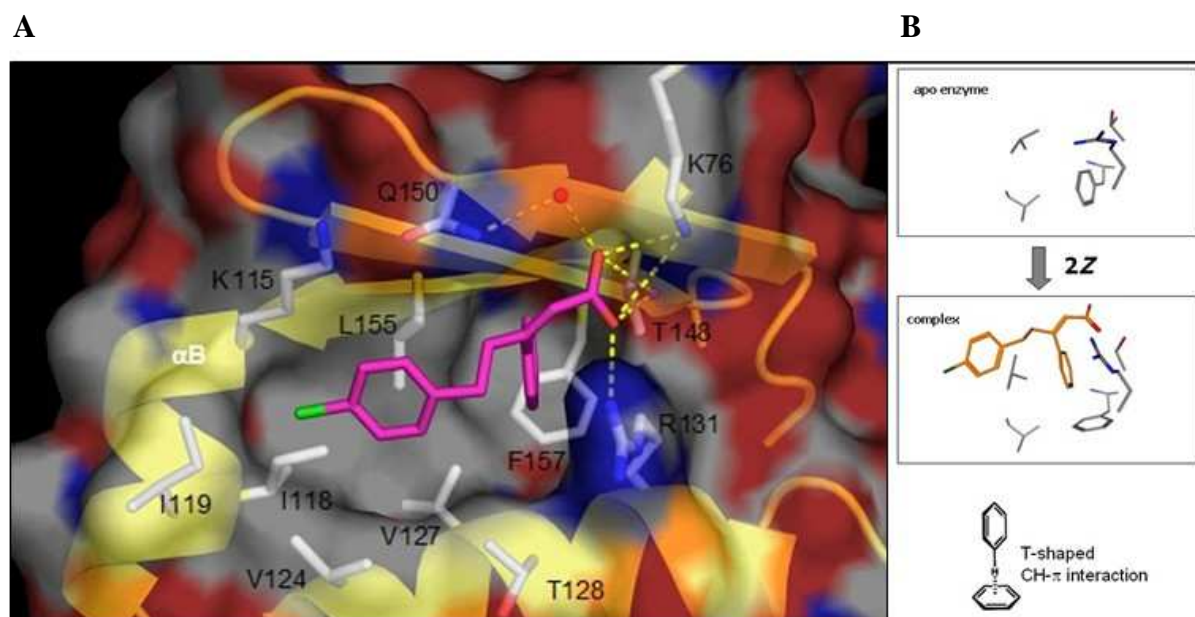
Biochemical evidence from site-directed mutagenesis that the PIF-binding pocket of PDK1 is the target site of **2Z**. The effect of **2Z** on PDK1 specific activity was measured with recombinant wild type enzyme and PIF pocket-binding mutants as indicated. Mutation of valine-127 to threonine abrogates the activation of PDK1 by **2Z** but not by the 22 amino acid residue peptide PIFtide. For comparison, results obtained with the original compound **1** are also given. Concentrations of the compounds used were 2 μ M for PIFtide and 20 μ M for **1** and **2Z**.

3.1.4. Cocrystallization of **2Z** with PDK1 as further biochemical evidence for binding of the small molecule compound in the PIF pocket.

In a further approach we cocrystallized **2Z** with PDK1 to confirm the localization of the compound **2Z** in the PIF-binding pocket. All crystallization experiments and analysis were carried out by Valerie Hindie at the Institute Pasteur in Paris supervised by Dr. Ricardo M. Biondi. The obtained results of the crystallographic data related to the allosteric mechanism of PDK1 activation by 3,5-diarylpent-2-enoic acids were published in more details parallel to

our SAR study by our project collaborators.¹²⁶ In this thesis the special focus is on the structural informations of the binding mode between **2Z** and the PIF pocket to elucidate the crucial interactions and to explain the differences in activity between the geometric isomers. In Figure 24A the resolved X-Ray structure indicates that **2Z** is bound in the PIF-binding pocket of PDK1. The crucial factors which may lead to enhancement of the kinase activity are the interactions of the carboxyl group with the amino acids of the PIF pocket. The carboxyl group forms hydrogen bonds with R131, T148 and K76 which are highlighted by dashed yellow lines. Additionally, the carboxyl forms a water mediated H-bond with Q150 (red ball). This was only achievable by the compounds that carry the carboxyl group on the *cis* position that is fixed by the double bond. The carboxyl group of the *trans* isomers appeared to be pointed to the opposite direction in case the phenyl moieties bind in the same modus in the PIF pocket as the *cis* isomers. Therefore, these compounds cannot make these activating interactions leading to loss or lack of activity. Moreover, the carboxyl group of the *trans* isomers cannot contribute to ionic interactions as is the case with compound **2Z** that appeared to mimic the phosphate group of phosphoserine/threonine residues from the natural ligands, which are expected to bind to the equivalent site. Furthermore, the cocrystal figure reveals that the two phenyl moieties of **2Z** occupy two hydrophobic subpockets that are separated by L155 and bordered by V127. This fact may explain the lack of activity of compound **2Z** on PDK1 proteins mutated at these sites (Figure 23). In contrast, the ethyl branch of I119 borders one side of the pocket and interacts only marginally with the chlorine of **2Z**, therefore, explaining why the substitution for a smaller hydrophobic residue did not affect the ability of **2Z** to activate PDK1. Moreover, the cocrystal structure discloses additional Van der Waals contacts, an edge to face CH- π interaction between the phenyl ring **B** and phenylalanine F157 that might increase the compound affinity to the allosteric pocket (Figure 24B). Therefore, having the activity assay results of compounds with varying substituents on the phenyl moiety **B** (Table 4) we decided to focus on modifying the phenyl ring **A** (Figure 22), especially the X-Ray structure suggested larger unfilled space in the ring **A** subpocket of the PIF pocket binding site.

Summing up, these results, together with the biochemical studies performed here in solution with PIF-binding pocket mutants of full length PDK1, provide evidence that the PIF-binding pocket serves as the binding site for **2Z**. The results indicated additionally that the broad range of interactions of the carboxyl moiety of the *cis* compounds with phosphate binding site residues is essential to prompt the activation of PDK1.

Figure 24: X-Ray structure of PDK1 in complex with **2Z** (PDB: 3HRF)

A: Compound **2Z** bound in the PIF-binding pocket of PDK1. The pocket is bordered by the α C helix and the short α B helix as indicated. Dashed yellow lines display the interactions of the carboxylate group with R131, T148 and K76 and with Q150 via a water molecule (red ball). L155 divides the hydrophobic groove into two subpockets which are occupied by the benzene rings. Phenyl ring **B** (3-phenyl, see Figure 21) additionally contributes to the binding energy by forming edge-to-face CH- π interactions with F157. As shown in Figure 23, mutation of V127 to threonine abolished the activation by **2Z**. The structure was generated using PYMOL. **B:** Scheme of the T-shaped CH- π interaction of the phenyl ring **B** with F157.

3.1.5. Validation of allosteric activators binding characteristics to PDK1 via Isothermal Titration Calorimetry (ITC).

To validate the affinity of the new identified activators to PDK1 we performed binding studies with selected compounds using ITC. We wanted to figure out whether the *trans* isomers lack binding to the PIF pocket or if there is binding that is uncoupled from allosteric activation.

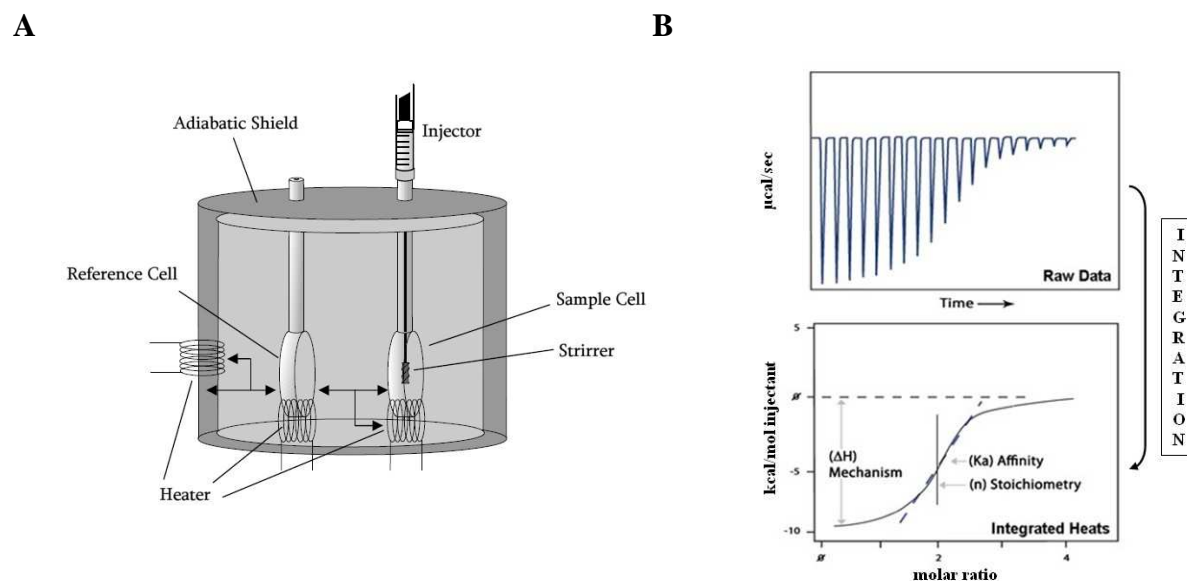
ITC is a biophysical measurement technique that has been widely applied to study biomolecular interactions in dilute solutions e.g. protein-ligand interactions. The measurements are carried out in an adiabatic ITC system (Figure 25A) and provide in a single experiment informations on thermodynamic quantities such as enthalpy (ΔH), entropy (ΔS), reaction stoichiometry (N) and binding affinity (K_a).¹³¹ These parameters are related to each other by the Gibbs-Helmholtz equation:

$$\Delta G = -RT \cdot \ln K_a \quad \rightarrow \quad \Delta G = \Delta H - T\Delta S$$

ΔH is released (or absorbed) upon the interaction between the ligand and the protein monitored over the time. Nonlinear regression fitting to the binding isotherm (ORIGIN software) gives the K_a . From the value of K_a , the free energy of binding ΔG and entropy of binding ΔS can be determined (Figure 25B).

Thus the results give information about the binding affinity of the ligand to the target and give insights into the mechanism of binding. Entropically driven binding is associated with hydrophobic interactions due to an increase in solvent entropy and release of water upon binding. In contrast, enthalpically binding is associated with Van der Waals and H-bonding interactions. Both entropy and enthalpy contribute to the free energy which is directly related to binding affinity and which has a negative value in case of spontaneous reactions. In medicinal chemistry the ITC method finds more and more application, since the thermodynamic data help to guide inhibitor optimization. Thermodynamic data aid to select lead compounds based on the balance between entropy and enthalpy. In general, a predominant enthalpy of binding indicates a high proportion of specific, directed bonds. In contrast, entropy driven ligands are too hydrophobic and thus it is difficult to increase their affinity to the binding pocket.¹³² However, high affinity can only be achieved if both enthalpy and entropy contribute favourably. Nezami *et al.* described that enthalpy-dominated binders are doubtlessly the preferred starting point for lead optimization. Characterizing allophenylnorstatine-based inhibitors of plasmepsin II, an antimalarial target, Nezami *et al.* found out that an optimal balance with the free energy partitioned approximately as one-third enthalpy and two-thirds entropy ($T\Delta S$) is required in order to overcome the enthalpy-entropy compensation effect. Thus only compounds with this combination reached nanomolar affinity to the target plasmepsin II.¹³³

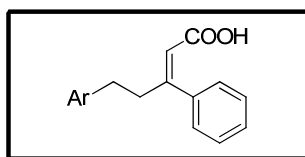
Figure 25: A: Schematic diagram of an ITC instrument. **B:** Typical ITC data. Top panel: raw ITC data. Lower panel: Binding isotherm



A: The ITC instrument contains of a sample cell and a reference cell that are enclosed by an adiabatic shield. The system maintains a constant temperature difference between both cells that is compensating by an electronic feedback mechanism that controls the heaters that are located adjacent to both cells. Endothermic reactions lead to an increase of the heat output and exothermic to a decrease. The amount of power that is required to maintain the constant temperature between the cells is measured.

B: In a typical ITC experiment a solution of a ligand is titrated into a cell containing a solution of the protein at constant temperature. During each injection heat is released or absorbed in direct proportion of the amount of bound ligand to the protein. At the beginning the ligand is completely bound to the protein leading to a maximal heat signal that diminishes as the protein becomes saturated until only background heat of dilution and mechanistic effects are observed. Integration of the heat changes of injections yield in resulting enthalpy H . A plot of the obtained heats from each injection against the molar ratio of the ligand leads to a sigmoidal binding curve.

In this study we performed the ITC experiments investigating the binding interactions of selected 3,5-diarylpent-2-enoic acids to PDK1₅₀₋₃₅₉. The measurements were conducted by injecting compound solution into the ITC cell containing the PDK1₅₀₋₃₅₉ solution in pH 7.5 media at 20 °C. Each experiment showed an exothermic course. The heat of the compound dilution that was involved at each injection was determined separately by injecting the corresponding compound solution into the buffer. To obtain the intrinsic binding isotherms we subtracted the dilution isotherm from the protein-compound-isotherm. The thermodynamic parameters obtained for the interactions are presented in Table 10.

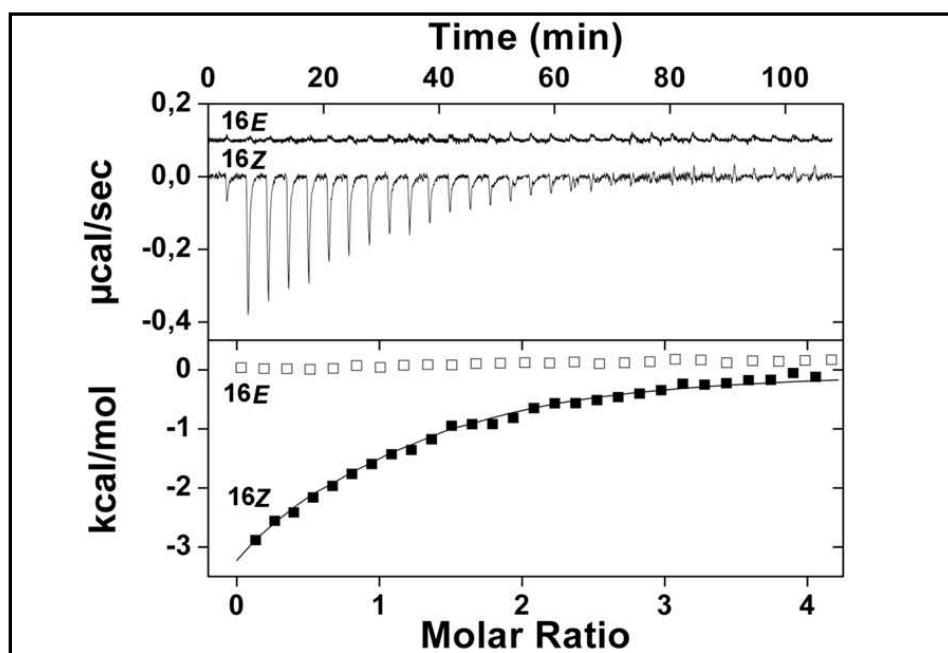
Table 10: Thermodynamic parameters for the binding interactions of selected compounds to PDK1 and their effects on catalytic activity of PDK1

No.	Ar	Kinase activity assay		ITC					
		A_{\max}^a fold	$AC_{50}^{a,b}$ μM	K_a^c M^{-1}	K_d^c μM	ΔH^d kcal/mol	$T\Delta S^e$ kcal/mol	ΔG^f kcal/mol	$\Delta H/\Delta G$ %
2Z		4.0 ^g	8.0 ^g	9.67E4	10.3	-1.82	4.87	-6.73	27.1
2E		ne	ne	-	nb				
3Z		2.2	9.5	-	nd				
3E		ne	ne	-	nd				
5Z		3.9	9.8	4.78E4	20.9	-3.07	3.20	-6.32	48.6
5E		ne	ne	-	nd				
6Z		4.4	7.1	9.66E4	10.4	-1.94	4.79	-6.73	28.8
6E		ne	ne	-	nd				
7Z		2.4	2.8	7.18E4	13.9	-3.71	2.80	-6.56	56.6
7E		ne	ne	-	nd				
8Z		2.1	4.7	1.71E5	5.9	-2.08	4.93	-7.07	29.5
8E		ne	ne	-	nd				
9Z		3.9	4.0	1.62E5	6.2	-1.79	5.19	-7.15	25.0
9E		ne	ne	-	nb				
16Z		3.5	6.0	7.26E4	13.8	-4.56	1.96	-6.67	68.3
16E		ne	ne	-	nb				
17Z		3.1	7.6	9.63E4	10	-4.09	2.60	-6.73	60.8
17E		2.2	8.8	-	nb				

^a: Mean value of at least two independent experiments, standard deviation <20%. ^b: As a particularity for compounds with activatory properties, it was necessary to indicate the maximum activation that was achievable with a compound, as compared to the basal activity of PDK1 (set to 100%). Based on two independent titrations of PDK1 with **16Z**, ^c: standard deviations for K_a and K_d are of 11%, error bars for ΔH , $T\Delta S$, and ΔG are of ^d + 0.30 kcal/mol, ^e + 0.37 kcal/mol, and ^f + 0.07 kcal/mol, respectively. ^g values were taken from¹²⁶. ^h mixture of isomers, ca. 75% Z/25% E for **16**, and 70% Z/30% E for **17**. ne: no effect; nb: no binding; nd: not determined.

Figure 26 depicts the binding isotherm obtained for the geometric isomers **16Z** and **16E** that we are using in the following to point out the general characteristics of the appropriate isomer interactions with PDK1. The typical curve shape of an ITC experiment is demonstrated in the top panel for compound **16Z** whereas each injection of the ligand to the protein resulted due to the occurred binding in exothermic pulses. These pulses decreased until a plateau is reached when the protein is saturated by the ligand. In case of the *trans* isomer, **16E**, there is no a characteristic curve shape. The only experiment signals resulted from the measurement of the background and dilution heats. The integrated peak intensities of compound **16Z** plotted against the molar ratio and their following fitting furnished $\Delta H = -4.56$ kcal/M, $K_d = 7.26 \times 10^4$ M⁻¹ or in terms of equilibrium dissociation constant $K_d = 13.8$ μ M ($K_d = 1/K_d$). The stoichiometry was near by 1 which applied for all *cis* isomers. For the *trans* isomer **16E** no thermodynamic data are obtained since no binding was detected.

Figure 26: Binding isotherm obtained by ITC



Characterization of **2Z** and **2E** isomers interactions with PDK1₅₀₋₃₅₉ by ITC. The top panel shows the raw heat signal for successive injections of dissolved compounds **16Z** and **16E** into a PDK1₅₀₋₃₅₉ solution at 20°C. The bottom panel shows the integrated heats of injections corrected for heats of dilution for **16Z** (filled squares) and **16E** (open squares), with solid lines corresponding to the best fit of the data to a bi-molecular binding model. No binding of compound **16E** to PDK1₅₀₋₃₅₉ is detected in conditions where **16Z** shows clear binding. Thermodynamic parameter values are given in Table 1.

In this context it is important to draw attention to the compound **17E**. The ITC experiment revealed that this compound did not bind to the PDK1. In contrast, in the biological *in vitro* assay **17E** exhibited a weak activation. Based on these results we can not explain this characteristic. We can only assume that the ATP could play a role. The ITC measurements were carried out in the absence of ATP, the radioactive kinase assays contained ATP. We speculate that the interaction of **17E** with the PIF-binding pocket in the activity assay can be given by the influence of ATP triggering allosteric cooperative effects. Consequently a slightly more active conformation of PDK1 becomes stabilized. Thereby the indole ring might promote the binding by H-bond interaction with Q150, thus distinguishing **17E** from the other *trans* configured compounds which were analyzed by ITC.

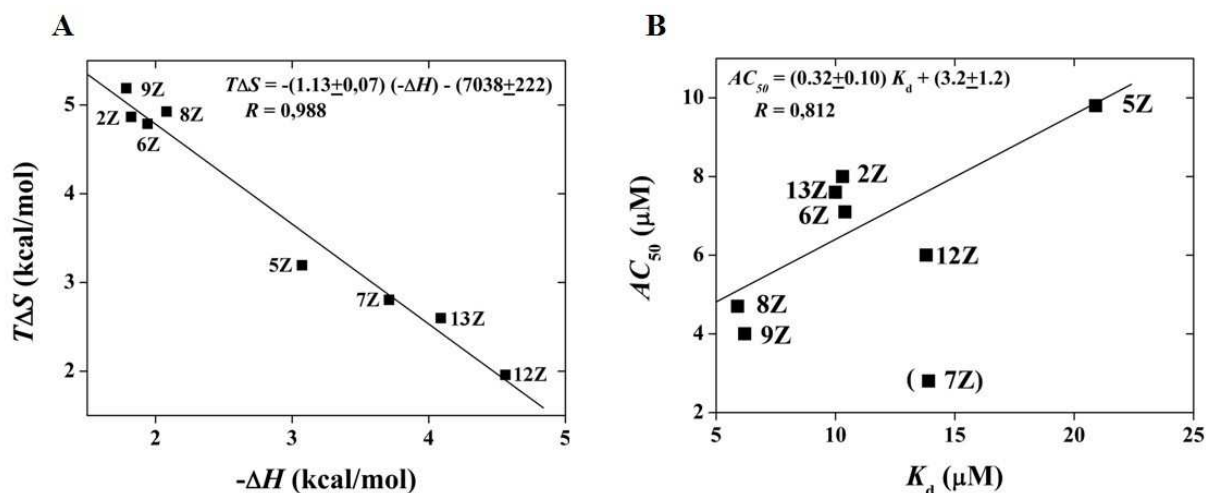
Summarizing, the ITC results confirmed the main potency of *cis* isomers we obtained already from the *in vitro* assays and the X-ray structure. The strong binding is only possible with the carboxyl group that has the *cis* configuration. Furthermore, we obtained similar results for all tested compounds (*E* and *Z* isomers of **2, 3, 5, 6, 7, 8, 9, 16, 17**) indicating that the phosphate binding site accommodated all *cis* compounds in a similar way leading to the same position of the phenyl ring **B** into the subpocket on the PDK1 PIF-binding pocket as experimentally described for **2Z**.

3.1.6. Interrelationships between Thermodynamic Binding Signature, Structure, and Activity of selected 3,5-diarylpent-2-enoic acids toward PDK1.

Analyzing the ITC experiments we found out that there is no general agreement between the estimated K_d values and the AC_{50} values from the activity assay. In the following we shed light on the consequential influences of structural features on the affinity and activity of selected compounds toward PDK1.

First of all, I would like to focus the attention on the edge-to-face CH- π interaction of the phenyl ring **B** with F157 that we already described in the chapter 3.1.4 presenting the cocrystal structure (Figure 24).¹³⁴ This kind of T-shaped interactions is found to be predominant among other aryl aryl interactions and plays a crucial role in stabilizing the ligand protein binding. The interaction energy of the T-shaped benzene dimers is - 2.4 kcal/mol.^{135, 136} Moreover, such hydrophobic interaction is found to be the most favored formation in solution.¹³⁴ Using the software PYMOL we calculated the separation between

the **2Z** C4 and the ring centre of F157 in the cocrystal that amounts 3.22 Å. The distance is significantly shorter than the sum of the C-H...C Van der Waals radii and thus indicative of a rather strong interaction. Moreover, insertion of substituents or heteroatoms influences T-shaped configurations.¹³⁷ Derivatization of the ring **B** by fluorine substituents on *para*, *ortho* and *meta* positions and by replacement of pyridine led effectively to a decrease of the activity of PDK1. Therefore, we decide for further investigations not to modify ring **B** but we focused our optimization approach on substitutions on ring **A**. This decision is based additionally on our crystal structure of the compound **2Z** suggesting larger unfilled space in the ring **A** subpocket of the binding site (Figure 24). Analyzing the calorimetric results we observed a further interesting issue. In chapter 3.1.3 we presented the biological activities of the halogen substituted derivatives and there was no major difference in activation potency (AC_{50}) among the compounds substituted with mono halogens on the ring **A** (**2Z**, **5Z**, **6Z**). However, the dichlorosubstituted compounds, **7Z** and **8Z**, emerged with distinct, remarkable properties. As shown in Figure 27 compound (*Z*)-5-(3,4-dichlorophenyl)-3-phenylpent-2-enoic acid (**7Z**) broke the general correlation between AC_{50} (= 2.8 μ M, Table 10) and K_d (= 13.9 μ M, Table 10). The thermodynamic data indicated additionally that **7Z** exhibited the biggest loss of binding entropy compared to **2Z**. We could not explain this feature but we suggested that the 3-Cl was impeding the hydrophobic interaction of the substituted phenyl ring with the pocket. In contrast, (*Z*)-5-(2,4-Dichlorophenyl)-3-phenylpent-2-enoic acid, **8E**, was characterized by a distinct and interesting behavior displaying the lowest K_d what correlated with the obtained AC_{50} value. Nevertheless, its potency to allosterically activate PDK1 was striking due to the decrease to about half of the A_{max} of **2Z**. We may suppose the *o*-chlorine of **8E** induced a rather “antagonist” like behavior of the compound.

Figure 27: General correlations based on calorimetric measurements

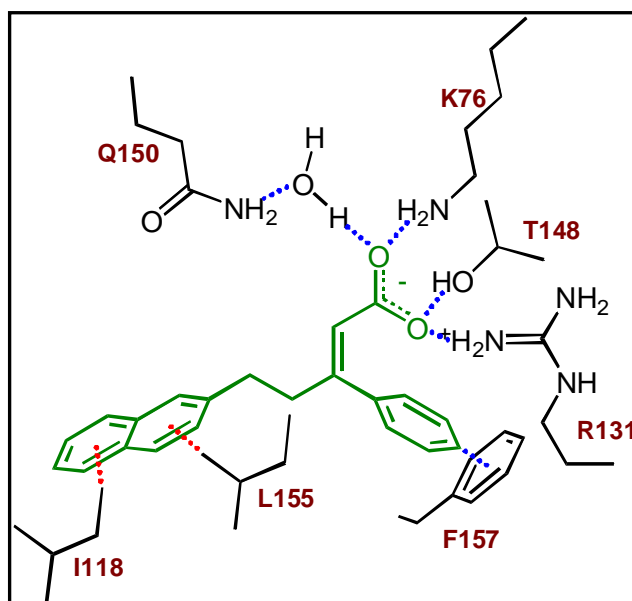
A: Enthalpy-entropy compensation phenomenon observed upon binding of Z isomers to PDK1. Large changes in the binding enthalpies (ΔH) and binding entropies ($T\Delta S$) were measured. However, the observed linear relationship between the ΔH and $T\Delta S$ values with a slope of 1 shows that a favourable increase in binding enthalpy was compensated by an equal unfavourable loss of entropy in the binding free energy ($\Delta G = \Delta H - T\Delta S$), which left nearly unchanged the binding affinity ($K_d = \exp[\Delta G/RT]$). **B:** A gross linear correlation was observed between the AC_{50} values for PDK1 activation and the dissociation constants as measured by ITC. This correlation suggested that for most compounds, the binding affinity to the intermediate active conformation of the kinase, which might be represented rather by the AC_{50} , does not differ strongly from the affinity to the activated conformation of the kinase, which might be described by the K_d . Only for compound **7Z** (not used to calculate the trend line), a low AC_{50} was associated with an over-proportionally high K_d .

Although entropically driven ligand-protein binding is usually attributed to structural features, in that case hydrophobic interactions, we observed that both dichloro substituted compounds (**7Z**, **8Z**) showed different thermodynamic profile. The 2,4-dichloro substituted analogue **8Z** displayed a predominantly entropy-driven binding and the 3,4-dichloro substituted analogue **7Z** did not (Table 1). We cannot provide a final answer based on our current data, but a possible reason for the difference could be due to the resulting location of the compounds within the hydrophobic pocket. The more entropy-driven binding of ring **A** in **8Z** might allow a greater flexibility of positioning within the hydrophobic pocket in order to avoid a steric clash of the 2-chlorine with either T128 or Q150 (compare with ring **A** position of **2Z**, Figure 3), whereas the binding positions might be more restricted in the case of highly directed H-bonds and dispersion forces which usually contribute to the enthalpy term. Such an entropy-enabled binding shift might propagate into sub-optimal interaction of the **8Z** carboxyl side chain with R131, resulting in a reduced allosteric activation without compromising binding affinity. Comparing compounds **8Z** with **9Z** we revealed that the “antagonist”-like properties result not only of entropy-driven binding alone. The steric impact like from the *o*-

chlorine plays also a significant role. This was corroborated by the fact that the maximum activation potency of the 4-bromo derivative **5Z** was not affected when a smaller *o*-fluorine was introduced (cf. **9Z**) despite the significant increase in the entropy/enthalpy ratio of binding. It will be interesting to see whether **8Z** binds to and stabilizes the intermediate active, basal conformation of the PIF pocket without causing major conformational changes.

As described in chapter 3.1.3.1 we decided to enlarge the ring **A** moiety motivated by the decrease of the AC₅₀ obtained with **7Z** in comparison to **2Z** (almost 3-fold). Using ITC we investigated the quality of the interactions between the extended aromatic rings and the PIF-binding pocket with the resulting naphthyl and indolyl derivatives (**16Z**, **17Z**) that did not abolish the PDK1 activity. The calorimetric data of these compounds showed the highest $\Delta H/\Delta G$ ratios in the analyzed series (**16Z**: 68.3%, **17Z**: 60.8%). The ratios resulted from a marked increase of the enthalpy relative to the entropy of binding (Table 10). All halogen-substituted phenyl analogues except **7Z** indicated completely different thermodynamic characteristics. We can suppose that the increase of the binding enthalpy is attributable to CH- π interactions resulting from higher π -electron density of the unsubstituted bicyclic rings combined with the larger surface. Although one unit CH- π interaction contributes around 1 kcal/mol to the total enthalpy,¹³⁸ we hypothesized that multiple CH groups participated simultaneously in interactions with π electrons, thus adding up to a significant increase in enthalpy, consistent with our experimental data. According to the cocrystal structure, the following residues of the PIF-binding pocket were possible candidates for a putative interaction with the extended π -electron system of **16Z** or **17Z**: most certainly the geminal dimethyl of L155, and – depending on which rotamer of the naphthyl or indolyl linking bond is preferred – either the terminal methyl of I118 or γ -methylene of the K115 side chain (cf. Figure 3). Both of the latter residues are within reach of the bicyclic rings of **16Z** and **17Z**, and the two possible corresponding rotamers could dock into the subpocket provided that the available space is slightly increased by a movement of the I119 chain. Since terminal methyls of Leu, Ile or Val are more commonly found in CH- π interactions,¹³⁸ we included a hypothetical interaction between the naphthyl of **16Z** and the methyl of I118 in the interaction scheme for **16Z** (Figure 28).

Figure 28: Binding scheme model summarizing interactions of activator compound **16Z** with the PDK1 PIF-binding pocket



Blue dotted lines denote interactions that have been identified for the analogue **2Z** in the cocrystal structure with PDK1; red dotted lines indicate the assumed interactions as inferred from the ITC experimental data.

Altogether, compounds with extended aromatic system interact substantially different from halogenated phenyl compounds, although the K_d values were in the same range what is due to the enthalpy-entropy compensation. We observed the enthalpy-entropy compensation effect also analyzing the thermodynamic parameters of the analogues **10Z** and **15Z** which displayed different activation potencies toward PDK1. It is most probable that both compounds can only bind to the PIF pocket in the same manner as the *p*-chlorophenyl ring of **2Z** when I119 moves away in order to avoid a steric clash (Figure 24). While the active compound **15Z** carries a *p*-phenyl substituent that contributes to additional CH- π interactions which could compensate for an entropic penalty, the *p*-ethyl substituted **10Z**, which is incapable of forming additional CH- π bonds, was nearly inactive. Summarizing, the less favourable entropy that is associated with potential movements of side chains could be compensated by the assumed reinforcement of CH- π interactions resulting in an enthalpy gain.

3.1.7. Overall Correlations between Enthalpy and Entropy of Binding and the Biological Activity Parameters of Allosteric PDK1 Activators.

Isothermal Titration Calorimetry provides information on the binding forces of ligands to the target proteins. It is increasingly apparent that the major contributor to binding of all

active compounds is ionic interaction. In our study, we found a surprisingly broad thermodynamic binding spectrum, from mainly entropy-driven to predominantly enthalpy-driven binding. We performed a correlation analysis plotting the thermodynamic binding signature against the activity data. The obtained plot revealed two strong relationships; as the most obvious correlation we identified a sharp enthalpy-entropy compensation effect, which has been described for many ligand-receptor systems such as agonists and antagonists interacting with membrane receptors¹³⁹⁻¹⁴¹ and inhibitors binding to HIV protease¹⁴² (see $\Delta H/\Delta S$ correlation, Figure 27A). This effect describes the fact that among a series of compound analogues with comparable size, any increase in binding enthalpy is accompanied by a loss of entropy to about the same degree, leading to little or no change in the binding affinity.^{143, 144} The compensation effect was most obvious when comparing the group of halogenated compounds (**2Z**, **6Z**, **8Z** and **9Z**) with **16Z** and **17Z** (Figure 27A). The bicyclic aromatic rings caused binding with highly favourable enthalpy, probably due to additional CH- π interactions as described above (Figure 28). Our ITC data indicated that the additional binding enthalpy was gained at the cost of entropy, accounting for the enthalpy-entropy compensation in the concrete case. A possible explanation for the concomitant loss of entropy with **16Z** and **17Z** could be that due to the higher polarity of the π -electron-rich rings, the contacting water molecules are less ordered and less entropy is gained upon water release from the compound. In contrast, fewer enthalpically favourable Van der Waals or CH- π interactions are possible with one phenyl ring where the density of the π -electrons is further decreased by halogen substituents. Apparently, this loss of H-bond capacity in the halogenated compounds was exactly balanced out by an opposite increase in hydrophobic interaction, giving raise to the entropy term. These mutual compensation processes prevented significant changes in the total binding free energies of compounds (compare e.g. **2Z**, $\Delta G = -6.73$ kcal/mol with **16Z**, $\Delta G = -6.67$ kcal/mol) which otherwise differed substantially in their $\Delta H/\Delta G$ ratio (Table 10). This phenomenon is not uncommon in the lead optimization process and has to be overcome in order to increase binding affinity (see chapter 3.1.8 below).

Another relationship became apparent when the thermodynamic binding profiles were correlated with the activatory potency of the compounds. We observed a rough correlation between the AC_{50} values for PDK1 activation and the dissociation constants as measured by ITC (Figure 27B). This correlation suggested that for most compounds, the binding affinity to the intermediate active conformation of the kinase, which might be represented rather by the AC_{50} , does not differ strongly from the affinity to the activated conformation of the kinase, which might be described by the K_d . The variations in activation efficacy (A_{max}) did not affect

this correlation. The relationship between AC_{50} and K_d was not self-evident since binding to the intermediate active state and dissociation of the complex after the conformational change could be perceived as two separate events characterized by divergent affinity constants. Our finding rather suggests that during the allosteric activation by the majority of compounds, only subtle and rapid changes occur within the PIF-binding pocket itself, while the overall geometry of the PIF-binding pocket remains unaltered.

3.1.8. Implication of the Calorimetric Characterization for Lead Selection and Optimization.

Since several years ITC has been enforced as a method to guide the lead evaluation and optimization in drug development providing a partition of the binding energy into its enthalpic and entropic components. Empirically obtained calorimetric data presented in numerous studies suggest that compounds that exhibit an enthalpy dominated binding are particularly suitable to increase ligand affinity.^{142, 145} Favourable binding enthalpy provides several advantages since Van der Waals and H-bonding interactions as enthalpy-driven interactions are more difficult to engineer. A good geometric complementary between the involved functional groups of drug and receptor is required for optimal electrostatic interactions between the ligand and the target. To optimize the entropy contribution on the other hand has proven much easier, as this is almost inevitably achieved by introducing non-polar groups which increase the hydrophobic effect. However, it is more difficult to increase ligand affinity when binding interactions become highly hydrophobic and rigid.¹⁴⁶ From the perspective of allosteric modulators, it might be worth discussing whether **8Z**, which displayed stronger binding in connection with the opposite trend in activation potency, should not be pursued in parallel as lead compounds toward the development of non-activators or even allosteric inhibitors. However, since very high affinity can only be achieved if both enthalpy and entropy contribute favourably and in a balanced manner to the binding free energy,^{133, 145} enthalpy-dominated binders are doubtlessly the preferred starting point for lead optimization. Moreover, it was reported by Nezami *et al.* that in order to overcome the enthalpy-entropy compensation effect, an optimal balance with the free energy partitioned approximately as one-third enthalpy and two-thirds entropy ($T\Delta S$) was required.¹³³ Only compounds with this combination reached nanomolar affinity to the target plasmepsin II in the reported case; the same conclusion could also be drawn for allosteric glycogen

phosphorylase inhibitors in a recent study.^{jmedchem38} In that sense, calorimetric analysis has disclosed **8Z** rather as a “dead end” since the balance has been reached already ($\Delta H/\Delta G = 29.5\%$) and any addition of another chemical moiety would provoke enthalpy/entropy compensation effects without substantially increasing ΔG . Similarly, the thermodynamic binding data for **9Z** revealed the compound as a less appropriate starting point to escape enthalpy-entropy compensation, even though the AC_{50} was two times lower than that of **2Z** (Table 10).

In summary, **16Z** and **17Z** were found to possess the most ideal thermodynamic lead profile among the compounds analyzed by ITC, since the enthalpic term strongly predominates the binding free energy.

3.1.9. Conclusion

In an effort to enhance the efficacy and the selectivity of the first identified hit compound **1** and the new lead compound **2Z** (Figure 22) toward PDK1 we developed a series of 3,5-diarylpent-2-enoic acid analogues. As **2Z** was the first analogue that we isolated from this compound family and that exhibited a good potency toward PDK1, it was selected for the evaluation of the actual binding site in a mutagenesis study and in a cocrystallization approach. Thus, we were successful to prove the PIF pocket, a protein kinase catalytic domain which is not adjacent to or overlapping with the ATP binding site as the binding site of **2Z**. Obtaining the cocrystal structure of **2Z** bound to the PIF pocket of PDK1 we confirmed the series of 3,5-diarylpent-2-enoic acid analogues as truly allosteric compounds. It should be mentioned that many inhibitors reported in the literature to be “allosteric” still bind to the ATP binding site at least partially. Like in the case of imatinib mesylate (Gleevec), the term is used to signify that an inactive, open conformation of the kinase is stabilized.⁷ Investigating the biological potency and utilizing an ITC approach with selected compounds we observed interesting structure-activity and interrelationships between thermodynamic profile, structure and activity of the set of compounds. First of all, the main potency showed compounds bearing the carboxyl moiety in the *cis* position. Moreover, the similar ITC results for all *cis* and *trans* isomers suggested that the phosphate binding site accommodated all *cis* compounds in a similar way. In general, the thermodynamic data of the new series revealed binding with variable proportions of entropy and enthalpy. This broad thermodynamic spectrum seemed to result from the enthalpy-entropy compensation effect we could prove comparing the analysis

plot of the halogenated compounds with the bicyclic compounds. Our ITC results indicated also some important CH- π interactions between ligand and receptor that can essentially contribute to increased selectivity and potency of PIF pocket-directed compounds which have been identified by virtue of their favourable binding enthalpy. The bicyclic analogues **16Z** and **17Z** turned out to have the highest $\Delta H/\Delta G$ ratio on the basis of favourable binding enthalpy values most likely due to the attributable CH- π interactions. Based on these best thermodynamic profiles and biological potencies toward PDK1 we selected **16Z** and **17Z** as new lead structures to further improve potency. Thus we achieved additional informations about structural requirements the compounds must have included to become good affinity and activity toward the PIF pocket of PDK1.

Altogether, we could confirm that compounds consist of two aromatic moieties connected by an aliphatic chain, bearing a two atom membered side chain with a free carboxylic group own the ability to function as a PDK1 activator. Thereby, in case of 3,5-diarylpent-2-enoic acid series only the carboxyl moiety of the *cis* analogues can exploit their carboxyl moiety to interact with the crucial phosphate binding site residues. And that's not all: we found out a V-shaped overall conformation of the aryl rings toward each other is required to achieve complementarity to the binding pocket. These prototype compounds – despite the low molecular masses – already displayed activities in the low micromolar range, suggesting that mass and ligand efficiency should remain in a reasonable range after lead optimization.

Nevertheless, to further confirm PDK1 as the target effects on the downstream proteins should be investigated. In the case of PDK1, activation of the catalytic activity is achieved by binding to the HM/PIF-binding pocket, which at the same time blocks the activation of all substrates (S6K, RSK and some PKC) with the exception of PKB. S6K, RSK and some PKC require transient interaction with the pocket. Thus the compounds might act differentially on the two subsets of PDK1 substrates which either require docking interaction with the PIF-binding pocket or not. Hence, in-depth investigation of the compounds' effects on the cellular signaling pathways – using genetic tools and detailed phosphorylation analysis – are required and will be subject of our future studies. In particular, detailed analysis in a cellular setting will be required to study the biological effects of PIF-binding pocket targeting compounds with high (e.g. **6Z**) vs. low (e.g. **8Z**) concomitant allosteric activation of PDK1 catalytic activity.

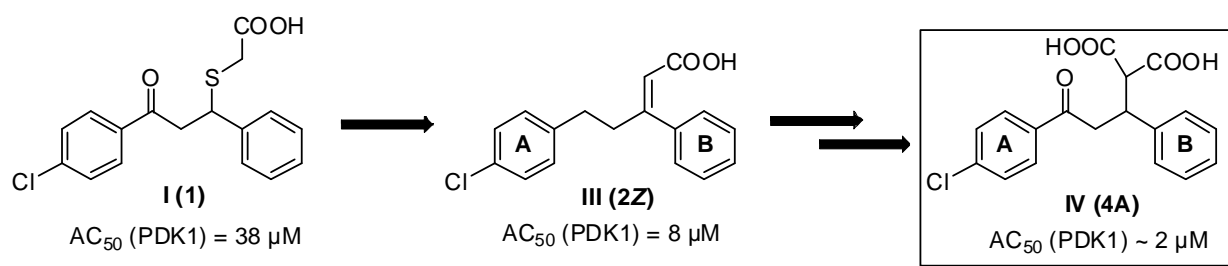
3.2. Prodrug approach of 2-(3-oxo-1,3-diphenylpropyl)malonic acids as potent allosteric activators of PDK1 to enable the bioavailability of the high polar dicarboxylic acids

3.2.1. Scientific rationale

Initial optimization of the allosteric PDK1 activator **1** (Scheme 9) identified from a library of commercial compounds led to the first larger series of 3,5-diphenylpent-2-enoic acids as PIF pocket-directed compounds. We were able to provide the activation characteristics in biophysical and biochemical assays, the SAR results and characterization of the cocrystal structure. Indeed, the results demonstrated that the compounds influenced PDK1's activity targeting the PIF pocket, but they displayed low affinity, rendering further studies difficult. For further improvement of the potency toward PDK1 we designed a chimeric compound combining the carbonyl function from the lead compound **1** with the short side chain from compound class **III** (Scheme 9). Another goal was to mimic better the two negative charges of the phosphate group present in natural ligands of the PIF pocket, the HM phosphopeptides of the PDK1 substrate proteins.

Thus, herein we present 2-(3-oxo-1,3-diphenyl-propyl)malonic acids (**IV**) as a new class of PDK1 activators with improved potency and high selectivity toward close homologues. Unfortunately, when used in cell assays these were completely inactive, presumably due to their highly dianionic structure. To overcome this transport barrier, a prodrug strategy was adapted and investigated as alternative approach for intracellular potency replacing the dicarboxylic functionality into the corresponding bisacetoxymethyl ester derivatives.

Scheme 9: Allosteric modulators design concept



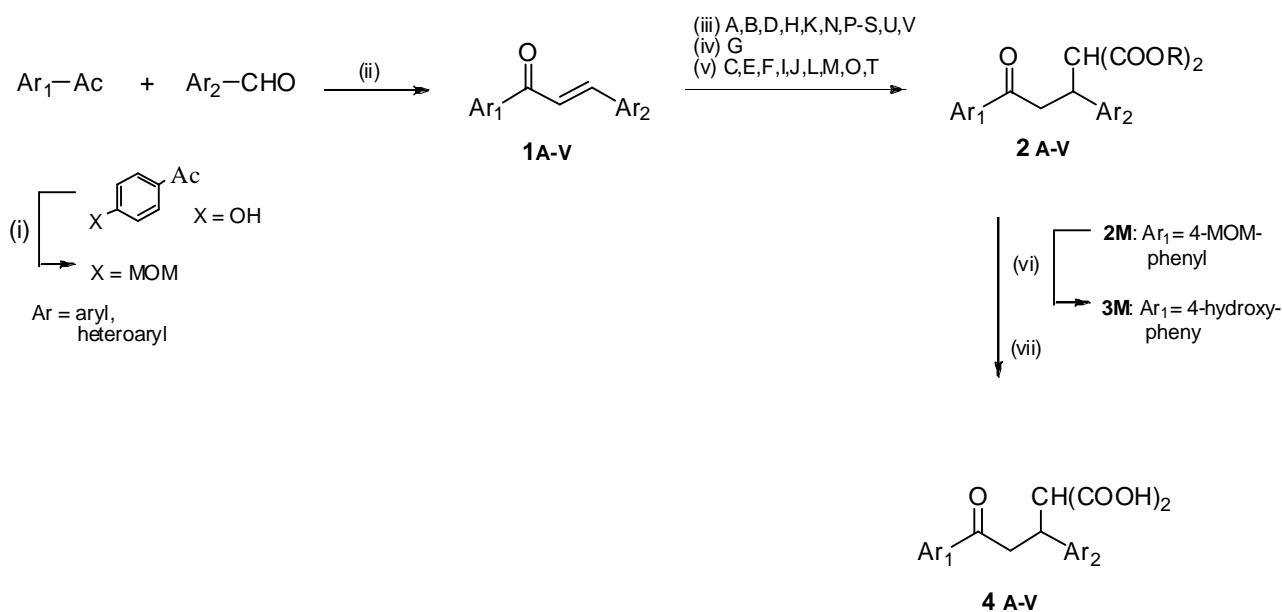
Furthermore, the malonic moiety of the 2-(3-oxo-1,3-diphenylpropyl)malonic acids provided a synthetic access to another substance class, the corresponding monoacid derivatives. A comparison with the corresponding 2-(3-oxo-1,3-diphenylpropyl)malonic acids should shed light on the significance of the polar moiety in relation to the PIF pocket of PDK1.

3.2.2. Synthesis

In our design strategy to create a chimeric compound we retained the carbonyl function from the hit compound **1** while keeping the short side chain from the new lead compound **2Z**. In addition, since the natural ligands of the PDK1-PIF pocket are phosphor peptides^{17, 26} we planned to introduce a second carboxyl function to better mimic the phosphate group.

The malonic acids derivatives (**IV**) were prepared by the synthetic route shown in Scheme 10.

Scheme 10: Synthesis of the compound class **IV (4 A-V)**.^a

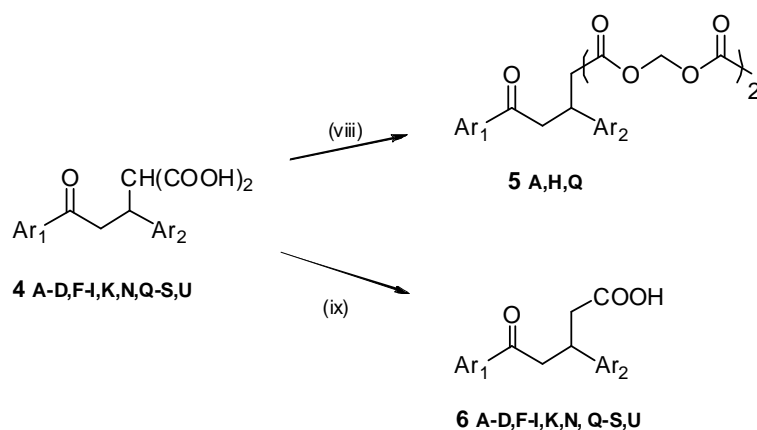


^a reagents and conditions: (i) Method G: bromomethyl-methylether, NaH, DME, 0 °C, 1 h; (ii) Method A: NaOH, EtOH, 1 h, rt; (iii) Method H: diethyl malonate, MgO, toluene, reflux, 2h; (iv) Method I: diethyl malonate, K₂CO₃, ethanol, reflux, 2 h; (v) Method J: diethyl malonate, NaH, methanol, reflux, 2 h; (vi) Method K: 10 % HCl, methanol, reflux, 2 h; (vii) Method L: NaOH, EtOH, reflux, 4 h; For substituents Ar₁ and Ar₂ see Table 11.

The target compounds were available in three steps starting from the already previously described 1,3-(heteroaryl/aryl)-prop-2-en-1-ones (chalcones) **1A-V** (see 3.1.2). These are available by classical Claisen-Schmitt condensation (Method A) of benzaldehydes or heteroarylaldehydes with acetophenones or heteroaryl methyl ketones and were converted to the corresponding dialkyl 2-(3-oxo-1,3-diheteroaryl-/arylpropyl)malonates via base-catalyzed Michael addition of CH-acidic malonates. Due to the mild base nature, ease of product isolation and good activity most of the Michael adducts **2A,B,D,H,K,N,P-S,U,V** could be obtained with magnesium oxide in toluene.¹⁴⁷ Because of the limited activity of magnesium oxide depending on the solvent and the substrate the remaining malonate derivatives were obtained using alternative catalysts, potassium carbonate for **2G** and sodium hydride for **2C,E-J,L,M,O,T**.^{148, 149} Treatment with diethylmalonate and magnesium oxide or potassium carbonate in ethanol gave the diethyl intermediates and with sodium hydride in methanol occurred transesterification leading to the dimethyl intermediates. Hydrolysis of these malonate analogues afforded the corresponding (3-oxo-1,3-diheteroaryl/arylpropyl)malonic acids **4A-V**.

The diacid functionality in turn provides the synthetic access on the one hand to the decarboxylated compounds and on the other hand to the cell permeable prodrug derivatives since the membrane transport barrier is presumably a major reason for the lack of cellular activity of the (3-oxo-1,3-diheteroaryl/arylpropyl)malonic acids. The corresponding synthetic route is outlined in Scheme 11.

Scheme 11: Synthesis of compounds **5 A,H,Q** and **6 A-D,F-I,K,N,Q-S,U**.^a



^a reagents and conditions: (viii) Method M: bromomethyl acetate, NEt₃, DMF, rt, 4 h; (ix) Method N: 160-170 °C, 2 h. For substituents Ar₁ and Ar₂ see Table 11.

Pyrolysis of the corresponding malonic acid analogue at about 165 °C gave rise to the decarboxylation leading to the 5-oxo-3,5-diheteroaryl/arylpentanoic acids **6A-D,F-I,K,N,Q-S,U**.¹⁵⁰ Treatment of the (3-oxo-1,3-diheteroaryl/arylpropyl)-malonic acids **4A-V** with bromo methylacetate and triethylamine in dimethylformamide afforded the bisacetoxymethyl ester derivatives **5A,E,G-I,L,N,O,Q,R** in modest yields.¹⁵¹

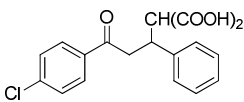
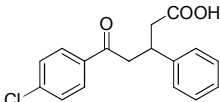
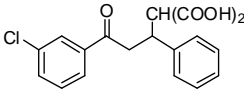
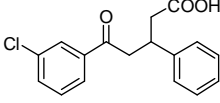
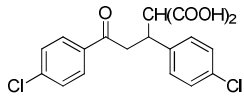
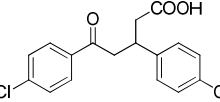
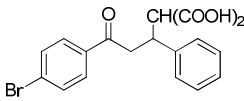
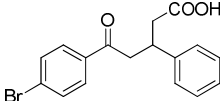
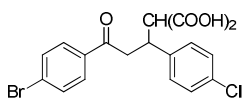
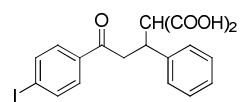
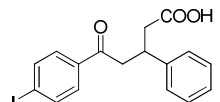
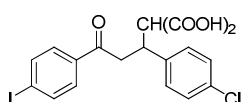
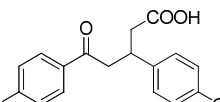
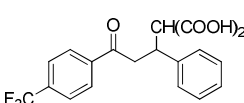
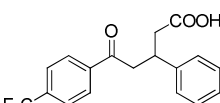
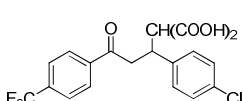
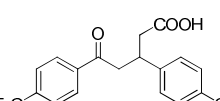
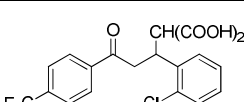
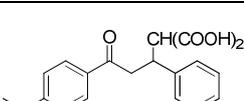
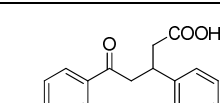
Synthesis of **4M** (Scheme 10), derived from the 4-hydroxyacetophenone, required protection of the nucleophilic alcohol function in order to obtain the corresponding chalcone **1M** and the malonate derivative **2M** in good yields. The methoxymethyl (MOM) group was chosen as protecting group and introduced by using bromomethyl-methylether with sodium hydride in dimethylformamide.¹⁵² Finally, the methoxymethyl group was cleaved under acidic conditions to give the desired dimethyl 2-(1-(4-chlorophenyl)-3-(4-hydroxyphenyl)-3-oxopropyl)-malonate **3M** followed by hydrolysis to furnish the target molecule **4M**.¹⁵²

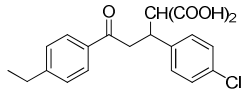
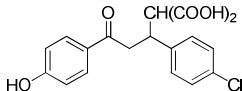
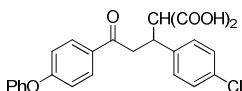
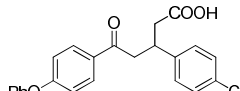
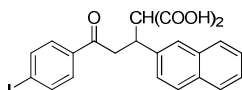
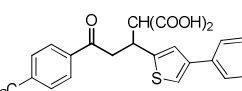
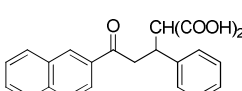
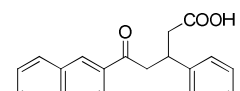
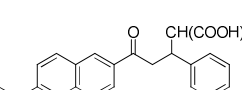
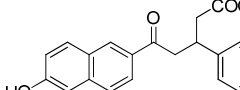
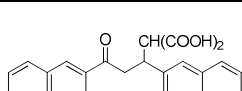
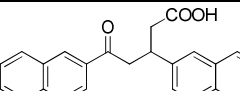
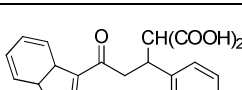
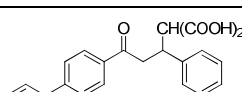
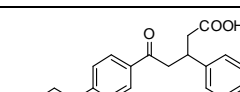
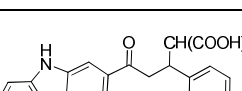
3.2.3. Biological results

3.2.3.1. Biological characterization *in vitro* of dicarboxyl PDK1 activators

I studied the effect of the malonic acid analogues on the activity of His-PDK1 50-556 using a radioactivity kinase assay. The kinase was incubated with the radiolabeled phosphate from [γ -³²P]ATP in the presence of T308tide as substrate peptide and the compounds. The amount of the radioactivity incorporated into the substrate was measured (see 3.1.3.1).¹⁵³ The concentration necessary to achieve half maximal activation (AC_{50}) and maximum activation (A_{max}) were determined using eight different concentrations. The results are summarized in Table 11. In parallel we measured the effect of **2Z** that possess only one carboxyl group but the same phenyl moieties as **4A**. As described previously **2Z** prompted a 3 fold increase in PDK1 activity.²⁰ Most of the dicarboxyl compounds raised the PDK1 activation to higher levels and had lower AC_{50} than **2Z**. Several potent analogues were produced.

Table 11: *In vitro* specificity of the 1,3-diaryl malonyl propanones and the corresponding monoacids.

No.	Structure	Kinase activity assay		No.	Structure	Kinase activity assay	
		A_{\max}^a fold	$AC_{50}^{a,b}$ μM			A_{\max}^a fold	$AC_{50}^{a,b}$ μM
4A		4.0	2.5	6A		3.0	> 20
4B		2.6	4.0	6B		nd	nd
4C		2.0	> 10	6C		nd	nd
4D		3.7	1.4	6D		nd	nd
4E		3.0	12.0	-	-	-	-
4F		4.0	0.4	6F		4.0	10
4G		3.8	2.0	6G		2.5	20
4H		5.5	2.0	6H		4.0	15
4I		3.5	10.0	6I		nd	nd
4J		nd	nd	-	-	-	-
4K		5.0	4.0	6K		nd	nd

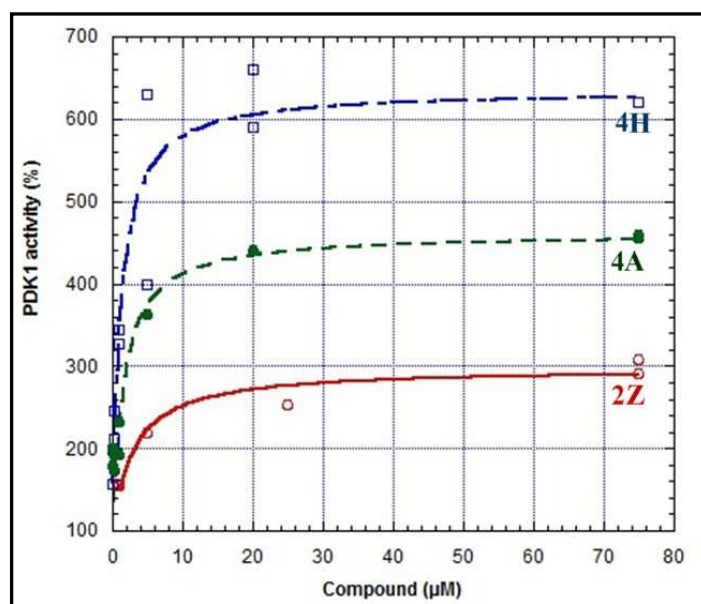
4L		3.0	6.8	-	-	-	-
4M		ne	ne	-	-	-	-
4N		7.0	16.0	6N		nd	nd
4O		3.6	0.2	-	-	-	-
4P		ne	ne	-	-	-	-
4Q		4.0	< 1.0	6Q		2.5	5.0
4R		3.6	3.3	6R		nd	nd
4S		4.8	2.0	6S		nd	nd
4T		3.0	14.0	-	-	-	-
4U		3.7	0.6	6U		1.5	0.5
4V		3.6	0.7	-	-	-	-

Values in % catalytic activity (DMSO-treated control = 100%)

nd: not determined; ne: no effect

The significant difference in activity between the compound class **III** and **IV** (Scheme 9) is shown in Figure 29 with three representative activation curves that were created using KaleidaGraph software. When we compared the compounds it was evident that both malonic acid analogues exhibited a pronounced increase of activation potency in comparison with the acrylic acid derivative **2Z**. Furthermore, the AC_{50} values which can be found explicitly in the Table 11 are lower.

Figure 29: Effect of **2Z** and the dicarboxylic compounds **4A** and **4H** on PDK1 activity



The predominant contribution of the dicarboxyl moiety to the affinity of the compounds to the PIF pocket of PDK1 is also clearly apparent from the Table 11. Nevertheless, we observed strong dependence on the AC_{50} to the ring substituents, too. Substitution in the *para* position of the phenyl ring **A** was appropriate to have higher potency and lower AC_{50} as we presented in the previous SAR analysis with the structure class **III**. The phenyl ring substituents were systematically varied, since the type and pattern of halogen substitutions were found to influence the potency of the PIF-binding compounds strongly. A chlorine substituent in *para* position (compound **4A**) induced a 4-fold increase in activity whereas an introduction of a chlorine atom in the *meta* position (compound **4B**) led merely to a 2.6-fold activation of PDK1. Within the halogen substituents the AC_{50} improved in the following order $\text{Cl} < \text{Br} < \text{I}$ at comparable 4-fold activation. The iodine analogue **4F** showed a significantly lowered AC_{50} in the high nanomolar range ($0.4 \mu\text{M}$). The potency of the iodine derivatives was slightly further enhanced by replacement of phenyl ring **B** by naphthyl **4O** ($AC_{50} = 0.2 \mu\text{M}$). An

extraordinarily high effect was observed in case of the *para*-trifluoromethyl malonic acid derivative **4H** displaying 5.5-fold activation potency toward PDK1. Although the 4-ethylphenyl malonic derivative **4K** exhibited also a pronounced activation it was less beneficial relating to the poor AC₅₀. Additional introduction of a halogen chlorine into the phenyl ring **B** in the 4-position of the above presented compounds **4A,D,F,H,K** abolished the activating effect on PDK1 considerably. Interestingly, the activity did not decrease introducing a chlorine atom in 2-position of the phenyl ring **B** (compound **4H**). **4M**, the hydroxyl analogue, and **4P**, the 4-phenylthiophene analogue, did not influence PDK1 activity at all. Besides introduction of small residues in *para* and *meta* position, further modification of the phenyl moiety **A** by naphthyl (**4Q**), its derivatization by 5-methoxylation (**4R**) or additional exchange of the phenyl ring **B** by naphthyl (**4S**) resulted in a 3-4.8-fold increase of potency. However, the AC₅₀ values were comparably high. Additionally, an indole derivative (**4T**), a phenanthrene derivative (**4U**) and also a carbazole compound (**4V**) were prepared. While **4T** exerted a moderate 3-fold activation, the replacement of the phenyl moiety by the condensed phenyl rings phenanthrene and carbazole led to potent activators with nanomolar AC₅₀ values.

Moreover, we studied the specificity of the 2-(3-oxo-1,3-diphenylpropyl)malonic acid **4A-V** toward a panel of AGC kinase. The series showed not only a high potency toward PDK1, most of them have also a high selectivity for the PDK1 PIF pocket over PIF pockets of closely related AGC kinases (Table 12).

Table 12: *In vitro* specificity of **2Z** and the dicarboxyl compounds **4A** and **4H**.

Cpd.	[μ M]	PDK1 (%)	S6K1 (%)	PKC ζ (%)	SGK (%)	PKB β (%)	PKA (%)	PRK2 (%)	RSK (%)	MSK (%)
2Z	2	100	ne	ne	ne	ne	ne	ne	-	-
	50	280	ne	40	ne	110	90	ne	-	-
	200	280	60	6	60	ne	60	ne	-	-
4A	2	280	ne	ne	ne	ne	ne	ne	ne	ne
	50	380	ne	80	ne	110	ne	ne	160	95
	200	400	130	50	ne	ne	ne	ne	142	100
4H	2	370	ne	ne	ne	ne	ne	ne	ne	ne
	50	570	90	ne	ne	83	180	110	140	100
	200	520	110	ne	ne	100	207	110	200	80

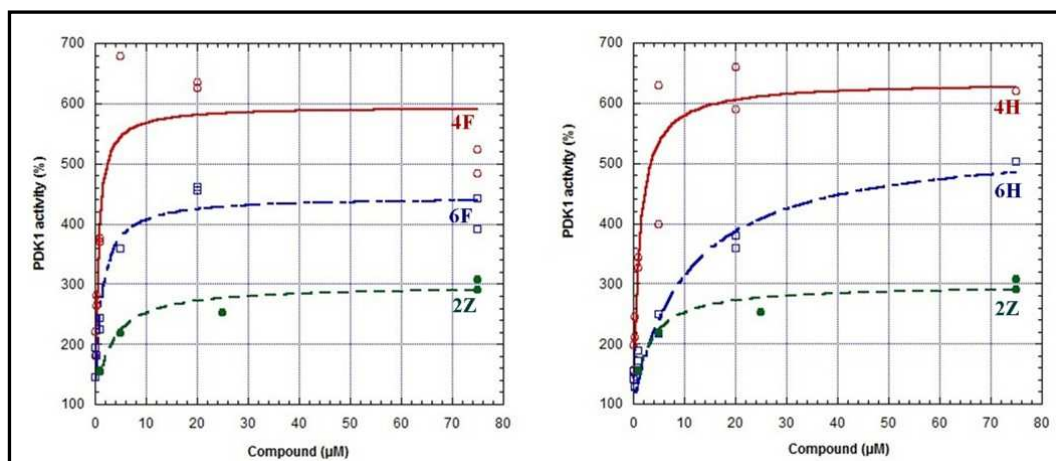
Values in % catalytic activity (DMSO-treated control = 100%)

ne = no effect

However, compounds **2Z** and **4A** displayed an inhibitory effect toward PKC ζ in the range of higher concentration. **2Z** induced also a slight inhibition of the AGC kinase PKA. **4A** exhibited additionally a slight activation effect toward RSK, and **4H** both RSK and PKA. Nevertheless, in conclusion with the compound class **IV** we were able to obtain several potent and selective compounds, especially since we are focused on allosteric modulation of kinase targeting the PIF pocket that is less conserved as the ATP binding site.

The second substance class presented here, the monoacid derivatives **6A-D,F-I,K,N,Q-S,U**, exhibited generally reduced activation potency and turned out to be weaker activators than the corresponding dicarboxyl analogues. In Figure 30 the differences between the monoacid and malonic acid analogues are shown with two representatives **4F** vs. **6F** (left panel) and **4H** vs. **6H** (right panel)). The effect of these compounds on PDK1 activity I measured in parallel in a radioactivity kinase assay. It is obvious that all four compounds prompted the PDK1 activation in higher levels than **2Z**, but the malonic acids were characterized by a more noticeable activation effect on PDK1. It must to be noted that we observed the highest activation potency with compounds **6F** and **6H** among the monoacid derivatives **6A-D,F-I,K,N,Q-S,U**. However, in our effort to obtain very potent and selective PDK1 activators we directed the attention to the malonic acid analogues for further experiments. For some compounds AC_{50} values could not be accurately determined because they went below the concentration of enzyme present in the assay. Attempts to measure K_d values by ITC failed because of the highly exergonic dilution behavior of the malonic acid derivatives. Instead, a novel technique called thermophoresis was employed to measure the K_d of **4H**, which was found to be 70 nM.

Figure 30: Comparison of the effect of the dicarboxylic compounds **4F** and **4H** on PDK1 activity versus the appropriate monoacid analogues **6F** and **6H**



3.2.3.2. PIF pocket Mutant Assay to confirm that compound 4H activates PDK1 by targeting the PIF-binding pocket

The series of 2-(3-oxo-1,3-diphenylpropyl)malonic acids (**IV**) reached higher levels of PDK1 activation *in vitro* in comparison with the first presented series of 3,5-diarylpent-2-enoic acids. In order to verify the binding site of the compounds we performed mutation experiments like we performed already for the previous compound class **III**. Laura Lopez Garcia (Biondi group) characterized the binding site of the compound **4H** on different PIF pocket-binding mutants of PDK1 measuring the activity in the presence or absence of **4H** and comparing the results with the PIFtide. The results gave the evidence that **4H** requires the PIF pocket of PDK1 as the target site.¹⁵⁴

In addition to the mutation analysis we utilized Alpha-screen technology to investigate the ability of the compounds to displace the PIFtide binding. In this way we could corroborate that the effects were mediated by binding of the compounds to the PIF-binding pocket. In fact, Laura Lopez Garcia was able to show that compound **4A** and **4H** displaced the binding of the PIFtide with comparable potency indicating that both compounds display the same affinity to the PIF pocket despite differences in their activation potency toward PDK1.¹⁵⁴

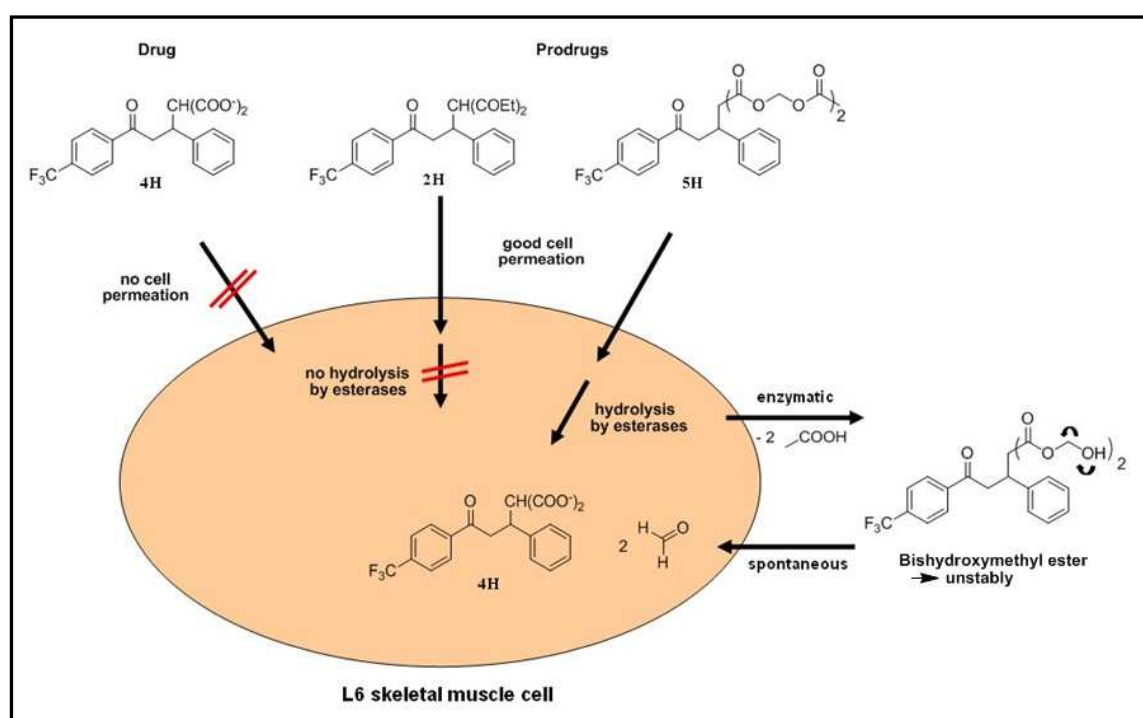
In summary, the *in vitro* data presented in 3.2.3.1, the biochemical studies performed with PIF pocket binding mutants and the Alpha-screen displacement study confirmed that the PIF-binding pocket serves as the binding site for compound class **IV**. Moreover, the results indicated once again the importance of the carboxyl moiety which is essential to prompt the activation of PDK1 targeting the phosphate binding site residues. And finally, two carboxylate groups enhanced the affinity to the PIF pocket.

3.2.3.3. Cell permeation studies using a prodrug strategy

All dicarboxylic acid compounds were inactive in cellular assays. Due to the high polarity of the carboxylate groups the free acid containing compounds did not penetrate the cell membrane. In an effort to improve the bioavailability a prodrug strategy was developed and investigated. In the past years the prodrug approach has been increasingly used when drugs have unattractive physicochemical properties such as poor aqueous solubility, low lipophilicity and chemical instability. Prodrugs as inactive derivatives will be converted into the pharmacologically active drug within the cells by chemical or enzymatic transformations.¹⁵⁵ Due to the fact that in most animal and human tissues esterase activity can

be found the esterification of the available carboxylate groups constituted an obvious and proven prodrug strategy. Since we wanted to explore the suitability of our compounds as potential enhancers of insulin signaling and glucose uptake in particular, the L6 skeletal muscle cell line was chosen as a model cell line.¹⁵⁶ Thus, we used the corresponding methyl and ethyl malonate derivatives of the diacids as prodrugs (Scheme 12), particularly because these kind of esters were available as the precursor of the 2-(3-oxo-1,3-diphenylpropyl)malonic acids. Nevertheless, this attempt failed due to the resistance to cleavage by esterase enzymes in the rat L6 skeletal muscle cell line. Indeed, the best known prodrugs are alkylesters,¹⁵³ however, many of them are not labile enough *in vivo* to ensure a sufficiently high rate and extent of prodrug conversion. For example, simple alkyl ester of penicillins have no therapeutic potential.^{153, 157} Another probable reason can be attributed to the steric crowding.

Scheme 12: Performed prodrug strategies and the hydrolysis of the bisacetoxymethyl ester analogue **6H**



Since there was no cell permeation of the malonic acid **4H** we tested the permeability of the corresponding prodrugs **2H** and **5H**. Prodrug **5H** was found to be metabolic labile and its enzymatic hydrolysis resulted in the free malonic analogue **4H**.

In case of this drug class these problems were overcome by preparing an acyloxyalkyl ester, which in general shows a higher enzymatic lability in cells than simple alkyl esters. Thereby the acyloxyalkyl ester undergo initial enzymatic cleavage of the terminal ester to

generate an unstable intermediate, the hydroxymethyl ester, which rapidly dissociates to the free acid analogue and formaldehyde.^{153, 157, 158}

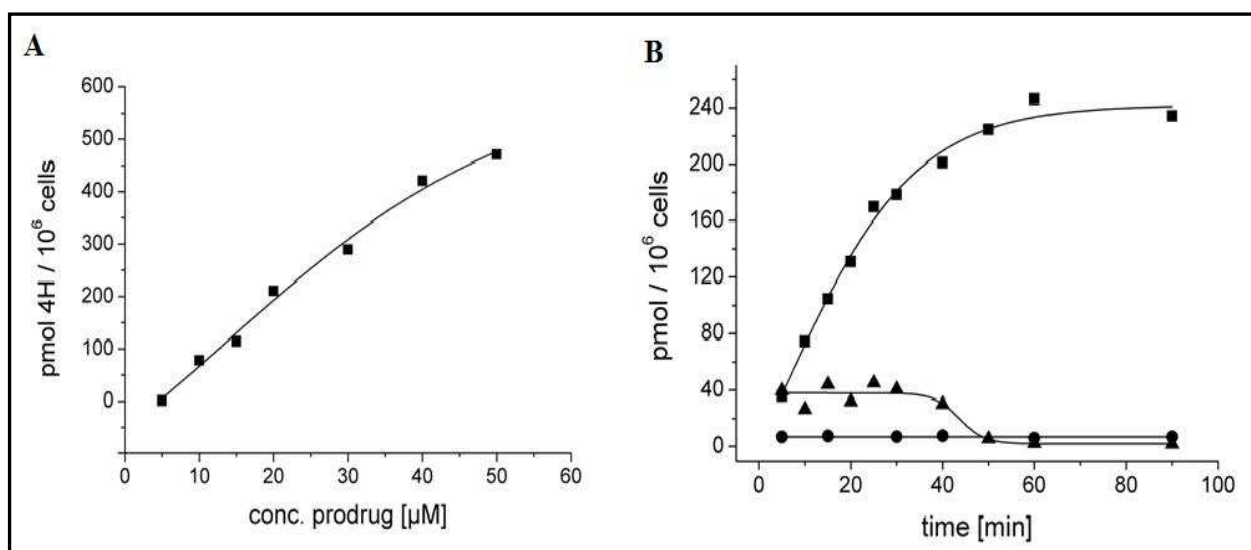
We synthesized the bisacetoxymethyl esters **5A,H** and **5Q** starting from selected malonic acid derivatives. As expected these ester derivatives were inactive in cell-free assays. The *para*-trifluoromethyl malonic acid analogue **4H** turned out to be the most potent PDK1 activator. Thus we selected its prodrug **5H** for the evaluation of its ability to cell permeation and hydrolysis to the potent analogue **4H** within the cells.

The cellular conversion of bis(acetoxymethyl) 2-(3-oxo-1-phenyl-3-(4 (trifluoromethyl)-phenyl)propyl) malonate was evaluated using the rat L6 skeletal muscle cell line which displays esterase activity in the differentiated form.³¹ Prior to each experiment, before treatment with compound **5H**, L6 cells were serum-starved (2 % FBS containing medium) for 4 days to transform them into myogen differentiated cells. The accumulation of the prodrug (**5H**) and the corresponding 2-(3-oxo-1-phenyl-3-(4-(trifluoromethyl)phenyl)propyl-)malonic acid (**4H**) in cells was monitored by mass spectrometry. The samples were subjected to the HPLC analysis after purification by extraction with ethyl acetate under acidic conditions, followed by subsequent separation of the supernatant, evaporation to dryness and resuspension in methanol. The bisacetoxymethyl ester displayed good membrane permeability and released to the free dicarboxylic acid form inside the cells upon enzymatic hydrolysis which occurred most likely in two steps, as already established for the acyloxyalkyl ester of penicillin. Firstly, enzymatic cleavage of the terminal ester formed the highly unstably bis(hydroxymethyl) 2-(3-(4-chlorophenyl)-3-oxo-1-phenylpropyl)malonate and secondly, the dissociation to **4H** and formaldehyde. The formation of the corresponding malonic acid **4H** occurred in a linear concentration-dependent increase after 3 hours (Figure 31A).

For the subsequent analysis of prodrug degradation and the release of the compound **4H** we chose a concentration of 20 μ M of the used prodrug. The prodrug degradation of **5H** appeared only in moderate concentrations in the cells and declined steadily, thereafter, most likely because of the rapid conversion of **5H** in the cytoplasm. In contrast, the accumulation of the malonic acid **4H** derivative increased and was maximal after approximately 60 min of incubation (Figure 31B). A disappearance of the corresponding prodrug, shown in the same figure, was noted. In a further experiment we measured the stability of the prodrug in tissue culture medium (DMEM). We observed that after one hour, the prodrug form was also degraded to more than 90 % in the cell medium, probably because of esterases leaking from the cells. However, the results of the hydrolysis of the prodrug to the free dicarboxylic acid with different concentrations and the enhanced formation of the corresponding malonic acid

despite the degradation of the prodrug suggest that the process of the intracellular release of the prodrug is not the limiting step. The above mentioned decay of the prodrug seems to be caused using the medium. Otherwise, an additional influence of the cell esterases would likely lead to an absence of the prodrug and drug in the cells leaving the disintegrated and high polar target compound in the medium.

Figure 31: **A:** Dependency of intracellular formation of **4H** on the prodrug concentration. **B:** Time course of the intracellular accumulation of **4H** and concomitant disappearance of the prodrug **5H**.



The prodrug **5H** is efficiently taken up by rat L6 cells and converted into the active compound **4H**. **A:** L6 cells were incubated for 2 h with the indicated concentrations of prodrug **5H**, then extracted with ethylacetate and the content of **4H** quantified using HPLC-MS/MS. **B:** L6 cells were incubated with 20 μM of the prodrug **5H** or with **4H** for the indicated times, the cells extracted and the compounds quantified. Analysis revealed that **4H** (▲) is released from **5H** (◆) in a time-dependent manner, whereas **4H** itself is not cell-permeable (●).

In parallel we analyzed whether the free malonic acid can accumulate in the cells using the same experiment conditions like for **5H**. This compound could not be detected neither in the soluble nor in the insoluble cell fractions indicating that it does not enter any cell compartment (data not shown).

Having established that **5H** accumulated in L6 cells and released large amounts of **4H**, we further characterized via cell fractionation the distribution of the prodrug **5H** and of the produced target molecule **4H**. For this purpose, the cells were incubated with **4H** and **5H**, then disrupted mechanically by an ultrasound sonotrode and the cell debris was separated by centrifugation. After the addition of HCl and the extraction with ethyl acetate the samples were quantified by LC-MS. As expected in case of incubation with **4H** there was no

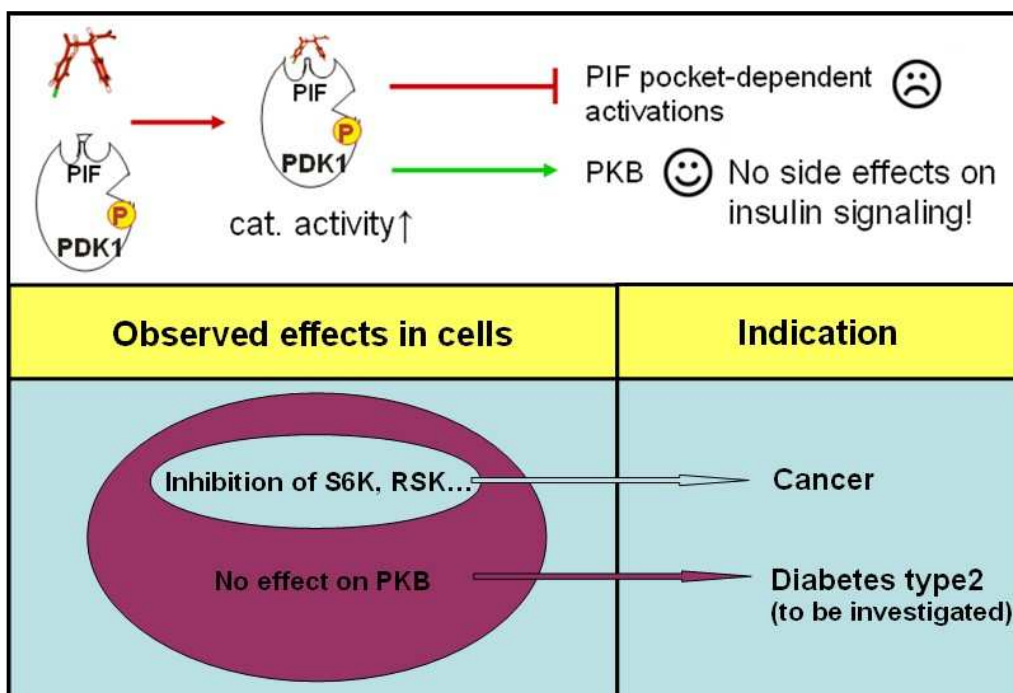
compound detectable both in the cell pellet and in the supernatant. In case of **5H** the converted malonic acid derivative was only detectable in the supernatant, thus ruling out enrichment in the cell membrane fraction.

Taken together, the bisacetoxymethyl ester analogues of **IV** has been shown to function as prodrug that is capable of increasing cell permeability as evaluated in rat L6 skeletal muscle cells and opened the way for evaluation of the activity of this kind of compounds in cells.

3.2.3.4. Proof of mechanism in cells: allosteric activators of PDK1 inhibit PIF pocket dependent pathway but not PKB pathway

The results from the prodrug approach showed that it is possible to improve significantly the cell permeability of 2-(3-oxo-1,3-diphenylpropyl)malonic acids. The bisacetoxymethyl ester prodrug (**5H**) exhibited good cell permeation and enzymatic hydrolysis to the free malonic acid analogue (**4H**). Having shown that **4H** is a very potent PDK1 activator in cell free assays, we focused to the next goal: the proof of mechanism in cells. It was essential to investigate if the compound that is directed to the PIF pocket in PDK1 would inhibit the phosphorylation of kinases whose require the docking of their P-HM to the PIF pocket of PDK1 (Figure 32, top panel). As described in more details in chapter 1.5 PDK1's PIF pocket is necessary for the docking with substrates such as S6K, SGK and RSK and results in full activation of these kinases. The only exception is PKB whose phosphorylation does not depend on docking interactions with the PIF pocket.

For this purpose, HEK293 cells were treated with the prodrug **5H** and the effects of the compounds analyzed by immunoblotting using fluorescence-labeled secondary antibodies.¹⁵⁴ Results showed an inhibition of S6K activation without affecting PKB (data not shown). The dicarboxylic compound **4H** that was measured in parallel did not show any effect in HEK293 cells, according to its high polarity and lack of ability to permeate cell membranes. These data supported that compound **5H** was cell permeable and that its active metabolite **4H** blocked the PIF pocket for interaction with S6K.

Figure 32: Proof of mechanism scheme.

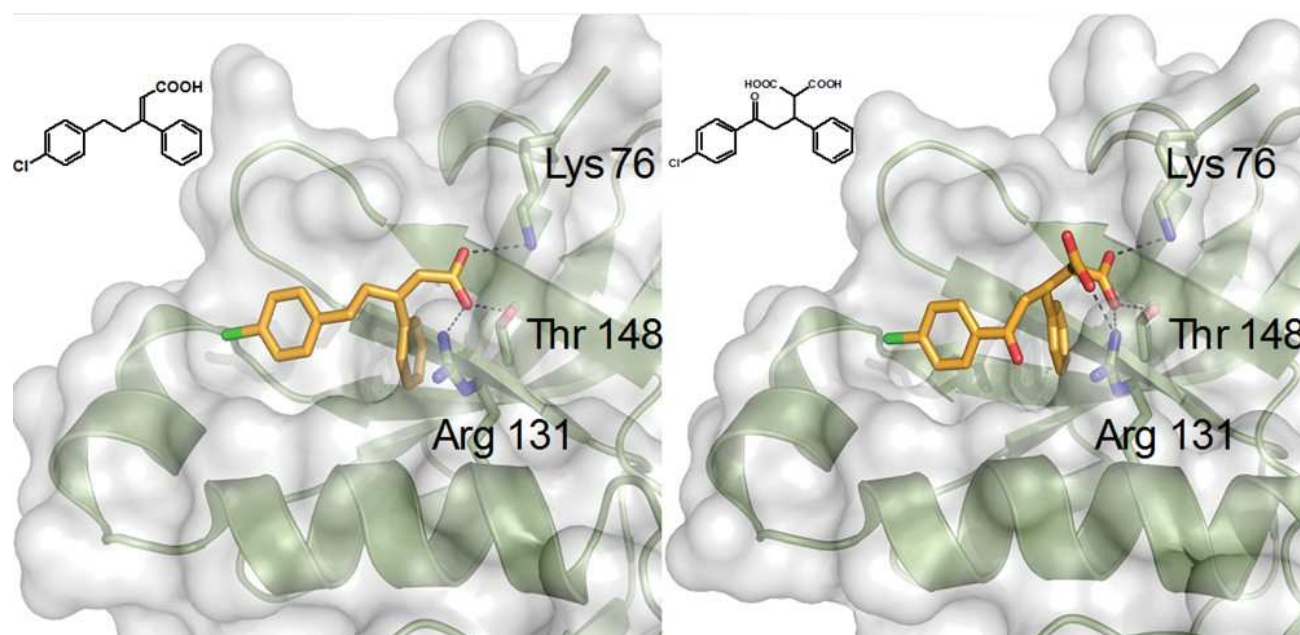
Thus we were able to proof for the first time the novel mechanism of action of a small molecule targeting the PIF pocket of PDK1. Furthermore, these experiments had confirmed **5H** as an invaluable tool to further analyze the effects of PIF pocket inhibition in a range of diseases in which PDK1 was involved. In this regard, we observed an inhibition of PDK1's substrate S6K (Figure 32, lower panel) that is involved in cell growth and survival processes playing an essential role in tumor cells.^{18, 19} Due to the lack of inhibition of PKB affecting the PDK1 PIF pocket and due to S6K's influence of the insulin receptor substrate-1 (IRS) **5H** has also become interesting for treatment of diabetes type-2. As already described in more details in chapter 1.3, S6K regulates the insulin action via a negative feedback mechanism and increased activity of S6K was observed in obesity and diabetes type-2. Nevertheless, for this purpose, more experiments are necessary and have to be performed.

3.2.4. Crystal structure of PDK1 in complex with 2-(3-(4-chlorophenyl)-3-oxo-1-phenylpropyl)malonic acid (4A)

To gain insight into the mode of binding of the dicarboxylic compounds with the protein cocrystallization of **4A** by soaking the compound with the His-PDK1 50-556 form was carried out by our collaborator Jörg Schulze from Biondi's group. The cocrystal structure

shows the location and interactions of the two carboxylates (Figure 33). **4A** contains the same two ring systems as **2Z**, previously published.²⁰ One carboxylate group occupies a position similar to **2Z**, interacting with Lys76, Thr148 and Arg131. The second carboxylate group forms an additional salt-bridge interaction with Arg131, which plays an important role in the allosteric activation mechanism. The structure highlights the importance of Arg131 in the mode of action of the allosteric activators of PDK1. The description of the allosteric changes and overall influence on the PDK1 conformation is beyond the scope of this work.

Figure 33: Crystal structures of PDK1 in complex with **2Z** and **4A**



3.2.5. Chromatographic Separation of the Enantiomers of **4H**

The compound class of 2-(3-oxo-1,3-diphenyl-propyl)malonic acids (**IV**) (Scheme 9) was obtained by an addition of malonic ester to the corresponding chalcone (chapter 3.2.2) resulting in a racemic mixture. All the synthesized compounds possess a chiral center which is expected to confer to the enantiomer distinct activities toward the kinase PDK1. To analyze whether the biological activity was more or less restricted to one of the distinct stereoisomers, we attempted to separate the enantiomers via chiral HPLC. For this experiment, we chose compound **4H** since it was the most potent analogue toward PDK1 and since it was selected for the prodrug evaluation. Within a student's project in the field of specialization in

medicinal chemistry Michael Zender had the challenge to separate different racemic mixtures in cooperation with Kazmaier's group. Besides other compounds, he was able to obtain the individual enantiomers of the compound **4H** using a chiral HPLC method (Figure 34 and Figure 35). Unfortunately, there was no time to assign the absolute stereochemistry of the stereoisomers. But, testing of the enantiomerically pure forms separated by chromatography *in vitro* toward PDK1 (Table 13) we proved that Enantiomer 2 was significantly more potent. Having additionally the cocrystal structure of the active compound **4H** with the PDK1 we can suggest that Enantiomer 2 is the (*S*)-2-(1-phenyl-3-(4-(trifluoromethyl)phenyl)-propyl)-malonic acid since the malonic acid moiety is turned toward the amino acids Arg131, Lys76 and Thr148 (Figure 33). Having found that the *S*-enantiomer is the eutomer, accounting for most of the biological activity of the racemate, future optimization schemes should include the enantioselective synthesis of the *S*-enantiomers.

Table 13: PDK1 activity of the individual enantiomers of **4H**.

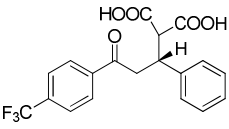
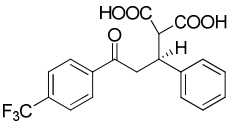
Cpd.	[μ M]	PDK1 (%)
Enantiomer 1 (<i>R</i>)	2	131
	50	268
	200	291
Enantiomer 2 (<i>S</i>)	2	326
	50	562
	200	545

Figure 34: Enantiomer 1

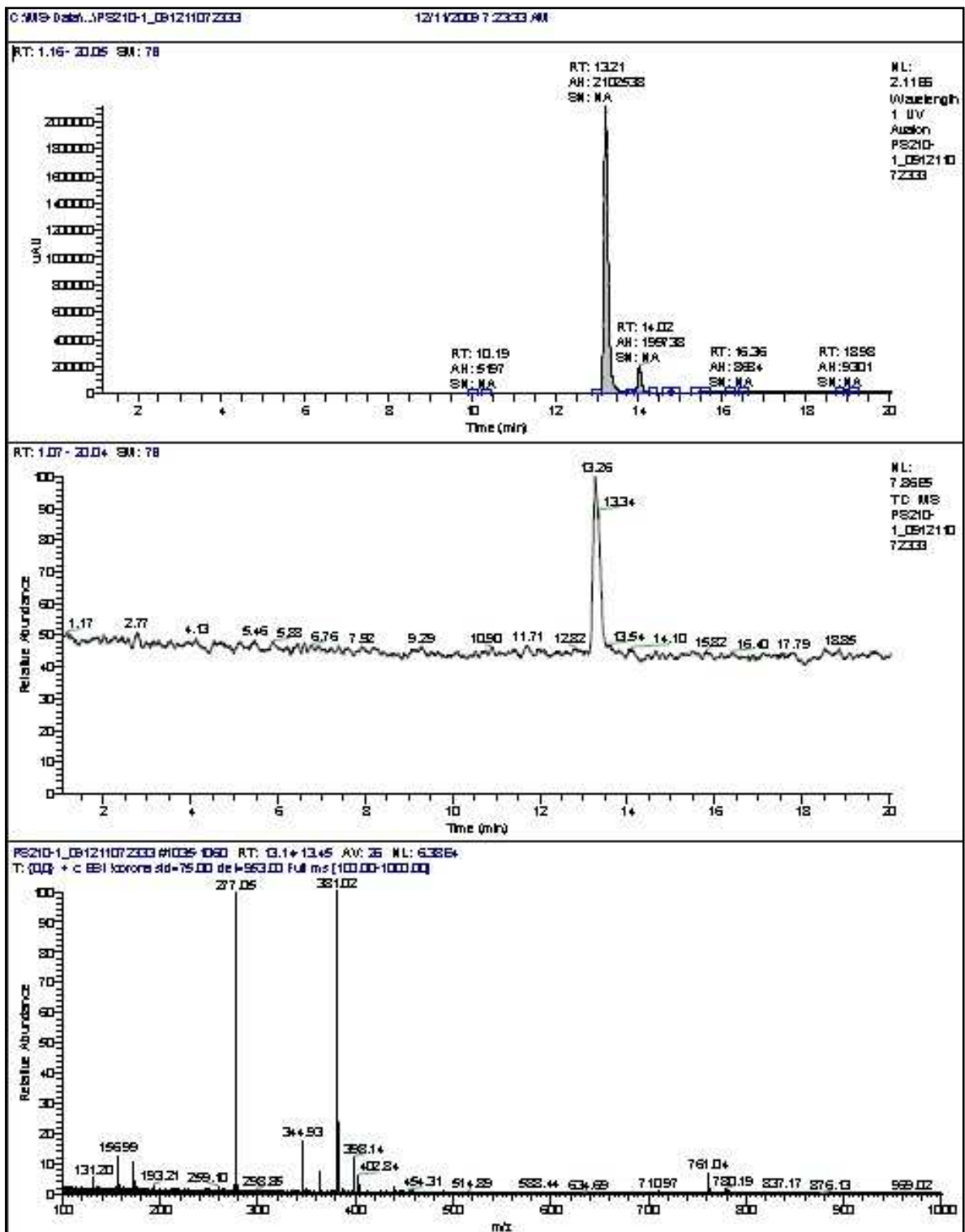
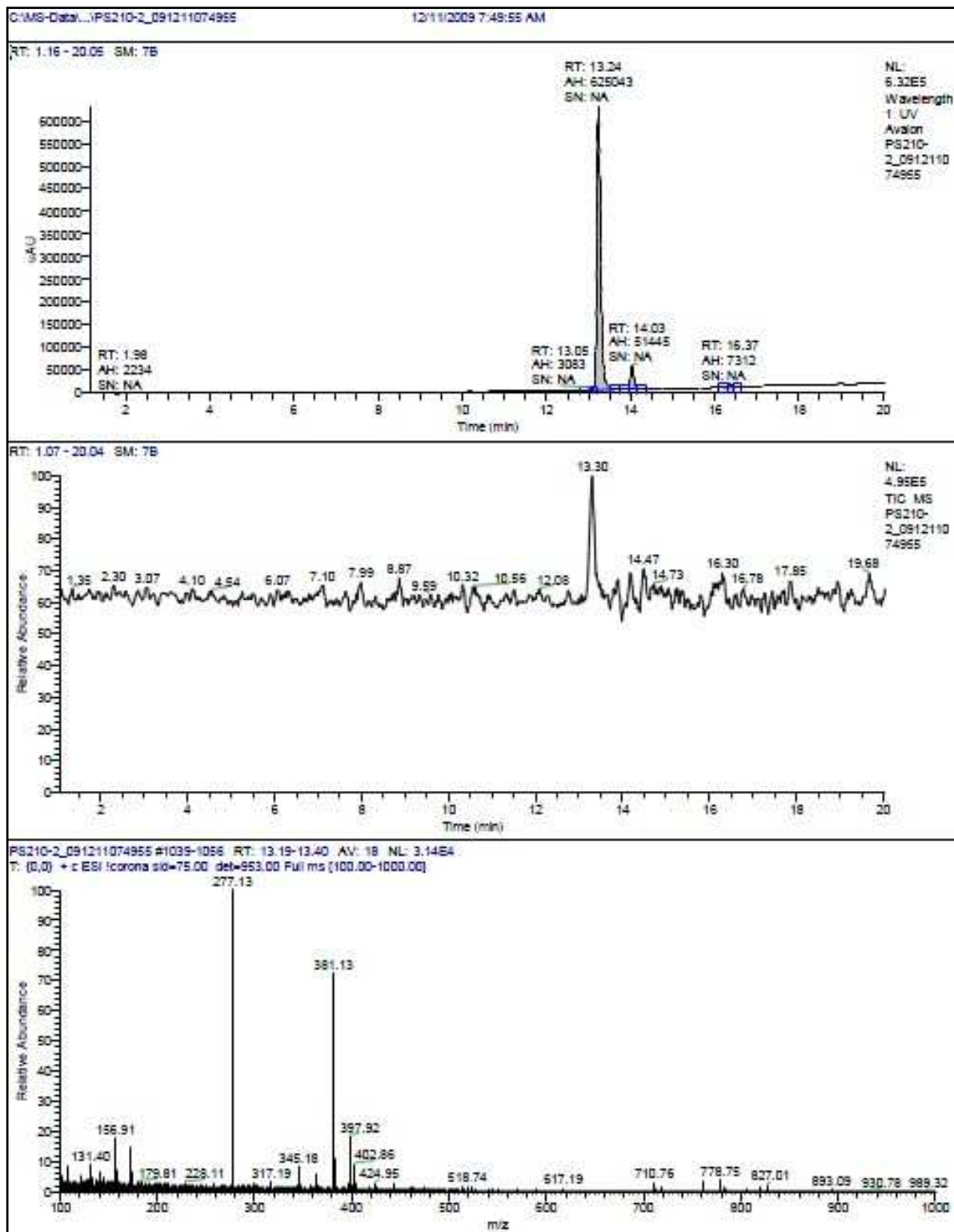


Figure 35: Enantiomer 2



3.2.6. Discussion and Conclusion

With the compound series of 3,5-diphenylpent-2-enoic acids (**III**) we have already provided evidence that compounds blocking the PIF-binding pocket might be able to prevent phosphorylation of PDK1 substrate proteins. An important requirement for potent activators of PDK1 is a carboxyl moiety that can mimic the phosphate group of phosphoserine/-threonine residues from natural ligands, which is expected to bind to the equivalent site. With the aim of further increasing potency, we modified the lead compounds **I** and **III** by introduction of a second carboxyl function. Indeed, compared to the monocarboxylic acids **I** and **III**, the dicarboxyl function generally caused a considerable increase in activatory potency and affinity. This observation might parallel several earlier reports on phosphotyrosine mimetics which also profited from two negative charges, e.g. malonic acid residue or combination of COOH and tetrazole. Cyclohexylmalonic acid as nonpeptidic tyrosine kinase, SykCSH2, inhibitor was identified as a potent phosphotyrosyl mimetic¹⁵⁹ and in the case of the growth factor receptor-bound protein-2 bicarboxyl analogues bind to the SH2 domain 2 with similar strength as the phosphonate-based phosphotyrosyl mimetics do.¹⁶⁰ However, it remains to be seen whether the malonic group of the here presented 2-(3-oxo-1,3-diphenylpropyl)malonic acids **4A-V** occupies the same space as the phosphate moiety of the natural peptide ligands of PDK1. A complex between PDK1 and a corresponding phosphopeptide has not been published so far.

Different 2-(3-oxo-1,3-diphenylpropyl)malonic acids were synthesized and tested for their potency toward PDK1 and other AGC kinases (Table 11 & Table 12). The most potent activators were **4F,O,U** and **4V** two of which contained a *p*-iodophenyl moiety. Halogen bonding has been demonstrated to increase the binding affinity. It is presumable that iodine mainly interacts with hydrophobic pocket space via Van der Waals attraction, however the data suggest that halogen bonding to carbonyl of Lys 115 might also contribute to the binding affinity. The increase in affinity as assumed based on the AC₅₀ values was only 1.8-fold from **4A** (4-Cl) to **4D** (4-Br), but 3.5-fold from **4D** to **4F** (4-I). This jump from 4-Br to 4-I is in accordance with the highest halogen binding potential of iodine but may also be a consequence of the shorter distance to the Lys115 carbonyl. Even though the cocrystal structure of **4F** with PDK1 showed the distance between *p*-iodine and the Lys-backbone carbonyl exceeds 4 Å, thus being too large for significant interaction according to the literature value 3.50 Å.¹⁶¹ This cannot rule out the possibility of halogen bonding in solution, which might just be impaired by the rigidity of the crystallized protein. At least, the cocrystal discloses a clear orientation of the iodine toward the carbonyl oxygen. Our experimental data

also argue for an iodine contribution to binding that exceeds the Van der Waals interactions seen in the cocrystal.

It can well be assumed that the conformation displayed in the cocrystal does not reflect the fully active conformation of PDK1 as induced by compound binding in solution. In this respect further experimental verification of the potential halogen bonding is required, e.g. by NMR techniques. An alternative explanation independent on halogen bonding might be that the size of the halogen determines the positioning of the compound which influences the interaction of the COOH groups and/or the carbonyl group with the protein.¹⁶² The activatory potency of **4O**, **4U** and **4V** was comparable to that of the 3 kDa peptide PIFtide, and the activation efficacy of the small compounds was also within the same range. Therefore, the degree of potency is now sufficient to perform studies in a cellular setting since PIFtide itself has been used for the same purpose previously.¹ Our small molecule compounds contain extended π -system which are participating in extended hydrophobic and Van der Waals interactions and may additionally contribute to a potential cation- π interaction with Lys115 (docking not shown).

A successful application of a prodrug approach was demonstrated by introducing an acetoxymethyl ester function to the corresponding malonic acid analogues. This was used to overcome various undesirable chemical properties of acidic compounds and to enhance their bioavailability. Increase in the lipophilicity of the parent hydrophilic compounds resulted in good membrane permeability and intracellular accumulation after esterase-catalyzed cleavage. In agreement, we observed that the prodrug disappeared concomitantly with increasing amount of the malonic acid analogue. In spite of the serum instability of **5H** a promising strategy for an efficient drug delivery and a promising starting point for the generation of cellular efficacy could be achieved. As demonstrated in previous reports, the stability of the prodrug toward serum esterases such as acetylcholin esterase can be fine tuned by variation of the acyl group; for instance, exchange to a pivaloyl function might increase serum stability while still permitting intracellular cleavage.¹⁶³⁻¹⁶⁵

Further experiments aiming to analyze the compounds' effect on the intracellular PDK1-dependent signaling pathways were additionally possible using the prodrug form. Especially, we were able to demonstrate the proof of mechanism applying the prodrug **5H** in HEK293 cells followed by western blot analysis. As expected, the intracellularly released compound **4H** blocked the PIF pocket of PDK1 for interaction with the substrate S6K without affecting the substrate PKB. This approach enabled with additional experiments to suggest these compound series (**IV**) for treatment of cancer and diabetes type-2.

The binding mode was elucidated by cocrystallization and X-ray analysis. Indeed it was very similar to **III** (Figure 33) binding mode with one of the carboxyl group (being located in the same pocket space) overlapping with the carboxyl group in **III**. The additional carboxyl function exclusively formed a salt bridge with Arg131 suggesting that this electrostatic interaction was mainly responsible for the observed increase in affinity. Maximum activation was higher on average than observed with the 3,5-diphenylpent-2-enoic acids, indicating that stronger allosteric changes must occur which can now be analyzed by comparing with cocrystals formed with weaker activators (not within the scope of this work). Thus, our compounds allow for the first time to investigate the conformational changes underlying the allosteric activation mechanism. Fixation of Arg 131 by strong electrostatic interactions is crucial for the activation mechanism not only for binding affinity. This is also corroborated by the mono carboxyl analogues of selected malonic acid derivatives, which display both weaker binding and lower activation efficacy (**4H** compared to **6H** in Table 11). Moreover, via chiral HPLC we were able to obtain specific chiral forms of the compound **4H**. Retesting for their effect on PDK1 and with the help of the cocrystal structure we suggested the *S*-Enantiomer as the bioactive chiral form.

In conclusion, we have shown that modifying the lead compounds **I** and **III** by introduction of an additional carboxyl group has clearly improved the activity and selectivity profile of the PDK1 activators. Finally the cocrystal structure has proven the importance and the influence of the second carboxyl group. Furthermore, we have provided an efficient prodrug strategy to deliver the highly polar compounds to the cellular cytoplasm, thus rendering them applicable to cellular studies. Thus, we were able to provide the proof of mechanism.

3.3. Evaluation of 3,5-diphenylpent-2-enoic acids' inhibitory effect toward PKC ζ : allosteric kinase inhibition targeting the PIF-binding pocket

3.3.1. Introduction

Regarding the specificity of the 3,5-diphenylpent-2-enoic acid class, **III** (presented in 3.1) against a panel of AGC kinases, we found out a tendency to affect the activity of the zeta isoform of the PKC family (PKC ζ). Thereby, compounds with the substitution pattern of the phenyl moiety **A** with expanded aromatic systems (Table 5, chapter 3.1.3.1) stood out. Interestingly, we have noticed that the PIF pocket-directed compounds are able not only to stabilize an active conformation of individual kinases, e.g. PDK1, but they are also able to inhibit kinase activity. These results induced us to invest more effort in this project in order to obtain further insight into the impact of explored aromatic systems on the inhibition of PKC ζ . Especially since PKC ζ constitutes an interesting target containing the unique feature to activate the eukaryotic transcription factor NF- κ B which is involved in the transcriptional activation of proinflammatory and anti-apoptotic genes.^{87, 95} The direct inhibition of NF- κ B would trigger toxic effects because of its numerous functionalities to the conservation of cell integrity in all tissues (chapter 1.11).^{104, 105} In contrast, PKC ζ performs the activating interaction only in selected cells and tissues (e.g. lung tissue). Hence, the inhibition of PKC ζ provides a promising strategy to treat chronic inflammatory diseases as well as different types of cancer without influencing a ubiquitous inhibition of NF- κ B. Also the PKC ζ knockout studies (chapter 1.11) have been suggested PKC ζ as a qualified target revealing viable mice with nearly normal developed organs only with the exception of a deficiency for the activation of NF- κ B that was observed e.g. in lymph cells and in lung.^{84, 90, 91}

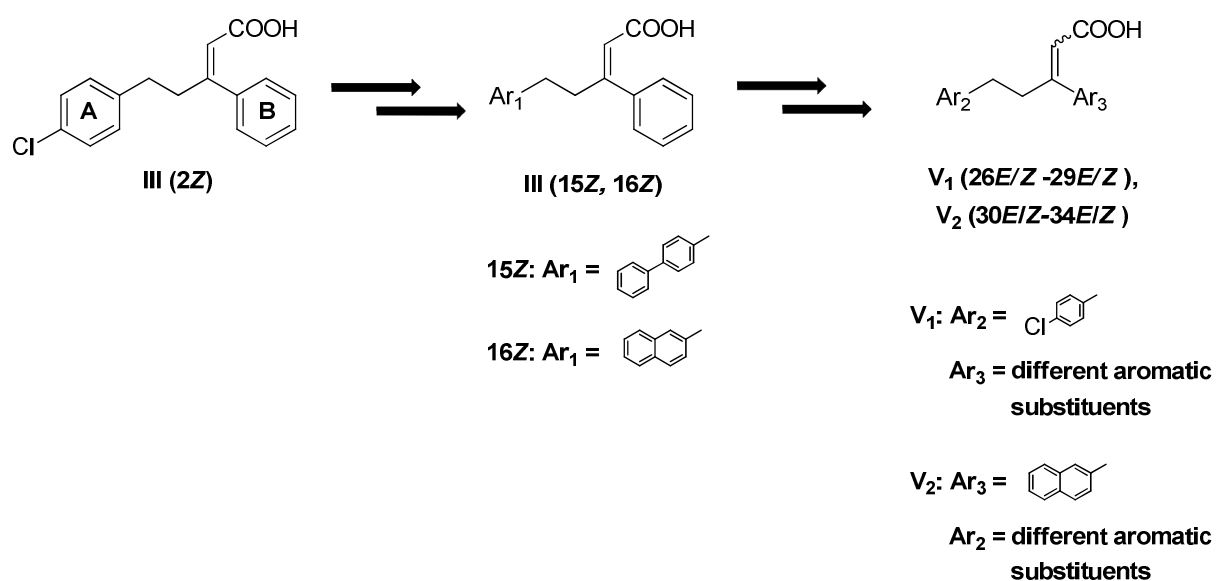
Usually, the drug design of protein kinase inhibitors is focused on the ATP-binding domain. But due to the existence of 11 isoenzymes of the PKC family the search for selective PKC ζ 's ATP-directed compounds has been proved to be more challenging. Moreover, the binding affinity for PKC ζ 's substrate, ATP, is measured as $K_M = 3.3 \mu\text{M}$. This value is relatively low and thus implies that the ATP-competitive inhibitors should have a K_i - value in a subnanomolar range to reach a significant inhibition *in vivo*. Consequently, there are no ATP-competitive inhibitors described so far.

Here we will present the structure optimization of 3,5-diphenylpent-2-enoic acids expanding the aromatic systems using the PIF pocket strategy as already presented for PDK1 in the previous chapters 3.1 and 3.2. First, the space availability in PKC ζ 's PIF pocket will be investigated varying the aromatic moieties in order to increase the inhibition effect and selectivity. Although the PIF pocket of PDK1 was relatively well filled by **2Z** as presented in the cocrystal structure in Figure 24, we suppose that the flexibility and ability to undergo an induced fit might differ between the two PIF pockets (PDK1 vs PKC ζ). Secondly, we will establish an adequate high-throughput screening assay which allows determination of the inhibitory activity toward PKC ζ in cells.

3.3.2. Synthesis

To develop small molecule inhibitors with enhanced activity toward PKC ζ compounds **15Z** and **16Z** (Figure 36) were chosen as leads for the design and synthesis. Thus, the preparation of the new structures was performed according to our previous procedure as presented in the optimization study of the class of 3,5-diphenylpent-2-enoic acids as activators of PDK1 (chapter 3.1.2).^{20, 75}

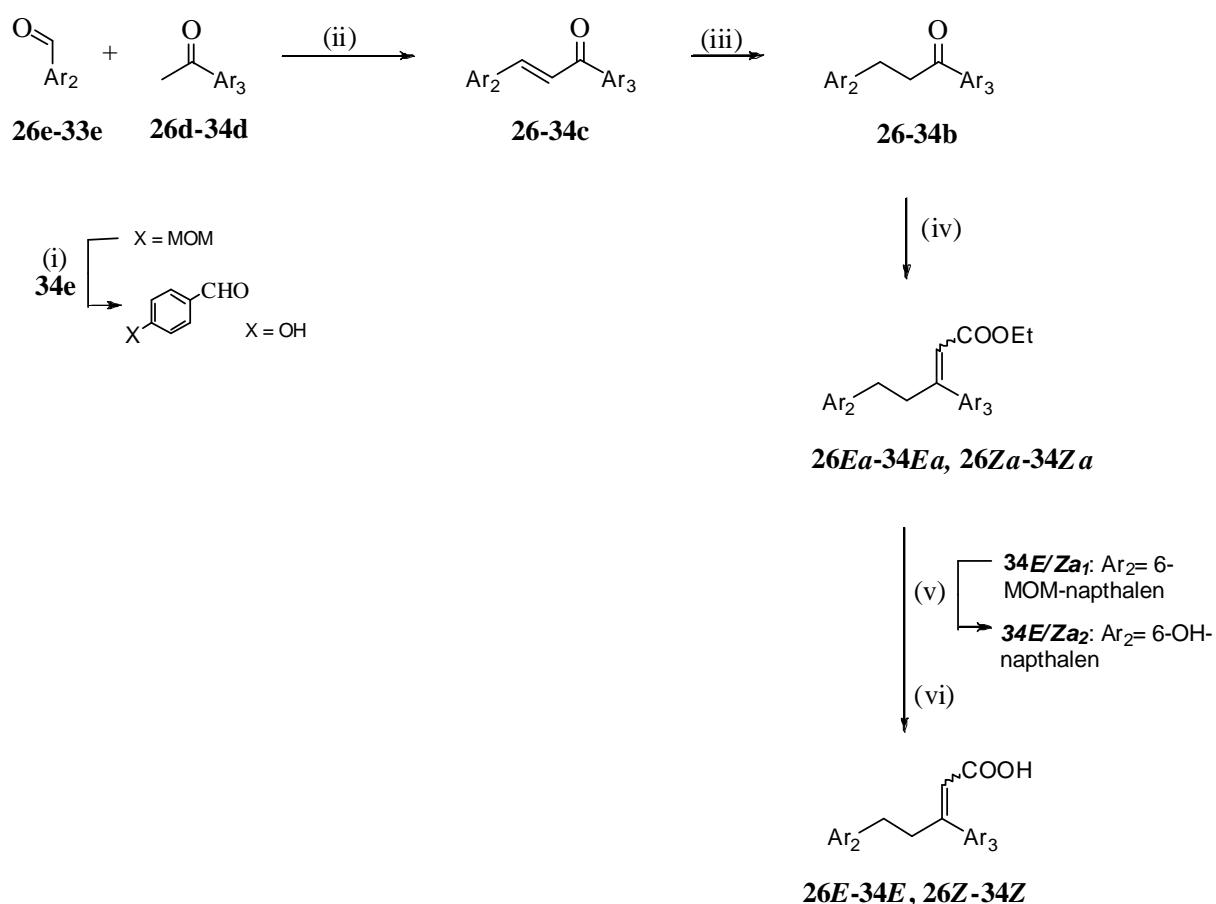
Figure 36: Allosteric inhibitors design concept



For substituents Ar₂ and Ar₃ see Table 14 and Table 15.

The synthetic pathway affording the final compounds **26E-33E** and **26Z-33Z** is depicted in Scheme 13. In pursuing our aim to further explore the aromatic systems we could retain the synthetic steps as already done in Scheme 5 expanding only the phenyl moieties. Thus, in the first step of the synthesis the corresponding, commercially available, benzaldehydes and acetophenones derivatives reacted together in a classical aldol condensation. This step was followed by a chemoselective reduction of the double bond of the individual chalcones. Via Horner-Wittig reaction using phosphonoacetate we introduced the acrylic acid side chain. This reaction led to *E/Z* mixtures which we were able to separate by flash chromatography. In the last step the pure geometric isomers were afforded by hydrolysis. More details of the synthetic route are described in chapter 3.1.2.

Scheme 13^a: Synthesis of compounds **26E-34E** and **26Z-34Z**



^a: Ar = aryl, heteroaryl; (i) bromomethyl-methylether, NaH, DME, 0 °C, 1 h; (ii) Method A: NaOH, EtOH, 1 h, rt; (iii) Method B: 3,5-bis(ethoxycarbonyl)-1,4-dihydro-2,6-dimethylpyridine, toluene, silica gel, 70 °C, 16 h; (iv) Method C: triethyl phosphonoacetate, NaH, DME, 80 °C, 4 h; (v) 10 % HCl, methanol, reflux, 2 h; (vi) Method D: NaOH, EtOH, rt, 3 h. For substituents Ar₂ and Ar₃ see Table 14 and Table 15.

The only one exception constituted the substances **34** (Scheme 13). The nucleophilic alcohol function of the aldehyde had to be protected for the synthetic pathway. For this purpose, we chose the methoxymethyl (MOM) group accordingly to the method already described for 2-(3-oxo-1,3-diphenylpropyl)malonic acid (**4M**) in 3.2.2.¹⁵² With the obtained 6-(methoxymethoxy)-2-naphthaldehyde (**34e**) and the 1-(naphthalen-2-yl)ethanone we were able to synthesize the corresponding chalcone **34c** which was converted to the desired *E* and *Z* ethyl 5-(6-hydroxynaphthalen-2-yl)-3-(naphthalen-2-yl)pent-2-enoates (**34Ea₁** and **34Za₁**) in two steps. Afterwards the cleavage of the protecting group was performed under acidic conditions furnishing **34Ea₂** and **34Za₂** which were in turn hydrolysed into the target molecules **34E** and **34Z**.¹⁵²

3.3.3. Biological results and Discussion

3.3.3.1. Biological characterization *in vitro* of the synthesized PKC ζ inhibitors

The activity of the compounds toward PKC ζ was determined by performing our previously described radioactivity kinase assay.⁷⁴ The radioactivity incorporation of ³²P phosphate from [γ -³²P]ATP into PKC ζ 's substrate myelin basic protein (MBP) was here measured (in duplicates) and was done by our collaborator group under the supervision of Dr. Ricardo M. Biondi. The biological results for the new compounds are shown in Table 14 and Table 15 (cell free), whereas the percent inhibition values were determined at concentrations 50 and 200 μ M and were compared to the control values with DMSO. To enable a better comparison of the structure-activity relationships we added also the SARs of the starting compounds **15** and **16** into the same table.

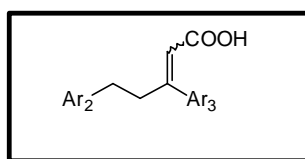
In our aim to investigate the spatial limitations of PKC ζ 's PIF pocket we extended our library with several compounds. These can be divided into two groups according to the Ar residues (Ar₂ and Ar₃). On the one hand; in the first group (I) we chose *para*-chlorophenyl as Ar₂ introducing different aromatic substituents on the Ar₃ moiety as presented in Table 14. This strategy arises from our previous results with the PIF-binding pocket of PDK1 which revealed that ring substitutions with halogens improved the enzyme activity within this series (Table 3). Consequently, we decided to investigate the impact of the nature of the *p*-chlorophenyl moiety on the potency and selectivity toward PKC ζ . On the other hand; our ITC study with the 3,5-diphenylpent-2-enoic acids disclosed compound **16Z** as enthalpically

favourable what can be attributed to the CH- π interactions most likely due to the high π -electron density of the unsubstituted fused rings combined with the large surface. Thus, in the second group (II) we varied the Ar₂ moiety focussing Ar₃ by naphthyl group (Table 15).

In contrast to the results obtained with the first 3,5-diphenylpent-2-enoic acid series when tested toward PDK1 (chapter 3.1.3.1) and despite the restricted bond rotation by the double bond, the new geometric isomers (**26-34Z** & **26-34E**) did not display a discernible trend to the difference in intrinsic potency toward PKC ζ . Already the parental compound **16** showed this characteristic. The isomer carrying the carboxyl group *cis* relatively to the Ar₃ moiety as well as the isomer with the opposite conformation disclosed a relatively similar inhibition efficacy toward PKC ζ . Nevertheless, the *E*- and *Z*-isomers of compounds **29-32** still differed in their PKC ζ 's activity. The *cis* isomers (**29-31Z**) displayed high inhibition potency. The corresponding *trans* isomers (**29-31E**) exhibited even an increase of activation potency of PKC ζ . The only exceptions represented the quinoline derivatives (**32Z** and **32E**) influencing PKC ζ with an opposite effect. **32Z** prompted an activation effect on PKC ζ and **32E** triggered an inhibition.

Among the group I, compounds bearing a naphthyl moiety (**26** and **27**) showed a similar inhibitory activity as the parental compound **16**. The inhibition was in the range of 90 % when tested at 200 μ M as well as at 50 μ M. The maximum inhibitory effect reached by the *para*-methoxy derivatives (**28Z** and **28E**) did not exceed 76 % at 200 μ M and decreased completely already at 50 μ M (**28Z**). The introduction of a biphenyl group on Ar₃ led in case of the *E* isomer to the absence of inhibitory effect turning out to be a weak PKC ζ activator.

These results suggest that an aromatic residue with fused rings as Ar₃ is favored for the inhibitory effect whereas the *para* substitution patterns led to an abolishment of the inhibition up to activation of the enzyme. Moreover, the contribution to the biological activity of both isomers (*cis* and *trans* of **26** and **27**) may be a result of additional space surrounding the hydrophobic PIF pocket which allowed greater flexibility of positioning of the naphthyl group. We can suppose that both arrangements of the naphthyl group in the PIF pocket enabled good electrostatic interactions of the carboxylic side chain with the corresponding amino acid (Lys301 that is equivalent to Arg131 in PDK1) what has to be investigated by co-crystallization experiments.

Table 14: Group I: Inhibition of recombinant PKC ζ and of the NF- κ B pathway in U937 cells

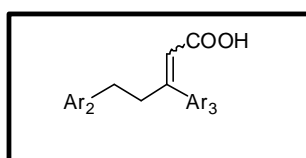
Cpd	Ar ₂	Ar ₃	PKC ζ		NF- κ B	
			cell free		reporter gene assay (U937 cells)	
			% inhibition		% inhibition	
			200 μ M	50 μ M	40 μ M	10-1 μ M
15Z			100	90	59	nd
15E			60	ne	87	nd
16Z			100	85	nd	nd
16E			100	70	84	nd
26Z			99	93	100	nd
26E			86	82	100	82 @ 5 μ M
27Z			95	89	100	nd
27E			99	93	100	nd
28Z			76	ne	18	nd
28E			55	10	26	nd
29Z			92	nd	nd	77 @ 5 μ M
29E			act	act	nd	78 @ 5 μ M

nd: not determined; ne: no effect; act: compound showed an activation of the enzyme

Group II includes compounds with extended aromatic residues on both Ar moieties leading to generally lower inhibitory potency than the analogues from group I. The good potency of compounds **26** and **27** prompted us to synthesize analogues with two naphthyl groups to figure out the variability of the PIF pocket shape. Indeed, the twofold naphthyl substitution resulted in good inhibition, but did not exceed the values of the mononaphthyl derivatives **26** and **27**. Moreover, the inhibition of 90 % at 50 μ M was only achieved by the *cis* isomer, the compound with the opposite conformation reached only 25 %. These results seem to demonstrate that enlarging the target compound size only the *cis* conformation might reach the position to interact with the hydrophobic moiety and amino acids relevant for the carboxyl moiety of the binding site. In order to further explore the ligand space and the structural features of the PIF pocket we introduced also a 6-hydroxynaphthalen as Ar₂ (**34**) and we transformed the naphthyl group into a quinoline (**32**). Compound **34** influenced the

PKC ζ activity by a less inhibition in comparison to the twofold naphthyl derivative (**30**) but with this substitution pattern, having a polar group, again both isomers affected the kinase. The *cis* quinoline derivative triggered activation and the *trans* isomer showed a moderate inhibition.

Table 15: Group II: Inhibition of recombinant PKC ζ and of the NF- κ B pathway in U937 cells



Cpd	Ar ₂	Ar ₃	PKC ζ		NF- κ B	
			cell free		reporter gene assay (U937 cells)	
			% inhibition		% inhibition	
			200 μ M	50 μ M	40 μ M	conc
15Z			100	90	59	nd
15E			60	ne	87	nd
16Z			100	85	nd	nd
16E			100	70	84	nd
30Z			nd	89	nd	83 @ 5 μ M
30E			nd	25	nd	98 @ 5 μ M
31Z			81	60	nd	67 @ 10 μ M
31E			8.0	nd	nd	67 @ 10 μ M
32Z			act	nd	nd	13 @ 10 μ M
32E			63	nd	nd	1 @ 10 μ M
33Z			20	nd	nd	9 @ 1 μ M
33E			act	nd	nd	4 @ 1 μ M
34Z			85	nd	nd	nd
34E			82	nd	nd	nd

conc: concentration; nd: not determined; ne: no effect; act: compound showed an activation of the enzyme;

To further investigate larger aromatic systems we synthesized 5-(4-phenoxyphenyl)-3-phenylpent-2-enoic acid isomers (**31Z** and **31E**), whereas **31Z** reached a moderate inhibition and **31E** showed hardly any effect. Moreover, we examine the influence of 5-(biphenyl-4-yl)-3-(naphthalen-2-yl)pent-2-enoic acid on the PKC ζ activity which exhibited only 20 % inhibition as *cis* isomer (**33Z**) and triggered a weak activation as *trans* isomer (**33E**).

However, the inhibitory potency among the compounds bearing extended aromatic functions on both Ar residues dropped in accordance with the *para* substitution of Ar₂. This fact is in contrast to the results of group I which revealed the *p*-chlorophenyl derivatives (**26** and **27**) as the most potent PKC ζ inhibitors *in vitro* in this study. It appears that the inductive effect of the halogen plays an important role in the hydrophobic subregion of the binding pocket. However, compounds **26**, **27** and **30Z** appear to be the best inhibitors in this series proving the fused rings (naphthyl) as a promising feature of the core structure to reach good affinity for the PIF pocket.

In order to examine the selectivity of the new PIF-binding pocket-directed compounds we screened them additionally against a panel of AGC kinases (Group of Ricardo M. Biondi). Since we observed both an inhibitory and an activatory effect toward PKC ζ , it was particularly interesting to know which effect the series would exert by binding to other AGC kinases. As already mentioned, by binding the PIF pocket the target compounds are able to stabilize the active conformation of the respective kinase or even lead to inhibition of the kinase activity. Table 16 shows the specificity of selected 3,5-diphenylpent-2-enoic acids. It should be noted that in contrast to the Table 14 and Table 15 the values are not given in percentage inhibition, but in percentage activation potency whereas the DMSO control were set at 100 % in order to simplify the comparison.

Within the investigated series we focused on analogues with the most impact on PKC ζ activity. It becomes apparent that compounds with the highest inhibitory efficacy toward PKC ζ revealed to be only slight (**26E**, **26Z**, **27E**, **27Z**) PDK1 activators. This fact we had already observed with the parental compounds. But it should be noted that these exhibited an elevated activation and the *E* isomers did not show any activity effect. Introduction of a chlorine atom and changing the position of the naphthyl moiety indicates that this substitution is more tolerated by the hydrophobic PIF pocket subregions of PKC ζ and lead to loss of affinity toward PDK1. Moreover, compounds **26Z** and **27Z** turned out to have not only a good inhibition effect toward PKC ζ but also a relatively good specificity toward its PIF pocket over the PIF pockets of the closely related AGC kinases. Both analogues influenced only slightly PDK1 and MSK, whereby **27Z** affected additionally the AGC kinases S6K1 and SGK. Nevertheless, our strategy seems to be along a right direction, especially since we are looking for allosteric modulators of PIF pocket that is in contrast to the ATP binding site less conserved and stands out through differences in the amino acid sequences among the AGC kinases (Figure 20, chapter 1.13). While the mentioned analogues possess a specific PIF pocket affinity, the *cis* isomer of 3,5-di(naphthalen-2-yl)pent-2-enoic acid displayed an

inhibitory effect toward almost all closely related AGC kinases we tested. The data shown for **31E** and **31Z** has not been yet completely investigated and thus these are not meaningful enough for the specificity.

Interestingly, the compounds affected several of the investigated AGC kinases with a contrary effect at 200 μ M in comparison with the values of 50 μ M concentration. This anomaly can be attributed to ATP-competitive inhibition which might occur at high concentrations of the target molecules. From this perspective further investigations such as mutant studies and cocrystallization are necessary to provide the binding of the compounds in the PIF pocket.

Table 16: *In vitro* specificity of selected analogues against a panel of AGC kinases

Cpd.	[μ M]	PDK1 (%)	S6K1 (%)	PKC ζ (%)	PKC ι (%)	SGK (%)	PKA (%)	PRK2 (%)	RSK (%)	MSK (%)
26Z	50	225	60	7	90	60	72	148	230	30
	200	17	25	1	10	2	10	160	50	10
26E	50	170	70	18	80	80	150	170	160	50
	200	58	100	14	30	40	50	114	60	80
27Z	50	280	37	11	73	40	120	170	130	15
	200	26	30	5	15	2	50	140	10	10
27E	50	220	45	7	62	30	24	160	80	15
	200	7	15	1	7	1	35	190	20	10
30Z	50	70	34	11	48	16	nd	135	42	4
	200	nd	nd	nd	3	nd	nd	nd	nd	nd
31Z	50	nd	nd	40	18	nd	nd	nd	nd	nd
	200	109	12	19	0	52	nd	54	6	nd
34Z	50	150	nd	nd	67	nd	nd	nd	nd	nd
	200	32	2	15	3	7	nd	ne	6	4
34E	50	nd	nd	nd	52	nd	nd	nd	nd	nd
	200	19	2	18	4	6	nd	30	5	4

Values in % catalytic activity (DMSO-treated control = 100%)

nd: not determined

A further essential item which has to be discussed is the comparison of the activity of the compounds toward the closely related atypical kinases PKC ζ and PKC ι . Interestingly, in the

presence of the compounds **26Z** and **26E** at 50 μ M the basal activity of PKC ι was hardly affected, suggesting high specificity for the PKC ζ PIF pocket. There is also a certain selectivity given for compounds **27Z** and **27E** whereby these showed a slight inhibition of PKC ι . In contrast, the remaining compounds seem not to be specific toward the target kinase.

Altogether, the above data suggest compound **26Z** as the most potent and specific toward PKC ζ *in vitro*. Thereby, an increase in lipophilicity by an inductive effect (-I) due to a *para*-phenyl substitution (Ar₂) by a halogen and a naphthyl group (Ar₃) proved to be important for enhancement of both potency and selectivity. Additionally, the results confirmed that the PIF pocket of PKC ζ could transduce inhibition. Nevertheless, we could also observe activation potency with the investigated molecules. The difference was already caused by screening of the compounds with the opposite conformation.

3.3.3.2. Biological characterization of 3,5-diphenylpent-2-enoic acids in U937 cells

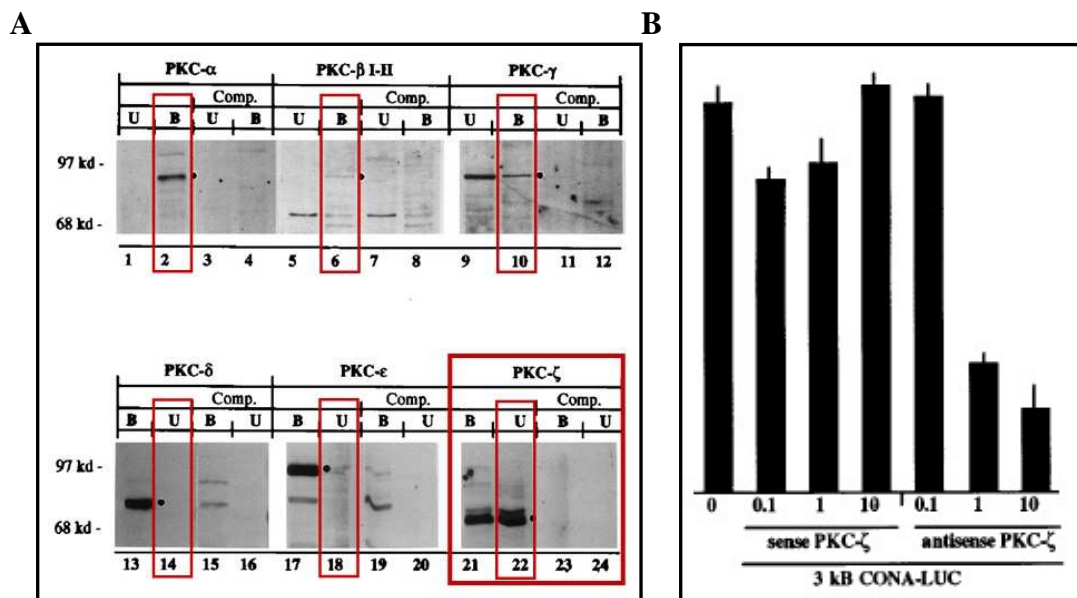
Since we observed inhibition potency screening compounds from our library toward PKC ζ in our routinary radioactivity kinase assay, we were interested to investigate their activity in cells on the target protein. For this purpose, we chose the human lymphoma cell line U937 because these cells displayed PKC ζ expression in immunoblotting experiments (Figure 37A) and antisense oligonucleotides to PKC ζ in turn was shown to control the HIV-induced NF- κ B activity (Figure 37B).^{106, 166} Additionally, Filamenco *et al.* performed immunoblotting experiments with lymphoma U937 cell line which revealed PKC ζ in a central position in the TNF α induced NF- κ B activation pathway.¹⁰⁷

In order to analyze the effect of the synthesized compounds in this cell model we developed a luciferase reporter gene assay according to the principle of the canonical TNF α induced NF- κ B activation pathway (Figure 17). The assay was established under the supervision of Dr. M. Engel by me and mainly by Nadja Weber who performed afterwards the screenings.

Firstly, we transfected the lymphoma U937 cells with plasmid containing luciferase coding sequence. This plasmid expressed luciferase under control by NF- κ B response elements as showed on the assay principle in Figure 38. Secondly, we validated the reporter gene assay with specific inducers to find out if the system would respond as expected. Therefore, we chose TNF α , C6 ceramide, an activator lipid of PKC ζ and bacterial

lipopolysaccharides (LPS). We observed a strong induction of NF- κ B activity using TNF α . C6 ceramide in turn influenced NF- κ B weakly and LPS not at all.

Figure 37: **A:** Immunoblotting experiment: PKC isoenzymes in U937 cells¹⁶⁶
B: Antisense oligonucleotides to PKC- ζ inhibit the HIV-mediated NF- κ B activation in U937 cells¹⁶⁶



A) Top panel: Within the group of classical PKC isoenzymes, only PKC- γ was detected in U937 cell lysates (U), while PKC- α , - β I and - β II, and - γ were present in the rat brain homogenate (B).

Bottom panel: PKC- δ and PKC- ϵ were present in rat brain (B) but not in U937 cells (U). The aPKC isoenzyme, PKC- ζ , was detected in both U937 cell lysates (U) and rat brain homogenate (B).

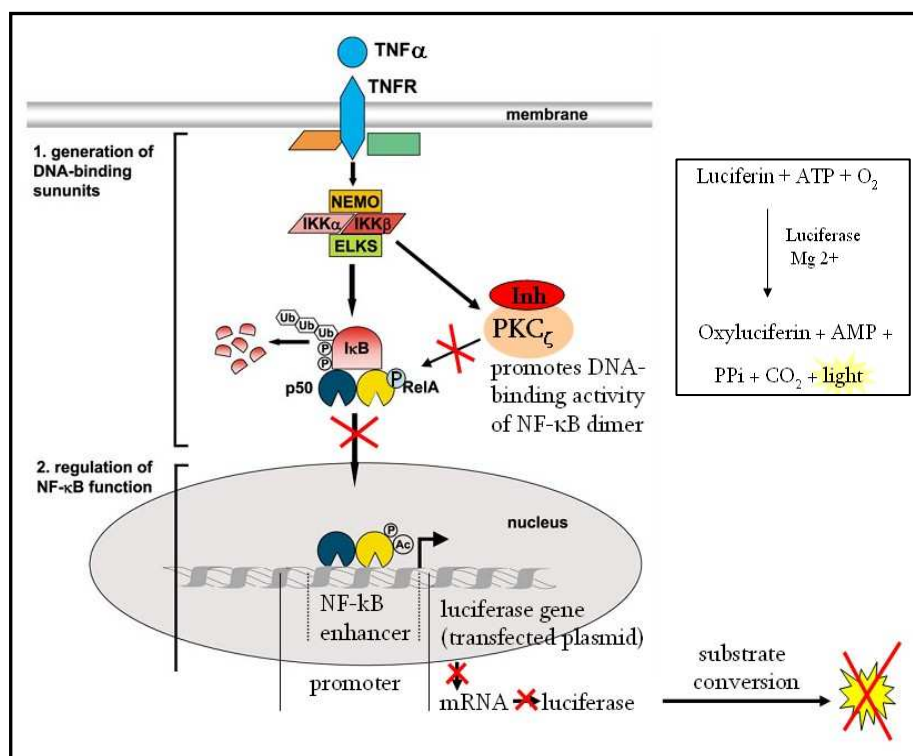
B) HIV infected U937 cells were co-transfected with a NF- κ B reporter gene plasmid (3 kB Cona Luc) and sense or antisense oligonucleotides to PKC- ζ .

In the next step we verified the inhibition of NF- κ B activation induced by TNF α treatment using known ATP-competitive protein kinase inhibitors. Among others we tested the broad range kinase inhibitor Staurosporine which inhibited the NF- κ B activation as expected. Moreover, we used UCN01 that inhibited only at high concentrations. Additionally, we chose known PI3K kinase pathway inhibitors, because many AGC kinases which also possess a PIF pocket are activated in the PI3 kinase pathway. Obtaining no inhibition effect with the known inhibitors LY294002 and Wortmannin, we were able to demonstrate that PI3K and PDK1 are not expressed and do not influence the assay.

Under these established conditions the luciferase transfected U937 cell line was incubated with the synthesized compounds for three hours and was activated with TNF α for further two

hours. Subsequently, the luciferase activity was measured based on light production (Figure 38).

Figure 38: Luciferase reporter gene assay principle in U937



Assay principle: $\text{TNF}\alpha$ treatment of the cells leads to stimulation of the transcription factor $\text{NF-}\kappa\text{B}$ (essential contribution from $\text{PKC}\zeta$) inducing an anti-apoptotic signal whereby light is produced by oxidation of luciferin. An inhibitor induces apoptosis and leads to decrease of the light production.

As already described the stimulation of the cells with $\text{TNF}\alpha$ affected a sharp activation of $\text{NF-}\kappa\text{B}$, so that we could determine the inhibition effect of tested compounds in comparison to DMSO as control. However, in Table 14 and Table 15 we summarized the cell data of our new developed target molecules which were incubated in duplicates and at different concentrations (40-1 μM). Several of the synthesized 3,5-diphenylpent-2-enoic acids inhibited the reporter gene activity. Comparing the potency of the compounds in the cell assay with the radioactivity assay it was obvious that compounds **26** and **27** did not only affect the target protein activity *in vitro* but also decreased the $\text{NF-}\kappa\text{B}$ activation, even totally at 40 μM in cells. Moreover, both geometric isomers of **29**, **30** and **31** decreased also the reporter gene activity being incubated in U937 cells. These results show a good correlation of the inhibition effect in luciferase activity with the $\text{PKC}\zeta$ inhibitory efficacy in cell free assay, but only for

the cis derivatives of **29**, **30** and **31**. The corresponding *E* isomers which had any inhibitory effect on PKC ζ *in vitro*, triggered NF- κ B inhibition. This fact indicates a non specific inhibition in cells. The remaining compounds did not affect the NF- κ B activation in cells showing a good correlation to the results of the cell free assay.

Another interesting point of view constitutes the disadvantages of the compounds. On the one hand, there is the carboxyl moiety that makes the cell permeability difficult and the hydrophobic aromatic moieties which are facing each other. Nevertheless, diffusion through biological membranes enabled the compounds to enter the cells. On the other hand, the high hydrophobicity of the compounds led to binding to the serum albumin what we found out performing the luciferase assay with and without bovine serum albumin. In further studies an important approach is to create the compound scaffold more drug-like via exchange of the naphthyl moiety with benzimidazole or -thiazole groups, especially since we know from our ITC experiments with PDK1 that fused rings are favored for enthalpy.

Summarizing, the presented results suggest that the target molecules are able to bind the PKC ζ PIF pocket in the cells. Furthermore, having the compounds **26** and **27** we present the most potent inhibitors in the reporter gene assay as well as in the kinase activity assay. Interestingly, we observed stronger inhibition of the compounds in cells than in the cell free assay. This might be due to the big advantage of allosteric inhibitors over the ATP site-directed compounds whereby the ATP concentration is often responsible of an increase of the IC₅₀. In conclusion there is again no activity difference between the isomers in cells.

3.3.4. Conclusion

This study demonstrates that analogues of 3,5-diphenylpent-2-enoic acids which were first identified as activators of PDK1 (chapter 3.1) have also a potential as PKC ζ modulators when extended on the phenyl moieties (**A**, **B**, Figure 36). Biological evaluation revealed that introduction of *p*-chlorophenyl as Ar₂ and 2- or 3-naphthyl as Ar₃ (**26**, **27**) led to potent PKC ζ inhibitors. These results provide herein new insights on inhibition efficacy on AGC kinases that can occur by binding the PIF pocket. We were already successful in development of allosteric PKC ζ inhibitors with an SAR study of 4-benzimidazolyl-3-phenylbutanoic acids as PIF pocket-directed compounds recently published by Dr. W. Fröhner *et al.*¹⁶⁷ Though, additional PIF pocket mutant study indicated that this class of compounds mediated their effects via the PIF pocket.^{154, 167}

In addition to the ability of the compounds to induce inhibition of the kinase targeting the PIF pocket both geometric isomers, **26Z**, **26E** and **27Z**, **27E**, turned out to be active substances. This is in contrast to the current results with PDK1 and applies especially to the most potent compounds **26** and **27**. Nevertheless, these results were confirmed also in the developed U937 cell assay. Thus we succeeded in proving the PKC ζ inhibition also in cells for **26Z**, **26E** and **27Z**, **27E**. With these most potent compounds *in vitro* as well as in cells we found also specific compounds as showed in our screening with several related AGC kinases. We achieved compounds with decreased activation potency toward PDK1 in comparison with the parental compounds and even a high degree of selectivity toward the PKC ι isoforms.

Further studies for the new described 3,5-diphenylpent-2-enoic acids such as the mutant study and cocrystallization are underway to confirm the binding site and the localization of the compounds. Having this evidence we could continue with further modifications to improve the affinity, selectivity and drug like features. Especially the cocrystal structure is of major importance since the here presented compound class bearing a double bond at the carboxylic side chain showed with both isomers good PIF pocket affinity. However, within the published the 4-benzimidazolyl-3-phenylbutanoic acid series two pure enantiomers showed also the characteristic displaying activity toward PKC ζ , but these compounds are able to reach the relevant electrostatic interactions only via single bond rotation what is not possible with the double bond.

4 Discussion

Previous work revealed a new allosteric regulatory site in PDK1, termed PIF pocket that is required for the recognition and phosphorylation of its substrates. It was found later that it serves as an important regulatory site in other AGC kinases as well, where the hydrophobic motif (HM), a C-terminal extension to the catalytic domain, folds back and binds into their own PIF pocket, thereby regulating the conformational transition between the active and inactive conformation and thus the activity of the kinases.^{12, 26} In contrast to other AGC kinases the PIF pocket of PDK1 is characterized by the lack of the HM and revealed as the docking site for the intramolecular HMs of PDK1's substrates. Hence, this docking interaction of PDK1 with its substrates triggers an intrinsic activity of PDK1 enabling ATP binding and phosphorylation of its substrates. Additional mutation and knock-in studies confirmed PDK1 as an upstream master kinase that controls the phosphorylation and activation of its substrate enzymes. These include S6K, SGK, RSK, MSK and the atypical PKCs. Only the phosphorylation of PKB does not depend on the interaction of the PIF pocket of PDK1.^{11, 32}

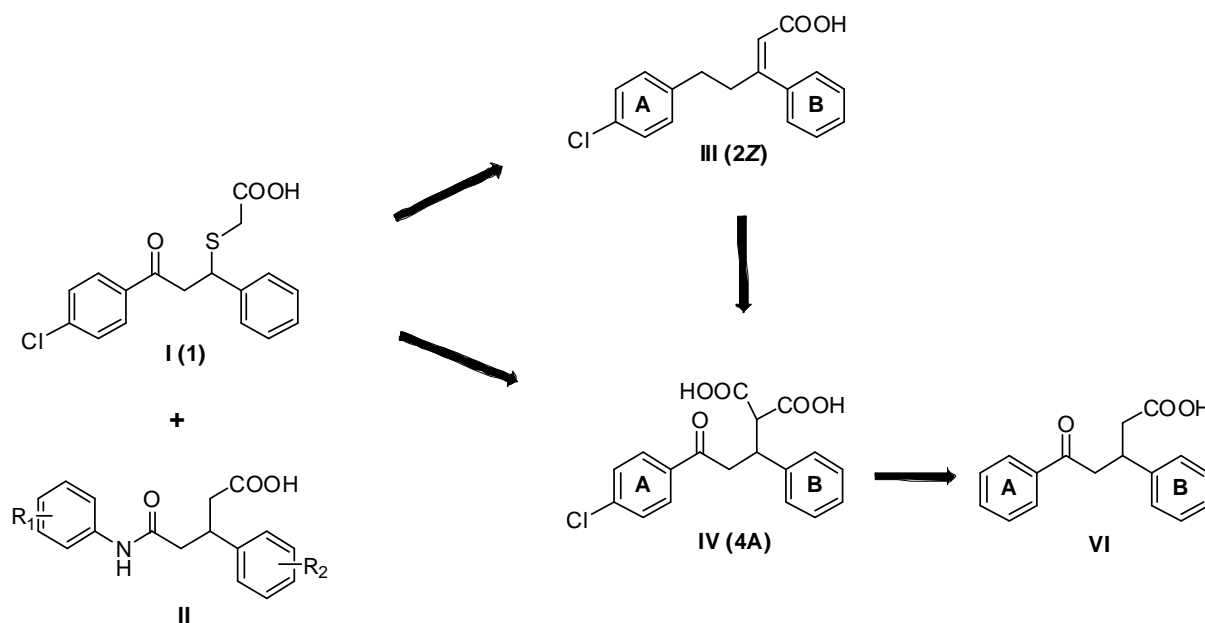
Supported by all these results the PIF pocket of PDK1 was suggested as a new allosteric target site for drug development. It is particularly interesting since the inhibition of PDK1 has gained high interest due to its crucial role in transducing the PI3K signaling pathway, where several of the substrates comprising PKB, RSK and S6K regulate processes which are essential for tumor cells, such as cell growth and survival. Deregulation of this signaling pathway leads in the majority of cases to cancer and also triggers diabetes type-2, autoimmune diseases, inflammation, neurological and metabolic disorders.²¹ Hence, proper regulation of PDK1 is critical for prevention of too high activity of its substrates. For that reason, targeted inhibition of PDK1 has emerged as an attractive strategy in treatment of a wide range of human cancers.^{17, 35, 36} Particularly, because the *in vivo* results suggested an incomplete inhibition of PDK1 in cancers where PTEN is mutated. Mice with 10-20 % of PDK1 protein were healthy although they were smaller. However, when they were crossed with knockout mice in a PTEN deficient background, they had spontaneous tumors, the mice with less PDK1 activity had less tumors and extended lifespan.¹⁷ As binding of ATP is essential for kinase activity, most therapeutic efforts have been focused on inactivation of PDK1 via ATP-competitive, small molecular weight compounds (Type I inhibitors) which block the enzymatic activity and thus interfere the phosphorylation of the cellular substrates.^{16, 35, 37-39, 41, 42} But, this approach has two main drawbacks. On the one side, due to

relative structural conservation of ATP binding sites for several protein kinases and resulting cross reactions with many different kinases, the risk of dose limiting off-target effects increases and it is a challenge to find a new candidate for clinical trials. In fact, not only in case of PDK1 the most ATP-competitive inhibitors show limited selectivity (e.g. staurosporine, UCN01)^{62, 63} Moreover, in general these inhibitors compete with the ATP for the same binding site.^{63, 168} On the other hand, this strategy proved inappropriate for several kinases because of the fact that therapeutic inactivation of essential protein kinases exerts a selective pressure resulting in development of mutations and thus inhibitor resistance.⁶ A prominent example is Gleevec. These observations prompted the search for new paths which have to be taken in order to succeed in specific and lasting regulation of kinase activity. Currently, the trend toward multi-kinase target strategy is increased in an attempt to become enhanced antitumor efficacy and safety profiles compared to single target drugs.⁶⁴ Moreover, the focus turned from the ATP binding site to intrinsic and unique regulation mechanisms of a protein kinase. In fact, increasing interest was observed based on many publications which included characterization of novel allosteric sites as drugable sites in kinases. Several focused on type II inhibitors, which do not really belong to allosteric inhibitors occupying at least partially the ATP binding site and acting only in some extent in a different non-competitive manner.⁶⁵ However, due to similar hydrophobic regions adjacent to the ATP binding site among the protein kinases these inhibitors exhibited again a lack of specificity. The next class of compounds presented in research studies are type III inhibitors. Type III inhibitors tend to exhibit the highest degree of kinase selectivity using an allosteric site, distant to the ATP binding site and exploiting regulatory mechanisms which are unique to a particular kinase.⁶⁵ Only few kinases from the kinome can be targeted by these allosteric, selective and potent inhibitors so far. Therefore, the development of further strategies remains urgent and provided us the motivation to identify first small compounds which bind to the PIF pocket. For this purpose, we defined a pharmacophore based on the crystals of the PIF pocket of PDK1 and of the closed PKA within the C-terminal HM and performed a virtual screening of a commercial compound data base. Selected compounds were subsequently tested on the activity of PDK1 and other AGC kinases. Two compound classes (**I**, **II**), (Scheme 14) revealed as activators of PDK1 and provided first evidence with further biochemical experiments that small compounds directed to the PIF pocket can be developed.

In this thesis a medicinal chemistry approach was used. Starting from compound class **I** the aim was to overcome its structural drawbacks in order to improve the activity and selectivity. Since no cocrystal structure was available, the rational drug design approach was

used. The goal was to discover new classes of PDK1 activators. In such manner, starting from the compound **1** we modified the structure by displacement of the chiral centre and the sulfanyl moiety to become more drug-like target molecules. Nevertheless, the general characteristic scaffold including two aromatic rings connected by a carbon chain with an attached carboxyl side chain should be maintained.

Scheme 14: Screening hits and designed, synthesized and evaluated classes through medicinal chemistry approach used



The structural refinement led to the series of 3,5-diphenylpent-2-enoic acids. Performing the radioactive kinase activity assay, it was apparent that the main potency showed mostly the *cis* isomers of the new synthesized 3,5-diphenylpent-2-enoic acids. Introduction of *para*-halogen substituents on the phenyl ring **A** revealed to increase the PDK1 activity and the potency was improved even more with compounds carrying additionally to the *para*-halogen one more halogen in *meta* or *ortho* position. In contrast, an ethyl substitution led to an abolishment of PDK1 activity. The same pattern could be observed by introduction of fluorine atoms on the phenyl moiety **B**. Furthermore, the replacement of the phenyl moiety **A** with different aromatic systems in order to explore the requirements of the PIF pocket led to a moderate potency toward PDK1. Only the naphthyl analogue (**16Z**) stood out showing the highest increase of potency. Derivatization of the backbone chain inserting polar groups (O, S) and the scaffold rigidification resulted in a significantly decrease of PDK1 activity.

Choosing compound **2Z** (Scheme 14), one of the first isolated analogue of the 3,5-diphenylpent-2-enoic acid series with good potency toward PDK1, the PIF pocket of PDK1 was proved as the binding site in a mutagenesis study. The cocrystal structure of **2Z** bound to the PIF pocket confirmed the compound as truly allosteric. Moreover, the cocrystal structure confirmed the interaction of the carboxyl moiety of the *cis* compounds with the phosphate binding site is essential to prompt the activation of PDK1.

The next particular part of this study provides the ITC approach. The relationships between the structural properties, binding affinity and allosteric activation with PIF pocket-directed small weight molecules could be evaluated for the first time. The ITC results again confirmed the main potency of the *cis* isomers obtaining a typical binding isotherm. In contrast, the *trans* isomers did not show a typical curve shape. The similar results for all tested compounds let suppose that the phosphate binding site accommodated all analogues in the same way. Thereby, the phenyl ring **B** of the *cis* analogues might bind into the subpocket on the PDK1 PIF pocket enabling good interactions with the carboxyl moiety. Furthermore, the ITC analysis revealed that there is no agreement between the estimated K_d - and the AC_{50} -values (Figure 27) from the radioactivity assay. For this reason, the attention was directed toward the influences of structural features on the affinity toward PDK1. There are three crucial aspects to be considered in terms of affinity and activity. In an agreement with the cocrystal analysis the edge-to-face CH- π interaction of the phenyl ring **B** with the amino acid F157 plays a crucial role in stabilizing the ligand protein binding, particularly since such hydrophobic interaction is found to be most favorable formation in solution. Thus, it was apparent why substitution of this phenyl ring led to an abolishment of activity toward PDK1. The next interesting issue represented the fact that in contrast to the *in vitro* activity assay results which did not show major differences between the activation potency of the halogen substituted derivatives, the dichloro analogues (**7Z** and **8Z**) emerged with distinct thermodynamic properties. **7Z** broke the general correlation between K_d and AC_{50} and exhibited the biggest loss of the binding entropy compared to **2Z**. The behavior can be attributed to the *meta*-chloro substituent which seemed to impede the hydrophobic interactions with the PIF pocket. In contrast, **8Z** displayed the lowest K_d that correlated with the AC_{50} value. But the *ortho*-chlorine substitution of **8Z** indicated an “antagonist” like behavior since its potency to allosterically activate PDK1 was striking due to the decrease to about half of the A_{max} of **2Z**. In the end, although entropically driven ligand protein binding is usually attributed to structural features **8Z** displayed the entropy-driven binding and **7Z** did not. This fact may be due to the differences in the position of these compounds within the PIF

pocket. Subsequently, extended aromatic system led to enthalpy-entropy compensation. These compounds showed K_d values similar to the halogen derivatives although these interacted differently to the PIF pocket. The highest $\Delta H/\Delta G$ ratios showed the naphthyl analogue (**16Z**) and the indol derivative (**17Z**) resulting from increase of enthalpy relative to entropy of binding. This might be attributed to the CH- π interaction resulting from the π -electron density of bicyclic rings combined with larger surface. In comparison with the cocrystal structure of **2Z** putative interaction of extended π -electron system of **16Z** and **17Z** was provided (Figure 24). In conclusion, the ITC approach resulted in a broad thermodynamic binding spectrum from mainly entropy-driven to predominantly enthalpy-driven binding. Among the 3,5-diphenylpent-2-enoic acid series with comparable size, the increase of the binding enthalpy is accompanied by a loss of entropy to about the same degree leading to little or no change in binding affinity. This compensation effect was obvious when comparing the halogen derivatives with the extended aromatic derivatives. In general, with the ITC method that is proved as a method to guide the lead evaluation and optimization in drug development, **16Z** and **17Z** were provided as compounds with the most ideal thermodynamic lead profile, since the enthalpic term strongly predominates the binding free energy. Thus, additional information about structural requirements was achieved in order to use them for further improvement of the affinity and activity toward the PIF pocket of PDK1.

Since a crucial point in development of PDK1 modulators is selectivity, the effect of the 3,5-diphenylpent-2-enoic acid series was tested on some related AGC kinases. Analyzing the results a slight inhibition of some compounds toward S6K and SGK and a tendency to stronger inhibition of PKC ζ was observed. This effect was exploited for a new approach to develop PKC ζ selective inhibitors.

The 3,5-diphenylpent-2-enoic acids proved as activators of PDK1 targeting the PIF pocket. But these compounds turned out to have low affinity rendering further studies difficult. In order to discover even more potent and selective PDK1 activators, the lead scaffold (**2Z**) was modified combining the short carboxyl side chain with the carbonyl function from the previous lead compound **1**. Additional aim to improve the activity of the compounds was to mimic the two negative charges of the phosphate groups present in natural ligands. For this purpose, we chose the malonic acid moiety as the short side chain. In the end, the synthesis of 2-(3-oxo-1,3-diphenyl-propyl)malonic acids (**IV**), (Scheme 14) as a new class of PDK1 activators and evaluation of its impact on the activatory potency toward PDK1's PIF pocket led to further increase of the PDK1 activation in both higher levels and lower AC₅₀ in comparison to **2Z**. There was a significant contribution of the dicarboxyl

moiety to the affinity and activity to the PIF pocket particularly when compared to the corresponding mono acid derivatives (Scheme 14). These were achieved via decarboxylation of the malonic acid derivatives and caused generally increased potency than **2Z**, but did not reach the pronounced increase of the activity like the malonic analogues did.

Supported by the results with the previous compound class, the focus was directed again toward compounds substituted with halogens on the phenyl moieties. In fact, the *para* substitution on ring **A** led in comparison to the structure class **III** to higher potency and lower AC₅₀ in the following order Cl < Br < I. The iodine analogue revealed as a particular good activator (AC₅₀ = 0.4 μM) and even improved by replacement of the phenyl ring **B** by a naphthyl group. An extraordinary high effect was observed also with the *para*-trifluoromethyl derivative. The introduction of condensed phenyl rings instead of phenyl ring **B** resulted also in potent activators. Concerning the selectivity the series showed not only high potency toward PDK1 but in most cases also a high selectivity over the closed related AGC kinases.

Going back to the monoacid derivatives (**VI**) that exhibited generally reduced potency than the malonic acid compounds it should be mentioned that both the *para*-iodo and the *para*-trifluoromethyl analogues were characterized by very good potency. Nevertheless, the focus was directed toward the malonic acid series in order to further succeed with potent and selective PDK1 activators.

In an effort to verify the binding site PIF pocket mutants experiments were done and proved the PIF pocket as the target site. These results were confirmed by displacement experiments utilizing the Alpha-Screen technology.

Furthermore, a prodrug strategy was adapted and investigated to overcome the membrane transport barrier that emerged due to the high polar malonic acid moiety. Therefore, the compounds were converted to bisacetoxymethyl esters and their cellular conversion in the L6 skeletal muscle cell line which displays esterase activity was evaluated. As expected, the prodrug derivatives remained inactive in our cell free kinase assay. The cell results data in turn revealed that the hydrolysis of the prodrug esters was occurring upon enzymatic activity leading to a good cell permeability and to intracellular accumulation, despite the serum instability of the prodrug. However, this prodrug concept provided a promising starting point for further development of PDK1 activators with efficient drug delivery and subsequently good cellular efficacy. Moreover, with the developed prodrugs the proof of mechanism could be demonstrated using a western blot analysis of pretreated HEK293 cells. In this manner, the influence of PDK1 PIF pocket-directed compounds toward the phosphorylation of the relevant kinases was investigated. These include S6K, SGK and RSK which require the PIF

pocket of PDK1 for docking interaction with their HM. The exception remains PKB. In fact, an inhibition of S6K without an influence of PKB activity was obtained. Accordingly, with further experiments these compounds could be proposed for treatment of cancer and diabetes type-2.

To gain insight into the mode of binding of the malonic acid derivatives cocrystals were generated. Their X-ray analysis revealed in comparison to the compound class **III** additional crucial interaction of the malonic moiety with the PIF pocket of PDK1 via a salt bridge. This salt bridge is essential for the allosteric activation mechanism as it became apparent due to increased affinity and activity toward PDK1. Finally, performing a chiral separation using HPLC and having the cocrystal results the *S*-enantiomer of the *para*-trifluoromethyl analogue could be suggested as the bioactive chiral form.

Altogether, the optimization approach starting with compound **1** was successful in improvement of the activity and selectivity profile of the PDK1 activators. With both compound series the importance of the carboxyl moiety and malonic acid moiety respectively, which mimic the phosphate group of the natural ligand, was confirmed as crucial for the affinity to the PIF pocket of PDK1. Moreover, the evidence that compounds blocking the PIF pocket might be able to prevent phosphorylation of PDK1's substrates was provided.

Discovering the PIF pocket's function in the molecular mechanism of kinase activation it became apparent that this site mediates conformational transition between active and inactive conformations in many AGC kinases. Therefore, the system provides the opportunity to influence the kinase activation both with an activity increase or inhibition depending on which conformation is stabilized. In fact, the optimization approach of the screening hit **1** revealed several compounds of the 3,5-diphenylpent-2-enoic acid series not only as PDK1 activators but they caused also an inhibitory effect toward PKC ζ . Thereby, compounds with expanded aromatic systems stood out. These results are interesting since the development of PKC ζ inhibitors arose interest due to its unique feature to activate the eukaryotic transcription factor NF- κ B which plays a crucial role in the transcriptional activation of proinflammatory and anti-apoptotic genes.^{86, 87} There are several advantages to inhibit PKC ζ instead of NF- κ B in order to treat inflammatory diseases. Firstly, PKC ζ performs the activating interaction only in selected cells and tissues. Secondly, knock-out studies revealed mice with nearly normal developed organs. Because there are not even ATP-competitive inhibitors described so far, the allosterical inhibition using the PIF pocket opened a promising strategy to develop selective inhibitors of PKC ζ . All these facts led to a new project. In an effort to investigate the impact of explored aromatic system on the PKC ζ activity the 3,5-diphenylpent-2-enoic acid

series was enlarged with the focus on improvement of the inhibitory effect. The biphenyl derivative (**15Z**) and the naphthyl derivative (**16Z**) served as leads in the aim to investigate the spatial limitations of PKC ζ 's PIF pocket. Two groups of derivatives were obtained. The first is characterized by the *para*-chlorophenyl moiety on the phenyl ring **A** position with varied aromatic substituents on phenyl ring **B**. For the second group the naphthyl function was set as phenyl ring **B** whereas the phenyl ring **A** was varied. The biological evaluation revealed several interesting characteristics. The geometric isomers of the potent analogues did not show a difference in intrinsic potency toward PKC ζ in most cases. These included (*E* and *Z*)-5-(4-chlorophenyl)-3-(naphthalen-2-yl)pent-2-enoic acid (**26**) and (*E* and *Z*)-5-(4-chlorophenyl)-3-(naphthalen-1-yl)pent-2-enoic acid (**27**) and indicated that the arrangements of the naphthyl group of both isomers enabled good electrostatic interactions of the carboxylic side chain with the relevant amino acid of the PIF pocket. Further derivatives demonstrated that enlarging the target compound size only the *cis* conformation might reach good inhibition potency toward PKC ζ . Moreover, further *para* substitution on the phenyl ring **A** led to a decrease of the PKC ζ effect and indicated the inductive effect of the halogen moiety as promising feature of the core structure to reach good affinity for the PIF pocket. This also applied for the naphthyl moiety on the phenyl ring **B** position.

Regarding the selectivity the most potent compounds turned out to be also specific toward PKC ζ . The particular challenge represented the aim to obtain molecules which specifically target the PIF pocket of PKC ζ but not of PDK1, especially since the lead compounds were found as PDK1 activators. The other challenge was to obtain selectivity toward the most closed PKC isoform PKC ι . Both compounds **26** and **27** revealed to have these features. These *in vitro* results increased the motivation to investigate the activity of the compounds in cells. Since the human lymphoma cell line U937 is known for the PKC ζ expression, and PKC ζ revealed to be involved in TNF α induced NF- κ B activation pathway, this cell line provided as a model to develop a luciferase reporter gene assay in order to find out the influence of the compounds on the TNF α induced NF- κ B activation. Again, **26** and **27** confirmed their *in vitro* inhibition toward PKC ζ also in cells. Nevertheless, due to the handicap of the derivatives, namely the limited cell membrane permeability due to the polar carboxyl moiety, the obtained results were attributable to diffusion through biological membranes. Interestingly, the cell results revealed stronger inhibition than in the cell free assay. This might be due to the advantage of allosteric inhibitors over the ATP site-directed compounds, whereby the ATP concentration is often responsible for an increase of the IC₅₀. Moreover, the isomers of the compounds showed again no activity differences in cells.

Altogether, to reach good potency and selectivity toward PDK1 an increase in lipophilicity by an inductive effect in *para*-phenyl position (ring **A**) by a halogen and a naphthyl moiety as phenyl ring **B** are important. Additionally, the luciferase reporter gene assay results proved these molecules as PKC ζ 's PIF pocket inhibitors in cells. However, mutant analysis and cocrystals would provide evidence about the targeting site and localization of the developed molecules.

5 Summary and Conclusion

The aim of the present thesis was the design and synthesis of small molecule compounds which act via an allosteric mode by binding to the PIF pocket of two AGC kinases, primarily, PDK1 and potentially the atypical PKC isoform PKC ζ . Based on the hit compound **1** derived from previous work of our group new compound classes (Scheme 15) were to be developed using structure based drug design. Our efforts were focused on selectivity toward a panel of related AGC kinases and on enhancement of potency of allosteric modulators to the nanomolar range in order to confirm the druggability of the PIF pocket. With potent allosteric modulators we could suggest an interesting alternative to traditional ATP-competitive drugs.

Chapter 3.1 deals with the synthesis and biological evaluation of 3,5-diphenylpent-2-enoic acids. This new compound class resulted from an effort to obtain more drug-like structure replacing the chiral center and the sulfanyl moiety of the hit compound **1**. The phenyl moiety was systematically modified to identify most favorable lead structure for further optimization. Since in the previous work the attention was focused on the ring substituents, here we examined in addition the structural features of the target site on PDK1 by extension and rigidification of the 3,5-diphenylpent-2-enoic acid scaffold.

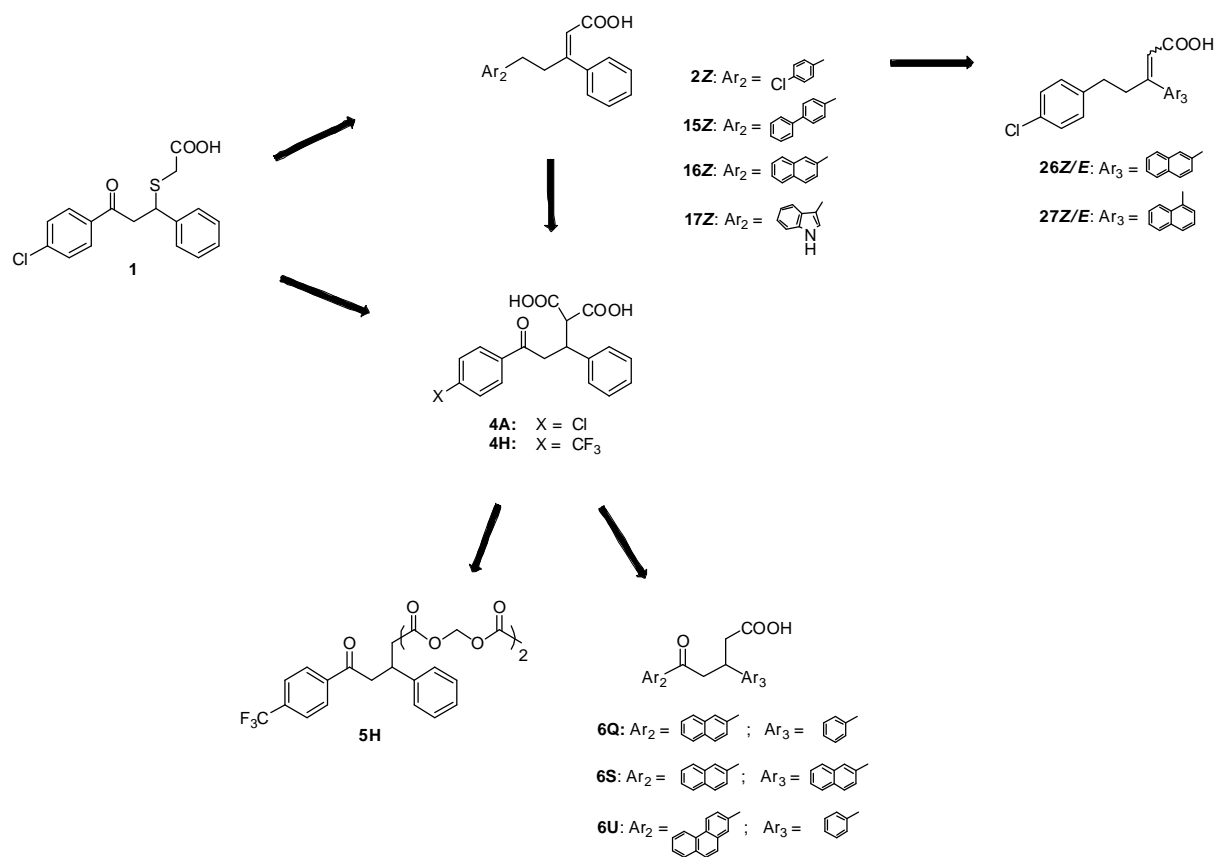
The structure-activity relationships clearly revealed that the obtained geometric isomers of the 3,5-diphenylpent-2-enoic acids exhibited different intrinsic activation potency toward PDK1. The analogues with the *cis* configuration were the active substances, whereas the compounds with the opposite configuration hardly displayed any potency. Among the *cis* isomers, the halogenated derivatives generally induced a stronger activation of PDK1, especially dihalogen substituted compounds. Similarly, bicyclic aromatic substituents turned out to improve potency toward PDK1. However, scaffold rigidification did not further increase the activity, suggesting that the some flexibility of the compounds was necessary to optimally accommodate to the hydrophobic surface of the PIF pocket. At the same time, polar groups inserted in the backbone chain of the molecules were poorly tolerated, leading to a substantial reduction of potency.

The binding site of modulators was finally confirmed using PDK1 mutated at the PIF pocket, and by cocrystallography with the selected compound **2Z**. It could be shown that **2Z** binds to the PIF pocket proving that the compounds were truly allosteric. Furthermore, the cocrystal structure emphasized the importance of the carboxyl moiety which seems to mimic the phosphate group of phosphoserine/threonine residues from the natural ligands. These results were confirmed by further experiments using isothermal titration calorimetry. Again,

only the *cis* isomers were observed as PIF pocket binding compounds. Moreover, the ITC study as an increasingly important method in drug development provided additional information about structure-dependent binding thermodynamics, useful for further improvement of the affinity and potency toward the PIF pocket. Compounds **16Z** and **17Z** (Scheme 15) showed the most ideal thermodynamic profile that might be attributable to their extended π -electron system and thus were selected as new lead structures. Both analogues turned out to compensate the loss of entropy gain by increased enthalpy resulting from additional CH- π interactions with the PIF pocket.

To obtain informations about selectivity, the 3,5-diphenylpent-2-enoic acids were tested toward a panel of selected, closely related AGC kinases. Interestingly, besides activation of the PDK1, inhibition of other AGC kinases, in particular PKC ζ were pursued further and refined in Chapter 3.3.

Scheme 15: Selected compounds of the optimization approach



In Chapter 3.2, rational optimization of the new structure **2Z**, also considering the previous hit compound **1** is described. We created a chimeric compound containing the carbonyl function from **1** and the shorter carboxyl side chain from **2Z**. In addition, the design concept was aimed to better mimic the phosphate moiety of the natural ligands by introduction of a second carboxyl group. These modifications led to 2-(3-oxo-1,3-diphenylpropyl)malonic acids which revealed to be very potent PDK1 activators reaching even submicromolar affinity. This compound class also showed a remarkable selectivity toward PDK1 when tested against a panel of related AGC kinases. Together with the mutagenesis study that confirmed the PIF pocket as binding site, we confirmed that specific modulators of even a single kinase can be developed using the less conserved, regulatory PIF pocket as a target site. Finally, the cocrystal structure of PDK1 in complex with **4A** corroborated the importance of the second carboxyl group with respect to potency and selectivity.

Separating the racemic mixture of **4H** by chiral HPLC and including the cocrystal structure we were able to suggest the *S*-enantiomer as the eutomer with the higher biological activity. The absolute conformation could be not determined due to limited amounts of material.

A prodrug approach allowed to investigate the activity of the highly polar compounds in cells, for which the bicacetoxymethyl ester of the most potent malonic acid analogue **4H** was synthesized (Scheme 15). In fact, the corresponding prodrug **5H** displayed good cellular delivery and was readily converted to the active malonic acid form **4H** upon enzymatic hydrolysis. This prodrug concept, combined with the high activity and selectivity of **4H**, the opened up the possibility to provide the proof of mechanism in cellular studies: indeed, the intracellular released **4H** blocked the PIF pocket of PDK1 for interaction with the substrate kinase S6K that requires the PIF pocket to become phosphorylated. As expected, the only one substrate PKB whose phosphorylation does not depend on PDK1's PIF pocket was not affected. Due to the essential role of S6K in insulin resistance the PIF pocket-directed compound **4H** might be applicable as a novel therapeutic for the treatment of diabetes type-2.

Moreover, Chapter 3.2 deals with a further compound class, the 5-oxo-3,5-diphenylpentanoic acids that were relatively easy to accessible via decarboxylation of the corresponding malonic acid derivatives. These monoacids exhibited generally reduced potency toward PDK1 than the corresponding dicarboxylic derivatives confirming the importance of the second carboxyl moiety for affinity and activity. Nevertheless, this series could be exploited to analyze the relative contribution of the second carboxylate group to the

overall potency toward PDK1. Combination of various fused aromatic rings with the mono-carboxyl group proved to retain the activity as observed with **6Q**, **6S** and **6U** (Scheme 15). These findings could be utilized for further optimization in order to render the molecules more drug-like.

The elaboration of the 3,5-diphenylpent-2-enoic acid structure with regard to inhibition efficacy on AGC kinases is described in Chapter 3.3. Since we found out that particularly **15Z** and **16Z** did not only trigger the PDK1 activity but also induced PKC ζ inhibition, the interest arose to optimize their scaffold in an effort to obtain more potent and selective inhibitors. For this purpose, the phenyl moieties were furthermore extended in order to investigate the spatial limitations of PKC ζ 's PIF pocket.

The biological evaluation demonstrated that the geometric isomers of the new synthesized analogues were still inhibiting PKC ζ whereas allosteric activation of PDK1 was abolished indicating that the PIF pockets of PDK1 and PKC ζ differ in their flexibility toward sterically demanding ligands. This was particularly the case with the most potent naphthyl analogues **26Z**, **26E** and **27Z**, **27E**. Enlarging the scaffold e.g. by two naphthyl groups (**30**) led to differences of potency between the isomers, so that only the *cis* isomers reached a good inhibitory effect. Further derivatizations of the aromatic moieties introducing polar groups abolished the potency toward PKC ζ .

The specificity profile of the most potent PKC ζ inhibitors was examined toward selected AGC kinases, with a main focus on PDK1 and the closely related PKC isoform PKC ι . In fact, **26Z**, **26E** and **27Z**, **27E** turned out to have not only good efficacy toward PKC ζ but also a decent specificity toward the other AGC kinases. **26Z** and **26E** did not even affect the most closely related isoenzyme PKC ι , indicating a remarkable selectivity for PKC ζ . In contrast, the remaining compounds were found to be not very specific. Altogether, the biological evaluation highlighted **26Z** as the most potent and specific inhibitor of PKC ζ *in vitro*.

In order to analyze the effect of the new PKC ζ inhibitors in cells, we used a luciferase reporter gene assay. Again, we observed no activity difference between the isomers. Moreover, a good correlation of the effect in cells with the PKC ζ inhibitory efficacy in cell free assay - particularly with the most potent compounds - was observed.

Altogether, our 3,5-diphenylpent-2-enoic acid series confirmed that PIF pocket-directed compounds are able besides stabilizing an active conformation of PDK1 also to allosterically inhibit PKC ζ 's activity. In further work, the actual binding mode of the inhibitors on PKC will be elucidated using cocrystallography.

In summary, this work describes the ligand- and structure-based design of truly allosteric compounds targeting the PIF pocket, a regulatory site on AGC protein kinases' catalytic domain. Compounds with such an alternative mode of action are still poorly represented. Since the PIF pocket is less conserved than the ATP binding site, we expect for the PIF pocket-directed modulators a distinct pharmacological profile, based on higher selectivity and a more subtle modulation of downstream signaling in particular of PDK1.

Extensive SAR studies to PDK1 and PKC ζ confirmed that the relevant structural requirements for PIF pocket-directed small molecules are two aromatic moieties connected by an aliphatic carbon chain, bearing a two atom membered side chain with a free carboxylic or dicarboxylic group. A V-shaped conformation of the aryl groups toward each other is required to achieve complementarity to the PIF-binding pocket. Moreover, the SAR results allowed for the first time to investigate conformational changes of the allosteric activation mechanism. We provided the evidence that it is possible to exploit the PIF pocket on the AGC kinases for the development of reversible allosteric activators and inhibitors. In the case of PDK1, the small molecules stabilize the active conformation leading to an increase of PDK1 activity. In contrast, the same molecules induced inhibition of the kinase targeting the PIF pocket of PKC ζ .

Furthermore, with allosteric activators directed to the PIF pocket of PDK1 we provided for the first time the proof of mechanism and the evidence that specific activators of a single kinase can be developed. Concerning further optimization of the potency, the most active compounds found in this work could serve as new lead structures. This may finally improve the biological activity in cells and enable the investigation of PDK1 activators *in vivo* using a suitable animal model.

6 Experimental Section

6.1. Chemistry

6.1.1. General descriptions

Solvents and reagents were obtained from commercial suppliers and were used without further purification. Flash column chromatography was carried out using silica-gel 40 (35/40-63/70 μM) with petroleum ether/ethyl acetate mixtures as eluents, and the reaction progress was determined by TLC analysis on Alugram® SIL G/UV₂₅₄ (Macherey-Nagel). Visualization was accomplished with UV light and KMnO_4 solution. ^1H -NMR and ^{13}C spectra were recorded at 500 MHz using a Bruker DRX-500 spectrometer. ^1H shifts are referenced to the residual protonated solvent signal (δ 2.50 for $\text{DMSO-}d_6$ and δ 7.26 for CDCl_3) and ^{13}C shifts are referenced to the deuterated solvent signal (δ 39.5 for $\text{DMSO-}d_6$ and δ 77.2 for CDCl_3). Chemical shifts are given in parts per million (ppm), and all coupling constants (J) are given in hertz (Hz). The purities of the tested compounds were determined by HPLC coupled with mass spectrometry and were higher than 95% for all compounds. Mass spectrometric analysis (HPLC-ESI-MS) was performed on a TSQ quantum (Thermo Electron Corporation) instrument equipped with an ESI source and a triple quadrupole mass detector (Thermo Finnigan, San Jose, CA). The MS detection was carried out at a spray voltage of 4.2 kV, a nitrogen sheath gas pressure of 4.0×10^5 Pa, an auxiliary gas pressure of 1.0×10^5 Pa, a capillary temperature of 400 °C, capillary voltage of 35 V and source CID of 10 V. All samples were injected by autosampler (Surveyor®, Thermo Finnigan) with an injection volume of 10 μL . A RP C18 NUCLEODUR ® 100-3 (125 x 3 mm) column (Macherey-Nagel) was used as stationary phase. The solvent system consisted of water containing 0.1 % TFA (A) and 0.1 % TFA in acetonitril (B). HPLC-Method: flow rate 400 $\mu\text{L}/\text{min}$. The percentage of B started at an initial of 5 %, was increased up to 100 % during 16 min, kept at 100 % for 2 min and flushed back to the 5 % in 2 min. All masses were reported as those of the protonated parent ions. Melting points were determined on a Mettler FP1 melting point apparatus and are uncorrected.

6.1.2. Synthetic procedures

Method A: Claisen-Schmitt condensation

The corresponding benzaldehyde (1 eq) was dissolved in EtOH (2 mL / 1 mmol), a 3 M NaOH_{aq} solution (3 eq) and the corresponding acetophenone (1 eq) were added and the resulting mixture was stirred at rt for 2 h forming a precipitate. The solid was separated by vacuum filtration and was washed three times with 10 mL ice water. The crude product was purified by recrystallization from MeOH.

Method B: Selective silica gel-catalyzed 1,4-reduction

The corresponding chalcone (1 eq) was stirred under the nitrogen atmosphere with 3,5-bis(ethoxycarbonyl)-1,4-dihydro-2,6-dimethylpyridine (HEH, 1.5 eq) in the presence of silica gel (0.2 g / 0.1 mmol) in toluene (2 mL / 1 mmol) at 70 °C in the dark for 17 h. After removal of toluene under vacuum, the crude mixture was purified by flash column chromatography on silica gel.

Method C: Horner-Wadsworth-Emmons reaction

Triethyl phosphonoacetate (1-3 eq) was added dropwise at 20 °C to a slurry of sodium hydride (abs. 60 % in oil) (1-3 eq) in anhydrous 1,2-dimethoxyethane under nitrogen. The reaction mixture was stirred at rt for 1 h until the gas evolution had ceased and the appropriate reduced chalcone (1 eq) was added. After stirring at 80 °C for 4 hours the resultant solution was poured into ice water (50 mL) and then extracted with dichloromethane (3 x 20 mL). The extract was washed with brine (20 mL), dried over anhydrous MgSO₄ and evaporated *in vacuo* to afford a crude which was purified by flash column chromatography to obtain the corresponding geometric isomers of the ethyl acrylate derivatives.

Method D: Hydrolysis I

A solution of the corresponding ester (1 eq) and NaOH_{aq} (3eq) in EtOH was refluxed for 4 hours. After the completion of reaction, the cooled mixture was poured into water (30 mL), acidified to pH 2 with 10 % HCl and extracted with ethyl acetate (3 x 20 mL). The organic layers were collected, washed with brine (20 mL), dried over MgSO₄ and evaporated to afford a residue, which was purified by crystallization to afford the acids.

Method E: Rap-Stoermer reaction

The corresponding salicylaldehyde (1 eq) and 2-bromoacetophenone (1 eq) were dissolved in ethanol and then treated with potassium carbonate (2.2 eq). The resultant mixture was heated at 80 °C for 1 hour, and the reaction mixture was taken up in water (50 mL) and extracted with dichloromethane (3 x 20 mL). The combined organic extracts were washed with brine (20 mL), dried over MgSO₄ and concentrated under reduced pressure. The resultant oil was subjected to silica gel chromatography to give the appropriate product.

Method F: Catalytic transfer hydrogenation

To a solution of the corresponding (*E*)-ethyl 3-(benzofuran-2-yl)-3-phenylacrylate (1eq) in ethanol (10 mL) was added Pd/C (10 %) and a solution of sodium hypophosphite (1.5 eq) in 7 mL of water. The mixture was stirred at 50 °C for 1.5 hours. After the completion of the reaction the catalyst was filtered off and the crude hydrolyzed (50 mL), extracted with dichloromethane (3 x 20 mL), dried over MgSO₄ and evaporated. The resultant oil was subjected to silica gel chromatography to give the appropriate product.

Method G: Synthesis of MOM-ether

Bromomethyl-methylether (1 eq) was added dropwise to a stirred suspension of the corresponding hydroxyl derivative (1.5 eq) and sodium hydride (1 eq) in dimethoxyethane at 0 °C. The mixture was stirred for 1h at room temperature. After the complete addition water was carefully added and it was extracted with ethylacetate (3x), dried over MgSO₄ and concentrated in vacuo.

Method H: Michael Addition Reaction I

The corresponding chalcone (1 eq) and magnesium oxide (0.1 g / 0.1 mmol) were dissolved in toluene and diethyl malonate (1 eq) was added. The reaction was stirred at rt for 2 hours. The magnesium oxide was separated by vacuum filtration and was washed three times with 10 mL dichloromethane. The solvent was evaporated and the crude product was crystallized from diethyl ether and hexane.

Method I: Michael Addition Reaction II

The corresponding chalcone (1 eq) and diethyl malonate (1.1 eq) were dissolved in ethanol and potassium carbonate (2 eq) was added. The mixture was heated at reflux for 2 hours. The reaction was quenched with H₂O (50 mL) and extracted with CH₂Cl₂ (3 x 20 mL). The

organic layer was washed with brine, dried with MgSO_4 and evaporated under vacuum. The crude product was crystallized from methylene chloride and hexane.

Method J: Michael Addition Reaction III

The corresponding chalcone (1 eq) and diethyl malonate (1 eq) were dissolved in methanol and sodium hydride (cat) was added. The mixture was heated at reflux for 2 hours. The reaction was quenched with H_2O (50 mL) and extracted with CH_2Cl_2 (3 x 20 mL). The organic layer was washed with brine, dried with MgSO_4 and evaporated under vacuum. The crude product was crystallized from methylene chloride and hexane.

Method K: Deprotection of MOM-ether

A solution of the corresponding MOM derivative was treated with 10 % HCl (2 mL) in methanol (10 mL) and the resulting mixture was refluxed for 2h. After cooling the solvent was removed, the residue was extracted with ethyl acetate (3x) and dried with MgSO_4 . Then the crude product was concentrated to obtain the product (quant, without further purification).

Method L: Hydrolysis II

A solution of the corresponding malon ester (1 eq) and NaOH_{aq} (3eq) in EtOH was refluxed for 4 hours. After the completion of reaction, the cooled mixture was poured into water (30 mL), acidified to pH 2 with 10 % HCl and extracted with ethyl acetate (3 x 20 mL). The ethyl acetate extracts were collected and further extracted with aqueous sodium bicarbonate solution (4 x 20 mL). The bicarbonate extractions were made acidic with 10 % HCl which was added until a pH of 2 was obtained. The white solids were formed which were further extracted with ethyl acetate (3x50 mL.). The organic solution was dried over MgSO_4 and evaporated to afford a residue, which was purified by crystallization to afford the acids.

Method M: Esterification

To a stirred solution of the corresponding malonic acid derivative (1 eq) and NEt_3 (5 eq) in anhydrous DMF (5 mL), bromomethyl acetate (3 eq) was added. After being stirred for 4h at rt, the mixture was hydrolyzed, extracted with ethyl acetate (3 x), washed with brine, dried over MgSO_4 , filtered and concentrated at reduced pressure. The residue was purified by flash column chromatography.

Method N: Decarboxylation

The corresponding malonic acid derivative (1 eq) was pyrolytic treated in an oil bath at 160 °C for 1 hour and the heating was stopped after the CO₂ evolution ceased. The crude acid was dissolved in acetone/methanol and precipitated with dichloromethane to afford the acid.

6.1.3. Analytical data**6.1.3.1. Compounds described in Chapter 3.1.****5-(4-Chlorophenyl)-3-phenylpent-2-enoic acids, (2E & 2Z):****3-(4-Chlorophenyl)-1-phenylprop-2-en-1-one, (2c):**

Synthesized according to Method A using 4-chlorobenzaldehyde **2d** (9.36 g, 67.0 mmol) and acetophenone (8.0 g, 67.0 mmol); pale yellow solid; yield: 15.3 g (94 %); Mp 113-114 °C;

¹H NMR (CDCl₃, 500 MHz): δ = 7.39 (d, ³J = 8.5 Hz, 2H), 7.47-7.51 (m, 3H), 7.58-7.60 (m, 3H), 7.75 (d, ³J = 15.7 Hz, 1H), 8.00-8.03 (m, 2H). ¹³C NMR (CDCl₃, 125 MHz): δ = 128.4, 128.7, 129.2, 129.5, 132.1, 132.9, 133.4, 136.4, 138.0, 144.7, 189.9.

3-(4-Chlorophenyl)-1-phenylpropan-1-one, (2b):

Synthesized according to Method B using compound **2c** (0.636 g, 2.62 mmol), HEH (1.0 g, 3.93 mmol) and silica gel (5.26 g); white solid; yield: 0.49 g (81 %); Mp 99-100 °C;

¹H NMR (CDCl₃, 500 MHz): δ = 2.95 (t, ³J = 7.6, 2H), 3.21 (t, ³J = 7.6, 2H), 7.17-7.19 (m, 2H), 7.19 (m, 2H), 7.44-7.47 (m, 2H), 7.55-7.58 (m, 1H), 7.96-7.94 (m, 2H). ¹³C NMR (CDCl₃, 125 MHz): δ = 29.6, 40.4, 128.2, 129.8, 128.9, 130.1, 132.1, 133.4, 137.0, 139.0, 199.1.

Ethyl 5-(4-chlorophenyl)-3-phenylpent-2-enoate, (2a):

Synthesized according to Method C using compound **2b** (0.346 g, 1.41 mmol), NaH (0.17 g, 4.23 mmol) and triethyl phosphonoacetate (0.96 mL, 4.23 mmol);

2Ea: colourless oil; yield: 0.19 g (42 %); ¹H NMR (CDCl₃, 500 MHz): δ = 1.30 (t, ³J = 7.2 Hz, 3H), 2.68-2.72 (m, 2H), 3.36-3.39 (m, ³J = 8.3 Hz, 2H), 4.20 (q, ³J = 7.2 Hz, 2H), 6.06 (s, 1H), 7.12-7.15 (m, 2H), 7.21-7.23 (m, 2H), 7.38-7.40 (m, 3H), 7.42-7.45 (m, 2H). ¹³C

NMR (CDCl₃, 125 MHz): δ = 14.3, 32.9, 34.4, 59.9, 118.1, 126.7, 128.3, 128.7, 129.0, 129.9, 131.6, 139.9, 140.9, 158.9, 165.9.

2Za: colourless oil; yield: 0.17 g (38 %); ¹H NMR (CDCl₃, 500 MHz): δ = 1.06 (t, ³J = 7.2 Hz, 3H), 2.65-2.68 (m, 2H), 2.69-2.72 (m, 2H), 4.98 (q, ³J = 7.2 Hz, 1H), 5.87 (s, 1H), 7.05 (d, ³J = 8.2 Hz, 2H), 7.17 (d, ³J = 7.8 Hz, 2H), 7.23 (d, ³J = 8.2 Hz, 2H), 7.37-7.34 (m, 3H). ¹³C NMR (CDCl₃, 125 MHz): δ = 13.9, 33.1, 41.8, 59.9, 118.1, 127.2, 127.8, 127.9, 128.5, 129.6, 131.9, 139.2, 139.6, 157.8, 164.9.

(E)-5-(4-Chlorophenyl)-3-phenylpent-2-enoic acid, (2E):

Synthesized according to Method D using compound **2Ea** (0.16 g, 0.51 mmol) and NaOH_{aq} (1.1 mL, 5.1 mmol); white solid; yield: 0.105 g (72 %); Mp 117-118 °C;

¹H NMR (CDCl₃, 500 MHz): δ = 2.70-2.74 (m, 2H), 3.37-3.41 (m, 2H), 6.11 (s, 1H), 7.12 (d, ³J = 8.5 Hz, 2H), 7.22 (d, ³J = 8.2 Hz, 2H), 7.39-7.42 (m, 3H), 7.44-7.48 (m, 2H); ¹³C NMR (CDCl₃, 125 MHz): δ = 17.2, 33.5, 60.2, 126.9, 127.6, 128.0, 128.1, 129.5, 131.2, 141.3, 144.8, 148.8, 180.5; NOESY experiment (¹H NMR (CDCl₃, 500 MHz) showed a cross peak between the signal at 7.44-7.48 (m, 2H) and the signal at 6.11 (s, 1H). LC/MS (+ESI): m/z = 287.6 [MH⁺], R_t = 14.13 (\geq 99 %).

(Z)-5-(4-Chlorophenyl)-3-phenylpent-2-enoic acid, (2Z):

Synthesized according to Method D using compound **2Za** (0.139 g, 0.44 mmol) and NaOH_{aq} (1.1 mL, 4.4 mmol); white solid; yield: 0.093 g (74 %); Mp 114-115 °C;

¹H NMR (CDCl₃, 500 MHz): δ = 2.64-2.67 (m, 2H), 2.71-2.77 (m, 2H), 5.87 (s, 1H), 7.04 (d, ³J = 8.5 Hz, 2H), 7.18 (m, 2H), 7.24 (d, ³J = 8.5 Hz, 2H), 7.34 (m, 3H); ¹³C NMR (CDCl₃, 125 MHz): δ = 15.9, 32.8, 60.2, 127.1, 127.6, 128.0, 129.7, 131.8, 139.8, 142.4, 145.3, 170.5; NOESY experiment (¹H NMR (CDCl₃, 500 MHz) showed a cross peak between the signals at 2.64-2.67 (m, 2H) and at 2.71-2.77 (m, 2H), and the signal at 5.87 (s, 1H). LC/MS (+ESI): m/z = 287.5 [MH⁺], R_t = 13.56 (\geq 99 %).

5-(3-Chlorophenyl)-3-phenylpent-2-enoic acids (3E & 3Z):

3-(3-Chlorophenyl)-1-phenylprop-2-en-1-one, (3c):

Synthesized according to Method A using 3-chlorobenzaldehyde **3d** (0.8 mL, 7.11 mmol) and acetophenone (0.83 mL, 7.11 mmol); pale yellow solid; yield: 1.62 g (94 %); Mp 110-111 °C;

¹H NMR (CDCl₃, 500 MHz): δ = 7.39-7.44 (m, 2H), 7.50-7.55 (m, 4H), 7.60-7.64 (m, 2H),

7.73 (d, $^3J = 15.3$ Hz, 1H), 8.02 (d, $^3J = 8.5$ Hz, 1H). ^{13}C NMR (CDCl_3 , 125 MHz): $\delta = 123.2$, 126.8, 127.9, 128.5, 128.7, 130.2, 130.3, 133.0, 134.9, 137.9, 143.0, 190.1.

3-(3-Chlorophenyl)-1-phenylpropan-1-one, (3b):

Synthesized according to Method B using compound **3c** (0.60 g, 2.47 mmol), HEH (0.94 g, 3.70 mmol) and silica gel (4.94 g); white solid; yield: 0.57 g (89 %); Mp 82-84 °C;

^1H NMR (CDCl_3 , 500 MHz): $\delta = 3.03$ -3.07 (m, 2H), 3.29-3.32 (m, 2H), 7.27-7.32 (m, 4H), 7.46 (t, $^3J = 7.9$ Hz, 2H), 7.57 (t, $^3J = 7.6$ Hz, 1H), 7.96 (d, $^3J = 7.9$ Hz, 2H). ^{13}C NMR (CDCl_3 , 125 MHz): $\delta = 29.7$, 40.0, 126.3, 126.7, 128.0, 128.6, 128.6, 129.7, 133.2, 134.3, 136.8, 143.3, 198.7.

Ethyl 5-(3-chlorophenyl)-3-phenylpent-2-enoate, (3a):

Synthesized according to Method C using compound **3b** (0.40 g, 1.63 mmol), NaH (0.20 g, 4.89 mmol) and triethyl phosphonoacetate (0.97 mL, 4.89 mmol);

3Ea: colourless oil; yield: 0.22 g (43 %); ^1H NMR (CDCl_3 , 500 MHz): $\delta = 1.32$ (t, $^3J = 6.9$ Hz, 3H), 2.69-2.74 (m, 2H), 3.37-3.41 (m, 2H), 4.21 (q, $^3J = 7.2$ Hz, 2H), 6.07 (s, 1H), 7.16-7.20 (m, 4H), 7.42-7.46 (m, 5H). ^{13}C NMR (CDCl_3 , 125 MHz): $\delta = 14.3$, 32.7, 34.7, 59.9, 118.1, 126.1, 126.7, 128.6, 128.7, 129.0, 129.5, 133.9, 140.9, 141.3, 143.5, 158.8, 166.3.

3Za: colourless oil; yield: 0.19 g (38 %); ^1H NMR (CDCl_3 , 500 MHz): $\delta = 1.07$ (t, $^3J = 7.2$ Hz, 3H), 2.66-2.70 (m, 2H), 2.74-2.79 (m, 2H), 3.98 (q, $^3J = 7.2$ Hz, 2H), 5.88 (s, 1H), 7.05 (d, $^3J = 7.2$ Hz, 1H), 7.11 (s, 1H), 7.16-7.21 (m, 4H), 7.30-7.37 (m, 3H). ^{13}C NMR (CDCl_3 , 125 MHz): $\delta = 13.9$, 33.5, 41.7, 59.9, 118.0, 126.3, 126.5, 127.8, 128.0, 128.4, 129.7, 134.2, 139.6, 142.8, 157.7, 165.8.

(E)-5-(3-Chlorophenyl)-3-phenylpent-2-enoic acid, (3E):

Synthesized according to Method D using compound **3Ea** (0.2 g, 0.63 mmol) and NaOH_{aq} (2.1 mL, 6.3 mmol); white solid; yield: 0.158 g (88 %); Mp 98-100 °C;

^1H NMR (CDCl_3 , 500 MHz): $\delta = 2.72$ -2.77 (m, 2H), 3.40-3.43 (m, 2H), 6.13 (s, 1H), 7.09 (d, $^3J = 7.2$ Hz, 1H), 7.19-7.15 (m, 3H), 7.41-7.45 (m, 3H), 7.46-7.50 (m, 2H); ^{13}C NMR (CDCl_3 , 125 MHz): $\delta = 33.0$, 34.8, 117.0, 126.6, 126.7, 126.8, 128.6, 129.5, 129.6, 134.0, 140.7, 143.3, 162.0, 170.8; LC/MS (+ESI): $m/z = 288.6$ [MH^+]; $R_t = 14.06$ ($\geq 97\%$).

(Z)-5-(3-Chlorophenyl)-3-phenylpent-2-enoic acid, (3Z):

Synthesized according to Method D using compound **3Za** (0.17 g, 0.54 mmol) and NaOH_{aq} (1.8 mL, 5.4 mmol); white solid; yield: 0.135 g (87 %); Mp 102-104 °C;

^1H NMR (CDCl_3 , 500 MHz) δ = 2.63-2.67 (m, 2H), 2.74-2.77 (m, 2H), 5.85 (s, 1H), 6.98 (td, 4J = 1.6, 3J = 7.2 Hz, 1H), 7.09-7.10 (m, 1H), 7.15-7.18 (m, 3H), 7.18-7.21 (m, 1H), 7.31-7.33 (m, 1H), 7.33-7.36 (m, 2H); ^{13}C NMR (CDCl_3 , 125 MHz): δ = 33.3, 42.0, 117.0, 126.0, 126.4, 127.2, 128.1, 128.2, 128.4, 128.6, 129.7, 138.8, 142.6, 160.6, 170.1; LC/MS (+ESI): m/z = 288.6 [MH^+]; R_t = 13.43 ($\geq 99\%$).

5-(4-Fluorophenyl)-3-phenylpent-2-enoic acids (4E & 4Z):

3-(4-Fluorophenyl)-1-phenylprop-2-en-1-one, (4c):

Synthesized according to Method A using 4-fluorobenzaldehyde **4d** (2.0 g, 16.11 mmol) and acetophenone (1.88 mL, 16.11 mmol); yellow solid; yield: 3.35 g (92 %); Mp 88-90 °C;

^1H NMR (CDCl_3 , 500 MHz): δ = 7.09-7.13 (m, 2H), 7.44-7.52 (m, 3H), 7.57-7.65 (m, 3H), 7.77 (d, 3J = 15.8 Hz, 1H), 8.00-8.02 (m, 2H). ^{13}C NMR (CDCl_3 , 125 MHz): δ = 116.1 (d, 2J (C, F) = 21.9 Hz, CH), 121.8, 128.4, 128.6, 130.3 (d, 3J (C, F) = 8.2 Hz, CH), 131.1 (d, 4J (C, F) = 3.7 Hz, CH), 132.8, 138.1, 143.4, 164.0 (d, 1J (C, F) = 252.0 Hz, C_{quat}), 190.3.

3-(4-Fluorophenyl)-1-phenylpropan-1-one, (4b):

Synthesized according to Method B using compound **4c** (0.50 g, 2.21 mmol), HEH (0.84 g, 3.31 mmol) and silica gel (4.42 g); pale yellow oil; yield: 0.476 g (94 %);

^1H NMR (CDCl_3 , 500 MHz): δ = 3.05 (t, 3J = 7.6, 2H), 3.29 (t, 3J = 7.6, 2H), 6.99-6.95 (m, 2H), 7.22-7.19 (m, 2H), 7.46 (t, 3J = 7.6 Hz, 2H), 7.58-7.54 (m, 1H), 7.95 (d, 3J = 8.5 Hz, 2H). ^{13}C NMR (CDCl_3 , 125 MHz): δ = 29.2, 40.4, 115.2 (d, J (C, F) = 21.1 Hz, CH), 127.9, 128.6, 129.8 (d, J (C, F) = 7.7 Hz, CH), 133.1, 136.7, 136.8, 161.0 (d, J (C, F) = 243.8 Hz, C_{quat}), 198.9.

Ethyl 5-(4-fluorophenyl)-3-phenylpent-2-enoate, (4a):

Synthesized according to Method C using compound **4b** (0.40 g, 1.75 mmol), NaH (0.21 g, 5.26 mmol) and triethyl phosphonoacetate (1.2 mL, 5.42 mmol);

4Ea: colourless oil; yield: 0.193 g (37%); ^1H NMR (CDCl_3 , 500 MHz): δ = 1.06 (t, 3J = 7.2 Hz, 3H), 2.65-2.75 (m, 4H), 3.98 (q, 3J = 7.2 Hz, 2H), 5.87 (s, 1H), 6.93-6.97 (m, 2H), 7.06-7.09 (m, 2H), 7.16-7.18 (m, 2H), 7.31-7.38 (m, 3H). ^{13}C NMR (CDCl_3 , 125 MHz): δ = 13.9, 32.9, 42.1, 59.8, 115.0, 115.1 (d, J (C, F) = 22.1 Hz, CH), 117.9, 127.2, 127.7, 127.8, 127.9,

129.6 (d, J (C, F) = 7.7 Hz, CH), 136.4, 139.7, 158.0, 161.0 (d, J (C, F) = 243.8 Hz, C_{quat}), 165.8.

4Za: colourless oil; yield: 0.189 g (36 %); ¹H NMR (CDCl₃, 500 MHz): δ = 1.29 (t, ³ J = 7.2 Hz, 3H), 2.69-2.72 (m, 2H), 3.36-3.39 (m, 2H), 4.20 (q, ³ J = 7.2 Hz, 2H), 6.06 (s, 1H), 6.92-6.96 (m, 2H), 7.15-7.18 (m, 2H), 7.46-7.35 (m, 5H). ¹³C NMR (CDCl₃, 125 MHz): δ = 14.3, 31.1, 34.3, 59.9, 115.0 (d, J (C, F) = 21.1 Hz, CH), 117.9, 126.7, 128.6, 129.0, 129.8 (d, J (C, F) = 7.7 Hz, CH), 137.1, 140.9, 159.1, 161.0 (d, J (C, F) = 243.8 Hz, C_{quat}), 166.3.

(E)-5-(4-Fluorophenyl)-3-phenylpent-2-enoic acid, (4E):

Synthesized according to Method D using compound **4Ea** (0.185 g, 0.62 mmol) and NaOH_{aq} (2.1 mL, 6.2 mmol); white solid; yield: 0.150 g (90 %); Mp 95-98 °C;

¹H NMR (CDCl₃, 500 MHz): δ = 2.72-2.75 (m, 2H), 3.38-3.42 (m, 2H), 6.12 (s, 1H), 6.92-6.96 (m, 2H), 7.13-7.16 (m, 2H), 7.41-7.42 (m, 3H), 7.46-7.48 (m, 2H); ¹³C NMR (CDCl₃, 125 MHz): δ = 33.4, 34.4, 115.0 (d, J (C, F) = 21.1 Hz, CH), 116.9, 126.8, 128.7, 129.4, 129.8 (d, J (C, F) = 8.6 Hz, CH), 136.9, 140.8, 149.5, 161.0 (d, J (C, F) = 240.9 Hz, C_{quat}), 170.9; LC/MS (+ESI): m/z = 271.5 [MH⁺]; R_t = 13.24 (\geq 99 %).

(Z)-5-(4-Fluorophenyl)-3-phenylpent-2-enoic acid, (4Z):

Synthesized according to Method D using compound **4Za** (0.18 g, 0.60 mmol) and NaOH_{aq} (2.0 mL, 5.4 mmol); white solid; yield: 0.135 g (83 %); Mp 90-92 °C;

¹H NMR (CDCl₃, 500 MHz): δ = 2.63-2.67 (m, 2H), 2.73-2.77 (m, 2H), 5.87 (s, 1H), 6.93-7.07 (m, 2H), 7.16-7.23 (m, 2H), 7.34-7.39 (m, 5H); ¹³C NMR (CDCl₃, 125 MHz): δ = 34.3, 42.4, 116.0 (d, J (C, F) = 21.1 Hz, CH), 117.9, 127.2, 128.2, 128.6, 129.6, 132.0 (, J (C, F) = 7.7 Hz, CH), 141.5, 160.4, 161.5 (d, J (C, F) = 264.9 Hz, C_{quat}), 168.2; LC/MS (+ESI): m/z = 271.5 [MH⁺]; R_t = 12.73 (\geq 98 %).

5-(4-Bromophenyl)-3-phenylpent-2-enoic acids, (5E & 5Z):

3-(4-Bromophenyl)-1-phenylprop-2-en-1-one, (5c):

Synthesized according to Method A using 4-bromobenzaldehyde **5d** (2.0 g, 10.81 mmol) and acetophenone (1.26 mL, 10.81 mmol); yellow solid; yield: 2.80 g (90 %); Mp 121-123 °C;

¹H NMR (CDCl₃, 500 MHz): δ = 7.50-7.61 (m, 8H), 7.74 (d, ³ J = 15.7 Hz, 1H), 8.01 (dd, ⁴ J = 1.4, ³ J = 7.2 Hz, 2H). ¹³C NMR (CDCl₃, 125 MHz): δ = 122.6, 124.8, 128.5, 128.7, 129.8, 132.2, 132.9, 133.8, 138.0, 143.4, 190.2.

3-(4-Bromophenyl)-1-phenylpropan-1-one, (5b):

Synthesized according to Method B using compound **5c** (0.50 g, 1.74 mmol), HEH (0.661 g, 2.61 mmol) and silica gel (3.48 g); pale yellow solid; yield: 0.479 g (95 %); Mp 73-75 °C; ¹H NMR (CDCl₃, 500 MHz): δ = 3.03 (t, ³J = 7.6 Hz, 2H), 3.28 (t, ³J = 7.6 Hz, 2H), 7.13 (d, ³J = 8.5 Hz, 2H), 7.30 (d, ³J = 8.5 Hz, 2H), 7.46 (t, ³J = 7.2 Hz, 2H), 7.58-7.55 (m, 1H), 7.94 (dd, ⁴J = 1.3, ³J = 7.2 Hz, 2H). ¹³C NMR (CDCl₃, 125 MHz): δ = 29.4, 40.0, 119.9, 128.0, 128.6, 130.2, 131.5, 133.2, 136.7, 140.2, 198.8.

Ethyl 5-(4-bromophenyl)-3-phenylpent-2-enoate, (5a):

Synthesized according to Method C using compound **5b** (0.40 g, 1.38 mmol), NaH (0.166 g, 4.15 mmol) and triethyl phosphonoacetate (0.94 mL, 4.15 mmol);

5Ea: colourless oil; yield: 0.226 g (46 %); ¹H NMR (CDCl₃, 500 MHz): δ = 1.30 (t, ³J = 7.2 Hz, 3H), 2.67-2.70 (m, 2H), 3.36-3.92 (m, 2H), 4.20 (q, ³J = 7.2 Hz, 2H), 6.06 (s, 1H), 7.08 (d, ³J = 8.5 Hz, 2H), 7.38-7.45 (m, 7H). ¹³C NMR (CDCl₃, 125 MHz): δ = 14.3, 32.8, 34.5, 59.9, 118.1, 119.7, 126.7, 128.7, 129.1, 130.3, 131.3, 140.9, 158.9, 166.2.

5Za: colourless oil; yield: 0.205 g (41 %); ¹H NMR (CDCl₃, 500 MHz): δ = 1.06 (t, ³J = 7.2 Hz, 3H), 2.63-2.75 (m, 4H), 3.98 (q, ³J = 7.2 Hz, 2H), 5.87 (s, 1H), 7.00 (d, ³J = 8.5 Hz, 1H), 7.16-7.18 (m, 2H), 7.31-7.40 (m, 5H). ¹³C NMR (CDCl₃, 125 MHz): δ = 12.2, 33.4, 42.0, 60.1, 118.3, 120.2, 127.4, 128.0, 128.2, 130.3, 131.7, 139.8, 140.0, 158.0, 166.1.

(E)-5-(4-Bromophenyl)-3-phenylpent-2-enoic acid, (5E):

Synthesized according to Method D using compound **5Ea** (0.20 g, 0.56 mmol) and NaOH_{aq} (0.56 mL, 1.68 mmol); white solid; yield: 0.162 g (88 %); Mp 137-140 °C; ¹H NMR (CDCl₃, 500 MHz): δ = 2.70-2.73 (m, 2H), 3.38-3.40 (m, 2H), 6.12 (s, 1H), 7.07 (d, ³J = 8.2 Hz, 2H), 7.37 (d, ³J = 8.5 Hz, 2H), 7.41-7.45 (m, 3H), 7.45-7.47 (m, 2H); ¹³C NMR (CDCl₃, 125 MHz): δ = 33.2, 34.5, 116.8, 126.8, 128.8, 129.5, 130.2, 131.4, 131.7, 140.2, 140.7, 162.1, 169.9; LC/MS (+ESI): *m/z* = 332.3 [MH⁺]; *R_t* = 14.53 (≥ 99 %).

(Z)-5-(4-Bromophenyl)-3-phenylpent-2-enoic acid, (5Z):

Synthesized according to Method D using compound **5Za** (0.18 g, 0.50 mmol) and NaOH_{aq} (0.5 mL, 1.5 mmol); white solid; yield: 0.148 g (90 %); Mp 120-122 °C; ¹H NMR (CDCl₃, 500 MHz): δ = 2.62-2.65 (m, 2H), 2.73-2.76 (m, 2H, ³J = 8.3 Hz, 2H), 5.85 (s, 1H), 6.98 (d, ³J = 8.5 Hz, 2H), 7.11 (d, ³J = 8.5 Hz, 2H), 7.29-7.42 (m, 5H); ¹³C NMR (CDCl₃, 125 MHz): δ = 33.1, 35.7, 116.9, 127.4, 128.5, 130.0, 130.5, 131.6, 133.1, 139.5, 141.4, 160.8, 169.9; LC/MS (+ESI): *m/z* = 332.3 [MH⁺]; *R_t* = 13.93 (≥ 99 %).

3-Phenyl-5-(4-(trifluoromethyl)phenyl)pent-2-enoic acids, (6E & 6Z):**3-(4-(Trifluoromethylphenyl)-1-phenylprop-2-en-1-one, (6c):**

Synthesized according to Method A using 4-trifluoromethylbenzaldehyde **6d** (2.00 g, 11.5 mmol) and acetophenone (1.34 mL, 11.5 mmol); yellow solid; yield: 3.05 g (94 %); Mp 129-131 °C;

¹H NMR (CDCl₃, 500 MHz): δ = 7.50-7.55 (m, 2H), 7.58-7.63 (m, 2H), 7.68 (d, ³J = 8.5 Hz, 2H), 7.74 (d, ³J = 8.5 Hz, 2H), 7.81 (d, ³J = 15.8 Hz, 1H), 8.02-8.04 (m, 2H). ¹³C NMR (CDCl₃, 125 MHz): δ = 124.3, 125.9 (q, J(C, F) = 3.7, CH), 128.5, 128.6, 128.7, 129.4, 131.9 (d, J(C-F) = 32.6), 132.1, 133.2, 138.1 (d, J(C, F) = 61.4 Hz, CH), 142.7, 190.6.

1-Phenyl-3-(4-(trifluoromethyl)phenyl)propan-1-one, (6b):

Synthesized according to Method B using compound **6c** (0.50 g, 1.81 mmol), HEH (0.687 g, 2.71 mmol) and silica gel (3.62 g); pale yellow oil; yield: 0.438 g (87 %);

¹H NMR (CDCl₃, 500 MHz): δ = 3.14 (t, ³J = 7.6 Hz, 2H), 3.32 (t, ³J = 7.6 Hz, 2H), 7.37 (d, ³J = 7.9 Hz, 2H), 7.46 (t, J = 7.9 Hz, 2H), 7.54-7.56 (m, 3H), 7.95 (d, ³J = 8.2 Hz, 2H). ¹³C NMR (CDCl₃, 125 MHz): δ = 29.8, 39.8, 125.2, 125.4, 127.9, 128.7, 128.8, 133.2, 136.7, 145.1, 145.4, 190.8.

Ethyl 3-phenyl-5-(4-(trifluoromethyl)phenyl)pent-2-enoate, (6a):

Synthesized according to Method C using compound **6b** (0.35 g, 1.26 mmol), NaH (0.151 g, 3.77 mmol) and triethyl phosphonoacetate (0.86 mL, 3.77 mmol);

6Ea: colourless oil; yield: 0.19 g (43 %); ¹H NMR (CDCl₃, 500 MHz): δ = 1.30 (t, ³J = 7.2 Hz, 3H), 2.79-2.81 (m, 2H), 3.40-3.44 (m, 2H), 4.20 (q, ³J = 7.2 Hz, 2H), 6.07 (s, 1H), 7.31 (d, ³J = 8.2 Hz, 2H), 7.39-7.45 (m, 5H), 7.50 (d, ³J = 8.2 Hz, 2H); ¹³C NMR (CDCl₃, 125 MHz): δ = 14.3, 32.6, 34.9, 59.9, 118.2, 125.0, 125.2 (d, J(C, F) = 3.9 Hz, CH), 126.7, 128.4, 128.5, 128.6, 128.8, 129.1, 140.8, 145.5, 158.8, 166.3;

6Za: colourless oil; yield: 0.162 g (36 %); ¹H NMR (CDCl₃, 500 MHz): δ = 1.06 (t, ³J = 7.2 Hz, 3H), 2.73-2.79 (m, 4H), 3.98 (q, ³J = 7.2 Hz, 2H), 5.89 (s, 1H), 7.18 (d, ³J = 8.2 Hz, 2H), 7.23 (d, ³J = 8.2 Hz, 2H), 7.32-7.39 (m, 3H), 7.52 (d, ³J = 7.9 Hz, 2H); ¹³C NMR (CDCl₃, 125 MHz): δ = 13.9, 33.6, 41.5, 59.9, 118.1, 125.2, 125.3 (d, J(C, F) = 3.9 Hz, CH), 125.4, 127.2, 127.9, 128.0, 128.4, 128.6, 139.4, 144.9, 157.5, 165.8;

(E)-3-Phenyl-5-(4-(trifluoromethyl)phenyl)pent-2-enoic acid, (6E):

Synthesized according to Method D using compound **6Ea** (0.19 g, 0.54 mmol) and NaOH_{aq} (1.80 mL, 5.45 mmol); white solid; yield: 0.163 g (95 %); Mp 127-129 °C;

¹H NMR (CDCl₃, 500 MHz): δ = 2.80-2.83 (m, 2H), 3.41-3.45 (m, 2H), 6.13 (s, 1H), 7.30 (d, ³J = 8.2 Hz, 2H), 7.41-7.48 (m, 5H), 7.51 (d, ³J = 8.2 Hz, 2H); ¹³C NMR (CDCl₃, 125 MHz): δ = 32.9, 34.9, 117.0, 125.2 (d, J (C, F) = 3.7 Hz, CH), 126.7, 128.3, 128.6, 128.8, 128.8, 129.1, 129.5, 140.6, 145.3 (d, J (C, F) = 1.9 Hz, CH), 162.0, 170.9; LC/MS (+ESI): m/z = 321.5 [MH⁺]; R_t = 14.27 (≥ 99 %).

(Z)-3-Phenyl-5-(4-(trifluoromethyl)phenyl)pent-2-enoic acid, (6Z):

Synthesized according to Method D using compound **6Za** (0.15 g, 0.43 mmol) and NaOH_{aq} (1.4 mL, 4.31 mmol); white solid; yield: 0.113 g (82 %); Mp 125-127 °C;

¹H NMR (CDCl₃, 500 MHz): δ = 2.70-2.78 (m, 4H), 5.85 (s, 1H), 7.14-7.16 (m, 2H), 7.19-7.29 (m, 2H), 7.30-7.37 (m, 3H), 7.49-7.54 (m, 2H); ¹³C NMR (CDCl₃, 125 MHz): δ = 33.5, 34.9, 125.3 (d, J (C, F) = 3.7 Hz, CH), 125.9, 127.2, 127.5, 128.1, 128.5, 128.6, 128.8, 130.0, 133.5, 144.6, 160.6, 170.0; LC/MS (+ESI): m/z = 321.5 [MH⁺]; R_t = 13.74 (≥ 95 %).

5-(3,4-Dichlorophenyl)-3-phenylpent-2-enoic acids, (7E & 7Z):**3-(3,4-Dichlorophenyl)-1-phenylprop-2-en-1-one, (7c):**

Synthesized according to Method A using 3,4-dichlorobenzaldehyde **7d** (2.00 g, 11.4 mmol) and acetophenone (1.33 mL, 11.4 mmol); pale yellow solid; yield: 3.00 g (94 %); Mp 110-113 °C;

¹H NMR (CDCl₃, 500 MHz): δ = 7.44-7.53 (m, 5H), 7.59-7.62 (m, 1H), 7.69 (d, ³J = 15.8 Hz, 1H), 7.72 (d, ³J = 1.9 Hz, 1H), 8.00-8.03 (m, 2H). ¹³C NMR (CDCl₃, 125 MHz): δ = 123.5, 127.5, 128.5, 128.7, 129.7, 131.0, 133.1, 133.3, 134.4, 134.9, 137.8, 141.9, 189.9.

3-(3,4-Dichlorophenyl)-1-phenylpropan-1-one, (7b):

Synthesized according to Method B using compound **7c** (0.50 g, 1.80 mmol), HEH (0.685 g, 2.70 mmol) and silica gel (3.60 g); pale yellow oil; yield: 0.416 g (83 %);

¹H NMR (CDCl₃, 500 MHz): δ = 3.03 (t, ³J = 7.2 Hz, 2H), 3.28 (t, ³J = 7.2 Hz, 2H), 7.09 (dd, ⁴J = 1.9, ⁴J = 8.5 Hz, 1H), 7.35-7.34 (m, 2H), 7.46 (t, ³J = 7.2 Hz, 2H), 7.59-7.55 (m, 1H), 7.96-7.94 (m, 2H). ¹³C NMR (CDCl₃, 125 MHz): δ = 29.9, 39.7, 127.9, 128.0, 128.7, 130.0, 130.3, 130.4, 132.3, 133.2, 136.6, 141.5, 198.4.

Ethyl 5-(3,4-dichlorophenyl)-3-phenylpent-2-enoate, (7a):

Synthesized according to Method C using compound **7b** (0.35 g, 1.25 mmol), NaH (0.15 g, 3.76 mmol) and triethyl phosphono-acetate (0.85 mL, 3.76 mmol);

7Ea: colourless oil; yield: 0.204 g (47 %); ^1H NMR (CDCl_3 , 500 MHz): δ = 1.30 (t, 3J = 7.2 Hz, 3H), 2.67-2.71 (m, 2H), 3.36-3.39 (m, 2H), 4.20 (q, 3J = 7.2 Hz, 2H), 6.06 (s, 1H), 7.04 (dd, 4J = 1.9, 3J = 8.2 Hz, 1H), 7.28 (d, 4J = 2.2, 3J = 8.2 Hz, 1H), 7.30 (d, 3J = 8.2 Hz, 1H), 7.38-7.44 (m, 5H); ^{13}C NMR (CDCl_3 , 125 MHz): δ = 14.3, 32.5, 34.1, 60.0, 118.3, 126.7, 128.1, 128.7, 129.1, 129.8, 130.1, 130.5, 132.0, 140.7, 141.6, 158.6, 166.3.

7Za: colourless oil; yield: 0.178 g (41 %); ^1H NMR (CDCl_3 , 500 MHz): δ = 1.01 (t, 3J = 6.9 Hz, 3H), 2.75-2.63 (m, 4H), 3.98 (q, 3J = 6.9 Hz, 2H), 5.87 (s, 1H), 6.96 (dd, 4J = 2.2, 3J = 8.2 Hz, 2H), 7.17 (d, 3J = 8.2 Hz, 2H), 7.20 (s, 1H), 7.32-7.38 (m, 4H); ^{13}C NMR (CDCl_3 , 125 MHz): δ = 13.9, 32.9, 41.5, 59.9, 118.2, 127.2, 127.8, 127.9, 128.0, 130.1, 130.2, 130.3, 132.3, 139.3, 141.0, 157.3, 165.8.

(E)-5-(3,4-Dichlorophenyl)-3-phenylpent-2-enoic acid, (7E):

Synthesized according to Method D using compound **7Ea** (0.10 g, 0.29 mmol) and NaOH_{aq} (0.96 mL, 2.86 mmol); white solid; yield: 0.09 g (95 %); Mp 120-123 °C;

^1H NMR (CDCl_3 , 500 MHz): δ = 2.70-2.73 (m, 2H), 3.38-3.41 (m, 2H), 6.13 (s, 1H), 7.02 (dd, 4J = 1.9, 3J = 8.2 Hz, 1H), 7.27 (d, 4J = 2.2 Hz, 1H), 7.31 (d, 3J = 8.2 Hz, 1H), 7.41-7.46 (m, 5H); ^{13}C NMR (CDCl_3 , 125 MHz): δ = 32.8, 34.2, 117.0, 126.7, 128.0, 128.8, 129.6, 130.0, 130.2, 130.4, 132.1, 140.5, 141.4, 170.4, 196.6; LC/MS (+ESI): m/z = 322.6 [MH^+]; R_t = 14.88 (≥ 99 %).

(Z)-5-(3,4-Dichlorophenyl)-3-phenylpent-2-enoic acid, (7Z):

Synthesized according to Method D using compound **7Za** (0.10 g, 0.29 mmol) and NaOH_{aq} (0.96 mL, 2.86 mmol); white solid; yield: 0.085 g (91 %); Mp 130-134 °C;

^1H NMR (CDCl_3 , 500 MHz): δ = 2.62-2.65 (m, 2H), 2.74-2.77 (m, 2H), 5.86 (s, 1H), 6.93 (dd, 4J = 2.2, 3J = 8.2 Hz, 2H), 7.16-7.21 (m, 2H), 7.31-7.39 (m, 4H); ^{13}C NMR (CDCl_3 , 125 MHz): δ = 32.5, 35.5, 116.8, 125.8, 126.9, 127.5, 127.9, 128.0, 128.2, 130.2, 133.3, 139.9, 140.4, 160.3, 169.9; LC/MS (+ESI): m/z = 322.7 [MH^+]; R_t = 14.32 (≥ 99 %).

5-(2,4-Dichlorophenyl)-3-phenylpent-2-enoic acids, (8E & 8Z):**3-(2,4-Dichlorophenyl)-1-phenylprop-2-en-1-one, (8c):**

Synthesized according to Method A using 2,4-dichlorobenzaldehyde **8d** (2.0 g, 11.43 mmol) and acetophenone (1.33 mL, 11.43 mmol); yellow solid; yield: 3.1 g (94 %); Mp 175-178 °C; ¹H NMR (CDCl₃, 500 MHz): δ = 7.39 (dd, ⁴J = 2.2, ³J = 8.5 Hz, 1H), 7.46-7.53 (m, 4H), 7.59-7.62 (m, 1H), 7.69 (d, ³J = 8.2 Hz, 1H), 8.00-8.10 (m, 2H), 8.10 (d, ³J = 15.8 Hz, 1H). ¹³C NMR (CDCl₃, 125 MHz): δ = 125.1, 127.6, 127.9, 128.5, 128.6, 128.7, 130.1, 133.1, 136.0, 136.5, 137.8, 139.3, 190.1.

3-(2,4-Dichlorophenyl)-1-phenylpropan-1-one, (8b):

Synthesized according to Method B using compound **8c** (0.50 g, 1.80 mmol), HEH (0.685 g, 2.70 mmol) and silica gel (3.60 g); pale green oil; yield: 0.363 g (72 %); ¹H NMR (CDCl₃, 500 MHz): δ = 3.15 (t, ³J = 7.6 Hz, 2H), 3.29 (t, ³J = 7.6 Hz, 2H), 7.17 (dd, ⁴J = 2.2, ³J = 8.2 Hz, 1H), 7.26 (d, ³J = 8.2 Hz, 2H), 7.37 (d, ³J = 2.2 Hz, 1H), 7.46 (t, ³J = 7.6 Hz, 2H), 7.54-7.59 (m, 1H), 7.95-7.97 (m, 2H). ¹³C NMR (CDCl₃, 125 MHz): δ = 27.7, 38.1, 127.3, 128.0, 128.6, 129.3, 131.7, 132.7, 133.2, 134.6, 136.6, 137.4, 198.6.

Ethyl 5-(2,4-dichlorophenyl)-3-phenylpent-2-enoate, (8a):

Synthesized according to Method C using compound **8b** (0.30 g, 1.07 mmol), NaH (0.13 g, 3.22 mmol) and triethyl phosphonoacetate (0.73 mL, 3.22 mmol);

8Ea: colourless oil; yield: 0.147 g (39 %); ¹H NMR (CDCl₃, 500 MHz): δ = 1.29 (t, ³J = 7.2 Hz, 3H), 2.83-2.86 (m, 2H), 3.35-3.38 (m, 2H), 4.20 (q, ³J = 7.2 Hz, 2H), 6.10 (s, 1H), 7.14 (dd, ³J = 2.2, ³J = 8.2 Hz, 1H), 7.23 (d, ³J = 8.2 Hz, 2H), 7.31 (d, ³J = 2.2 Hz, 1H), 7.37-7.41 (m, 3H), 7.48-7.50 (m, 2H); ¹³C NMR (CDCl₃, 125 MHz): δ = 14.3, 30.9, 32.3, 60.0, 118.1, 126.7, 127.0, 128.6, 129.0, 129.1, 131.5, 132.3, 134.4, 137.7, 140.6, 158.6, 166.3.

8Za: colourless oil; yield: 0.179 g (48 %); ¹H NMR (CDCl₃, 500 MHz): δ = 1.07 (t, ³J = 7.2 Hz, 3H), 2.70-2.79 (m, 4H), 3.99 (q, ³J = 7.2 Hz, 2H), 5.91 (s, 1H), 7.05 (d, ³J = 8.2 Hz, 1H), 7.15 (dd, ⁴J = 2.2, ³J = 8.2 Hz, 1H), 7.19-7.21 (m, 2H), 7.31-7.38 (m, 4H). ¹³C NMR (CDCl₃, 125 MHz): δ = 13.9, 31.4, 39.8, 59.9, 118.0, 127.1, 127.3, 127.9, 128.0, 129.3, 131.1, 132.6, 134.5, 137.0, 139.4, 157.6, 165.9.

(E)-5-(2,4-Dichlorophenyl)-3-phenylpent-2-enoic acid, (8E):

Synthesized according to Method D using compound **8Ea** (0.10 g, 0.31 mmol) and NaOH_{aq} (0.32 mL, 0.93 mmol); white solid; yield: 0.09 g (87 %); Mp 118-120 °C;

¹H NMR (CDCl₃, 500 MHz): δ = 2.85-2.89 (m, 2H), 3.40-3.72 (m, 2H), 6.16 (s, 1H), 7.14 (dd, ⁴J = 2.2, ³J = 8.2 Hz, 2H), 7.19 (d, ³J = 8.2 Hz, 2H), 7.32 (d, ³J = 1.9 Hz, 1H), 7.40-7.41 (m, 3H), 7.51-7.53 (m, 2H); ¹³C NMR (CDCl₃, 125 MHz): δ = 31.1, 32.4, 116.8, 125.9, 126.8, 127.1, 128.7, 129.1, 129.6, 131.5, 132.5, 137.1, 137.5, 140.0, 169.9; LC/MS (+ESI): *m/z* = 322.2 [MH⁺]; *R_t* = 13.12 (≥ 93 %).

(Z)-5-(2,4-Dichlorophenyl)-3-phenylpent-2-enoic acid, (8Z):

Synthesized according to Method D using compound **8Za** (0.10 g, 0.31 mmol) and NaOH_{aq} (0.32 mL, 0.93 mmol); white solid; yield: 0.09 g (87 %); Mp 122-124 °C;

¹H NMR (CDCl₃, 500 MHz): δ = 2.67-2.74 (m, 4H), 5.88 (s, 1H), 7.03 (d, ³J = 8.2 Hz, 1H), 7.14 (dd, ³J = 2.2, ⁴J = 8.2 Hz, 1H), 7.19-7.21 (m, 2H), 7.33-7.39 (m, 4H); ¹³C NMR (CDCl₃, 125 MHz): δ = 32.5, 40.2, 116.9, 127.1, 127.3, 128.2, 128.4, 129.4, 131.1, 132.7, 134.5, 138.7, 141.4, 160.5, 176.5; LC/MS (+ESI): *m/z* = 322.7 [MH⁺]; *R_t* = 14.63 (≥ 98 %).

5-(4-Bromo-2-fluorophenyl)-3-phenylpent-2-enoic acids, (9E & 9Z):**3-(4-Bromo-2-fluorophenyl)-1-phenylprop-2-en-1-one, (9c):**

Synthesized according to Method A using 4-bromo-2-fluoro-benzaldehyde **9d** (1.50 g, 7.39 mmol) and acetophenone (0.86 mL, 7.39 mmol); yellow solid; yield: 1.81 g (80 %); Mp 166-168 °C;

¹H NMR (CDCl₃, 500 MHz): δ = 7.33-7.36 (m, 2H), 7.51 (t, ³J = 7.6 Hz, 3H), 7.56-7.63 (m, 1H), 7.63 (d, ³J = 15.8 Hz, 1H), 7.82 (d, ³J = 16.1 Hz, 1H), 8.03-8.00 (m, 2H). ¹³C NMR (CDCl₃, 125 MHz): δ = 119.9 (d, *J* (C, F) = 24.9 Hz, CH), 120.1 (d, *J* (C, F) = 1.6 Hz, CH), 122.2, 124.6 (d, *J* (C, F) = 9.6 Hz, CH), 125.0 (d, *J* (C, F) = 3.8 Hz, CH), 128.0 (d, *J* (C, F) = 7.7 Hz, CH), 128.6, 128.7, 130.6 (d, *J* (C, F) = 3.8 Hz, CH), 133.0, 136.3, 161.0 (d, *J* (C, F) = 252.0 Hz, C_{quat}), 190.2.

3-(4-Bromo-2-fluorophenyl)-1-phenylpropan-1-one, (9b):

Synthesized according to Method B using compound **9c** (0.50 g, 1.64 mmol), HEH (0.623 g, 2.46 mmol) and silica gel (3.28 g); pale green oil; yield: 0.395 g (78 %);

^1H NMR (CDCl_3 , 500 MHz): δ = 3.06 (t, 3J = 7.6 Hz, 2H), 3.28 (t, 3J = 7.6 Hz, 2H), 7.15-7.21 (m, 3H), 7.46 (t, 3J = 7.9 Hz, 2H), 7.54-7.59 (m, 1H), 7.91-7.97 (m, 2H). ^{13}C NMR (CDCl_3 , 125 MHz): δ = 23.5, 38.4, 118.8, 119.0, 120.0 (d, J (C, F) = 9.6 Hz, CH), 127.3, (t, J (C, F) = 2.9 Hz, CH), 128.0, 128.6, 132.0 (d, J (C, F) = 5.8 Hz, CH), 133.2, 136.6, 161.0 (d, J (C, F) = 249.5 Hz, C_{quat}), 198.6.

Ethyl 5-(4-bromo-2-fluorophenyl)-3-phenylpent-2-enoate, (9a):

Synthesized according to Method C using compound **9b** (0.30 g, 0.98 mmol), NaH (0.117 g, 2.93 mmol) and triethyl phosphonoacetate (0.67 mL, 3.05 mmol);

9Ea: colourless oil; yield: 0.145 g (39 %); ^1H NMR (CDCl_3 , 500 MHz): δ = 1.30 (t, 3J = 6.9 Hz, 3H), 2.73-2.76 (m, 2H), 3.35-3.38 (m, 2H), 4.19 (q, 3J = 6.9 Hz, 2H), 6.09 (s, 1H), 7.10-7.18 (m, 3H), 7.37-7.39 (m, 3H), 7.45-7.47 (m, 2H). ^{13}C NMR (CDCl_3 , 125 MHz): δ = 14.3, 28.0, 31.1, 60.0, 118.2, 118.6 (d, J (C, F) = 24.9 Hz, CH), 119.7 (d, J (C, F) = 9.6 Hz, CH), 126.7, 127.1 (d, J (C, F) = 3.9 Hz, CH), 127.4, 128.6, 129.1, 131.9, 132.0, 140.6, 158.4, 160.5 (d, J (C, F) = 249.5 Hz, C_{quat}).

9Za: colourless oil; yield: 0.154 g (42 %); ^1H NMR (CDCl_3 , 500 MHz): δ = 1.06 (t, 3J = 7.2 Hz, 3H), 2.66-2.75 (m, 4H), 3.98 (q, 3J = 7.2 Hz, 2H), 5.87 (s, 1H), 6.96 (t, 3J = 8.2 Hz, 1H), 7.18 (d, 3J = 8.8 Hz, 4H), 7.31-7.38 (m, 3H). ^{13}C NMR (CDCl_3 , 125 MHz): δ = 13.9, 27.1, 40.1, 60.0, 118.1, 118.9, 119.0, 119.5 (d, J (C, F) = 9.6 Hz, CH), 126.8, 127.1, 127.2, 127.3, 127.9 (d, J (C, F) = 9.6 Hz, CH), 131.5 (d, J (C, F) = 5.8 Hz, CH), 139.4, 158.5 (d, J (C, F) = 299.4 Hz, C_{quat}), 165.8.

(E)-5-(4-Bromo-2-fluorophenyl)-3-phenylpent-2-enoic acid, (9E):

Synthesized according to Method D using compound **9Ea** (0.10 g, 0.26 mmol) and NaOH_{aq} (0.27 mL, 0.79 mmol); white solid; yield: 0.075 g (82 %); Mp 110-113 °C;

^1H NMR (CDCl_3 , 500 MHz): δ = 2.76-2.79 (m, 2H), 3.37-3.41 (m, 2H), 6.14 (s, 1H), 7.08 (d, 3J = 8.2 Hz, 1H), 7.14-7.19 (m, 2H), 7.40-7.41 (m, 3H), 7.48-7.50 (m, 2H); ^{13}C NMR (CDCl_3 , 125 MHz): δ = 28.1, 31.4, 117.0, 118.7, 118.9, 119.9, 126.7, 127.2 (d, J (C, F) = 2.8 Hz, CH), 127.3, 128.7, 129.5, 131.9 (d, J (C, F) = 6.4 Hz, CH), 160.9 (d, J (C, F) = 250.2 Hz, C_{quat}), 161.6, 170.9; LC/MS (+ESI): m/z = 350.3 [MH^+]; R_t = 12.90 (\geq 98 %).

(Z)-5-(4-Bromo-2-fluorophenyl)-3-phenylpent-2-enoic acid, (9Z):

Synthesized according to Method D using compound **9Za** (0.10 g, 0.26 mmol) and NaOH_{aq} (0.27 mL, 0.79 mmol); white solid; yield: 0.078 g (85 %); Mp 82-84 °C;

^1H NMR (CDCl_3 , 500 MHz): δ = 2.65-2.68 (m, 2H), 2.74-2.78 (m, 2H), 5.86 (s, 1H), 7.18-7.22 (m, 3H), 7.27-7.38 (m, 4H); ^{13}C NMR (CDCl_3 , 125 MHz): δ = 27.0, 28.0, 35.6, 40.5, 116.9, 118.8 (d, J (C, F) = 5.5 Hz, CH), 119.2 (d, J (C, F) = 9.2 Hz, CH), 120.1, 126.0, 127.5 (d, J (C, F) = 3.7 Hz, CH), 128.5, 131.4 (d, J (C, F) = 5.5 Hz, CH), 141.4, 161.0 (d, J (C, F) = 258.4 Hz, C_{quat}), 169.8; LC/MS (+ESI): m/z = 350.3 [MH^+]; R_t = 14.00 ($\geq 99\%$).

5-(4-Ethylphenyl)-3-phenylpent-2-enoic acids, (10E &10Z):

3-(4-Ethylphenyl)-1-phenylprop-2-en-1-one, (10c):

Synthesized according to Method A using 4-ethylbenzaldehyde **10d** (2.00 g, 14.9 mmol) and acetophenone (1.79 g, 14.9 mmol); yellow oil; yield: 2.60 g (74 %);

^1H NMR (CDCl_3 , 500 MHz): δ = 1.04 (t, 3J = 7.6 Hz, 3H), 2.47 (q, 3J = 7.6 Hz, 2H), 7.02-7.04 (m, 2H), 7.26-7.32 (m, 3H), 7.34-7.37 (m, 3H), 7.58 (d, 3J = 15.8 Hz, 1H), 7.77-7.81 (m, 2H). ^{13}C NMR (CDCl_3 , 125 MHz): δ = 15.3, 28.8, 121.2, 128.4, 128.5, 128.6, 131.6, 132.4, 132.6, 138.4, 145.0, 147.4, 190.7.

3-(4-Ethylphenyl)-1-phenylpropan-1-one, (10b):

Synthesized according to Method B using compound **10c** (0.50 g, 2.11 mmol), HEH (0.84 g, 3.17 mmol) and silica gel (4.22 g); pale yellow oil; yield: 0.284 g (57 %);

^1H NMR (CDCl_3 , 500 MHz): δ = 1.23 (t, 3J = 7.6 Hz, 3H), 2.63 (q, 3J = 7.6 Hz, 2H), 3.05 (t, 3J = 7.6 Hz, 2H), 3.30 (t, 3J = 7.6 Hz, 2H), 7.14 (d, 3J = 8.2 Hz, 2H), 7.18 (d, 3J = 8.2 Hz, 2H), 7.46 (t, 3J = 7.2 Hz, 2H), 7.54-7.57 (m, 1H), 7.95-7.98 (m, 2H). ^{13}C NMR (CDCl_3 , 125 MHz): δ = 15.6, 28.4, 29.7, 40.6, 127.9, 128.0, 128.3, 128.6, 133.0, 136.9, 138.4, 142.0, 199.3.

Ethyl 5-(4-ethylphenyl)-3-phenylpent-2-enoate, (10a):

Synthesized according to Method C using compound **10b** (0.25 g, 1.05 mmol), NaH (0.126 g, 3.15 mmol) and triethyl phosphonoacetate (0.72 mL, 3.15 mmol);

10Ea: colourless oil; yield: 0.143 g (44 %); ^1H NMR (CDCl_3 , 500 MHz): δ = 1.25 (d, 3J = 7.6 Hz, 3H), 1.30 (t, 3J = 7.2 Hz, 3H), 2.61 (q, 3J = 7.6 Hz, 2H), 2.69-2.72 (m, 2H), 3.37-3.40 (m, 2H), 4.21 (q, 3J = 7.2 Hz, 2H), 6.07 (s, 1H), 7.10 (d, 3J = 8.2 Hz, 2H), 7.15 (d, 3J = 8.2 Hz, 2H), 7.38-7.41 (m, 3H), 7.46-7.48 (m, 2H). ^{13}C NMR (CDCl_3 , 125 MHz): δ = 14.3, 15.7, 28.5, 33.3, 34.8, 59.9, 117.8, 126.7, 127.8, 128.4, 128.6, 128.9, 138.8, 141.1, 141.8, 159.5, 166.3.

10Za: colourless oil; yield: 0.133 g (41 %); ^1H NMR (CDCl_3 , 500 MHz): $\delta = 1.06$ (t, $^3J = 7.2$ Hz, 3H), 1.22 (t, $^3J = 7.6$ Hz, 3H), 2.60 (q, $^3J = 7.6$ Hz, 2H), 2.72-2.76 (m, 4H), 3.98 (q, $^3J = 7.2$ Hz, 2H), 5.90 (s, 1H), 7.05 (d, $^3J = 7.9$ Hz, 2H), 7.10 (d, $^3J = 7.9$ Hz, 2H), 7.20-7.18 (m, 2H), 7.38-7.30 (m, 3H). ^{13}C NMR (CDCl_3 , 125 MHz): $\delta = 13.9, 15.6, 28.4, 33.4, 42.1, 59.8, 117.6, 127.2, 127.7, 127.9, 128.2, 138.1, 139.9, 142.0, 158.6, 166.0$.

(E)-5-(4-Ethylphenyl)-3-phenylpent-2-enoic acid, (10E):

Synthesized according to Method D using compound **10Ea** (0.10 g, 0.32 mmol) and NaOH_{aq} (1.07 mL, 3.24 mmol); white solid; yield: 0.085 g (94 %); Mp 98-100 °C;

^1H NMR (CDCl_3 , 500 MHz): $\delta = 1.22$ (t, $^3J = 7.6$ Hz, 3H), 2.62 (q, $^3J = 7.6$ Hz, 2H), 2.72-2.76 (m, 2H), 3.39-3.42 (m, 2H), 6.13 (s, 1H), 7.11 (d, $^3J = 8.2$ Hz, 2H), 7.15 (d, $^3J = 8.2$ Hz, 2H), 7.40-7.41 (m, 3H), 7.48-7.50 (m, 2H); ^{13}C NMR (CDCl_3 , 125 MHz): $\delta = 15.7, 28.5, 33.6, 34.9, 116.7, 126.8, 127.8, 128.3, 128.7, 129.3, 140.9, 141.9, 145.5, 162.6, 170.8$; LC/MS (+ESI): $m/z = 289.4$ [MH^+]; $R_t = 14.68$ ($\geq 97\%$).

(Z)-5-(4-Ethylphenyl)-3-phenylpent-2-enoic acid, (10Z):

Synthesized according to Method D using compound **10Za** (0.10 g, 0.32 mmol) and NaOH_{aq} (1.07 mL, 3.24 mmol); white solid; yield: 0.083 g (92 %); Mp 96-98 °C;

^1H NMR (CDCl_3 , 500 MHz): $\delta = 1.15$ (t, $^3J = 7.6$ Hz, 3H), 2.54 (q, $^3J = 7.6$ Hz, 2H), 2.64-2.68 (m, 2H), 3.34 (m, 2H), 6.05 (s, 1H), 7.03 (d, $^3J = 8.2$ Hz, 2H), 7.07 (d, $^3J = 8.2$ Hz, 2H), 7.33-7.35 (m, 3H), 7.41-7.43 (m, 2H); ^{13}C NMR (CDCl_3 , 125 MHz): $\delta = 15.7, 28.5, 33.6, 34.8, 116.5, 126.8, 127.8, 128.2, 128.3, 128.7, 129.3, 140.9, 141.9, 162.2, 170.8$; LC/MS (+ESI): $m/z = 289.4$ [MH^+]; $R_t = 14.15$ ($\geq 97\%$).

5-(4-Chlorophenyl)-3-(3-fluorophenyl)pent-2-enoic acids, (11E & 11Z):

(E)-3-(4-Chlorophenyl)-1-(2-fluorophenyl)prop-2-en-1-one, (11c):

Synthesized according to Method A using 4-chlorobenzaldehyde (2.00 g, 14.3 mmol) and 2-fluoroacetophenone (1.74 mL, 14.3 mmol); pale yellow solid; yield: 1.85 g (49 %);

^1H NMR (CDCl_3 , 500 MHz) $\delta = 7.18$ (t, $J = 8.5$ Hz, 2H), 7.40 (d, $J = 8.5$ Hz, 2H), 7.47 (d, $J = 15.4$ Hz, 1H), 7.57 (d, $J = 8.5$ Hz, 2H), 7.76 (d, $J = 15.8$ Hz, 1H), 8.06 (d, $J = 8.5$ Hz, 2H);

3-(4-Chlorophenyl)-1-(2-fluorophenyl)propan-1-one, (11b):

Synthesized according to Method B using **11c** (1.0 g, 3.85 mmol), HEH (1.46 g, 5.75 mmol) and silica gel (7.67 g); colourless solid; yield: 0.75 g (75 %);

^1H NMR (CDCl_3 , 500 MHz) δ 3.04 (t, $J = 7.2$ Hz, 2H), 3.30 (dt, $J = 3.1, 7.6$ Hz, 2H), 7.12-7.3 (m, 6H), 7.50-7.55 (m, 1H), 7.88 (dd, $J = 1.6, 8.5$ Hz, 1H). ^{13}C NMR (CDCl_3 , 125 MHz) δ 29.2, 44.9, 116.6 (d, $^2J_{\text{C-F}} = 23.4$ Hz), 124.5 (d, $^4J_{\text{C-F}} = 2.9$ Hz), 125.5 (d, $^3J_{\text{C-F}} = 13.4$ Hz), 128.5, 129.8, 130.6 (d, $^4J_{\text{C-F}} = 2.9$ Hz), 131.8, 134.6 (d, $^3J_{\text{C-F}} = 9.6$ Hz), 139.6, 161.9 (d, $^1J_{\text{C-F}} = 254.3$ Hz), 197.1.

Ethyl 5-(4-chlorophenyl)-3-(2-fluorophenyl)pent-2-enoate, (11a):

Synthesized according to Method C using **11b** (0.60 g, 2.28 mmol), NaH (0.28 g, 6.85 mmol) and triethyl phosphonoacetate (1.51 mL, 6.85 mmol);

11Ea: colourless oil; yield: 0.14 g (19 %); ^1H NMR (CDCl_3 , 500 MHz) δ 1.30 (t, $J = 7.2$ Hz, 3H), 2.66-2.70 (m, 2H), 3.32-3.35 (m, 2H), 4.19 (q, $J = 7.2$ Hz, 2H), 5.94 (s, 1H), 7.07-7.11 (m, 3H), 7.14 (d, $J = 8.5$ Hz, 1H), 7.17-7.21 (m, 3H), 7.31-7.35 (m, 1H). ^{13}C NMR (CDCl_3 , 125 MHz) δ 14.3, 33.7, 33.9, 60.1, 116.1 (d, $^2J_{\text{C-F}} = 23.0$ Hz), 117.9, 119.4, 122.0 (d, $^4J_{\text{C-F}} = 2.9$ Hz), 124.2 (d, $^4J_{\text{C-F}} = 3.8$ Hz), 128.3, 129.8, 129.9, 130.2, 139.7, 155.1, 167.9 (d, $^1J_{\text{C-F}} = 250.5$ Hz), 169.4.

11Za: colourless oil; yield: 0.18 g (24 %); ^1H NMR (CDCl_3 , 500 MHz) δ 1.07 (t, $J = 7.2$ Hz, 3H), 2.69-2.74 (m, 4H), 4.00 (q, $J = 7.2$ Hz, 2H), 5.98 (s, 1H), 7.06-7.14 (m, 5H), 7.23 (d, $J = 8.5$ Hz, 2H), 7.29-7.33 (m, 1H).

(E)-5-(4-Chlorophenyl)-3-(3-fluorophenyl)pent-2-enoic acid, (11E):

Synthesized according to Method D using (*E*)-ethyl **11Ea** (0.14 g, 0.42 mmol) and NaOH_{aq} (1.4 mL, 4.20 mmol); white solid; yield: 0.09 g (70 %);

^1H NMR (CDCl_3 , 500 MHz) δ 2.69-2.72 (m, 2H), 3.34-3.38 (m, 2H), 6.01 (s, 1H), 7.08-7.21 (m, 7H), 7.37-7.38 (m, 1H). MS (+ESI): $m/z = 306$ (M+H).

(Z)-5-(4-Chlorophenyl)-3-(3-fluorophenyl)pent-2-enoic acid, (11Z):

Synthesized according to Method D using **11Za** (0.18 g, 0.55 mmol) and NaOH_{aq} (1.8 mL, 5.5 mmol); white solid; yield: 0.07 g (40 %);

^1H NMR (CDCl_3 , 500 MHz) δ 2.60-2.63 (m, 2H), 2.67-2.70 (m, 2H), 5.91 (s, 1H), 6.93-7.10 (m, 4H), 7.17-7.23 (m, 4H); MS (+ESI): $m/z = 306$ (M+H).

5-(4-Chlorophenyl)-3-(3-fluorophenyl)pent-2-enoic acids, (12E & 12Z):**(E)-3-(4-Chlorophenyl)-1-(3-fluorophenyl)prop-2-en-1-one, (12c):**

Synthesized according to Method A using 4-chlorobenzaldehyde (1.02 g, 7.24 mmol) and 3-fluoroacetophenone (1.0 g, 7.24 mmol); pale yellow solid; yield: 1.68 g (45 %);

^1H NMR (CDCl_3 , 500 MHz) δ 7.18 (t, $J = 8.5$ Hz, 2H), 7.40 (d, $J = 8.5$ Hz, 2H), 7.47 (d, $J = 15.4$ Hz, 1H), 7.57 (d, $J = 8.5$ Hz, 2H), 7.76 (d, $J = 15.8$ Hz, 1H), 8.06 (d, $J = 8.5$ Hz, 2H); ^{13}C NMR (CDCl_3 , 125 MHz) δ 116.5 (d, $^2J_{\text{C-F}} = 23.0$ Hz), 124.5 (d, $^4J_{\text{C-F}} = 3.8$ Hz), 126.0 (d, $^3J_{\text{C-F}} = 6.7$ Hz), 126.9, 129.2, 129.7, 131.0 (d, $^4J_{\text{C-F}} = 2.9$ Hz), 133.2, 134.1 (d, $^3J_{\text{C-F}} = 8.6$ Hz), 136.6, 143.2, 161.2 (d, $^1J_{\text{C-F}} = 253.3$ Hz), 188.7.

3-(4-Chlorophenyl)-1-(3-fluorophenyl)propan-1-one, (12b):

Synthesized according to Method B using 3-(4-chlorophenyl)-1-(3-fluorophenyl)prop-2-en-1-one (1.0 g, 3.85 mmol), HEH (1.46 g, 5.75 mmol) and silica gel (7.67 g); colourless solid; yield: 0.88 g (88 %);

^1H NMR (CDCl_3 , 500 MHz) δ 3.03 (t, $J = 7.6$ Hz, 2H), 3.23 (t, $J = 7.6$ Hz, 2H), 7.17 (d, $J = 8.5$ Hz, 1H), 7.23-7.28 (m, 3H), 7.40-7.48 (m, 1H), 7.60-7.63 (m, 1H), 7.71 (d, $J = 7.9$ Hz, 1H). ^{13}C NMR (CDCl_3 , 125 MHz) δ 29.3, 40.3, 114.7 (d, $^2J_{\text{C-F}} = 22.1$ Hz), 120.1 (d, $^2J_{\text{C-F}} = 21.1$ Hz), 123.7, 128.6, 129.8, 130.3 (d, $^3J_{\text{C-F}} = 7.7$ Hz), 131.9, 138.8 (d, $^3J_{\text{C-F}} = 5.8$ Hz), 139.4, 162.8 (d, $^1J_{\text{C-F}} = 248.5$ Hz), 197.5.

Ethyl 5-(4-chlorophenyl)-3-(3-fluorophenyl)pent-2-enoate, (12a):

Synthesized according to Method C using **12b** (0.60 g, 2.28 mmol), NaH (0.28 g, 6.85 mmol) and triethyl phosphonoacetate (1.51 mL, 6.85 mmol);

12Ea: colourless oil; yield: 0.34 g (45 %); ^1H NMR (CDCl_3 , 500 MHz) δ 1.29 (t, $J = 7.0$ Hz, 3H), 2.69-2.71 (m, 2H), 3.33-3.36 (m, 2H), 4.19 (q, $J = 7.0$ Hz, 2H), 6.05 (s, 1H), 7.04 (t, $J = 8.5$ Hz, 1H), 7.10-7.14 (m, 3H), 7.20-7.23 (m, 3H), 7.33-7.36 (m, 1H). ^{13}C NMR (CDCl_3 , 125 MHz) δ 14.3, 32.8, 34.3, 60.1, 113.7 (d, $^2J_{\text{C-F}} = 23.0$ Hz), 115.8 (d, $^2J_{\text{C-F}} = 22.1$ Hz), 119.0, 122.4 (d, $^4J_{\text{C-F}} = 2.9$ Hz), 128.3, 129.9, 130.2 (d, $^3J_{\text{C-F}} = 8.6$ Hz), 131.7, 139.6, 143.2 (d, $^3J_{\text{C-F}} = 6.7$ Hz), 157.4, 160.0 (d, $^1J_{\text{C-F}} = 253.3$ Hz), 166.0.

12Za: colourless oil; yield: 0.3 g (40 %); ^1H NMR (CDCl_3 , 500 MHz) δ 1.07 (t, $J = 7.2$ Hz, 3H), 2.65-2.72 (m, 4H), 3.99 (q, $J = 7.2$ Hz, 2H), 5.88 (s, 1H), 6.87-6.89 (m, 1H), 6.94 (d, $J = 7.6$ Hz, 1H), 7.00-7.01 (m, 1H), 7.04 (d, $J = 8.5$ Hz, 2H), 7.24 (d, $J = 8.2$ Hz, 2H), 7.30-7.35 (m, 1H). ^{13}C NMR (CDCl_3 , 125 MHz) δ 13.9, 33.0, 41.6, 60.0, 114.4 (d, $^2J_{\text{C-F}} = 22.1$ Hz),

114.7, 118.7, 123.0 (d, $^4J_{C-F} = 2.9$ Hz), 128.6, 129.5, 129.6, 132.0, 156.2 (d, $^4J_{C-F} = 1.9$ Hz), 161.4 (d, $^1J_{C-F} = 2465.7$ Hz), 162.6, 163.2, 165.5.

(E)-5-(4-Chlorophenyl)-3-(3-fluorophenyl)pent-2-enoic acid, (12E):

Synthesized according to Method D using **12Ea** (0.25 g, 0.75 mmol) and NaOH_{aq} (2.5 mL, 7.5 mmol); white solid; yield: 0.16 g (72 %);

^1H NMR (CDCl₃, 500 MHz) δ 2.71-2.74 (m, 2H), 3.34-3.38 (m, 2H), 6.11 (s, 1H), 7.09-7.16 (m, 4H), 7.21-7.24 (m, 3H), 7.36-7.40 (m, 1H). ^{13}C NMR (CDCl₃, 125 MHz) δ 33.1, 34.4, 113.8 (d, $^2J_{C-F} = 22.1$ Hz), 116.3 (d, $^2J_{C-F} = 21.1$ Hz), 117.9, 122.5 (d, $^4J_{C-F} = 2.9$ Hz), 128.5, 129.8, 130.3 (d, $^3J_{C-F} = 8.6$ Hz), 131.9, 139.4, 143.0, 160.5, 164.6 (d, $^1J_{C-F} = 261.0$ Hz), 170.5; MS (+ESI): m/z = 306 (M+H).

(Z)-5-(4-Chlorophenyl)-3-(3-fluorophenyl)pent-2-enoic acid, (12Z):

Synthesized according to Method D using **12Za** (0.25 g, 0.87 mmol) and NaOH_{aq} (2.5 mL, 7.5 mmol); white solid; yield: 0.11 g (40 %);

^1H NMR (CDCl₃, 500 MHz) δ 2.64-2.67 (m, 2H), 2.71-2.74 (m, 2H), 5.86 (s, 1H), 6.91-7.10 (m, 4H), 7.24-7.27 (m, 3H), 7.31-7.34 (m, 1H). ^{13}C NMR (CDCl₃, 125 MHz) δ 32.9, 41.9, 114.2, 114.9 (d, $^2J_{C-F} = 21.1$ Hz), 117.5, 122.9, 128.6, 129.6, 129.7, 131.7, 132.1, 141.1, 143.0, 159.3, 168.3 (d, $^1J_{C-F} = 255.3$ Hz); MS (+ESI): m/z = 306 (M+H).

5-(4-Chlorophenyl)-3-(4-fluorophenyl)pent-2-enoic acids, (13E & 13Z):

(E)-3-(4-Chlorophenyl)-1-(4-fluorophenyl)prop-2-en-1-one, (13c):

Synthesized according to Method A using 4-chlorobenzaldehyde (2.00 g, 14.3 mmol) and 4-fluoroacetophenone (1.74 mL, 14.3 mmol); pale yellow solid; yield: 3.44 g (92 %);

^1H NMR (CDCl₃, 500 MHz) δ 7.18 (t, $J = 8.5$ Hz, 2H), 7.40 (d, $J = 8.5$ Hz, 2H), 7.47 (d, $J = 15.4$ Hz, 1H), 7.57 (d, $J = 8.5$ Hz, 2H), 7.76 (d, $J = 15.8$ Hz, 1H), 8.06 (d, $J = 8.5$ Hz, 2H); ^{13}C NMR (CDCl₃, 125 MHz) δ 115.8 (d, $^2J_{C-F} = 22.1$ Hz), 121.9, 129.3, 129.6, 131.1 (d, $^3J_{C-F} = 9.6$ Hz), 133.2, 134.4, 136.6, 143.5, 165.6 (d, $^1J_{C-F} = 255.3$ Hz), 188.5.

3-(4-Chlorophenyl)-1-(4-fluorophenyl)propan-1-one, (13b):

Synthesized according to Method B using **13c** (1.0 g, 3.85 mmol), HEH (1.46 g, 5.75 mmol) and silica gel (7.67 g); colourless solid; yield: 0.82 g (82 %);

^1H NMR (CDCl_3 , 500 MHz) δ 3.05 (t, $J = 7.5$ Hz, 2H), 3.26 (t, $J = 7.5$ Hz, 2H), 7.13 (d, $J = 8.5$ Hz, 2H), 7.18 (d, $J = 8.8$ Hz, 2H), 7.27 (d, $J = 8.5$ Hz, 2H), 7.98 (t, $J = 8.8$ Hz, 2H).

Ethyl 5-(4-chlorophenyl)-3-(4-fluorophenyl)pent-2-enoate, (13a):

Synthesized according to Method C using **13b** (0.60 g, 2.28 mmol), NaH (0.28 g, 6.85 mmol) and triethyl phosphonoacetate (1.51 mL, 6.85 mmol);

13Ea: colourless oil; yield: 0.301 g (30 %); ^1H NMR (CDCl_3 , 500 MHz) δ 1.30 (t, $J = 7.2$ Hz, 3H), 2.67-2.71 (m, 2H), 3.33-3.37 (m, 2H), 4.20 (q, $J = 7.2$ Hz, 2H), 6.01 (s, 1H), 7.06 (t, $J = 8.5$ Hz, 2H), 7.10 (d, $J = 8.5$ Hz, 2H), 7.22 (d, $J = 8.5$ Hz, 2H), 7.39-7.42 (m, 2H). ^{13}C NMR (CDCl_3 , 125 MHz) δ 14.3, 32.8, 34.3, 60.0, 115.5 (d, $^2J_{\text{C-F}} = 22.1$ Hz), 118.1, 128.3, 128.5 (d, $^4J_{\text{C-F}} = 7.7$ Hz), 129.8, 131.7, 136.8 (d, $^3J_{\text{C-F}} = 6.7$ Hz), 157.8, 163.2 (d, $^1J_{\text{C-F}} = 248.5$ Hz), 166.1.

13Za: colourless oil; yield: 0.299 g (39 %); ^1H NMR (CDCl_3 , 500 MHz) δ 1.10 (t, $J = 6.9$ Hz, 3H), 2.63-2.66 (m, 2H), 2.70-2.73 (m, 2H), 3.99 (q, $J = 6.9$ Hz, 2H), 5.87 (s, 1H), 7.02-7.07 (m, 4H), 7.13-7.16 (m, 2H), 7.23 (d, $J = 8.5$ Hz, 2H). ^{13}C NMR (CDCl_3 , 125 MHz) δ 14.0, 33.1, 41.8, 59.9, 115.0 (d, $^2J_{\text{C-F}} = 21.1$ Hz), 118.4, 128.6, 129.6 (d, $^3J_{\text{C-F}} = 7.7$ Hz), 131.9, 135.3, 139.0, 156.8, 164.4 (d, $^1J_{\text{C-F}} = 246.6$ Hz), 165.7.

(E)-5-(4-Chlorophenyl)-3-(4-fluorophenyl)pent-2-enoic acid, (13E):

Synthesized according to Method D using **13Ea** (0.3 g, 0.90 mmol) and NaOH_{aq} (3.01 mL, 9.01 mmol); white solid; yield: 0.19 g (69 %);

^1H NMR (CDCl_3 , 500 MHz) δ 2.70-2.72 (m, 2H), 3.35-3.38 (m, 2H), 6.07 (s, 1H), 7.08-7.12 (m, 4H), 7.22 (d, $J = 8.5$ Hz, 2H), 7.42-7.45 (m, 2H). ^{13}C NMR (CDCl_3 , 125 MHz) δ 33.1, 34.4, 111.4 (d, $^4J_{\text{C-F}} = 2.9$ Hz), 113.9, 115.8 (d, $^2J_{\text{C-F}} = 21.1$ Hz), 128.4, 128.6, 129.8, 131.9, 135.3, 139.5, 143.2, 157.2 (d, $^2J_{\text{C-F}} = 250.5$ Hz), 162.5, 169.3; MS (+ESI): $m/z = 306$ (M+H).

(Z)-5-(4-Chlorophenyl)-3-(4-fluorophenyl)pent-2-enoic acid, (13Z):

Synthesized according to Method D using **13Za** (0.29 g, 0.87 mmol) and NaOH_{aq} (2.9 mL, 8.7 mmol); white solid; yield: 0.09 g (35 %);

^1H NMR (CDCl_3 , 500 MHz) δ 2.61-2.65 (m, 2H), 2.72-2.75 (m, 2H), 5.85 (s, 1H), 6.98-7.04 (m, 4H), 7.22 (d, $J = 8.5$ Hz, 2H), 7.23-7.27 (m, 2H). ^{13}C NMR (CDCl_3 , 125 MHz) δ 33.0, 42.1, 115.1 (d, $^2J_{\text{C-F}} = 21.1$ Hz), 117.2, 127.7, 128.6 (d, $^3J_{\text{C-F}} = 7.7$ Hz), 129.1 (d, $^3J_{\text{C-F}} = 9.6$ Hz), 129.6, 129.8, 138.2, 138.8, 159.8, 164.8 (d, $^1J_{\text{C-F}} = 250.5$ Hz), 167.6, 169.3; MS (+ESI): $m/z = 306$ (M+H).

(E)-5-(4-Chlorophenyl)-3-(pyridin-2-yl)pent-2-enoic acid, (14E):**(E)-3-(4-Chlorophenyl)-1-(acetylpyridin)prop-2-en-1-one, (14c):**

Synthesized according to Method A using 4-chlorobenzaldehyde (2.00 g, 14.3 mmol) and acetylpyridine (1.60 mL, 14.3 mmol); pale yellow solid; yield: 1.2 g (34 %);

^1H NMR (CDCl_3 , 500 MHz) δ 7.39 (d, $J = 8.5$ Hz, 2H), 7.48-7.51 (m, 1H), 7.66 (d, $J = 8.8$ Hz, 2H), 7.86-7.90 (m, 2H), 8.19 (td, $J = 0.9, 7.9$ Hz, 1H), 8.28 (d, $J = 16.1$ Hz, 1H), 8.73-8.75 (m, 1H);

3-(4-Chlorophenyl)-1-(acetylpyridin)propan-1-one, (14b):

Synthesized according to Method B using **14c** (1.0 g, 4.1 mmol), HEH (1.56 g, 5.75 mmol) and silica gel (8.20 g); pale yellow solid; yield: 0.56 g (52 %);

^1H NMR (CDCl_3 , 500 MHz) δ 3.04 (t, $J = 7.6$ Hz, 2H), 3.55 (t, $J = 7.6$ Hz, 2H), 7.19-7.25 (m, 4H), 7.45-7.48 (m, 1H), 7.82 (dt, $J = 7.6$ Hz, 1H), 8.03 (td, $J = 1.3, 7.9$ Hz, 1H), 8.66-8.70 (m, 1H).

Ethyl 5-(4-chlorophenyl)-3-(pyridin-2-yl)pent-2-enoate, (14a):

Synthesized according to Method C using **14b** (0.56 g, 2.28 mmol), NaH (0.28 g, 6.85 mmol) and triethyl phosphonoacetate (1.30 mL, 6.85 mmol);

14Ea: colourless oil; yield: 0.15 g (21 %); ^1H NMR (CDCl_3 , 500 MHz) δ 1.32 (t, $J = 7.2$ Hz, 3H), 2.75-2.79 (m, 2H), 3.47-3.50 (m, 2H), 4.21 (q, $J = 7.2$ Hz, 2H), 6.51 (s, 1H), 7.16-7.21 (m, 4H), 7.22-7.27 (m, 1H), 7.50 (d, $J = 7.9$ Hz, 1H), 7.70 (dt, $J = 1.6, 7.9$ Hz, 1H), 8.65-8.67 (m, 1H).

14Za: colourless oil; yield: 0.08 g (11 %); ^1H NMR (CDCl_3 , 500 MHz) δ 1.09 (t, $J = 7.2$ Hz, 3H), 2.77-2.79 (m, 2H), 3.01-3.04 (m, 2H), 4.05 (q, $J = 7.2$ Hz, 2H), 6.30 (s, 1H), 7.06-7.08 (m, 1H), 7.16-7.27 (m, 5H), 7.54 (dt, $J = 1.6, 7.9$ Hz, 1H), 8.49-8.51 (m, 1H).

(E)-5-(4-Chlorophenyl)-3-(pyridin-2-yl)pent-2-enoic acid, (14E):

Synthesized according to Method D using **13Ea** (0.15 g, 0.46 mmol) and NaOH_{aq} (0.5 mL, 1.4 mmol); yellow solid; yield: 0.09 g (68 %);

^1H NMR (CDCl_3 , 500 MHz) δ 2.76-2.79 (m, 2H), 3.49-3.52 (m, 2H), 6.51 (s, 1H), 7.13 (d, $J = 8.5$ Hz, 2H), 7.20 (d, $J = 7.9$ Hz, 2H), 7.26-7.33 (m, 1H), 7.51 (d, $J = 7.9$ Hz, 1H), 7.74 (dt, $J = 1.6, 7.9$ Hz, 1H), 8.69-8.70 (m, 1H). ^{13}C NMR (CDCl_3 , 125 MHz) δ 31.4, 34.6, 118.8,

121.6, 123.9, 128.3, 129.9, 137.0, 139.8, 141.4, 149.4, 157.2, 159.8, 164.2. MS (+ESI): m/z = 288 (M+H).

5-(Biphenyl-4-yl)-3-phenylpent-2-enoic acids, (15E & 15Z):

3-(Biphenyl-4-yl)-1-phenylprop-2-en-1-one, (15c):

Synthesized according to Method A using 2-biphenylcarboxaldehyde **15d** (2.00 g, 10.9 mmol) and acetophenone (1.28 g, 10.9 mmol); pale yellow solid; yield: 1.90 g (63 %); Mp 102-104 °C;

^1H NMR (CDCl_3 , 500 MHz): δ = 7.37-7.41 (m, 1H), 7.47 (t, 3J = 7.6 Hz, 2H), 7.52 (t, 3J = 7.6 Hz, 2H), 7.56-7.65 (m, 6H), 7.73 (d, 3J = 8.2 Hz, 2H), 7.86 (d, 3J = 15.8 Hz, 1H), 8.03-8.06 (m, 2H). ^{13}C NMR (CDCl_3 , 125 MHz): δ = 121.9, 127.0, 127.6, 127.9, 128.5, 128.6, 128.9, 129.0, 132.8, 133.8, 138.3, 140.1, 143.3, 144.4, 190.2.

3-(Biphenyl-4-yl)-1-phenylpropan-1-one, (15b):

Synthesized according to Method B using compound **15c** (0.50 g, 1.76 mmol), HEH (0.686 g, 2.63 mmol) and silica gel (3.52 g); pale yellow solid; yield: 0.446 g (88 %);

^1H NMR (CDCl_3 , 500 MHz): δ = 3.13 (t, 3J = 7.6 Hz, 2H), 3.35 (t, 3J = 7.6 Hz, 2H), 7.31-7.35 (m, 3H), 7.42-7.48 (m, 4H), 7.55-7.59 (m, 5H), 7.97-8.00 (m, 2H). ^{13}C NMR (CDCl_3 , 125 MHz): δ = 29.7, 40.4, 126.9, 127.0, 127.2, 128.0, 128.6, 128.7, 128.9, 133.1, 136.9, 139.1, 140.4, 140.9, 199.1.

Ethyl 5-(biphenyl-4-yl)-3-phenylpent-2-enoate, (15a):

Synthesized according to Method C using compound **15b** (0.35 g, 1.22 mmol), NaH (0.147 g, 3.67 mmol) and triethyl phosphonoacetate (0.83 mL, 3.67 mmol);

15Ea: colourless oil; yield: 0.171 g (39 %); ^1H NMR (CDCl_3 , 500 MHz): δ = 1.31 (t, 3J = 7.2 Hz, 3H), 2.77-2.81 (m, 2H), 3.42-3.46 (m, 2H), 4.22 (q, 3J = 7.2 Hz, 2H), 6.09 (s, 1H), 7.30-7.37 (m, 3H), 7.38-7.48 (m, 5H), 7.49-7.51 (m, 4H), 7.56-7.59 (m, 2H); ^{13}C NMR (CDCl_3 , 125 MHz): δ = 14.3, 33.1, 34.8, 59.9, 157.9, 126.7, 126.9, 127.0, 127.1, 128.6, 128.7, 128.9, 129.0, 138.9, 140.7, 141.0, 141.1, 159.3, 166.3.

15Za: colourless oil; yield: 0.194 g (45 %); ^1H NMR (CDCl_3 , 500 MHz): δ = 1.07 (t, 3J = 7.2 Hz, 3H), 2.73-2.82 (m, 4H), 3.99 (q, 3J = 7.2 Hz, 2H), 5.93 (s, 1H), 7.20-7.22 (m, 4H), 7.31-7.39 (m, 4H), 7.42 (t, 3J = 7.5 Hz, 2H), 7.49-7.51 (m, 2H), 7.56-7.59 (m, 2H). ^{13}C NMR

(CDCl₃, 125 MHz): δ = 13.9, 33.4, 42.0, 59.8, 117.8, 127.0, 127.1, 127.2, 127.3, 127.7, 127.9, 128.7, 138.6, 139.0, 139.8, 139.9, 140.9, 158.3, 166.0.

(E)-5-(Biphenyl-4-yl)-3-phenylpent-2-enoic acid, (15E):

Synthesized according to Method D using compound **15Ea** (0.16 g, 0.45 mmol) and NaOH_{aq} (1.50 mL, 4.49 mmol); white solid; yield: 0.125 g (85 %); Mp 139-141 °C;

¹H NMR (CDCl₃, 500 MHz): δ = 2.79-2.83 (m, 2H), 3.44-3.48 (m, 2H), 6.15 (s, 1H), 7.29-7.32 (m, 3H), 7.39-7.44 (m, 5H), 7.50-7.52 (m, 4H), 7.55-7.57 (m, 2H); ¹³C NMR (CDCl₃, 125 MHz): δ = 33.5, 34.9, 116.8, 126.6, 126.8, 127.0, 127.1, 128.7, 128.7, 128.9, 129.4, 139.0, 140.5, 140.8, 141.1, 162.3, 170.7; LC/MS (+ESI): m/z = 329.8 [MH⁺]; R_t = 12.60 (\geq 97 %).

(Z)-5-(Biphenyl-4-yl)-3-phenylpent-2-enoic acid, (15Z):

Synthesized according to Method D using compound **15Za** (0.185 g, 0.52 mmol) and NaOH_{aq} (1.75 mL, 5.19 mmol); white solid; yield: 0.145 g (85 %); Mp 185-188 °C; ¹H NMR (CDCl₃, 500 MHz): δ = 2.72-2.75 (m, 2H), 2.78-2.83 (m, 2H), 5.91 (s, 1H), 7.20 (t, ³J = 7.9 Hz, 4H), 7.30-7.39 (m, 4H), 7.42 (t, ³J = 7.9 Hz, 2H), 7.50 (d, ³J = 8.2 Hz, 2H), 7.56-7.58 (m, 2H); ¹³C NMR (CDCl₃, 125 MHz): δ = 33.4, 42.3, 116.6, 127.0, 127.1, 127.2, 127.2, 128.1, 128.1, 128.7, 128.8, 139.1, 139.7, 140.9, 141.5, 160.9, 173.7; LC/MS (+ESI): m/z = 329.8 [MH⁺]; R_t = 14.70 (\geq 96 %).

5-(Naphthalen-2-yl)-3-phenylpent-2-enoic acids, (16E & 16Z):

3-(Naphthalen-2-yl)-1-phenylprop-2-en-1-one, (16c).

Synthesized according to Method A using 2-naphthaldehyde **16d** (2.00 g, 12.8 mmol) and acetophenone (1.49 g, 12.8 mmol); pale yellow solid; yield: 2.85 g (86 %); Mp 158-160 °C;

¹H NMR (CDCl₃, 500 MHz): δ = 7.51-7.55 (m, 4H), 7.59-7.62 (m, 1H), 7.65 (d, ³J = 15.4 Hz, 1H), 7.80 (dd, ⁴J = 1.7, ³J = 8.5 Hz, 1H), 7.85-7.90 (m, 3H), 7.98 (d, ³J = 15.4 Hz, 1H), 8.04-8.08 (m, 3H). ¹³C NMR (CDCl₃, 125 MHz): δ = 122.3, 123.7, 126.8, 127.4, 127.8, 128.5, 128.6, 128.7, 130.6, 132.4, 132.8, 133.4, 134.4, 138.3, 144.9, 190.5.

3-(Naphthalen-2-yl)-1-phenylpropan-1-one, (16b):

Synthesized according to Method B using compound **16c** (0.50 g, 1.936 mmol), HEH (0.735 g, 2.90 mmol) and silica gel (3.86 g); white solid; yield: 0.426 g (85 %); Mp 68-70 °C;

^1H NMR (CDCl_3 , 500 MHz): $\delta = 3.25$ (t, $^3J = 8.5$ Hz, 2H), 3.40 (t, $^3J = 8.5$ Hz, 2H), 7.39-7.48 (m, 5H), 7.56 (m, 1H), 7.70 (s, 1H), 7.78-7.82 (m, 3H), 7.98 (dd, $^4J = 1.26$, $^3J = 8.5$ Hz, 2H). ^{13}C NMR (CDCl_3 , 125 MHz): $\delta = 30.2$, 40.3, 125.3, 126.0, 126.5, 127.1, 127.4, 127.6, 128.0, 128.1, 128.6, 132.1, 133.1, 133.6, 136.9, 138.8, 187.9.

Ethyl 5-(naphthalen-2-yl)-3-phenylpent-2-enoate, (16a):

Synthesized according to Method C using compound **16b** (0.35 g, 1.34 mmol), NaH (0.161 g, 4.03 mmol) and triethyl phosphonoacetate (0.91 mL, 4.03 mmol);

16Ea: colourless oil; yield: 0.178 g (40 %); ^1H NMR (CDCl_3 , 500 MHz): $\delta = 1.29$ (t, $^3J = 7.2$ Hz, 3H), 2.89-2.92 (m, 2H), 3.48-3.52 (m, 2H), 4.20 (q, $^3J = 7.2$ Hz, 2H), 6.08 (s, 1H), 7.39-7.50 (m, 8H), 7.63 (s, 1H), 7.75-7.80 (m, 3H). ^{13}C NMR (CDCl_3 , 165 MHz): $\delta = 14.3$, 33.0, 35.3, 59.9, 118.0, 125.1, 125.8, 126.4, 126.8, 127.4, 127.5, 127.6, 127.8, 128.6, 129.0, 132.1, 133.6, 139.1, 141.1, 159.3, 166.4.

16Za: colourless oil; yield: 0.188 g (42 %); ^1H NMR (CDCl_3 , 500 MHz): $\delta = 1.06$ (t, $^3J = 7.2$ Hz, 3H), 2.83-2.90 (m, 4H), 3.98 (q, $^3J = 7.2$ Hz, 2H), 5.94 (s, 1H), 7.21 (dd, $^4J = 1.7$, $^4J = 8.2$ Hz, 2H), 7.23-7.28 (m, 2H), 7.32-7.47 (m, 5H), 7.56 (s, 1H), 7.76 (d, $^3J = 7.9$ Hz, 2H), 7.80 (d, $^3J = 7.9$ Hz, 1H). ^{13}C NMR (CDCl_3 , 125 MHz): $\delta = 13.9$, 34.0, 41.9, 59.8, 117.8, 125.3, 126.0, 126.4, 127.0, 127.3, 127.4, 127.6, 127.8, 127.9, 128.0, 132.1, 133.6, 138.3, 139.8, 158.4, 165.9.

(E)-5-(Naphthalen-2-yl)-3-phenylpent-2-enoic acid, (16E):

Synthesized according to Method D using compound **16Ea** (0.17 g, 0.51 mmol) and NaOH_{aq} (1.70 mL, 5.14 mmol); white solid; yield: 0.143 g (93 %); Mp 147-150 °C;

^1H NMR (CDCl_3 , 500 MHz): $\delta = 2.91$ -2.94 (m, 2H), 3.49-3.53 (m, 2H), 6.14 (s, 1H), 7.38-7.44 (m, 6H), 7.51-7.53 (m, 2H), 7.62 (s, 1H), 7.74-7.79 (m, 3H); ^{13}C NMR (CDCl_3 , 125 MHz): $\delta = 33.3$, 35.4, 116.5, 125.2, 126.5, 126.8, 127.2, 127.4, 127.9, 128.4, 128.7, 128.7, 129.4, 130.9, 132.1, 138.6, 138.7, 162.4, 170.9; LC/MS (+ESI): $m/z = 303.6$ [MH^+]; $R_t = 14.54$ ($\geq 99\%$).

(Z)-5-(Naphthalen-2-yl)-3-phenylpent-2-enoic acid, (16Z):

Synthesized according to Method D using compound **16Za** (0.180 g, 0.54 mmol) and NaOH_{aq} (1.80 mL, 5.45 mmol); white solid; yield: 0.150 g (92 %); Mp 117-120 °C;

^1H NMR (CDCl_3 , 500 MHz): $\delta = 2.84$ -2.89 (m, 4H), 5.92 (s, 1H), 7.21 (dd, $^4J = 1.7$, $^3J = 8.2$ Hz, 2H), 7.30-7.47 (m, 6H), 7.47-7.52 (m, 1H), 7.55 (s, 1H), 7.74-7.82 (m, 2H); ^{13}C NMR (CDCl_3 , 125 MHz): $\delta = 34.1$, 42.5, 116.9, 125.6, 126.3, 126.7, 127.2, 127.5, 127.7, 127.9,

128.3, 128.4, 128.5, 128.7, 133.8, 138.3, 139.4, 159.8, 173.3; LC/MS (+ESI): $m/z = 303.5$ [MH⁺]; $R_f = 14.02$ ($\geq 98\%$).

5-(1H-Indol-3-yl)-3-phenylpent-2-enoic acids, (17E & 17Z):

3-(1H-Indol-3-yl)-1-phenylprop-2-en-1-one, (17c):

Indole-3-aldehyde **17d** (1 g, 6.89 mmol) was dissolved in EtOH (14 mL). Then the acetophenone (0.8 mL, 6.89 mmol) and afterwards piperidine (0.37 mL, 3.82 mmol) were added. The resulting solution was refluxed for 16 h. The reaction mixture was neutralized with 10 % HCl to pH 7. The formed precipitate was collected by vacuum filtration and purified by recrystallization from MeOH to give **17c**. Deep yellow solid; yield: 1.18 g (68 %); Mp 161-163 °C;

¹H NMR (CDCl₃, 500 MHz): $\delta = 7.29$ -7.33 (m, 2H), 7.44-7.46 (m, 1H), 7.50-7.54 (m, 2H), 7.56-7.62 (m, 3H), 8.01-8.06 (m, 1H), 8.06-8.08 (m, 2H), 8.12 (d, ³ $J = 15.5$ Hz, 1H), 8.84 (s, NH). ¹³C NMR (CDCl₃, 125 MHz): $\delta = 112.0$, 114.5, 117.9, 120.7, 121.8, 123.5, 125.4, 128.3, 128.5, 130.3, 132.3, 137.3, 139.0, 139.0, 191.9.

3-(1H-Indol-3-yl)-1-phenylpropan-1-one, (17b):

Synthesized according to Method B using compound **17c** (1.0 g, 4.04 mmol), HEH (1.53 g, 6.06 mmol) and silica gel (8.08 g); white solid; yield: 0.85 g (84 %); Mp 127-130 °C;

¹H NMR (CDCl₃, 500 MHz): $\delta = 3.23$ (t, ³ $J = 7.6$ Hz, 2H), 3.39 (t, ³ $J = 7.6$ Hz, 2H), 7.05-7.06 (m, 1H), 7.14 (dt, ⁴ $J = 0.9$, ³ $J = 7.2$ Hz, 1H), 7.21 (dt, ⁴ $J = 1.3$, ⁴ $J = 8.2$ Hz, 1H), 7.36 (d, ³ $J = 8.2$ Hz, 1H), 7.43-7.47 (m, 2H), 7.53-7.57 (m, 1H), 7.64 (d, ³ $J = 8.5$ Hz, 1H), 7.96-7.99 (m, 2H). ¹³C NMR (CDCl₃, 125 MHz): $\delta = 19.7$, 39.3, 111.1, 115.5, 118.7, 119.3, 121.5, 122.0, 127.3, 128.0, 128.5, 132.9, 136.3, 137.0, 199.9.

Ethyl 5-(1H-indol-3-yl)-3-phenylpent-2-enoate, (17a):

Synthesized according to Method C using compound **17b** (0.50 g, 2.0 mmol), NaH (0.250 g, 6.01 mmol) and triethyl phosphonoacetate (1.2 mL, 6.01 mmol);

17Ea: pale brown oil; yield: 0.175 g (27 %); ¹H NMR (CDCl₃, 500 MHz): $\delta = 1.29$ (t, ³ $J = 7.2$ Hz, 3H), 2.87-2.91 (m, 2H), 3.49-3.52 (m, 2H), 4.19 (q, ³ $J = 7.2$ Hz, 2H), 6.09 (s, 1H), 7.00-7.01 (m, 1H), 7.10 (dt, ⁴ $J = 1.3$, ³ $J = 8.2$ Hz, 1H), 7.17 (dt, ⁴ $J = 1.3$, ³ $J = 8.2$ Hz, 1H), 7.33 (d, ³ $J = 8.2$ Hz, 2H), 7.37-7.41 (m, 3H), 7.48-7.50 (m, 2H), 7.63 (d, ³ $J = 7.9$ Hz, 1H),

7.91 (s, NH). ^{13}C NMR (CDCl_3 , 125 MHz): $\delta = 14.3, 24.7, 31.9, 59.9, 110.9, 116.1, 117.7, 119.0, 119.1, 121.3, 121.8, 126.7, 127.4, 128.5, 128.9, 136.2, 141.2, 159.8, 166.4$.

17Za: pale brown oil; yield: 0.189 g (30 %); ^1H NMR (CDCl_3 , 500 MHz): $\delta = 1.07$ (t, $^3J = 6.9$ Hz, 3H), 2.82-2.90 (m, 4H), 3.99 (q, $^3J = 6.9$ Hz, 2H), 5.94 (s, 1H), 6.96 (s, 1H), 7.10 (dt, $^4J = 0.9$, $^3J = 7.9$ Hz, 1H), 7.19-7.23 (m, 3H), 7.31-7.38 (m, 4H), 7.51 (d, $^3J = 7.9$ Hz, 1H), 7.93 (s, NH). ^{13}C NMR (CDCl_3 , 125 MHz): $\delta = 13.9, 23.3, 40.8, 59.8, 111.1, 115.1, 117.5, 118.6, 119.2, 121.2, 121.9, 127.2, 127.9, 128.0, 128.5, 136.2, 140.0, 159.1, 166.1$.

(E)-5-(1H-Indol-3-yl)-3-phenylpent-2-enoic acid, (17E):

Synthesized according to Method D using compound **17Ea** (0.20 g, 0.63 mmol) and NaOH_{aq} (0.65 mL, 1.89 mmol); white solid; yield: 0.135 g (73 %); Mp 157-160 °C;

^1H NMR (CD_3OD , 500 MHz): $\delta = 2.72$ -2.75 (m, 2H), 3.39-3.43 (m, 2H), 6.05 (s, 1H), 6.95 (dt, $^3J = 0.9, 8.2$ Hz, 1H), 7.05 (dt, $^4J = 0.9, ^4J = 7.9$ Hz, 1H), 7.11-7.12 (d, $^3J = 2.2$ Hz, 1H), 7.31 (d, $^3J = 8.2$ Hz, 1H), 7.39-7.46 (m, 3H), 7.57-7.60 (m, 3H), 10.76 (s, NH), 12.29 (s, OH); ^{13}C NMR (CD_3OD , 125 MHz): $\delta = 34.3, 40.9, 120.8, 123.6, 127.5, 127.6, 128.0, 130.3, 131.6, 136.1, 136.6, 138.2, 138.5, 145.8, 150.1, 168.0, 176.8$; LC/MS (+ESI): $m/z = 292.5$ [MH^+]; $R_t = 12.37$ ($\geq 96\%$).

(Z)-5-(1H-Indol-3-yl)-3-phenylpent-2-enoic acid, (17Z):

Synthesized according to Method D using compound **17Za** (0.20 g, 0.63 mmol) and NaOH_{aq} (0.65 mL, 1.89 mmol); white solid; yield: 0.135 g (73 %); Mp 160-162 °C;

^1H NMR (CD_3OD , 500 MHz): $\delta = 2.68$ -2.71 (m, 2H), 2.79-2.82 (m, 2H), 5.89 (s, 1H), 7.05 (t, $^3J = 7.9$ Hz, 1H), 6.95 (dt, $^4J = 0.9, ^3J = 7.6$ Hz, 1H), 7.05 (dt, $^4J = 0.9, ^3J = 7.6$ Hz, 1H), 7.10-7.11 (d, $^4J = 2.2$ Hz, 1H), 7.23-7.25 (m, 2H), 7.29-7.38 (m, 4H), 7.41 (d, $^3J = 7.9$ Hz, 1H), 10.78 (s, NH), 11.85 (s, OH); ^{13}C NMR (CD_3OD , 125 MHz): $\delta = 24.6, 42.3, 112.2, 115.1, 118.7, 119.2, 119.5, 122.3, 123.0, 128.5, 128.6, 128.7, 128.9, 138.2, 141.4, 160.7, 169.8$; LC/MS (+ESI): $m/z = 292.5$ [MH^+]; $R_t = 11.93$ ($\geq 94\%$).

4-(4-Chlorophenoxy)-3-phenylbut-2-enoic acids, (18Z & 18E):

2-(4-Chlorophenoxy)-1-phenylethanone, (18b):

4-Chlorophenol **18c** (0.774 g, 6.02 mmol) was refluxed with 2-bromoacetophenone (1.0 g, 5.02 mmol) in DMF (10 mL) with potassium carbonate (3.5 g, 25.1 mmol) for 2 hours. The reaction mixture was taken up in water (50 mL) and extracted with dichloromethane (3 x 20

mL). The combined organic layers were washed with water (20 mL) and brine (20 mL), dried over MgSO_4 and the solvent was removed under reduced pressure. The crude product was purified by flash column chromatography on silica gel [PE / EtOAc (10:1)]; pale yellow solid; yield: 1.22 g (99 %);

^1H NMR (CDCl_3 , 500 MHz): δ = 5.26 (s, 2H), 6.85-6.89 (m, 2H), 7.22-7.25 (m, 2H), 7.51 (t, 3J = 7.4 Hz, 2H), 6.09-6.42 (m, 1H), 7.97-8.00 (m, 2H); ^{13}C NMR (CDCl_3 , 125 MHz): δ = 71.0, 116.2, 126.6, 128.0, 128.9, 129.4, 133.9, 134.5, 156.7, 194.1.

Ethyl 4-(4-chlorophenoxy)-3-phenylbut-2-enoate, (18a):

Synthesized according to Method C using compound **18b** (0.60 g, 2.43 mmol), NaH (0.29 g, 7.30 mmol) and triethyl phosphonoacetate (1.61 mL, 7.30 mmol);

18Za: colourless oil; yield: 0.135 g (18 %); ^1H NMR (CDCl_3 , 500 MHz): δ = 1.01 (t, 3J = 6.9 Hz, 3H), 3.94 (q, 3J = 6.9 Hz, 2H), 4.63 (d, 3J = 1.9 Hz, 2H), 6.19 (t, 3J = 1.9 Hz, 1H), 6.77-6.82 (m, 2H), 7.16-7.20 (m, 4H), 7.28-7.35 (m, 3H). ^{13}C NMR (CDCl_3 , 125 MHz): δ = 13.9, 60.1, 71.1, 116.1, 117.4, 126.4, 127.5, 128.2, 128.4, 129.5, 136.6, 152.4, 156.5, 165.6.

18Ea: colourless oil; yield: 0.40 g (52 %); ^1H NMR (CDCl_3 , 500 MHz): δ = 1.32 (t, 3J = 7.2 Hz, 3H), 4.25 (q, 3J = 7.2 Hz, 2H), 5.56 (s, 1H), 6.25 (s, 1H), 6.81-6.83 (m, 2H), 7.17-7.21 (m, 2H), 7.35-7.38 (m, 3H), 7.46-7.48 (m, 2H). ^{13}C NMR (CDCl_3 , 125 MHz): δ = 14.2, 60.5, 64.4, 116.3, 120.5, 125.9, 127.2, 128.4, 129.2, 129.3, 138.2, 153.5, 157.0, 165.6.

(Z)-4-(4-Chlorophenoxy)-3-phenylbut-2-enoic acid, (18Z):

Synthesized according to Method D using compound **18Za** (0.15 g, 0.47 mmol) and NaOH_{aq} (1.6 mL, 4.7 mmol); white solid; yield: 0.10 g (74 %); Mp 115-117 °C;

^1H NMR (CDCl_3 , 500 MHz): δ = 5.48 (s, 2H), 6.21 (s, 1H), 6.71-6.74 (m, 2H), 7.10-7.13 (m, 2H), 7.28-7.33 (m, 3H), 7.38-7.42 (m, 2H); ^{13}C NMR (CDCl_3 , 125 MHz): δ = 64.5, 116.3, 119.2, 126.1, 127.3, 128.5, 129.3, 129.7, 137.8, 156.7, 156.9, 170.4; LC/MS (+ESI): m/z = 289.4 [MH^+]; R_t = 13.26 (≥ 95 %).

(E)-4-(4-Chlorophenoxy)-3-phenylbut-2-enoic acid, (18E):

Synthesized according to Method D using compound **18Ea** (0.06 g, 0.18 mmol) and NaOH_{aq} (0.61 mL, 1.8 mmol); white solid; yield: 0.05 g (86 %); Mp 110-112 °C;

^1H NMR (CDCl_3 , 500 MHz): δ = 3.43 (s, 2H), 6.61 (s, 1H), 7.00 (d, 3J = 9.1 Hz, 2H), 7.25-7.27 (m, 1H), 7.28 (d, 3J = 8.8 Hz, 2H), 7.33-7.36 (m, 2H), 7.53-7.55 (m, 2H); ^{13}C NMR (CDCl_3 , 125 MHz): δ = 38.0, 115.8, 118.1, 127.4, 127.9, 128.3, 128.4, 129.6, 135.4, 141.2, 155.7, 177.4; LC/MS (+ESI): m/z = 289.4 [MH^+]; R_t = 13.01 (≥ 99 %).

(Z)-4-(4-Chlorophenylthio)-3-phenylbut-2-enoic acid, (19Z):**2-(4-Chlorophenylthio)-1-phenylethanone, (19b):**

2-Bromoacetophenone (1.0 g, 6.91 mmol), 4-chlorothiophenol **19c** (1.37 g, 6.91 mmol) and 5 % benzyltriethylammonium chloride (0.078 g, 0.35 mmol) were dissolved in 20 mL dichloromethane. Under vigorous stirring sodium hydroxide (0.61 g, 15.21 mmol) in 2 mL water was added and the stirring maintained for 16 hours. The mixture was diluted with water (50 mL), the dichloromethane organic layer (60 mL) separated and washed successively with brine (20 mL), dried over MgSO₄ and evaporated. The resultant oil was further purified by column chromatography on silica gel [PE / EtOAc (12:1)]; pale yellow solid; yield 0.74 g (41 %); Mp 82-84 °C;

¹H NMR (CDCl₃, 500 MHz): δ = 4.26 (s, 2H), 7.24-7.28 (m, 2H), 7.31-7.34 (m, 2H), 7.46-7.50 (m, 2H), 7.58-7.62 (m, 1H), 7.92-7.97 (m, 2H).

(Z)-Ethyl 4-(4-chlorophenylthio)-3-phenylbut-2-enoate, (19Za):

Synthesized according to Method C using compound **19b** (0.50 g, 1.90 mmol), NaH (0.228 g, 5.71 mmol) and triethyl phosphonoacetate (1.26 mL, 5.71 mmol); pale yellow oil; yield: 0.401 g (63 %);

¹H NMR (CDCl₃, 500 MHz): δ = 1.23 (t, ³J = 7.2 Hz, 3H), 3.77 (s, 2H), 4.14 (q, ³J = 7.2 Hz, 2H), 6.69 (s, 1H), 7.27-7.31 (m, 3H), 7.32-7.36 (m, 4H), 7.38-7.42 (m, 2H). ¹³C NMR (CDCl₃, 125 MHz): δ = 14.1, 37.8, 61.0, 124.8, 125.8, 127.7, 128.6, 129.2, 130.5, 132.6, 134.3, 136.1, 140.1, 170.3.

(Z)-4-(4-Chlorophenylthio)-3-phenylbut-2-enoic acid, (19Z):

Synthesized according to Method D using compound **19Za** (0.20 g, 0.60 mmol) and NaOH_{aq} (1.0 mL, 3 mmol); white solid; yield: 0.11 g (60 %); Mp 137-139 °C;

¹H NMR (CDCl₃, 500 MHz): δ = 3.76 (s, 2H), 6.66 (s, 1H), 6.71-6.74 (m, 2H), 7.20-7.35 (m, 9H); ¹³C NMR (CDCl₃, 125 MHz): δ = 37.3, 125.6, 125.7, 127.9, 128.7, 129.3, 130.7, 133.1, 134.0, 134.8, 139.7, 176.2; LC/MS (+ESI): *m/z* = 305.6 [MH⁺]; *R_t* = 13.84 (≥ 99 %).

(E/Z)-3-(5-Chlorobenzofuran-2-yl)-3-phenylacrylic acid, (20E/Z):**Benzofuran-2-yl-(4-chlorophenyl)methanone, (20b):**

Synthesized according to Method E using compound **20c** (2.0 g, 12.77 mmol), 2-bromoacetophenone (1.85 g, 12.77 mmol) and K_2CO_3 (3.53 g, 25.54 mmol); white solid, yield: 1.85 g (57 %);

1H NMR ($CDCl_3$, 500 MHz): δ = 7.44-7.48 (m, 2H), 7.53-7.58 (m, 13), 7.64-7.68 (m, 1H), 7.70 (d, 3J = 2.2 Hz, 1H), 8.03-8.06 (m, 2H); ^{13}C NMR ($CDCl_3$, 125 MHz): δ = 113.7, 115.4, 122.6, 126.5, 128.2, 128.6, 128.7, 129.5, 129.6, 133.2, 136.9, 154.2, 184.1.

(E/Z)-Ethyl 3-(5-chlorobenzofuran-2-yl)-3-phenylacrylate, (20E/Za):

Synthesized according to Method C using compound **20b** (0.60 g, 2.34 mmol), NaH (0.187 g, 4.68 mmol) and triethyl phosphonoacetate (1.08 mL, 4.91 mmol); pale yellow oil; yield: 0.702 g (92 %; 3:1, *E/Z*);

1H NMR ($CDCl_3$, 500 MHz): δ = 1.12 (t, 3J = 7.2 Hz, 1H, *Z*), 1.24 (t, 3J = 7.2 Hz, 3H, *E*), 4.06 (q, 3J = 7.2 Hz, 0.6H, *Z*), 4.24 (q, 3J = 7.2 Hz, 2H, *E*), 6.27 (s, 1H, *E*), 6.36 (s, 0.3H, *Z*), 6.78 (s, 0.3H, *Z*), 6.83 (s, 1H, *E*), 7.45-7.26 (m, 10H), 7.55 (d, 3J = 2.2 Hz, 1H). ^{13}C NMR ($CDCl_3$, 125 MHz): δ = 13.9, 14.2, 60.2, 60.7, 109.5, 110.6, 112.3, 116.8, 121.0, 121.1, 125.5, 126.4, 128.0, 128.4, 128.5, 128.6, 129.6, 128.4, 141.5, 143.9, 153.4, 154.2, 165.6, 165.9.

(E/Z)-3-(5-Chlorobenzofuran-2-yl)-3-phenylacrylic acid, (20E/Z):

Synthesized according to Method D using compound **20E/Za** (0.20 g, 0.63 mmol) and $NaOH_{aq}$ (2.1 mL, 6.3 mmol); pale yellow solid; yield: 0.147 g (78 %; 3:1, *E/Z*); Mp 164-166 °C;

1H NMR ($CDCl_3$, 500 MHz): δ = 6.27 (s, 1H, *E*), 6.39 (s, 0.3H, *Z*), 6.78 (s, 0.3H, *Z*), 6.88 (s, 1H, *E*), 7.26-7.47 (m, 10H), 7.55 (d, 4J = 1.8 Hz, 1H); ^{13}C NMR ($CDCl_3$, 125 MHz): δ = 110.4, 110.4, 111.6, 112.5, 115.5, 119.4, 121.1, 121.3, 125.8, 126.8, 128.0, 128.6, 128, 7, 128.8, 129.4, 129.6, 130.0, 138.3, 144.2, 153.5, 156.6, 170.3, 207.6, 210.0; LC/MS (+ESI): m/z = 299.4 [MH^+]; $R_t(E)$ = 13.39, $R_t(Z)$ = 14.33; (≥ 99 %).

(E/Z)-3-(5-Methylbenzofuran-2-yl)-3-phenylacrylic acid, (21E/Z):**Benzofuran-2-yl-(p-tolyl)methanone, (21b):**

Synthesized according to Method E using compound **21c** (1.0 g, 7.35 mmol), 2-bromoacetophenone (1.06 g, 7.35 mmol) and K₂CO₃ (2.03 g, 14.69 mmol); pale yellow solid, yield: 1.1 g (64 %);

¹H NMR (CDCl₃, 500 MHz): δ = 2.47 (s, 3H), 7.31 (dd, ⁴J = 1.9, ³J = 8.2 Hz, 1H), 7.46 (s, 1H), 7.49-7.55 (m, 4H), 7.61-7.66 (m, 1H), 8.03-8.06 (m, 2H); ¹³C NMR (CDCl₃, 125 MHz): δ = 21.3, 112.1, 116.4, 122.7, 128.5, 129.4, 130.0, 132.8, 133.6, 137.3, 152.4, 154.6, 184.4.

(E/Z)-Ethyl 3-(5-methylbenzofuran-2-yl)-3-phenylacrylate, (21E/Za):

Synthesized according to Method C using compound **21b** (0.60 g, 2.54 mmol), NaH (0.204 g, 5.10 mmol) and triethyl phosphonoacetate (1.18 mL, 5.33 mmol); pale yellow oil; yield: 0.721 g (93 %; 2.5:1, E/Z);

¹H NMR (CDCl₃, 500 MHz): δ = 1.12 (t, ³J = 7.0 Hz, 1.2H, Z), 1.25 (t, ³J = 7.0 Hz, 3H, E), 2.41 (s, 1.2H, Z), 2.44 (s, 3H, E), 4.06 (q, ³J = 7.0 Hz, 0.8H, Z), 4.26 (q, ³J = 7.0 Hz, 2H, E), 6.20 (s, 1H, E), 6.35 (s, 0.4H, Z), 6.77 (s, 0.4H, Z), 6.81 (s, 1H, E), 7.17-7.14 (m, 1.4H), 7.24 (s, 0.4H), 7.32-7.45 (m, 10H). ¹³C NMR (CDCl₃, 125 MHz): δ = 13.9, 14.2, 21.2, 21.3, 60.0, 60.7, 110.0, 110.8, 111.3, 115.6, 120.0, 121.2, 126.7, 127.6, 127.9, 128.3, 128.4, 128.7, 128.8, 129.4, 132.4, 132.7, 136.2, 138.9, 141.8, 144.6, 152.9, 153.5, 153.9, 155.6, 165.8, 166.3.

(E/Z)-3-(5-Methylbenzofuran-2-yl)-3-phenylacrylic acid, (21E/Z):

Synthesized according to Method D using compound **21E,Za** (0.25 g, 0.63 mmol) and NaOH_{aq} (2.73 mL, 8.2 mmol); pale yellow solid; yield: 0.189 g (83 %; 2.5:1, E/Z); Mp 200-204 °C;

¹H NMR (CDCl₃, 500 MHz): δ = 2.41 (s, 1.3H, Z), 2.44 (s, 3H, E), 6.21 (s, 1H, E), 6.37 (s, 0.4H, Z), 6.76 (s, 0.4H, Z), 6.88 (s, 1H, E), 7.13-7.19 (m, 1.5H), 7.24 (s, 0.4H), 7.33-7.46 (m, 10H); ¹³C NMR (CDCl₃, 125 MHz): δ = 21.1, 21.3, 110.0, 110.9, 111.0, 111.2, 114.2, 118.4, 121.2, 121.3, 126.9, 127.1, 127.9, 128.5, 128.6, 128.9, 129.2, 129.8, 132.6, 133.6, 137.9, 138.8, 143.1, 143.8, 144.6, 145.4, 146.6, 152.2, 152.4, 154.3, 154.8, 169.7, 169.9; LC/MS (+ESI): m/z = 279.5 [MH⁺]; R_t = 14.09 (≥ 98 %).

3-(5-Chlorobenzo[b]thiophen-2-yl)-3-phenylacrylic acids, (22Z & 22E):**1-Benzothiophen-2-yl-(4-chlorophenyl)methanone, (22b):**

To a cold solution (ice bath) containing 5-chloro-2-nitrobenzaldehyde (0.2 g, 1.31 mmol) and anhydrous potassium carbonate (0.221 g, 1.60 mmol) in DMF was added dropwise a solution of thioacetophenone (0.243 g, 1.31 mmol). The mixture was stirred from 0 °C to rt within 3 hours. The mixture was then poured into ice water, extracted with dichloromethane and dried over MgSO₄. The oily crude product was purified by column chromatography on silica gel [PE / EtOAc (10:1)]; pale yellow solid; yield 0.31 g (87 %);

¹H NMR (CDCl₃, 500 MHz): δ = 7.45 (dd, ⁴J = 1.9, ³J = 8.8 Hz, 1H), 7.53-7.56 (m, 2H), 7.63-7.67 (m, 1H), 7.79 (s, 1H), 7.83-7.86 (m, 2H), 7.91-7.94 (m, 2H); ¹³C NMR (CDCl₃, 125 MHz): δ = 124.0, 124.9, 125.3, 126.7, 127.9, 128.6, 129.3, 130.9, 131.3, 132.7, 137.5, 144.9, 189.3.

Ethyl 3-(5-chlorobenzo[b]thiophen-2-yl)-3-phenylacrylate, (22E/Za):

Synthesized according to Method C using compound **22b** (0.17 g, 0.62 mmol), NaH (0.05 g, 1.24 mmol) and triethyl phosphonoacetate (0.29 mL, 1.24 mmol);

22Za: pale yellow oil; yield: 0.086 g (41 %); ¹H NMR (CDCl₃, 500 MHz): δ = 1.17 (t, ³J = 6.9 Hz, 3H), 4.14 (q, ³J = 6.9 Hz, 2H), 6.39 (s, 1H), 7.27 (s, 1H), 7.27-7.32 (m, 2H), 7.34-7.41 (m, 5H), 7.71-7.74 (m, 2H). ¹³C NMR (CDCl₃, 125 MHz): δ = 14.0, 60.5, 120.4, 123.2, 123.4, 125.2, 125.4, 128.2, 128.5, 128.7, 130.6, 138.8, 139.0, 140.4, 141.9, 147.9, 165.5.

22Ea: pale yellow oil; yield: 0.077 g (36 %); ¹H NMR (CDCl₃, 500 MHz): δ = 1.11 (t, ³J = 6.9 Hz, 3H), 4.04 (q, ³J = 6.9 Hz, 2H), 6.46 (s, 1H), 6.90 (s, 1H), 7.29-7.31 (m, 3H), 7.35-7.46 (m, 3H), 7.59 (d, ⁴J = 1.9 Hz, 1H) 7.69 (d, ³J = 8.5 Hz, 1H). ¹³C NMR (CDCl₃, 125 MHz): δ = 13.9, 60.2, 118.0, 123.3, 123.8, 126.3, 126.9, 128.0, 128.4, 128.6, 135.0, 137.4, 138.0, 140.7, 146.5, 156.8, 165.3.

(Z)-3-(5-Chlorobenzo[b]thiophen-2-yl)-3-phenylacrylic acid, (22Z):

Synthesized according to Method D using compound **22Za** (0.075 g, 0.22 mmol) and NaOH_{aq} (0.75 mL, 2.28 mmol); pale yellow solid; yield: 0.05 g (74 %); Mp 210-212 °C;

¹H NMR ((CD₃)₂SO, 500 MHz): δ = 6.48 (s, 1H), 7.38-7.41 (m, 2H), 7.41-7.43 (m, 4H), 7.43-7.46 (m, 1H), 7.97 (d, ⁴J = 2.2 Hz, 1H), 8.00 (d, ³J = 8.5 Hz, 1H); ¹³C NMR ((CD₃)₂SO, 125 MHz): δ = 122.3, 123.1, 123.8, 124.6, 124.8, 125.8, 127.7, 128.5, 129.4, 129.5, 138.4, 139.4, 140.4, 141.9, 166.3; LC/MS (+ESI): m/z = 315.4 [MH⁺]; R_t = 14.14 (\geq 99 %).

(E)-3-(5-Chlorobenzo[b]thiophen-2-yl)-3-phenylacrylic acid, (22E):

Synthesized according to Method D using compound **22Ea** (0.085 g, 0.26 mmol) and NaOH_{aq} (0.9 mL, 2.61 mmol); pale yellow solid; yield: 0.06 g (74 %); Mp 208-210 °C;

¹H NMR (CDCl₃, 500 MHz): δ = 6.26 (s, 1H), 7.16-7.29 (m, 7H), 7.58-7.61 (m, 2H); ¹³C NMR (CDCl₃, 125 MHz): δ = 120.9, 123.3, 123.5, 125.3, 125.5, 128.4, 128.6, 129.9, 130.7, 139.3, 140.9, 140.5, 142.1, 148.0, 167.8; LC/MS (+ESI): m/z = 315.4 [MH⁺]; R_t = 14.70 (\geq 99 %).

3-(5-Chlorobenzofuran-2-yl)-3-phenylpropanoic acid, (23):**Ethyl 3-(5-chlorobenzofuran-2-yl)-3-phenylpropanoate, (23a):**

Synthesized according to Method F using compound **20E/Z** (0.4 g, 1.22 mmol), sodium hypophosphite (0.194 g, 1.83 mmol) and Pd/C (0.13 g, 0.12 mmol); pale yellow oil; yield: 0.249 g (88 %); ¹H NMR (CDCl₃, 500 MHz): δ = 1.16 (t, ³J = 7.2 Hz, 3H), 2.95-3.01 (m, 1H), 3.17-3.24 (m, 1H), 4.03-4.13 (m, 2H), 4.69 (t, ³J = 7.9 Hz, 1H), 6.45 (s, 1H), 7.16-7.32 (m, 4H), 7.38-7.49 (m, 4H); ¹³C NMR (CDCl₃, 125 MHz): δ = 14.1, 41.8, 60.6, 102.8, 111.0, 120.6, 122.6, 123.9, 127.4, 127.8, 128.2, 128.7, 129.8, 140.4, 153.2, 159.3, 171.0.

3-(5-Chlorobenzofuran-2-yl)-3-phenylpropanoic acid, (23).

Synthesized according to Method D using compound **23a** (0.2 g, 0.61 mmol) and NaOH_{aq} (2.0 mL, 6.01 mmol); white solid; yield: 0.14 g (76 %); Mp 135-138 °C;

¹H NMR (CDCl₃, 500 MHz): δ = 3.03-3.06 (m, 1H), 3.25-3.29 (m, 1H), 4.67 (t, ³J = 7.6 Hz, 1H), 6.45 (s, 1H), 7.15-7.30 (m, 4H), 7.39-7.47 (m, 4H); ¹³C NMR (CDCl₃, 125 MHz): δ = 38.9, 41.4, 102.9, 112.0, 117.8, 120.6, 122.7, 123.8, 127.4, 127.7, 127.8, 128.4, 128.9, 154.8, 160.5; LC/MS (+ESI): m/z = 301.6 [MH⁺]; R_t = 13.45 (\geq 99 %).

3-(5-Methylbenzofuran-2-yl)-3-phenylpropanoic acid, (24):**Ethyl 3-(5-methylbenzofuran-2-yl)-3-phenylpropanoate, (24a):**

Synthesized according to Method F using compound **21E/Z** (0.2 g, 0.65 mmol), sodium hypophosphite (0.103 g, 0.98 mmol) and Pd/C (0.07 g, 0.065 mmol); white oil; yield: 0.182 g (91 %);

^1H NMR (CDCl_3 , 500 MHz): δ = 1.15 (t, 3J = 7.2 Hz, 3H), 2.40 (s, 3H), 2.95-3.00 (m, 1H), 3.17-3.22 (m, 1H), 4.02-4.12 (m, 2H), 4.67 (t, 3J = 7.9 Hz, 1H), 6.37 (s, 1H), 7.02 (dd, 4J = 1.6, 3J = 9.1 Hz, 1H), 7.23-7.33 (m, 7H); ^{13}C NMR (CDCl_3 , 125 MHz): δ = 14.1, 21.2, 39.5, 41.8, 60.6, 102.6, 110.5, 120.5, 124.8, 127.2, 127.9, 128.5, 128.6, 132.0, 140.4, 153.2, 159.4, 171.1.

3-(5-Methylbenzofuran-2-yl)-3-phenylpropanoic acid, (24):

Synthesized according to Method D using compound **24a** (0.15 g, 0.48 mmol) and NaOH_{aq} (1.6 mL, 4.86 mmol); white solid; yield: 0.101 g (75 %); Mp 124-127 °C;

^1H NMR (CDCl_3 , 500 MHz): δ = 2.40 (s, 3H), 2.99-3.04 (m, 1H), 3.23-3.28 (m, 1H), 4.64 (t, 3J = 8.2 Hz, 1H), 6.37 (s, 1H), 7.01 (dd, 4J = 1.6, 3J = 8.8 Hz, 1H), 7.23-7.33 (m, 8H); ^{13}C NMR (CDCl_3 , 125 MHz): δ = 21.3, 38.8, 41.5, 102.7, 110.6, 120.1, 120.5, 124.9, 125.7, 127.3, 127.8, 128.5, 128.8, 132.1, 153.3, 158.9, 175.6; LC/MS (+ESI): m/z = 281.5 [MH^+]; R_f = 13.03 (\geq 99 %).

(E)-2-(2-(4-Chlorobenzyl)-2,3-dihydro-1H-inden-1-ylidene)acetic acid, (25E):

2-(4-Chlorobenzylidene)-2,3-dihydro-1H-inden-1-one, (25c):

Synthesized according to Method A using 4-chlorobenzaldehyde **2d** (1.06 g, 7.57 mmol) and 1-indanone (1.0 g, 7.57 mmol); white solid; yield: 1.6 g (83 %); Mp 156-160 °C;

^1H NMR (CDCl_3 , 500 MHz): δ = 4.02 (s, 2H), 7.42-7.45 (m, 3H), 7.55-7.64 (m, 5H), 7.91 (d, 3J = 7.6 Hz, 1H). ^{13}C NMR (CDCl_3 , 125 MHz): δ = 32.3, 124.5, 126.2, 127.8, 129.2, 131.8, 132.4, 133.9, 134.8, 135.1, 135.6, 137.9, 149.4, 194.0.

2-(4-Chlorobenzyl)-2,3-dihydro-1H-inden-1-one, (25b):

Synthesized according to Method B using compound **25c** (0.435 g, 1.71 mmol), HEH (0.650 g, 2.56 mmol) and silica gel (3.42 g); white solid; yield: 0.359 g (82 %); Mp 80-82 °C;

^1H NMR (CDCl_3 , 500 MHz): δ = 2.68-2.73 (m, 1H), 2.81-2.86 (m, 1H), 2.95-3.00 (m, 1H), 3.16-3.21 (m, 1H), 3.32-3.36 (m, 1H), 7.15-7.19 (m, 2H), 7.25-7.29 (m, 2H), 7.36-7.42 (m, 2H), 7.58 (dt, 4J = 1.2, 3J = 7.2 Hz, 1H), 7.78 (d, 3J = 7.2 Hz, 1H). ^{13}C NMR (CDCl_3 , 125 MHz): δ = 32.0, 36.2, 48.7, 124.0, 126.6, 127.5, 128.6, 130.3, 132.2, 134.9, 136.5, 138.0, 153.4, 207.3.

(E)-Ethyl 2-(2-(4-chlorobenzyl)-2,3-dihydro-1H-inden-1-ylidene)acetate, (25Ea):

Synthesized according to Method C using compound **25b** (0.30 g, 1.17 mmol), NaH (0.234 g, 3.51 mmol) and triethyl phosphonoacetate (0.70 mL, 3.51 mmol); pale yellow oil; yield: 0.126 g (33 %); ^1H NMR (CDCl_3 , 500 MHz): δ = 1.33 (t, 3J = 7.2 Hz, 3H), 2.22 (t, 3J = 11.0 Hz, 1H), 2.72 (d, 3J = 17.0 Hz, 1H), 2.95 (m, 1H), 3.17 (dd, 4J = 3.5, 3J = 13.2 Hz, 1H), 4.09-4.17 (m, 1H), 4.25 (q, 3J = 7.2 Hz, 2H), 6.32 (d, 3J = 1.6 Hz, 1H), 7.24-7.30 (m, 6H), 7.35 (t, 3J = 7.6 Hz, 1H) 7.59 (d, 3J = 7.6 Hz, 1H). ^{13}C NMR (CDCl_3 , 125 MHz): δ = 14.4, 35.6, 40.7, 44.2, 59.9, 108.1, 122.0, 125.2, 126.0, 127.0, 128.2, 128.3, 130.6, 131.0, 131.9, 139.2, 139.2, 165.8.

(E)-2-(2-(4-Chlorobenzyl)-2,3-dihydro-1H-inden-1-ylidene)acetic acid, (25E):

Synthesized according to Method D using compound **25Ea** (0.10 g, 0.30 mmol) and NaOH_{aq} (1.0 mL, 3.06 mmol); white solid; yield: 0.07 g (79 %); Mp 216-219 °C; ^1H NMR ($(\text{CD}_3)_2\text{SO}$, 500 MHz): δ = 2.23 (dd, 3J = 11.0 Hz, 1H), 2.68 (d, 3J = 17.0 Hz, 1H), 2.94 (dd, 3J = 7.2 Hz, 1H), 3.08 (dd, 4J = 2.8, 3J = 12.9 Hz, 1H), 3.98-4.04 (m, 1H), 6.39 (s, 1H), 7.26-7.32 (m, 1H), 7.34-7.41 (m, 6H), 7.77 (d, 3J = 7.9 Hz, 1H); ^{13}C NMR ($(\text{CD}_3)_2\text{SO}$, 125 MHz): δ = 34.9, 40.1, 43.4, 109.2, 122.0, 125.9, 126.9, 128.1, 130.6, 130.9, 138.7, 139.4, 146.7, 164.8, 167.4; Mp 115-118 °C; LC/MS (+ESI): m/z = 299.5 [MH^+]; R_t = 14.6 (≥ 96 %).

6.1.3.2. Compounds described in Chapter 3.2.**2-(3-(4-Chlorophenyl)-3-oxo-1-phenylpropyl)malonic acid, (4A):****(E)-1-(4-Chlorophenyl)-3-phenylprop-2-en-1-one, (1A):**

Synthesized according to Method A using benzaldehyde (2.0 g, 18.8 mmol) and 4'-chloroacetophenone (2.91 g, 18.8 mmol); pale yellow solid; yield: 4.2 g (93 %); ^1H -NMR (500 MHz, CDCl_3): δ (ppm) = 7.42-7.43 (m, 3H), 7.47-7.50 (m, 3H), 7.63-7.65 (m, 2H), 7.82 (d, J = 15.8 Hz, 1H), 7.96 (d, J = 8.8 Hz, 2H). ^{13}C -NMR (125 MHz, CDCl_3): δ (ppm) = 121.5, 128.5, 128.9, 129.0, 129.9, 130.7, 134.7, 136.5, 139.2, 145.3, 189.2.

Diethyl 2-(3-(4-chlorophenyl)-3-oxo-1-phenylpropyl)malonate, (2A):

Synthesized according to Method H using **1A** (1.0 g, 4.12 mmol) and diethyl malonate (0.62 mL, 4.12 mmol) and magnesium oxide (0.41 g); white solid; yield: 1.5 g (89 %);

$^1\text{H-NMR}$ (500 MHz, CDCl_3): δ (ppm) = 1.01 (t, J = 7.2 Hz, 3H), 1.23 (t, J = 7.2 Hz, 3H), 3.38 (dd, J = 9.2, 9.2 Hz, 1H), 3.53 (dd, J = 4.4, 4.4 Hz, 1H), 3.80 (d, J = 9.7 Hz, 1H), 3.95 (q, J = 7.2 Hz, 2H), 4.12-4.25 (m, 3H), 7.14-7.19 (m, 1H), 7.22-7.25 (m, 4H), 7.39 (d, J = 8.8 Hz, 2H), 7.83 (d, J = 8.8 Hz, 2H). $^{13}\text{C-NMR}$ (125 MHz, CDCl_3): δ (ppm) = 13.7, 14.0, 40.9, 42.6, 57.5, 61.4, 61.7, 127.2, 128.2, 128.4, 128.8, 129.5, 135.1, 139.4, 140.2, 167.6, 168.3, 196.4.

2-(3-(4-Chlorophenyl)-3-oxo-1-phenylpropyl)malonic acid, (4A):

Synthesized according to Method L using **2A** (0.9 g, 2.22 mmol) and NaOH_{aq} (7.5 mL); white solid; yield: 0.5 g (64 %); mp 143-145 °C.

$^1\text{H-NMR}$ (500 MHz, CD_3OD): δ (ppm) = 3.33 (dd, J = 3.5, 16.7 Hz, 1H), 3.60 (dd, J = 10.1, 10.1 Hz, 1H), 3.73 (d, J = 3.5, 16.7 Hz, 1H), 3.87 (dt, J = 3.8, 10.4 Hz, 1H), 7.11 (t, J = 7.2 Hz, 1H), 7.19 (t, J = 7.2 Hz, 2H), 7.27 (d, J = 7.2 Hz, 2H), 7.54 (d, J = 8.5 Hz, 2H), 7.87 (d, J = 8.5 Hz, 2H), 12.67 (s, 2H). $^{13}\text{C-NMR}$ (125 MHz, CD_3OD): δ (ppm) = 40.4, 42.4, 57.2, 126.4, 127.8, 128.3, 128.7, 129.6, 135.2, 137.9, 141.0, 169.0, 169.6, 196.4; LC/MS (+ESI): m/z = 347.2 [MH^+]; R_t = 4.17 (≥ 97 %).

Bis(acetoxymethyl) 2-(3-(4-chlorophenyl)-3-oxo-1-phenylpropyl)malonate, (5A):

Synthesized according to Method M **4A** (0.5 g, 1.44 mmol), bromomethyl acetate (0.42 mL, 4.32 mmol) and triethylamine (1.0 mL, 7.2 mmol); white solid; yield: 0.46 g (65 %); mp 92-93 °C;

$^1\text{H-NMR}$ (500 MHz, CD_3OD): δ (ppm) = 1.99 (s, 3H), 2.10 (s, 3H), 3.47 (dd, J = 8.9 Hz, 1H), 3.54 (dd, J = 4.72 Hz, 1H), 3.96 (d, J = 9.1 Hz, 1H), 4.17-4.21 (m, 1H), 5.67 (q, J = 5.7 Hz, 2H), 5.76 (q, J = 5.7 Hz, 2H), 7.19-7.23 (m, 1H), 7.25-7.28 (m, 4H), 7.41 (d, J = 8.5 Hz, 2H), 7.83 (d, J = 8.5 Hz, 2H); $^{13}\text{C-NMR}$ (125 MHz, CD_3OD): δ (ppm) = 20.5, 20.53, 40.42, 42.1, 56.3, 79.4, 79.8, 127.5, 128.1, 128.6, 128.9, 129.5, 134.9, 139.6, 139.64, 166.0, 166.5, 169.1, 169.3, 196.0; LC/MS (+ESI): m/z = 491.2 [MH^+]; R_t = 5.24 (≥ 97 %).

5-(4-Chlorophenyl)-5-oxo-3-phenylpentanoic acid, (6A):

Synthesized according to Method N using **4A** (0.30 g, 0.86 mmol); white solid; yield: 0.19 g (75 %); mp 135-137 °C;

$^1\text{H-NMR}$ (500 MHz, CDCl_3): δ (ppm) = 2.73 (dd, J = 7.6, 7.6 Hz, 1H), 2.85 (dd, J = 6.9, 6.9 Hz, 1H), 3.28-3.37 (m, 2H), 3.81-3.87 (m, 1H), 7.18-7.22 (m, 1H), 7.24-7.31 (m, 4H), 7.39 (d, J = 8.8 Hz, 2H), 7.82 (d, J = 8.8 Hz, 2H); $^{13}\text{C-NMR}$ (125 MHz, CDCl_3): δ (ppm) = 37.2.

40.1, 44.5, 127.0, 127.3, 128.7, 128.9, 129.5, 135.1, 139.6, 142.8, 176.9, 196.9; LC/MS (+ESI): $m/z = 303.2$ [MH^+]; $R_t = 4.69$ ($\geq 98\%$).

2-(3-(3-Chlorophenyl)-3-oxo-1-phenylpropyl)malonic acid, (4B):

(E)-1-(3-Chlorophenyl)-3-phenylprop-2-en-1-one, (1B):

Synthesized according to Method A using benzaldehyde (3.4 g, 32.34 mmol) and 3'-chloroacetophenone (5.0 g, 32.34 mmol); pale yellow solid; yield: 6.48 g (83 %);

1H -NMR (500 MHz, $CDCl_3$): δ (ppm) = 7.43-7.45 (m, 4H), 7.47 (d, $J = 15.4$ Hz, 1H), 7.55-7.57 (m, 1H), 7.65-7.67 (m, 2H), 7.82 (d, $J = 15.4$ Hz, 1H), 7.88-7.90 (m, 1H), 7.99 (t, $J = 1.7$ Hz, 1H). ^{13}C -NMR (125 MHz, $CDCl_3$): δ (ppm) = 121.5, 126.5, 128.4, 128.6, 129.0, 129.9, 130.8, 132.7, 134.5, 134.9, 139.8, 145.7, 189.2.

Diethyl 2-(3-(3-chlorophenyl)-3-oxo-1-phenylpropyl)malonate, (2B):

Synthesized according to Method H using **1B** (2.0 g, 8.25 mmol) and diethyl malonate (1.26 mL, 8.25 mmol) and magnesium oxide (0.82 g); white solid; yield: 2.66 g (80 %);

1H -NMR (500 MHz, $CDCl_3$): δ (ppm) = 1.02 (t, $J = 7.2$ Hz, 3H), 1.25 (t, $J = 7.2$ Hz, 3H), 3.43 (dd, $J = 9.2, 9.2$ Hz, 1H), 3.53 (dd, $J = 4.45, 4.5$ Hz, 1H), 3.80 (d, $J = 9.5$ Hz, 1H), 3.97 (q, $J = 7.2$ Hz, 2H), 4.13-4.24 (m, 3H), 7.16-7.19 (m, 1H), 7.24-7.27 (m, 4H), 7.36 (t, $J = 8.2$ Hz, 1H), 7.48-7.50 (m, 1H), 7.77-7.79 (m, 1H), 7.84 (t, $J = 1.6$ Hz, 1H). ^{13}C -NMR (125 MHz, $CDCl_3$): δ (ppm) = 13.8, 14.0, 40.7, 42.7, 57.4, 61.4, 61.7, 126.2, 127.2, 128.2, 128.4, 129.9, 132.9, 134.9, 138.4, 167.7, 168.3, 182.9.

2-(3-(3-Chlorophenyl)-3-oxo-1-phenylpropyl)malonic acid, (4B):

Synthesized according to Method L using **2B** (2.0 g, 4.96 mmol) and $NaOH_{aq}$ (8.3 mL); white solid; yield: 1.3 g (76 %); mp 155-158 °C.

1H -NMR (500 MHz, CD_3OD): δ (ppm) = 3.50 (d, $J = 7.6$ Hz, 2H), 3.84 (d, $J = 10.4$ Hz, 1H), 4.00-4.05 (m, 1H), 7.14 (t, $J = 7.2$ Hz, 1H), 7.21 (t, $J = 7.6$ Hz, 2H), 7.27 (d, $J = 7.2$ Hz, 2H), 7.44 (t, $J = 7.9$ Hz, 1H), 7.55 (d, $J = 8.8$ Hz, 1H), 7.8-7.83 (m, 2H). ^{13}C -NMR (125 MHz, CD_3OD): δ (ppm) = 42.7, 44.1, 58.8, 127.6, 128.1, 128.6, 129.0, 129.3, 129.6, 131.4, 134.0, 140.1, 142.1, 171.4, 171.8, 199.0; LC/MS (+ESI): $m/z = 347.2$ [MH^+]; $R_t = 4.08$ ($\geq 96\%$).

5-(3-Bromophenyl)-5-oxo-3-phenylpentanoic acid, (6B):

Synthesized according to Method N using **4B** (0.75 g, 2.16 mmol); white solid; yield: 0.49 g (75 %); mp 118-120 °C;

¹H-NMR (500 MHz, CDCl₃): δ (ppm) = 2.73 (dd, *J* = 7.6, 7.6 Hz, 1H), 2.85 (dd, *J* = 7.2, 7.2 Hz, 1H), 3.29-3.38 (m, 2H), 3.82-3.88 (m, 1H), 7.21 (t, *J* = 6.9 Hz, 1H), 7.25-7.31 (m, 3H), 7.37 (t, *J* = 7.6 Hz, 1H), 7.50-7.52 (m, 2H), 7.76 (d, *J* = 8.8 Hz, 1H), 7.84-7.86 (t, *J* = 1.6 Hz, 1H); ¹³C-NMR (125 MHz, CDCl₃): δ (ppm) = 37.1, 39.9, 44.0, 126.2, 126.4, 127.4, 127.5, 128.0, 130.6, 132.7, 133.5, 138.4, 143.6, 156.9, 190.2; LC/MS (+ESI): *m/z* = 303.1 [MH⁺]; *R_t* = 4.62 (≥ 98 %).

2-(1,3-Bis(4-chlorophenyl)-3-oxopropyl)malonic acid, (4C):**(E)-1,3-Bis(4-chlorophenyl)prop-2-en-1-one, (1C):**

Synthesized according to Method A using 4-chlorobenzaldehyde (3.0 g, 21.34 mmol) and 4'-chloroacetophenone (2.77 mL, 21.34 mmol); pale yellow solid; yield: 5.60 g (95 %);

¹H-NMR (500 MHz, CDCl₃): δ (ppm) = 7.38 (d, *J* = 8.2 Hz, 2H), 7.45 (d, *J* = 15.8 Hz, 1H), 7.48 (d, *J* = 8.8 Hz, 2H), 7.57 (d, *J* = 8.2 Hz, 2H), 7.76 (d, *J* = 15.8 Hz, 1H), 7.98 (d, *J* = 8.8 Hz, 2H). ¹³C-NMR (125 MHz, CDCl₃): δ (ppm) = 121.9, 128.9, 129.3, 129.6, 129.9, 133.2, 126.3, 126.6, 139.4, 143.8, 188.8.

Dimethyl 2-(1,3-Bis(4'-chlorophenyl)-3-oxopropyl)malonate, (2C):

Synthesized according to Method J using **1C** (2.0 g, 7.2 mmol) and diethyl malonate (1.10 μL, 14.4 mmol) and sodium hydride (cat.); white solid; yield: 2.32 g (74 %);

¹H-NMR (500 MHz, CDCl₃): δ (ppm) = 3.40 (dd, *J* = 9.2, 9.2 Hz, 1H), 3.51 (dd, *J* = 4.4, 4.4 Hz, 1H), 3.53 (s, 3H), 3.72 (s, 3H), 3.81 (d, *J* = 9.1 Hz, 1H), 7.20 (q, *J* = 8.8 Hz, 4H), 7.40 (d, *J* = 8.8 Hz, 2H), 7.82 (d, *J* = 8.8 Hz, 2H). ¹³C-NMR (125 MHz, CDCl₃): δ (ppm) = 40.1, 42.1, 52.5, 52.7, 56.9, 128.7, 128.9, 129.4, 129.5, 133.1, 134.9, 138.7, 139.7, 167.9, 168.5, 196.1.

2-(1,3-Bis(4-chlorophenyl)-3-oxopropyl)malonic acid, (4C):

Synthesized according to Method L using **2C** (2.0 g, 4.57 mmol) and NaOH_{aq} (7.62 mL); white solid; yield: 0.11 g (74 %); mp 140-142 °C.

¹H-NMR (500 MHz, CD₃OD): δ (ppm) = 3.53 (d, *J* = 6.9 Hz, 2H), 3.84 (d, *J* = 10.4 Hz, 1H), 4.03-4.07 (m, 1H), 7.24 (d, *J* = 8.5 Hz, 2H), 7.30 (d, *J* = 8.5 Hz, 2H), 7.49 (d, *J* = 8.8 Hz, 2H), 7.92 (d, *J* = 8.8 Hz, 2H). ¹³C-NMR (125 MHz, CD₃OD): δ (ppm) = 42.0, 43.8, 58.6, 129.3, 130.0, 130.9, 131.3, 133.8, 136.8, 140.6, 141.0, 171.3, 171.6, 198.8. LC/MS (+ESI): *m/z* = 382.8 [MH⁺]; *R_t* = 4.08 (≥ 98 %).

3,5-Bis(4-chlorophenyl)-5-oxopentanoic acid, (6C):

Synthesized according to Method N using **4C** (0.70 g, 1.84 mmol); white solid; yield: 0.5 g (80 %); mp 149-151 °C; ¹H-NMR (500 MHz, CDCl₃): δ (ppm) = 2.68 (dd, *J* = 7.9 Hz, 1H), 2.83 (dd, *J* = 6.9 Hz, 1H), 3.24-3.35 (m, 2H), 3.79-3.85 (m, 1H), 7.18 (d, *J* = 8.5 Hz, 2H), 7.25 (d, *J* = 8.5 Hz, 2H), 7.40 (d, *J* = 8.8 Hz, 2H), 7.81 (d, *J* = 8.8 Hz, 2H); ¹³C-NMR (125 MHz, CDCl₃): δ (ppm) = 36.5, 40.0, 44.3, 128.7, 128.8, 129.0, 129.4, 132.7, 135.0, 139.8, 141.3, 176.7, 196.4; LC/MS (+ESI): *m/z* = 339.2 [MH⁺]; *R_t* = 4.97 (≥ 98 %).

2-(3-(4-Bromophenyl)-3-oxo-1-phenylpropyl)malonic acid, (4D):

(E)-1-(4-Bromophenyl)-3-phenylprop-2-en-1-one, (1D):

Synthesized according to Method A using benzaldehyde (2.55 mL, 25.1 mmol) and 4'-bromoacetophenone (5.0 g, 25.1 mmol); pale yellow solid; yield: 5.84 g (81 %);

¹H-NMR (500 MHz, CDCl₃): δ (ppm) = 7.40-7.43 (m, 3H), 7.48 (d, *J* = 15.6 Hz, 1H), 7.63-7.66 (m, 4H), 7.81 (d, *J* = 15.6 Hz, 1H), 7.89 (d, *J* = 8.5 Hz, 2H). ¹³C-NMR (125 MHz, CDCl₃): δ (ppm) = 121.5, 127.9, 128.5, 129.0, 130.0, 130.7, 131.9, 134.7, 136.9, 145.4, 189.3.

Diethyl 2-(3-(4-bromophenyl)-3-oxo-1-phenylpropyl)malonate, (2D):

Synthesized according to Method H using **1D** (2.0 g, 6.96 mmol) and diethyl malonate (1.06 mL, 6.96 mmol) and magnesium oxide (0.70 g); white solid; yield: 2.56 g (82 %);

¹H-NMR (500 MHz, CDCl₃): δ (ppm) = 1.01 (t, *J* = 7.2 Hz, 3H), 1.23 (t, *J* = 7.2 Hz, 3H), 3.39 (dd, *J* = 9.2, 9.2 Hz, 1H), 3.52 (dd, *J* = 4.4, 4.4 Hz, 1H), 3.94 (d, *J* = 9.5 Hz, 1H), 3.95 (q, *J* = 7.2 Hz, 2H), 4.11-4.25 (m, 3H), 7.15-7.19 (m, 1H), 7.22-7.25 (m, 4H), 7.56 (d, *J* = 8.8 Hz, 2H), 7.75 (d, *J* = 8.8 Hz, 2H). ¹³C-NMR (125 MHz, CDCl₃): δ (ppm) = 13.7, 14.0, 40.9, 42.6, 57.5, 61.4, 61.7, 127.2, 128.2, 128.4, 129.6, 131.8, 135.5, 140.2, 167.6, 168.3, 190.6, 196.6.

2-(3-(4-Bromophenyl)-3-oxo-1-phenylpropyl)malonic acid, (4D):

Synthesized according to Method L using **2D** (2.0 g, 4.47 mmol) and NaOH_{aq} (7.45 mL); white solid; yield: 1.27 g (72 %); mp 159-161 °C.

¹H-NMR (500 MHz, (CD₃)₂SO): δ (ppm) = 3.29-3.33 (m, 1H), 3.59 (dd, *J* = 10.1, 10.1 Hz, 1H), 3.74 (d, *J* = 10.7 Hz, 1H), 3.83-3.88 (m, 1H), 7.11 (t, *J* = 7.2 Hz, 1H), 7.18 (t, *J* = 7.2 Hz, 2H), 7.26 (d, *J* = 7.2 Hz, 2H), 7.70 (d, *J* = 8.6 Hz, 2H), 7.78 (d, *J* = 8.6 Hz, 2H). ¹³C-NMR (125 MHz, (CD₃)₂SO): δ (ppm) = 40.4, 42.3, 57.2, 126.4, 127.1, 127.8, 128.3, 129.7, 131.6, 135.5, 141.0, 168.9, 169.9, 197.1; LC/MS (+ESI): *m/z* = 392.6 [MH⁺]; *R_t* = 4.2 (≥ 98 %).

5-(4-Bromophenyl)-5-oxo-3-phenylpentanoic acid, (6D):

Synthesized according to Method N using **4D** (0.5 g, 1.28 mmol); white solid; yield: 0.39 g (89 %);

¹H-NMR (500 MHz, CD₃OD): δ (ppm) = 2.64-2.71 (m, 1H), 2.78-2.85 (m, 1H), 3.39 (d, *J* = 6.9 Hz, 2H), 3.75-3.81 (m, 1H), 7.16 (t, *J* = 6.9 Hz, 1H), 7.23-7.29 (m, 4H), 7.63 (d, *J* = 8.8 Hz, 2H), 7.83 (d, *J* = 8.8 Hz, 2H), ¹³C-NMR (125 MHz, CD₃OD): δ (ppm) = 37.2, 40.1, 44.4, 127.0, 127.3, 128.3, 128.7, 129.6, 131.9, 135.5, 142.8, 176.8, 197.1; LC/MS (+ESI): *m/z* = 348.2 [MH⁺]; *R_t* = 4.74 (≥ 98 %).

2-(3-(4-Bromophenyl)-1-(4-chlorophenyl)-3-oxopropyl)malonic acid, (4E):**(E)-1-(4-Bromophenyl)-3-(4-chlorophenyl)prop-2-en-1-one, (1E):**

Synthesized according to Method A using 4-chlorobenzaldehyde (3.53 mL, 25.11 mmol) and 4-bromoacetophenone (5.0 g, 25.11 mmol); pale yellow solid; yield: 6.51 g (81 %);

¹H-NMR (500 MHz, CDCl₃): δ (ppm) = 7.39 (d, *J* = 8.5 Hz, 2H), 7.44 (d, *J* = 15.5 Hz, 1H), 7.57 (d, *J* = 8.5 Hz, 2H), 7.65 (d, *J* = 8.5 Hz, 2H), 7.76 (d, *J* = 15.5 Hz, 1H), 7.88 (d, *J* = 8.5 Hz, 2H). ¹³C-NMR (125 MHz, CDCl₃): δ (ppm) = 121.9, 128.0, 129.3, 129.6, 130.0, 132.0, 133.2, 136.7, 136.8, 143.8, 189.0.

Dimethyl 2-(3-(4-bromophenyl)-1-(4-chlorophenyl)-3-oxopropyl)malonate, (2E):

Synthesized according to Method J using **1E** (3.0 g, 9.32 mmol) and diethyl malonate (1.56 mL, 10.26 mmol) and sodium hydride (cat.); white solid; yield: 3.20 g (76 %);

$^1\text{H-NMR}$ (500 MHz, CDCl_3): δ (ppm) = 3.39 (dd, $J = 9.1, 9.1$ Hz, 1H), 3.50 (dd, $J = 4.7, 4.7$ Hz, 1H), 3.53 (s, 3H), 3.73 (s, 3H), 3.80 (d, $J = 9.1$ Hz, 1H), 4.11-4.16 (m, 1H), 7.21 (q, $J = 8.5$ Hz, 4H), 7.57 (d, $J = 8.5$ Hz, 2H), 7.75 (d, $J = 8.8$ Hz, 2H). $^{13}\text{C-NMR}$ (125 MHz, CDCl_3): δ (ppm) = 40.1, 42.1, 52.5, 52.7, 56.9, 128.4, 128.7, 129.4, 129.6, 131.9, 133.1, 135.3, 138.7, 167.9, 168.5, 196.2.

2-(3-(4-Bromophenyl)-1-(4-chlorophenyl)-3-oxopropyl)malonic acid, (4E):

Synthesized according to Method L using **2E** (2.0 g, 4.41 mmol) and 10M NaOH_{aq} (4.4 mL); white solid; yield: 1.2 g (64 %); mp 154-155 °C;

$^1\text{H-NMR}$ (500 MHz, $(\text{CD}_3)_2\text{SO}$): δ (ppm) = 3.32 (dd, $J = 3.5, 17.3$ Hz, 1H), 3.62 (dd, $J = 10.1$ Hz, 1H), 3.74 (d, $J = 10.7$ Hz, 1H), 3.82 (dt, $J = 3.8, 10.4$ Hz, 1H), 7.26 (d, $J = 8.5$ Hz, 2H), 7.31 (d, $J = 8.5$ Hz, 2H), 7.70 (d, $J = 8.8$ Hz, 2H), 7.79 (d, $J = 8.8$ Hz, 2H), 12.60 (s, OH), 13.00 (s, OH). $^{13}\text{C-NMR}$ (125 MHz, $(\text{CD}_3)_2\text{SO}$): δ (ppm) = 30.6, 42.2, 57.0, 127.3, 127.8, 129.74, 130.3, 131.1, 131.7, 135.4, 140.1, 168.9, 169.4, 197.0. LC/MS (+ESI): $m/z = 426.9$ [MH^+]; $R_t = 4.56$ ($\geq 99\%$).

2-(3-(4-Iodophenyl)-3-oxo-1-phenylpropyl)malonic acid, (4F):

(E)-1-(4-Iodophenyl)-3-phenylprop-2-en-1-one, (1F):

Synthesized according to Method A using benzaldehyde (1.03 g, 10.2 mmol) and 4'-iodoacetophenone (2.5g, 10.2 mmol); pale beige solid; yield: 1.6 g (47 %);

$^1\text{H-NMR}$ (500 MHz, CDCl_3): δ (ppm) = 7.42-7.44 (m, 3H), 7.46 (d, $J = 15.5$ Hz, 1H), 7.62-7.67 (m, 2H), 7.73 (d, $J = 8.2$ Hz, 2H), 7.82 (d, $J = 15.5$ Hz, 1H), 7.87 (d, $J = 8.5$ Hz, 2H). $^{13}\text{C-NMR}$ (125 MHz, CDCl_3): δ (ppm) = 100.6, 121.4, 128.5, 129.0, 129.9, 130.7, 134.7, 137.4, 137.9, 145.3, 189.6.

Dimethyl 2-(3-(4-iodophenyl)-3-oxo-1-phenylpropyl)malonate, (2F):

Synthesized according to Method J using **1F** (1.0 g, 2.99 mmol) and diethyl malonate (0.50 mL, 3.29 mmol) and sodium hydride (cat.); pale yellow solid; yield: 0.96 g (69 %);

$^1\text{H-NMR}$ (500 MHz, CDCl_3): δ (ppm) = 3.41 (dd, $J = 4.8, 16.7$ Hz, 1H), 3.50 (s, 3H), 3.52 (dd, $J = 4.8, 16.7$ Hz, 1H), 3.72 (s, 3H), 3.83 (d, $J = 9.4$ Hz, 1H), 4.12-4.17 (m, 1H), 7.16-7.20 (m, 1H), 7.21-7.27 (m, 4H), 7.60 (d, $J = 8.5$ Hz, 2H), 7.79 (d, $J = 8.5$ Hz, 2H). $^{13}\text{C-NMR}$

(125 MHz, CDCl₃): δ (ppm) = 40.8, 42.2, 52.4, 52.7, 57.2, 127.9, 128.5, 129.5, 137.9, 140.2, 142.8, 145.1, 158.8, 177.0, 177.3, 199.6.

2-(3-(4-Iodophenyl)-3-oxo-1-phenylpropyl)malonic acid, (4F):

Synthesized according to Method L using **2F** (0.6 g, 1.29 mmol) and 10M NaOH_{aq} (1.3 mL); white solid; yield: 0.48 g (86 %); mp 174-175 °C;

¹H-NMR (500 MHz, (CD₃)₂SO): δ (ppm) = 3.28 (dd, J = 3.6, 17.1 Hz, 1H), 3.58 (dd, J = 10.5 Hz, 1H), 3.73 (d, J = 10.7 Hz, 1H), 3.84 (dt, J = 3.6, 10.3 Hz, 1H), 7.11 (t, J = 7.3 Hz, 1H), 7.19 (t, J = 7.9 Hz, 2H), 7.26 (d, J = 7.3 Hz, 2H), 7.61 (d, J = 8.5 Hz, 2H), 7.87 (d, J = 8.5 Hz, 2H), 12.61 (s, OH), 12.90 (s, OH). ¹³C-NMR (125 MHz, (CD₃)₂SO): δ (ppm) = 40.4, 42.3, 57.3, 101.6, 126.4, 127.8, 128.3, 129.4, 135.8, 137.5, 141.0, 168.9, 169.9, 197.4; LC/MS (+ESI): m/z = 439.1 [MH⁺]; R_t = 4.32 (\geq 99 %).

5-(4-Iodophenyl)-5-oxo-3-phenylpentanoic acid, (6F):

Synthesized according to Method N using **4F** (0.11 g, 0.25 mmol); white solid; yield: 0.60 g (71 %). mp 183-184 °C;

¹H-NMR (500 MHz, CDCl₃): δ (ppm) = 2.73 (dd, J = 7.3, 16.0 Hz, 1H), 2.85 (dd, J = 7.3, 16.0 Hz, 1H), 3.28 (dd, J = 7.2, 16.7 Hz, 1H), 3.34 (dd, J = 7.2, 16.7 Hz, 1H), 3.81-3.87 (m, 1H), 7.20 (tt, J = 1.3, 7.2 Hz, 1H), 7.24-7.31 (m, 4H), 7.59 (d, J = 8.6 Hz, 2H), 7.79 (d, J = 8.6 Hz, 2H). ¹³C-NMR (125 MHz, (CD₃)₂SO): δ (ppm) = 37.1, 40.2, 43.8, 101.6, 126.1, 127.4, 129.5, 135.8, 137.5, 172.7, 197.9; LC/MS (+ESI): m/z = 396.0 [MH⁺]; R_t = 4.85 (\geq 98).

2-(1-(4-Chlorophenyl)-3-(4-iodophenyl)-3-oxopropyl)malonic acid, (4G):

(E)-3-(4-Chlorophenyl)-1-(4-iodophenyl)prop-2-en-1-one, (1G):

Synthesized according to Method A using 4-chlorobenzaldehyde (1.14 mL, 8.13 mmol) and 4'-iodoacetophenone (2.0 g, 8.13 mmol); pale beige solid; yield: 2.65 g (89 %);

¹H-NMR (500 MHz, CDCl₃): δ (ppm) = 7.39 (d, J = 8.5, 2H), 7.42 (d, J = 15.8, 1H), 7.57 (d, J = 8.5, 2H), 7.71 (d, J = 8.5, 2H), 7.77 (d, J = 15.8, 1H), 7.85 (d, J = 8.5 Hz, 2H). ¹³C-NMR (125 MHz, CDCl₃): δ (ppm) = 100.8, 121.8, 129.2, 129.6, 129.9, 133.2, 136.7, 137.3, 138.0, 143.8, 189.3.

Diethyl 2-(1-(4-chlorophenyl)-3-(4-iodophenyl)-3-oxopropyl)malonate, (2G):

Synthesized according to Method I using **1G** (2.0 g, 4.07 mmol) and diethyl malonate (0.68 mL, 4.47 mmol) and potassium carbonate (1.12 g, 8.14 mmol); pale beige solid; yield: 0.86 g (40 %);

$^1\text{H-NMR}$ (500 MHz, CDCl_3): δ (ppm) = 1.05 (t, $J = 7.2$ Hz, 3H), 1.25 (t, $J = 7.2$ Hz, 3H), 3.35 (dd, $J = 9.5, 9.5$ Hz, 1H), 3.49 (dd, $J = 4.1, 4.1$ Hz, 1H), 3.76 (d, $J = 9.8$ Hz, 1H), 3.98 (q, $J = 7.2$ Hz, 2H), 4.09-4.25 (m, 3H), 7.18 (d, $J = 8.8$ Hz, 2H), 7.22 (d, $J = 8.8$ Hz, 2H), 7.59 (d, $J = 8.8$ Hz, 2H), 7.79 (d, $J = 8.8$ Hz, 2H). $^{13}\text{C-NMR}$ (125 MHz, CDCl_3): δ (ppm) = 13.8, 14.0, 40.1, 42.3, 57.2, 61.5, 61.8, 101.2, 128.6, 129.5, 129.6, 133.0, 133.9, 138.0, 138.8, 167.5, 168.1, 196.6.

2-(1-(4-Chlorophenyl)-3-(4-iodophenyl)-3-oxopropyl)malonic acid, (4G):

Synthesized according to Method L using **2G** (0.59 g, 1.11 mmol) and 10M NaOH_{aq} (2 mL); pale yellow solid; yield: 0.35 g (67 %); mp 167-168 °C;

$^1\text{H-NMR}$ (500 MHz, $(\text{CD}_3)_2\text{SO}$): δ (ppm) = 3.31 (dd, $J = 3.5, 17.0$ Hz, 1H), 3.59 (dd, $J = 9.9$ Hz, 1H), 3.73 (d, $J = 10.8$ Hz, 1H), 3.82 (dt, $J = 3.5, 10.42$ Hz, 1H), 7.26 (d, $J = 8.5$ Hz, 2H), 7.29 (d, $J = 8.5$ Hz, 2H), 7.62 (d, $J = 8.5$ Hz, 2H), 7.88 (d, $J = 8.5$ Hz, 2H), 12.62 (s, OH), 12.89 (s, OH). $^{13}\text{C-NMR}$ (125 MHz, $(\text{CD}_3)_2\text{SO}$): δ (ppm) = 39.8, 42.1, 57.0, 101.8, 127.8, 129.4, 130.3, 131.0, 135.6, 137.5, 140.1, 168.9, 169.5, 197.3; LC/MS (+ESI): $m/z = 473.1$ [MH^+]; $R_t = 4.66$ (≥ 95 %).

3-(4-Chlorophenyl)-5-(4-iodophenyl)-5-oxopentanoic acid, (6G):

Synthesized according to Method N using **4G** (0.15 g, 0.32 mmol); white solid; yield: 0.12 g (88 %); mp 145-147 °C;

$^1\text{H-NMR}$ (500 MHz, CDCl_3): δ (ppm) = 2.67 (dd, $J = 7.9$ Hz, 1H), 2.82 (dd, $J = 6.6$ Hz, 1H), 3.25 (dd, $J = 7.2$ Hz, 1H), 3.32 (dd, $J = 6.6$ Hz, 1H), 3.79-3.85 (m, 1H), 7.18 (d, $J = 8.4$ Hz, 2H), 7.25 (d, $J = 8.4$ Hz, 2H), 7.59 (d, $J = 8.8$ Hz, 2H), 7.80 (d, $J = 8.8$ Hz, 2H); $^{13}\text{C-NMR}$ (125 MHz, CDCl_3): δ (ppm) = 36.5, 40.0, 44.2, 101.3, 128.7, 128.8, 129.4, 132.7, 135.9, 138.0, 141.3, 176.2, 197.0; LC/MS (+ESI): $m/z = 429.1$ [MH^+]; $R_t = 5.16$ (≥ 99 %).

2-(3-Oxo-1-phenyl-3-(4-(trifluoromethyl)phenyl)propyl)malonic acid, (4H):**(E)-3-Phenyl-1-(4-(trifluoromethyl)phenyl)prop-2-en-1-one, (1H):**

Synthesized according to Method A using benzaldehyde (1.62 mL, 15.95 mmol) and 1-(4'-(trifluoromethyl)phenyl)ethanone (3.0 g, 15.95 mmol); pale yellow solid; yield: 3.05 g (70 %);

¹H-NMR (500 MHz, CDCl₃): δ (ppm) = 7.49-7.43 (m, 3H), 7.50 (d, *J* = 15.8 Hz, 1H), 7.67-7.65 (m, 2H), 7.77 (d, *J* = 8.0 Hz, 2H), 7.84 (d, *J* = 15.8 Hz, 1H), 8.10 (d, *J* = 8.0 Hz, 2H). ¹³C-NMR (125 MHz, CDCl₃): δ (ppm) = 121.6, 123.6 (q, ¹*J*_{C-F} = 272.9 Hz), 125.69 (q, ³*J*_{C-F} = 4.3 Hz), 128.6, 128.8, 129.0, 130.9, 133.9 (q, ²*J*_{C-F} = 32.3 Hz), 134.5, 141.1, 146.1, 189.7.

Diethyl 2-(3-oxo-1-phenyl-3-(4-(trifluoromethyl)phenyl)propyl)malonate, (2H):

Synthesized according to Method H using **1H** (1.5 g, 5.42 mmol) and diethyl malonate (0.82 mL, 5.92 mmol) and magnesium oxide (0.54 g); white solid; yield: 1.8 g (76 %);

¹H-NMR (500 MHz, (CD₃)₂SO): δ (ppm) = 0.85 (t, *J* = 7.2 Hz, 3H), 1.16 (t, *J* = 7.2 Hz, 3H), 3.46 (dd, *J* = 3.8, 17.0 Hz, 1H), 3.69 (dd, *J* = 3.8, 17.0 Hz, 1H), 3.83 (q, *J* = 7.2 Hz, 2H), 3.90-3.98 (m, 2H), 4.08-4.18 (m, 2H), 7.15 (t, *J* = 7.6 Hz, 1H), 7.22 (d, *J* = 7.6 Hz, 2H), 7.29 (d, *J* = 7.8 Hz, 2H), 7.87 (d, *J* = 8.2 Hz, 2H), 8.05 (d, *J* = 8.2 Hz, 2H). ¹³C-NMR (125 MHz, (CD₃)₂SO): δ (ppm) = 13.4, 13.7, 40.4, 56.7, 60.6, 61.2, 116.2, 116.4, 125.6 (q, ³*J*_{C-F} = 3.7 Hz), 126.8, 127.9, 128.2, 128.5, 140.2, 167.7, 168.4, 197.2.

2-(3-Oxo-1-phenyl-3-(4-(trifluoromethyl)phenyl)propyl)malonic acid, (4H):

Synthesized according to Method L using **2H** (1.76 g, 4.03 mmol) and NaOH_{aq} (6.71 mL); white solid; yield: 1.25 g (82 %); mp 128-130 °C;

¹H-NMR (500 MHz, CD₃OD): δ (ppm) = 3.53 (d, *J* = 9.7 Hz, 1H), 3.56 (d, *J* = 6.9 Hz, 1H), 3.83 (d, *J* = 10.9 Hz, 1H), 4.02-4.08 (m, 1H), 7.14 (t, *J* = 7.2 Hz, 1H), 7.21 (t, *J* = 7.6 Hz, 2H), 7.27 (d, *J* = 7.9 Hz, 2H), 7.75 (d, *J* = 8.2 Hz, 2H), 8.05 (d, *J* = 8.2 Hz, 2H). ¹³C-NMR (125 MHz, CD₃OD): δ (ppm) = 42.6, 44.3, 58.7, 125.2 (q, ¹*J*_{C-F} = 272.2 Hz), 126.7 (q, ³*J*_{C-F} = 3.7 Hz), 128.0, 129.3, 129.6, 129.8, 135.2 (d, ²*J*_{C-F} = 32.9 Hz), 141.3, 142.0 (d, ⁴*J*_{C-F} = 1.8 Hz), 171.5, 171.8, 199.2; LC/MS (+ESI): *m/z* = 381.2 [MH⁺]; *R*_t = 4.35 (≥ 96 %).

Bis(acetoxymethyl) 2-(3-oxo-1-phenyl-3-(4-(trifluoromethyl)-phenyl)propyl)-malonate, (5H):

Synthesized according to Method M using **4H** (0.2 g, 0.52 mmol), bromo methylacetate (0.206 mL, 2.10 mmol) and triethylamine (0.44 mL, 3.12 mmol); white solid; yield: 0.17 g (62 %); mp 89-90 °C;

¹H-NMR (500 MHz, CD₃OD): δ (ppm) = 1.98 (s, 3H), 2.09 (s, 3H), 3.50 (dd, *J* = 8.8 Hz, 1H), 3.60 (dd, *J* = 4.2 Hz, 1H), 3.96 (d, *J* = 9.1 Hz, 1H), 4.17-4.21 (m, 1H), 5.55 (q, *J* = 5.7 Hz, 2H), 5.76 (d, *J* = 5.7 Hz, 2H), 7.18-7.21 (m, 1H), 7.23-7.28 (m, 4H), 7.69 (d, *J* = 8.2 Hz, 2H), 7.98. ¹³C-NMR (125 MHz, CD₃OD): δ (ppm) = 20.5, 20.6, 40.4, 40.5, 56.5, 79.4, 79.8, 118.0, 125.6 (q, ³*J*_{C-F} = 4.6 Hz), 127.6, 128.1, 128.4, 128.7, 164.9, 165.8, 166.0, 166.5, 169.2, 169.3, 196.4; LC/MS (+ESI): *m/z* = 525.3 [MH⁺]; *R*_t = 5.31 (≥ 99 %).

5-Oxo-3-phenyl-5-(4-(trifluoromethyl)phenyl)pentanoic acid, (6H):

Synthesized according to Method N **4H** (0.10 g, 0.26 mmol); white solid; yield: 0.70 g (68%); mp 99-101 °C;

¹H-NMR (500 MHz, CDCl₃): δ (ppm) = 2.75 (dd, *J* = 7.0, 16.1 Hz, 1H), 2.87 (dd, *J* = 7.0, 16.1 Hz, 1H), 3.36 (dd, *J* = 6.8, 17.0 Hz, 1H), 3.42 (dd, *J* = 6.8, 17.0 Hz, 1H), 3.83-3.89 (m, 1H), 7.20 (tt, *J* = 1.6, 6.9 Hz, 1H), 7.22-7.31 (m, 4H), 7.69 (d, *J* = 8.2 Hz, 2H), 7.90 (d, *J* = 8.2 Hz, 2H). ¹³C-NMR (125 MHz, CDCl₃): δ (ppm) = 37.2, 39.9, 44.8, 114.8, 115.3, 116.0, 116.5, 125.7 (q, ³*J*_{C-F} = 3.7 Hz), 127.1, 127.3, 128.4, 128.8, 175.6, 199.4. LC/MS (+ESI): *m/z* = 337.2 [MH⁺]; *R*_t = 4.80 (≥ 99 %).

2-(1-(4-Chlorophenyl)-3-oxo-3-(4-(trifluoromethyl)phenyl)propyl) malonic acid, (4I):

(E)-3-(4-Chlorophenyl)-1-(4-(trifluoromethyl)phenyl)prop-2-en-1-one, (1I):

Synthesized according to Method A using 4-chlorobenzaldehyde (1.12 g, 7.97 mmol) and 1-(4'-(trifluoromethyl)phenyl)ethanone (1.5 g, 7.97 mmol); pale beige solid; yield: 1.90 g (77 %);

¹H-NMR (500 MHz, CDCl₃): δ (ppm) = 7.41 (d, *J* = 8.5 Hz, 2H), 7.46 (d, *J* = 15.8 Hz, 1H), 7.58 (q, *J* = 8.5 Hz, 2H), 7.77 (d, *J* = 8.2 Hz, 2H), 7.78 (d, *J* = 15.8 Hz, 1H), 8.10 (d, *J* = 8.2 Hz, 2H). ¹³C-NMR (125 MHz, CDCl₃): δ (ppm) = 122.0, 123.7 (q, ¹*J*_{C-F} = 273.1 Hz), 125.7 (q, ³*J*_{C-F} = 3.7 Hz), 128.8, 129.4, 129.7, 133.0, 134.3, 136.9, 140.9, 144.5, 189.3.

Dimethyl 2-(1-(4-chlorophenyl)-3-oxo-3-(4-(trifluoromethyl)phenyl)propyl)malonate, (2I):

Synthesized according to Method J using **1I** (1.0 g, 3.22 mmol), diethyl malonate (0.54 mL, 3.54 mmol) and sodium hydride (cat.); white solid; yield: 1.35 g (95%);

$^1\text{H-NMR}$ (500 MHz, CDCl_3): δ (ppm) = 3.45 (dd, $J = 9.1, 17.0$ Hz, 1H), 3.54 (s, 3H), 3.59 (dd, $J = 4.4, 17.0$ Hz, 1H), 3.74 (s, 3H), 3.81 (d, $J = 9.1$ Hz, 1H), 4.13-4.17 (m, 1H), 7.18-7.24 (q, $J = 8.5$ Hz, 4H), 7.70 (d, $J = 8.2$ Hz, 2H), 7.99 (d, $J = 8.2$ Hz, 2H). $^{13}\text{C-NMR}$ (125 MHz, CDCl_3): δ (ppm) = 40.0, 42.4, 52.6, 52.8, 56.9, 122.4, 125.7 (q, $^3J_{\text{C-F}} = 3.7$ Hz), 128.4, 128.8, 129.4, 133.2, 134.7, 138.6, 139.2, 167.8, 168.5, 196.4.

2-(1-(4-Chlorophenyl)-3-oxo-3-(4-(trifluoromethyl)phenyl)propyl) malonic acid, (4I):

Synthesized according to Method L using **2I** (0.8 g, 1.18 mmol) and 10M NaOH_{aq} (1.8 mL); white solid; yield: 0.41 g (55 %); mp 147-148 °C;

$^1\text{H-NMR}$ (500 MHz, $(\text{CD}_3)_2\text{SO}$): δ (ppm) = 3.49 (dd, $J = 3.8, 17.9$ Hz, 1H), 3.67 (dd, $J = 3.8, 9.8$ Hz, 1H), 3.76 (d, $J = 10.7$ Hz, 1H), 3.85 (dt, $J = 3.8, 10.4$ Hz, 1H), 7.30 (q, $J = 8.5$ Hz, 4H), 7.87 (d, $J = 8.5$ Hz, 2H), 8.05 (d, $J = 8.5$ Hz, 2H). $^{13}\text{C-NMR}$ (125 MHz, $(\text{CD}_3)_2\text{SO}$): δ (ppm) = 40.0, 42.6, 57.0, 124.0 (q, $^1J_{\text{C-F}} = 272.9$ Hz), 125.7 (q, $^3J_{\text{C-F}} = 4.3$ Hz), 127.8, 128.6, 130.3, 131.1, 139.5, 140.0, 140.7, 168.9, 169.5, 197.4; LC/MS (+ESI): $m/z = 415.1$ [MH^+]; $R_t = 4.68$ (≥ 98 %).

3-(4-Chlorophenyl)-5-oxo-5-(4-(trifluoromethyl)phenyl)pentanoic acid, (6I):

Synthesized according to Method N using **4I** (0.10 g, 0.24 mmol); white solid; yield: 0.75 g (84 %);

$^1\text{H-NMR}$ (500 MHz, $(\text{CD}_3)_2\text{SO}$): δ (ppm) = 2.70 (dd, $J = 7.4, 16.1$ Hz, 1H), 2.85 (dd, $J = 7.4, 16.1$ Hz, 1H), 3.34 (dd, $J = 7.0, 17.1$ Hz, 1H), 3.40 (dd, $J = 7.0, 17.1$ Hz, 1H), 3.82-3.88 (m, 1H), 7.20 (d, $J = 8.5$ Hz, 2H), 7.27 (d, $J = 8.5$ Hz, 2H), 7.70 (d, $J = 8.2$ Hz, 2H), 7.99 (d, $J = 8.2$ Hz, 2H). $^{13}\text{C-NMR}$ (125 MHz, $(\text{CD}_3)_2\text{SO}$): δ (ppm) = 36.5, 39.8, 44.6, 122.4, 125.7 (q, $^3J_{\text{C-F}} = 4.3$ Hz), 128.3, 128.7, 128.72, 128.9, 132.8, 139.3, 141.1, 175.4, 196.8; LC/MS (+ESI): $m/z = 371.2$ [MH^+]; $R_t = 5.06$ (≥ 95 %).

2-(1-(2-Chlorophenyl)-3-oxo-3-(4-(trifluoromethyl)phenyl)propyl) malonic acid, (4J):**(E)-3-(2-Chlorophenyl)-1-(4-(trifluoromethyl)phenyl)prop-2-en-1-one, (1J):**

Synthesized according to Method A using 2-chlorobenzaldehyde (1.64 g, 11.7 mmol) and 1-(4'-(trifluoromethyl)phenyl)ethanone (1.3 mL, 11.7 mmol); pale beige solid; yield: 1.28 g (35 %);

$^1\text{H-NMR}$ (500 MHz, CDCl_3): δ (ppm) = 7.32-7.38 (m, 2H), 7.43 (d, $J = 15.8$ Hz, 1H), 7.46 (d, $J = 8.2$ Hz, 1H), 7.75-7.79 (m, 3H), 8.10 (d, $J = 7.9$ Hz, 2H), 8.20 (d, $J = 15.8$ Hz, 1H).

Dimethyl 2-(1-(2-chlorophenyl)-3-oxo-3-(4-(trifluoromethyl)phenyl)propyl)malonate, (2J):

Synthesized according to Method J using **1J** (0.64 g, 2.10 mmol), diethyl malonate (0.35 mL, 2.30 mmol) and sodium hydride (cat.); white solid; yield: 0.511 g (55%);

$^1\text{H-NMR}$ (500 MHz, CDCl_3): δ (ppm) = 3.60 (s, 3H), 3.68-3.71 (m, 5H), 4.08 (d, $J = 8.2$ Hz, 1H), 4.63-4.68 (m, 1H), 7.12-7.19 (m, 2H), 7.27 (dd, $J = 2.2, 7.2$ Hz, 1H), 7.35 (dd, $J = 2.2, 7.2$ Hz, 2H), 7.70 (d, $J = 8.2$ Hz, 2H), 8.03 (d, $J = 8.8$ Hz, 2H). $^{13}\text{C-NMR}$ (125 MHz, CDCl_3): δ (ppm) = 37.2, 40.6, 52.6, 54.7, 60.3, 122.4, 122.6 (q, $^1J_{\text{C-F}} = 269.4$ Hz), 125.7 (q, $^3J_{\text{C-F}} = 3.7$ Hz), 126.9, 128.4, 128.5, 130.2, 134.0, 134.3, 134.5, 137.4, 139.3, 168.1, 168.6, 196.6.

2-(1-(2-Chlorophenyl)-3-oxo-3-(4-(trifluoromethyl)phenyl)propyl) malonic acid, (4J):

Synthesized according to Method L using **2J** (0.45 g, 1.10 mmol) and 10M NaOH_{aq} (1.1 mL); white solid; yield: 0.33 g (71 %); mp 149-151 °C;

$^1\text{H-NMR}$ (500 MHz, $(\text{CD}_3)_2\text{SO}$): δ (ppm) = 3.56 (dd, $J = 4.7, 4.7$ Hz, 1H), 3.63 (dd, $J = 9.1, 9.1$ Hz, 1H), 3.85 (d, $J = 9.8$ Hz, 1H), 4.39-4.44 (m, 1H), 7.16 (t, $J = 8.8$ Hz, 1H), 7.23 (t, $J = 8.5$ Hz, 1H), 7.32 (d, $J = 9.1$ Hz, 1H), 7.51 (d, $J = 8.8$ Hz, 1H), 7.86 (d, $J = 8.2$ Hz, 2H), 8.06 (d, $J = 8.2$ Hz, 2H). $^{13}\text{C-NMR}$ (125 MHz, $(\text{CD}_3)_2\text{SO}$): δ (ppm) = 36.5, 42.2, 56.1, 123.8 (q, $^1J_{\text{C-F}} = 272.2$ Hz), 125.7 (q, $^3J_{\text{C-F}} = 3.7$ Hz), 127.1, 128.2, 128.8, 129.4, 132.4, 132.6, 133.6, 138.6, 139.7, 169.0, 169.6, 197.3; LC/MS (+ESI): $m/z = 415.2$ [MH^+]; $R_t = 4.46$ (≥ 99 %).

2-(3-(4-Ethylphenyl)-3-oxo-1-phenylpropyl)malonic acid, (4K):**(E)-1-(4-Ethylphenyl)-3-phenylprop-2-en-1-one, (1K):**

Synthesized according to Method A using benzaldehyde (3.43 mL, 34.0 mmol) and 4'-ethylacetophenone (5.0 g, 34.0 mmol); pale yellow solid; yield: 6.9 g (85 %);

¹H-NMR (500 MHz, CDCl₃): δ (ppm) = 1.28 (t, *J* = 7.6 Hz, 3H), 2.74 (d, *J* = 7.6 Hz, 2H), 7.33 (d, *J* = 8.5 Hz, 2H), 7.41-7.44 (m, 3H), 7.54 (d, *J* = 15.8 Hz, 1H), 7.64-7.66 (m, 2H), 7.81 (d, *J* = 15.8 Hz, 1H), 7.97 (d, *J* = 8.2 Hz, 2H). ¹³C-NMR (125 MHz, CDCl₃): δ (ppm) = 15.2, 28.9, 122.2, 128.1, 128.4, 128.7, 128.9, 130.4, 130.1, 135.9, 144.4, 149.8, 190.1.

Diethyl 2-(3-(4-ethylphenyl)-3-oxo-1-phenylpropyl)malonate, (2K):

Synthesized according to Method H using **1K** (2.0 g, 8.46 mmol) and diethyl malonate (1.28 mL, 8.46 mmol) and magnesium oxide (0.85 g); white solid; yield: 1.85 g (55 %);

¹H-NMR (500 MHz, CDCl₃): δ (ppm) = 1.01 (t, *J* = 7.2 Hz, 3H), 1.24 (t, *J* = 7.2 Hz, 6H), 2.69 (q, *J* = 7.6 Hz, 2H), 3.42-3.43 (dd, *J* = 9.1, 9.1 Hz, 1H), 3.50 (dd, *J* = 4.7, 4.7 Hz, 1H), 3.82 (d, *J* = 9.5 Hz, 1H), 3.95 (q, *J* = 7.2 Hz, 2H), 4.18-4.25 (m, 3H), 7.16 (t, *J* = 7.2 Hz, 1H), 7.21-7.27 (m, 6H), 7.82 (d, *J* = 8.2 Hz, 2H). ¹³C-NMR (125 MHz, CDCl₃): δ (ppm) = 13.7, 14.1, 15.1, 28.9, 40.8, 42.5, 57.6, 61.3, 61.6, 127.1, 128.0, 128.2, 128.3, 128.3, 134.6, 140.6, 149.9, 167.7, 168.4, 197.1.

2-(3-(4-Ethylphenyl)-3-oxo-1-phenylpropyl)malonic acid, (4K):

Synthesized according to Method L using **2K** (2.7 g, 7.33 mmol) and NaOH_{aq} (1.1 mL, 12.2 mmol); white solid; yield: 1.5 g (60 %); mp 127-128 °C.

¹H-NMR (500 MHz, DMSO-d₆): δ (ppm) = 1.17 (t, *J* = 7.6 Hz, 3H), 2.64 (q, *J* = 7.6 Hz, 2H), 3.27 (q, *J* = 3.5, 16.7 Hz, 1H), 3.59 (dd, *J* = 10.4, 10.4 Hz, 1H), 3.74 (d, *J* = 10.7 Hz, 1H), 3.86-3.90 (m, 1H), 7.11 (t, *J* = 7.2 Hz, 1H), 7.19 (t, *J* = 7.9 Hz, 2H), 7.27 (d, *J* = 6.9 Hz, 2H), 7.30 (d, *J* = 7.9 Hz, 2H), 7.78 (d, *J* = 8.2 Hz, 2H), 12.78 (s, 2H, OH). ¹³C-NMR (125 MHz, DMSO-d₆): δ (ppm) = 15.0, 28.0, 30.6, 40.4, 42.2, 57.3, 126.3, 127.8, 127.9, 128.3, 134.3, 141.2, 149.4, 169.0, 169.6, 197.3; LC/MS (+ESI): *m/z* = 341.2 [MH⁺]; *R*_t = 4.23 (≥ 95 %).

5-(4-Ethylphenyl)-5-oxo-3-phenylpentanoic acid, (6K):

Synthesized according to Method N using **4K** (0.2 g, 0.67 mmol); white solid; yield: 0.11 g (56 %); mp 118-119 °C;

¹H-NMR (500 MHz, CDCl₃): δ (ppm) = 1.24 (t, *J* = 7.6 Hz, 3H), 2.67-2.74 (m, 3H), 2.86 (dd, *J* = 6.6, 6.9 Hz, 1H), 3.33 (d, *J* = 8.2 Hz, 2H), 3.83-3.89 (m, 1H), 7.18-7.20 (m, 1H), 7.28-7.30 (m, 6H), 7.83 (d, *J* = 8.2 Hz, 2H), 10.25 (s, 1H, OH); ¹³C-NMR (125 MHz, CDCl₃): δ (ppm) = 15.1, 28.9, 37.2, 40.0, 44.4, 126.9, 127.3, 128.1, 128.3, 128.6, 134.5, 143.1, 150.1, 173.5, 197.7; LC/MS (+ESI): *m/z* = 297.2 [MH⁺]; *R_t* = 4.76 (≥ 97 %).

2-(1-(4-Chlorophenyl)-3-(4-ethylphenyl)-3-oxopropyl)malonic acid, (4L):**(E)-3-(4-Chlorophenyl)-1-(4-ethylphenyl)prop-2-en-1-one, (1L):**

Synthesized according to Method A using 4-chlorobenzaldehyde (1.90 g, 12.19 mmol) and 4-ethylacetophenone (3.0 g, 12.19 mmol); pale yellow solid; yield: 3.90 g (83 %);

¹H-NMR (500 MHz, CDCl₃): δ (ppm) = 1.28 (t, *J* = 7.9 Hz, 3H), 2.73 (q, *J* = 7.9 Hz, 2H), 7.33 (d, *J* = 8.2 Hz, 2H), 7.39 (d, *J* = 8.5 Hz, 2H), 7.50 (d, *J* = 15.8 Hz, 1H), 7.57 (d, *J* = 8.8 Hz, 2H), 7.75 (d, *J* = 15.8 Hz, 1H), 7.95 (d, *J* = 8.2 Hz, 2H). ¹³C-NMR (125 MHz, CDCl₃): δ (ppm) = 15.2, 29.0, 122.6, 128.2, 128.7, 129.2, 129.5, 133.5, 135.7, 136.3, 142.1, 150.0, 189.7.

Dimethyl 2-(1-(4-chlorophenyl)-3-(4-ethylphenyl)-3-oxopropyl)malonate (2L):

Synthesized according to Method J using **1L** (3.0 g, 11.10 mmol) and diethyl malonate (1.85 mL, 12.19 mmol) and sodium hydride (cat.); pale yellow solid; yield: 3.40 g (76 %);

¹H-NMR (500 MHz, CDCl₃): δ (ppm) = 1.24 (t, *J* = 7.8 Hz, 3H), 2.69 (q, *J* = 7.8 Hz, 2H), 3.42 (dd, *J* = 8.8, 16.7 Hz, 1H), 3.48 (dd, *J* = 4.7, 16.7 Hz, 1H), 3.53 (s, 3H), 3.73 (s, 3H), 3.82 (d, *J* = 9.5 Hz, 1H), 4.14-4.19 (m, 1H), 7.19-7.23 (m, 4H), 7.25 (d, *J* = 8.5 Hz, 2H), 7.81 (d, *J* = 8.2 Hz, 2H). ¹³C-NMR (125 MHz, CDCl₃): δ (ppm) = 15.1, 28.9, 40.2, 42.0, 52.5, 52.7, 57.1, 128.1, 128.3, 128.6, 129.5, 132.9, 134.4, 139.1, 150.2, 168.0, 168.5, 196.8.

2-(1-(4-Chlorophenyl)-3-(4-ethylphenyl)-3-oxopropyl)malonic acid, (4L):

Synthesized according to Method L using **2L** (2.0 g, 4.96 mmol) and 10M NaOH_{aq} (5.0 mL, 14.89 mmol); white solid; yield: 1.53 g (83 %); mp 153-154 °C;

$^1\text{H-NMR}$ (500 MHz, $(\text{CD}_3)_2\text{SO}$): δ (ppm) = 1.17 (t, $J = 7.6$ Hz, 3H), 2.65 (q, $J = 7.6$ Hz, 2H), 3.28 (dd, $J = 3.5, 16.7$ Hz, 1H), 3.60 (dd, $J = 10.4, 16.7$ Hz, 1H), 3.75 (d, $J = 10.7$ Hz, 1H), 3.86 (dt, $J = 3.5, 10.4$ Hz, 1H), 7.26 (d, $J = 8.5$ Hz, 2H), 7.30-7.32 (m, 4H), 7.79 (d, $J = 8.2$ Hz, 2H), 12.80 (s, 2OH). $^{13}\text{C-NMR}$ (125 MHz, $(\text{CD}_3)_2\text{SO}$): δ (ppm) = 15.0, 28.0, 42.1, 46.4, 57.1, 127.7, 127.9, 128.0, 132.3, 131.0, 134.2, 140.2, 149.5, 168.9, 169.5, 197.2; LC/MS (+ESI): $m/z = 375.1$ [MH^+]; $R_t = 4.55$ ($\geq 95\%$).

2-(1-(4-Chlorophenyl)-3-(4-hydroxyphenyl)-3-oxopropyl)malonic acid, (4M):

1-(4-(Methoxymethoxy)phenyl)ethanone, (0M):

Synthesized according to Method G using bromomethyl-methylether (0.87 mL, 11.01 mmol), 4-hydroxyacetophenone (1.0 g, 7.34 mmol) and sodium hydride (0.44 g, 11.01 mmol); yellow solid; yield: 1.25 g (95%).

$^1\text{H-NMR}$ (500 MHz, CDCl_3): δ (ppm) = 2.55 (s, 3H), 3.47 (s, 3H), 5.22 (s, 2H), 7.06 (d, $J = 8.8$ Hz, 2H), 7.92 (d, $J = 8.8$ Hz, 2H). $^{13}\text{C-NMR}$ (125 MHz, CDCl_3): δ (ppm) = 26.3, 56.2, 94.0, 115.7, 130.4, 131.2, 161.0, 196.8.

(E)-3-(4-Chlorophenyl)-1-(4-(methoxymethoxy)phenyl)prop-2-en-1-one, (1M):

Synthesized according to Method A using 4-chlorobenzaldehyde (0.78 mL, 5.5 mmol) and 1-(4-(methoxymethoxy)phenyl)ethanone (1.0 g, 5.5 mmol); pale yellow solid; yield: 0.84g (50 %);

$^1\text{H-NMR}$ (500 MHz, CDCl_3): δ (ppm) = 3.50 (s, 3H), 5.26 (s, 2H), 7.12 (d, $J = 8.8$ Hz, 2H), 7.39 (d, $J = 8.2$ Hz, 2H), 7.50 (d, $J = 15.5$ Hz, 1H), 7.57 (d, $J = 8.2$ Hz, 2H), 7.74 (d, $J = 15.5$ Hz, 1H), 8.02 (d, $J = 8.8$ Hz, 2H). $^{13}\text{C-NMR}$ (125 MHz, CDCl_3): δ (ppm) = 56.3, 94.1, 115.9, 122.3, 129.2, 129.5, 130.7, 131.8, 133.5, 136.2, 142.6, 161.1, 188.5.

Dimethyl 2-(1-(4-chlorophenyl)-3-(4-(methoxymethoxy)phenyl)-3-oxopropyl)-malonate, (2M):

Synthesized according to Method J using **1M** (0.4 g, 1.32 mmol) and diethyl malonate (0.22 mL, 1.45 mmol) and sodium hydride (cat.); white solid; yield: 0.45 g (88 %);

$^1\text{H-NMR}$ (500 MHz, CDCl_3): δ (ppm) = 3.38 (dd, $J = 9.1, 9.1$ Hz, 1H), 3.46 (d, $J = 4.7$ Hz, 1H), 3.47 (s, 3H), 3.52 (s, 3H), 3.72 (s, 3H), 3.82 (d, $J = 9.1$ Hz, 1H), 4.13-4.17 (m, 1H), 5.21 (s, 2H), 7.04 (d, $J = 8.8$ Hz, 2H), 7.19-7.27 (m, 4H), 7.86 (d, $J = 8.8$ Hz, 2H). $^{13}\text{C-NMR}$ (125

MHz, CDCl₃): δ (ppm) = 40.25, 41.8, 52.5, 52.7, 56.2, 57.0, 94.0, 115.7, 128.6, 129.5, 130.2, 130.6, 132.9, 139.0, 161.2, 168.0, 168.5, 195.7.

Dimethyl 2-(1-(4-chlorophenyl)-3-(4-hydroxyphenyl)-3-oxopropyl)malonate, (3M):

Synthesized according to Method K using **2M** (0.3 g, 0.71 mmol) and 2 mL 10 % HCl; yellow oil; yield: 0.30 g (quant, without further purification);

¹H-NMR (500 MHz, CDCl₃): δ (ppm) = 3.37 (dd, J = 9.1 Hz, 1H), 3.46 (d, J = 4.6 Hz, 1H), 3.53 (s, 3H), 3.73 (s, 3H), 3.81 (d, J = 9.1 Hz, 1H), 4.14-4.17 (m, 2H), 6.82 (d, J = 8.8 Hz, 2H), 7.18-7.22 (m, 4H), 7.82 (d, J = 8.8 Hz, 2H). ¹³C-NMR (125 MHz, CDCl₃): δ (ppm) = 40.3, 41.7, 52.6, 52.8, 57.1, 115.3, 128.6, 129.5, 130.7, 133.0, 137.4, 138.9, 139.8, 168.1, 168.6, 195.4.

2-(1-(4-Chlorophenyl)-3-(4-hydroxyphenyl)-3-oxopropyl)malonic acid, (4M):

Synthesized according to Method L using **3M** (0.25 g, 0.64 mmol) and 10M NaOH_{aq} (1.1 mL); white solid; yield: 0.15 g (63 %); mp 151-152 °C;

¹H-NMR (500 MHz, (CD₃)₂SO): δ (ppm) = 3.18 (dd, J = 3.3, 16.7 Hz, 1H), 3.53 (dd, J = 10.3, 16.7 Hz, 1H), 3.73 (d, J = 11.0 Hz, 1H), 3.85 (dt, J = 3.3, 10.3 Hz, 1H), 6.79 (d, J = 8.8 Hz, 2H), 7.28 (q, J = 8.5 Hz, 4H), 7.75 (d, J = 8.8 Hz, 2H), 10.3 (s, OH), 12.60 (s, OH), 12.98 (s, OH). ¹³C-NMR (125 MHz, (CD₃)₂SO): δ (ppm) = 40.0, 41.6, 57.1, 115.1, 127.7, 128.1, 130.3, 130.4, 130.9, 140.3, 162.0, 169.0, 196.5, 195.7; LC/MS (+ESI): m/z = 363.2 [MH⁺]; R_t = 3.30 (\geq 96 %).

2-(3-Oxo-3-(4-phenoxyphenyl)-1-phenylpropyl)malonic acid, (4N):

(E)-3-(4-Chlorophenyl)-1-(4-phenoxyphenyl)prop-2-en-1-one, (1N):

Synthesized according to Method A using 4-chlorobenzaldehyde (5.0 g, 23.56 mmol) and 4'-phenoxyacetophenone (5.0 g, 23.56 mmol); pale yellow solid; yield: 5.1 g (72 %).

¹H-NMR (500 MHz, CDCl₃): δ (ppm) = 7.06 (d, J = 8.5 Hz, 2H), 7.10 (d, J = 8.5 Hz, 2H), 7.21 (t, J = 7.2 Hz, 1H), 7.39-7.43 (m, 5H), 7.54 (d, J = 15.8 Hz, 1H), 7.63-7.66 (m, 2H), 8.82 (d, J = 15.8 Hz, 1H), 8.04 (d, J = 8.5 Hz, 2H). ¹³C-NMR (125 MHz, CDCl₃): δ (ppm) = 117.5, 120.1, 121.8, 124.5, 128.4, 128.9, 130.0, 130.4, 130.8, 132.8, 134.9, 144.4, 155.6, 161.8, 188.8.

Diethyl 2-(3-oxo-3-(4-phenoxyphenyl)-1-phenylpropyl)malonate, (2N):

Synthesized according to Method H using **1N** (2.0 g, 6.66 mmol) and diethyl malonate (1.01 mL, 6.66 mmol) and magnesium oxide (0.67 g); white solid; yield: 2.52 g (82 %);

¹H-NMR (500 MHz, CDCl₃): δ (ppm) = 1.01 (t, *J* = 6.9 Hz, 3H), 1.24 (t, *J* = 6.9 Hz, 3H), 3.39 (dd, *J* = 9.1, 9.1 Hz, 1H), 3.49 (dd, *J* = 4.4, 4.4 Hz, 1H), 3.81 (d, *J* = 9.8 Hz, 1H), 3.96 (q, *J* = 7.2 Hz, 2H), 4.14-4.23 (m, 3H), 6.95 (d, *J* = 8.9 Hz, 2H), 7.05 (d, *J* = 8.9 Hz, 1H), 7.15-7.27 (m, 6H), 7.38 (t, *J* = 7.6 Hz, 1H), 7.88 (d, *J* = 9.1 Hz, 2H). ¹³C-NMR (125 MHz, CDCl₃): δ (ppm) = 13.7, 14.0, 41.0, 42.4, 57.6, 61.3, 61.6, 117.3, 120.1, 124.6, 127.1, 128.2, 128.4, 130.0, 130.4, 131.5, 140.4, 125.5, 161.9, 167.7, 168.4, 196.1

2-(3-Oxo-3-(4-phenoxyphenyl)-1-phenylpropyl)malonic acid, (4N):

Synthesized according to Method L using **2N** (2.0 g, 4.34 mmol) and NaOH_{aq} (7.3 mL); white solid; yield: 1.26 g (72 %); mp 131-134 °C.

¹H-NMR (500 MHz, CD₃OD): δ (ppm) = 3.44 (m, 2H), 3.86 (d, *J* = 10.4 Hz, 1H), 4.05-4.10 (m, 1H), 6.97 (d, *J* = 8.5 Hz, 2H), 7.08 (d, *J* = 7.2 Hz, 2H), 7.16 (t, *J* = 7.9 Hz, 1H), 7.20-7.30 (m, 5H), 7.44 (t, *J* = 7.6 Hz, 2H), 7.92 (d, *J* = 8.2 Hz, 2H); ¹³C-NMR (125 MHz, CD₃OD): δ (ppm) = 42.8, 43.8, 58.9, 118.2, 121.3, 125.8, 128.0, 129.3, 129.6, 131.2, 131.7, 133.0, 142.2, 156.9, 163.6, 171.4, 171.8, 199.0; LC/MS (+ESI): *m/z* = 405.2 [MH⁺]; *R_t* = 4.59 (≥ 95 %).

5-Oxo-5-(4-phenoxyphenyl)-3-phenylpentanoic acid, (6N):

Synthesized according to Method N using **4N** (0.3 g, 0.74 mmol); white solid; yield: 0.25 g (93 %); mp 135-136 °C;

¹H-NMR (500 MHz, CDCl₃): δ (ppm) = 2.71 (dd, *J* = 7.9, 7.9 Hz, 1H), 2.86 (dd, *J* = 6.8, 6.8 Hz, 1H), 3.27-3.35 (m, 2H), 3.82-3.88 (m, 1H), 6.96 (d, *J* = 9.1 Hz, 1H), 7.05 (d, *J* = 8.5 Hz, 2H), 7.20 (t, *J* = 7.2 Hz, 2H), 7.25-7.30 (m, 4H), 7.39 (t, *J* = 7.6 Hz, 2H), 7.88 (d, *J* = 8.8 Hz, 2H). ¹³C-NMR (125 MHz, CDCl₃): δ (ppm) = 37.1, 39.7, 44.0, 117.1, 119.9, 124.4, 126.6, 127.0, 128.4, 129.8, 130.1, 131.3, 142.8, 155.2, 161.8, 175.7, 196.4; LC/MS (+ESI): *m/z* = 361.2 [MH⁺]; *R_t* = 5.05 (≥ 99 %).

2-(3-(4-Iodophenyl)-1-(naphthalen-2-yl)-3-oxopropyl)malonic acid, (4O):**(E)-1-(4-Iodophenyl)-3-(naphthalen-2-yl)prop-2-en-1-one, (1O):**

Synthesized according to Method A using 2-naphthaldehyde (1.90 g, 12.19 mmol) and 4'-iodoacetophenone (3.0 g, 12.19 mmol); pale yellow solid; yield: 3.90 g (83 %);

¹H-NMR (500 MHz, CDCl₃): δ (ppm) = 7.51-7.56 (m, 2H), 7.58 (d, *J* = 15.6 Hz, 1H), 7.76 (d, *J* = 8.5 Hz, 2H), 7.76-7.80 (m, 1H), 7.82-7.89 (m, 3H), 7.88 (d, *J* = 8.5 Hz, 2H), 7.98 (d, *J* = 15.6 Hz, 1H), 8.04 (s, 1H). ¹³C-NMR (125 MHz, CDCl₃): δ (ppm) = 100.6, 121.6, 123.6, 126.8, 127.5, 127.8, 128.7, 128.8, 129.9, 130.8, 132.2, 133.4, 134.5, 137.6, 137.9, 145.5, 189.6.

Dimethyl 2-(3-(4-iodophenyl)-1-(naphthalen-2-yl)-3-oxopropyl)malonate, (2O):

Synthesized according to Method J using **1O** (1.5 g, 3.90 mmol) and diethyl malonate (0.59 mL, 3.90 mmol) and sodium hydride (cat.); pale yellow solid; yield: 1.10 g (55 %);

¹H-NMR (500 MHz, CDCl₃): δ (ppm) = 3.47 (s, 3H), 3.53 (dd, *J* = 8.8, 16.9 Hz, 1H), 3.59 (dd, *J* = 4.7, 16.9 Hz, 1H), 3.73 (s, 3H), 3.95 (d, *J* = 9.1 Hz, 1H), 4.31-4.36 (m, 1H), 7.39 (dd, *J* = 1.9, 8.5 Hz, 1H), 7.41-7.45 (m, 2H), 7.60 (d, *J* = 8.5 Hz, 2H), 7.67 (ds, *J* = 1.26 Hz, 1H), 7.74-7.77 (m, 3H), 7.78 (d, *J* = 8.5 Hz, 2H). ¹³C-NMR (125 MHz, CDCl₃): δ (ppm) = 40.8, 42.2, 52.4, 52.7, 57.2, 101.1, 125.9, 126.0, 126.1, 127.6, 127.8, 128.3, 129.5, 132.6, 133.3, 136.0, 137.8, 137.9, 168.0, 168.7, 196.5.

2-(3-(4-Iodophenyl)-1-(naphthalen-2-yl)-3-oxopropyl)malonic acid, (4O):

Synthesized according to Method L using **2O** (0.7 g, 1.36 mmol) and 10M NaOH_{aq} (4.4 mL); white solid; yield: 0.5 g (75 %); mp 150-151 °C;

¹H-NMR (500 MHz, (CD₃)₂SO): δ (ppm) = 3.41 (dd, *J* = 3.5, 17.02 Hz, 1H), 3.71 (dd, *J* = 10.4 Hz, 1H), 3.85 (d, *J* = 10.7 Hz, 1H), 4.02 (dt, *J* = 3.8, 10.4 Hz, 1H), 7.41-7.46 (m, 2H), 7.50 (dd, *J* = 1.6, 8.5 Hz, 1H), 7.74-7.77 (m, 2H), 7.79-7.82 (m, 2H), 7.86 (d, *J* = 8.5 Hz, 2H), 12.84 (s, 2OH). ¹³C-NMR (125 MHz, (CD₃)₂SO): δ (ppm) = 40.2, 40.5, 57.3, 101.7, 125.5, 125.8, 126.7, 126.9, 127.2, 127.3, 127.4, 129.5, 131.8, 132.6, 134.4, 135.7, 137.5, 138.7, 168.9, 169.6, 192.4; LC/MS (+ESI): *m/z* = 489.2 [MH⁺]; *R*_t = 5.05 (≥ 97 %).

2-(3-Oxo-1-(4-phenylthiophen-2-yl)-3-(4-(trifluoromethyl)phenyl)propyl)malonic acid, (4P):

(E)-3-(4-Phenylthiophen-2-yl)-1-(4-(trifluoromethyl)phenyl)prop-2-en-1-one, (1P):

Synthesized according to Method A using 4-phenylthiophene-2-carbaldehyde (0.50 g, 2.66 mmol) and 1-(4'-(trifluoromethyl)phenyl)ethanone (0.49 g, 2.66 mmol); yellow solid; yield: 0.86 g (90 %);

¹H-NMR (500 MHz, CDCl₃): δ (ppm) = 7.31 (d, *J* = 15.3, 1H), 7.34 (tt, *J* = 1.3, 7.6, 1H), 7.43 (t, *J* = 7.9, 2H), 7.58 (dt, *J* = 8.2, 3H), 7.66 (ds, *J* = 1.3 Hz, 1H), 7.78 (d, *J* = 8.2 Hz, 2H), 7.99 (d, *J* = 15.3 Hz, 1H), 8.10 (d, *J* = 7.9 Hz, 2H). ¹³C-NMR (125 MHz, (CD₃)₂SO): δ (ppm) = 117.0, 117.2, 120.4, 125.6 (q, ³*J*_{C-F} = 3.7 Hz), 125.9, 127.6, 128.9, 129.1, 131.3, 132.4, 132.5, 134.1, 137.6, 139.9, 142.4, 188.1.

Diethyl 2-(3-oxo-1-(4-phenylthiophen-2-yl)-3-(4-(trifluoromethyl)phenyl)propyl)malonate, (2P):

Synthesized according to Method H using **1P** (0.5 g, 1.39 mmol) and diethyl malonate (0.37 mL, 1.53 mmol) and magnesium oxide (0.14 g); yellow oil; yield: 0.67 g (93 %);

¹H-NMR (500 MHz, (CD₃)₂SO): δ (ppm) = 0.99 (t, *J* = 7.1 Hz, 3H), 1.16 (t, *J* = 7.1 Hz, 3H), 3.31 (s, 3H), 3.56 (dd, *J* = 4.1, 17.8 Hz, 1H), 3.80 (dd, *J* = 9.5, 17.8 Hz, 1H), 3.95-3.98 (m, 2H), 3.99 (m, 2H), 4.12-4.18 (m, 2H), 4.27 (dt, *J* = 4.1, 9.1 Hz, 1H), 7.26 (tt, *J* = 1.3, 7.3 Hz, 1H), 7.37 (t, *J* = 7.6 Hz, 2H), 7.45 (ds, *J* = 1.3 Hz, 1H), 7.60 (dd, *J* = 1.3, 8.2 Hz, 2H), 7.62 (ds, *J* = 1.6 Hz, 1H), 7.89 (d, *J* = 8.5 Hz, 2H), 8.13 (d, *J* = 8.5 Hz, 2H). ¹³C-NMR (125 MHz, (CD₃)₂SO): δ (ppm) = 13.5, 13.7, 35.4, 43.1, 57.0, 60.9, 61.3, 119.4, 122.5, 124.6, 125.61, 125.63, 125.7, 126.9, 128.7, 128.71, 135.0, 138.5, 140.4, 144.0, 167.0, 167.4, 196.9.

2-(3-Oxo-1-(4-phenylthiophen-2-yl)-3-(4-(trifluoromethyl)phenyl)propyl)malonic acid, (4P):

Synthesized according to Method L using **2P** (0.4 g, 0.77 mmol) and 10M NaOH_{aq} (0.8 mL); white solid; yield: 0.21 g (59 %); mp 162-163 °C;

¹H-NMR (500 MHz, (CD₃)₂SO): δ (ppm) = 3.53 (dd, *J* = 3.8, 17.3 Hz, 1H), 3.79 (dd, *J* = 9.5, 17.3 Hz, 1H), 3.80 (d, *J* = 9.8 Hz, 1H), 4.20 (dt, *J* = 4.1, 9.5 Hz, 1H), 7.26 (t, *J* = 7.3 Hz, 1H), 7.37 (t, *J* = 7.6 Hz, 2H), 7.41 (ds, *J* = 1.3 Hz, 1H), 7.58-7.60 (m, 3H), 7.88 (d, *J* = 8.2 Hz, 2H), 8.12 (d, *J* = 8.2 Hz, 2H), 12.92 (s, 2OH). ¹³C-NMR (125 MHz, (CD₃)₂SO): δ (ppm) = 35.5, 43.3, 57.7, 119.2, 124.3, 125.6, 126.9, 128.6, 128.7, 135.0, 138.9, 140.3, 144.8, 168.9,

169.2, 175.0, 183.1, 194.0, 194.2, 197.1; LC/MS (+ESI): $m/z = 463.2$ [MH^+]; $R_t = 4.92$ (≥ 95 %).

2-(3-(Naphthalen-2-yl)-3-oxo-1-phenylpropyl)malonic acid, (4Q):

(E)-1-(Naphthalen-2-yl)-3-phenylprop-2-en-1-one, (1Q):

Synthesized according to Method A using benzaldehyde (2.99 mL, 29.4 mmol) and 2-acetylnaphthalene (5.0 g, 29.4 mmol); pale yellow solid; yield: 6.1 g (80 %);

1H -NMR (500 MHz, $CDCl_3$): δ (ppm) = 7.44-7.46 (m, 3H), 7.56-7.63 (m, 2H), 7.68-7.72 (m, 3H), 7.87-7.96 (m, 3H), 7.95 (d, $J = 7.9$ Hz, 1H), 8.11 (d, $J = 8.5$ Hz, 1H), 8.55 (s, 1H). ^{13}C -NMR (125 MHz, $CDCl_3$): δ (ppm) = 122.1, 124.5, 126.8, 127.8, 128.4, 128.5, 128.6, 129.0, 129.5, 129.9, 130.5, 132.6, 135.0, 135.5, 135.6, 144.7, 190.3.

Diethyl 2-(3-(naphthalen-2-yl)-3-oxo-1-phenylpropyl)malonate, (2Q):

Synthesized according to Method H using **1Q** (2.0 g, 7.74 mmol) and malonate diethyl malonate (1.17 mL, 7.74 mmol) and magnesium oxide (0.77 g); white solid; yield: 2.76 g (85 %);

1H -NMR (500 MHz, $CDCl_3$): δ (ppm) = 1.02 (t, $J = 7.2$ Hz, 3H), 1.25 (t, $J = 7.2$ Hz, 3H), 3.60 (dd, $J = 9.5, 9.5$ Hz, 1H), 3.67 (dd, $J = 4.4, 4.4$ Hz, 1H), 3.87 (d, $J = 9.5$ Hz, 1H), 3.97 (q, $J = 6.9$ Hz, 2H), 4.19-4.28 (m, 3H), 7.17 (t, $J = 7.2$ Hz, 1H), 7.23-7.30 (m, 4H), 7.52-7.60 (m, 2H), 7.84 (d, $J = 8.5$ Hz, 2H), 7.93-7.96 (m, 2H), 8.44 (s, 1H). ^{13}C -NMR (125 MHz, $CDCl_3$): δ (ppm) = 13.7, 14.0, 41.0, 42.7, 57.6, 61.3, 61.6, 123.9, 126.7, 127.1, 127.7, 128.2, 128.4, 128.4, 129.6, 129.8, 132.5, 134.2, 135.5, 140.5, 153.0, 167.6, 167.8, 197.5.

2-(3-(Naphthalen-2-yl)-3-oxo-1-phenylpropyl)malonic acid, (4Q):

Synthesized according to Method L using **2Q** (2.0 g, 4.78 mmol) and $NaOH_{aq}$ (8.0 mL); white solid; yield: 1.5 g (87 %); mp 147-149 °C.

1H -NMR (500 MHz, $DMSO-d_6$): δ (ppm) = 3.44 (dd, $J = 3.5, 16.7$ Hz, 2H), 3.74-3.80 (m, 2H), 3.93-3.98 (m, 1H), 7.10 (t, $J = 7.6$ Hz, 1H), 7.20 (t, $J = 7.9$ Hz, 2H), 7.31 (d, $J = 8.5$ Hz, 2H), 7.60-7.67 (m, 2H), 7.86 (dd, $J = 1.9, 8.8$ Hz, 1H), 7.96 (dd, $J = 2.5, 7.9$ Hz, 1H), 8.07 (d, $J = 7.9$ Hz, 1H), 8.59 (s, 1H). ^{13}C -NMR (125 MHz, $DMSO-d_6$): δ (ppm) = 40.6, 42.4, 57.4, 123.3, 126.4, 126.8, 127.5, 127.8, 128.1, 128.3, 128.5, 129.4, 129.6, 132.0, 133.8, 134.8, 141.2, 168.9, 169.7, 197.7; LC/MS (+ESI): $m/z = 363.2$ [MH^+]; $R_t = 4.26$ (≥ 95 %).

Bis(acetoxymethyl) 2-(3-(naphthalen-2-yl)-3-oxo-1-phenylpropyl)malonate, (5Q):

Synthesized according to Method M using **4Q** (0.3 g, 0.83 mmol), bromo methylacetate (0.24 mL, 2.48 mmol) and triethylamine (0.57 mL, 4.14 mmol); white solid; yield: 0.12 g (30 %); mp 100-102 °C;

¹H-NMR (500 MHz, DMSO-d₆): δ (ppm) = 1.97 (s, 3H), 2.10 (s, 3H), 3.61-3.71 (m, 2H), 4.02 (d, *J* = 9.1 Hz, 1H), 4.27-4.32 (m, 1H), 5.58 (q, *J* = 5.7 Hz, 2H), 5.76-5.78 (m, 2H), 7.19 (t, *J* = 7.2 Hz, 1H), 7.24-7.31 (m, 4H), 7.53-7.61 (m, 2H), 7.85 (d, *J* = 8.5 Hz, 2H), 7.92-7.97 (m, 2H), 8.43 (s, 1H); ¹³C-NMR (125 MHz, DMSO-d₆): δ (ppm) = 20.5, 20.54, 40.6, 42.2, 56.6, 79.4, 79.8, 123.7, 126.8, 127.4, 127.7, 128.2, 128.4, 128.51, 128.58, 129.6, 129.9, 132.5, 134.0, 135.6, 139.8, 166.1, 166.6, 169.2, 169.3, 197.1; LC/MS (+ESI): *m/z* = 507.3 [MH⁺]; *R_t* = 5.33 (≥ 96 %).

5-(naphthalen-2-yl)-5-oxo-3-phenylpentanoic acid, (6Q):

Synthesized according to Method N using **4Q** (0.55 g, 1.52 mmol); white solid; yield: 0.30 g (61 %); mp 169-170 °C;

¹H-NMR (500 MHz, CDCl₃): δ (ppm) = 2.77 (dd, *J* = 7.6, 7.9 Hz, 1H), 2.92 (dd, *J* = 6.9, 6.9 Hz, 1H), 3.45-3.55 (m, 2H), 3.91-3.96 (m, 1H), 7.20-7.22 (m, 1H), 7.29-7.31 (m, 4H), 7.52 (t, *J* = 8.2 Hz, 1H), 7.59 (t, *J* = 8.2 Hz, 1H), 7.86 (d, *J* = 8.8 Hz, 1H), 7.92-7.98 (m, 2H), 8.42 (s, 1H); ¹³C-NMR (125 MHz, CDCl₃): δ (ppm) = 37.4, 40.1, 44.6, 123.8, 126.8, 126.9, 127.4, 127.7, 128.4, 128.5, 128.7, 129.6, 129.8, 132.5, 134.2, 135.6, 143.1, 176.5, 198.0; LC/MS (+ESI): *m/z* = 319.2 [MH⁺]; *R_t* = 4.80 (≥ 96 %).

2-(3-(6-Methoxynaphthalen-2-yl)-3-oxo-1-phenylpropyl)malonic acid, (4R):**(E)-1-(6-Methoxynaphthalen-2-yl)-3-phenylprop-2-en-1-one, (1R):**

Synthesized according to Method A using benzaldehyde (1.52 mL, 14.98 mmol) and 2-acetyl-6-methoxynaphthalene (3.0 g, 14.98 mmol); pale beige solid; yield: 4.0 g (93 %);

¹H-NMR (500 MHz, CDCl₃): δ (ppm) = 3.95 (s, 3H), 7.18 (d, *J* = 2.2, 1H), 7.22 (dd, *J* = 2.5, 11.3, 1H), 7.43-7.45 (m, 3H), 7.67-7.71 (m, 3H), 7.81 (d, *J* = 8.5 Hz, 1H), 7.86-7.89 (m, 2H), 8.10 (dd, *J* = 1.60, 1.89, 8.5 Hz, 1H), 8.48 (s, 1H). ¹³C-NMR (125 MHz, CDCl₃): δ (ppm) = 55.4, 105.8, 119.7, 122.1, 125.2, 127.3, 127.9, 128.4, 128.9, 129.8, 130.4, 131.1, 133.5, 135.1, 137.2, 144.3, 159.7, 189.8.

Diethyl 2-(3-(6-methoxynaphthalen-2-yl)-3-oxo-1-phenylpropyl)malonate (2R):

Synthesized according to Method H using **1R** (2.0g, 6.94 mmol) and diethyl malonate (1.05 mL, 6.94 mmol) and magnesium oxide (0.694 g); pale beige solid; yield: 2.10 g (68 %);

¹H-NMR (500 MHz, CDCl₃): δ (ppm) = 1.01 (t, *J* = 7.2 Hz, 3H), 1.25 (t, *J* = 7.2 Hz, 3H), 3.56 (dd, *J* = 9.1, 9.1 Hz, 1H), 3.64 (dd, *J* = 4.4, 4.4 Hz, 1H), 3.87 (d, *J* = 9.8 Hz, 1H), 3.94 (s, 3H), 3.96 (q, *J* = 7.2 Hz, 2H), 4.16-4.27 (m, 3H), 7.12-7.30 (m, 7H), 7.71 (d, *J* = 8.8 Hz, 1H), 7.83 (d, *J* = 9.1 Hz, 1H), 7.91 (dd, *J* = 1.9, 8.5 Hz, 1H), 8.37 (d, *J* = 1.6 Hz, 1H). ¹³C-NMR (125 MHz, CDCl₃): δ (ppm) = 13.7, 14.0, 41.0, 42.5, 55.4, 57.6, 61.3, 61.6, 105.7, 119.6, 124.6, 127.0, 127.1, 127.8, 128.3, 128.4, 129.7, 131.1, 132.2, 137.2, 140.6, 159.7, 167.8, 168.4, 197.1.

2-(3-(6-Methoxynaphthalen-2-yl)-3-oxo-1-phenylpropyl)malonic acid, (4R):

Synthesized according to Method L using **2R** (1.0 g, 2.22 mmol) and 10M NaOH_{aq} (5 mL); pale yellow solid; yield: 0.74 g (85 %); mp 164-165 °C.

¹H-NMR (500 MHz, (CD₃)₂SO): δ (ppm) = 3.38 (dd, *J* = 3.5, 16.7 Hz, 1H), 3.71-3.79 (m, 2H), 3.95 (s, 3H), 3.96 (dt, *J* = 3.5, 10.7 Hz, 1H), 7.10 (t, *J* = 7.2 Hz, 1H), 7.20 (t, *J* = 7.6 Hz, 2H), 7.25 (dd, *J* = 2.2, 8.8 Hz, 1H), 7.31 (d, *J* = 7.2 Hz, 2H), 7.37 (d, *J* = 2.2 Hz, 1H), 7.83 (q, *J* = 8.8 Hz, 2H), 7.98 (d, *J* = 8.8 Hz, 1H), 8.51 (s, 1H), 12.53 (s, OH), 12.92 (s, OH). ¹³C-NMR (125 MHz, (CD₃)₂SO): δ (ppm) = 40.6, 42.3, 55.4, 57.5, 106.0, 119.5, 124.0, 126.4, 126.9, 127.3, 127.9, 128.4, 129.6, 131.1, 131.9, 136.8, 141.3, 159.3, 169.1, 169.8, 197.3; LC/MS (+ESI): *m/z* = 393.2 [MH⁺]; *R_f* = 4.25 (≥ 96 %).

5-(6-Hydroxynaphthalen-2-yl)-5-oxo-3-phenylpentanoic acid, (6R):

A mixture of **4R** (0.15 g, 0.45 mmol) in glacial acetic acid (5 mL) was treated with 48% aqueous HBr (2 mL) and heated to 150 °C for 2 h. The solvent and acid were then distilled off and the residue hydrolyzed, acidified to pH 2 with 10 % HCl and extracted with ethyl acetate (3 x 20 mL). The organic layers were collected, washed with brine (20 mL), dried over MgSO₄ and evaporated to afford a residue, which was purified by flash column chromatography on silica gel; pale yellow solid; yield: 0.10 g (67 %);

¹H-NMR (500 MHz, (CD₃)₂SO): δ (ppm) = 2.59 (dd, *J* = 8.5 Hz, 1H), 2.73 (dd, *J* = 6.3 Hz, 1H), 3.43 (dd, *J* = 6.3 Hz, 1H), 3.52 (dd, *J* = 8.5 Hz, 1H), 3.69-3.74 (m, 1H), 7.12-7.18 (m, 3H), 7.25 (t, *J* = 7.6 Hz, 2H), 7.32 (d, *J* = 8.2 Hz, 2H), 7.71 (d, *J* = 8.8 Hz, 1H), 7.82 (dd, *J* = 1.9, 8.8 Hz, 1H), 7.94 (d, *J* = 9.8 Hz, 1H), 8.51 (d, *J* = 1.6 Hz, 1H), 10.19 (s, OH), 12.20 (s, OH). ¹³C-NMR (125 MHz, (CD₃)₂SO): δ (ppm) = 37.3, 40.3, 43.6, 108.6, 119.4, 123.7, 126.1,

126.2, 126.4, 127.4, 128.0, 129.9, 131.1, 131.4, 136.7, 143.9, 157.7, 172.8, 197.7; LC/MS (+ESI): $m/z = 335.2$ [MH^+]; $R_t = 3.99$ ($\geq 96\%$).

2-(1,3-Di(naphthalen-2-yl)-3-oxopropyl)malonic acid, (4S):

(E)-1,3-Di(naphthalen-2-yl)prop-2-en-1-one, (1S):

Synthesized according to Method A using 2-naphthaldehyde (10.9 g, 64.03 mmol) and 1-(naphthalen-2-yl)ethanone (11.9 g, 64.03 mmol); yellow solid; yield: 18.8 g (95 %);

1H -NMR (500 MHz, $CDCl_3$): δ (ppm) = 7.52-7.55 (m, 2H), 7.56-7.65 (m, 2H), 7.82 (d, $J = 15.8$ Hz, 1H), 7.86-7.92 (m, 5H), 7.97 (d, $J = 8.8$ Hz, 1H), 8.02-8.07 (m, 2H), 8.08 (s, 1H), 8.14 (dd, $J = 1.6, 8.5$ Hz, 1H), 8.59 (s, 1H). ^{13}C -NMR (125 MHz, $CDCl_3$): δ (ppm) = 117.7, 122.2, 123.7, 124.5, 126.8, 127.4, 127.81, 127.84, 128.4, 128.6, 128.7, 128.8, 129.5, 129.9, 130.7, 132.5, 132.6, 133.4, 134.4, 35.5, 135.7, 144.9, 190.2.

Diethyl 2-(1,3-di(naphthalen-2-yl)-3-oxopropyl)malonate, (2S):

Synthesized according to Method H using **1S** (2.0 g, 6.48 mmol) and diethyl malonate (0.98 mL, 6.48 mmol) and magnesium oxide (0.65 g); white solid; yield: 1.32 g (43 %);

1H -NMR (500 MHz, $CDCl_3$): δ (ppm) = 0.95 (t, $J = 7.1$ Hz, 3H), 1.25 (t, $J = 7.1$ Hz, 3H), 3.72 (dd, $J = 9.1, 16.7$ Hz, 1H), 3.77 (dd, $J = 4.9, 16.7$ Hz, 1H), 3.90-3.96 (m, 2H), 3.98 (d, $J = 9.7$ Hz, 1H), 4.18-4.27 (m, 2H), 4.41-4.46 (m, 1H), 7.39-7.44 (m, 2H), 7.47 (dd, $J = 1.5, 8.5$ Hz, 1H), 7.53 (t, $J = 7.9$ Hz, 1H), 7.58 (t, $J = 8.2$ Hz, 1H), 7.73-7.77 (m, 4H), 7.83-7.85 (m, 2H), 7.93-7.95 (m, 2H), 8.47 (s, 1H). ^{13}C -NMR (125 MHz, $CDCl_3$): δ (ppm) = 13.5, 13.8, 40.8, 42.4, 57.4, 61.1, 61.4, 123.6, 125.4, 125.7, 126.1, 126.4, 126.9, 127.3, 127.5, 127.6, 127.9, 128.1, 128.2, 129.3, 129.6, 132.2, 132.3, 133.0, 133.9, 135.3, 137.8, 167.5, 168.2, 197.1.

2-(1,3-Di(naphthalen-2-yl)-3-oxopropyl)malonic acid, (4S):

Synthesized according to Method L using **2S** (1.0 g, 2.13 mmol) and 10M $NaOH_{aq}$ (5.0 mL, 6.39 mL); white solid; yield: 0.6 g (68 %); mp 174-175 °C;

1H -NMR (500 MHz, $(CD_3)_2SO$): δ (ppm) = 3.61 (dd, $J = 3.8, 16.85$ Hz, 1H), 3.85 (dd, $J = 9.8, 16.85$ Hz, 1H), 3.92 (d, $J = 10.4$ Hz, 1H), 4.17 (dt, $J = 3.8, 10.1$ Hz, 1H), 7.39-7.45 (m, 2H), 7.53 (dd, $J = 1.9, 8.5$ Hz, 1H), 7.59 (dt, $J = 1.3, 8.2$ Hz, 1H), 7.64 (dt, $J = 1.3, 8.2$ Hz, 1H), 7.76 (d, $J = 8.5$ Hz, 1H), 7.78-7.80 (m, 3H), 7.86 (dd, $J = 1.6, 8.8$ Hz, 1H), 7.93-7.95 (m,

2H), 8.06 (d, $J = 8.2$ Hz, 1H), 8.58 (s, 1H), 12.78 (s, 2OH). ^{13}C -NMR (125 MHz, $(\text{CD}_3)_2\text{SO}$): δ (ppm) = 40.7, 42.4, 57.5, 123.3, 125.4, 125.7, 126.7, 126.8, 126.9, 127.1, 127.2, 127.4, 127.5, 128.1, 128.5, 129.4, 129.7, 131.8, 132.0, 133.7, 134.9, 138.8, 169.0, 169.7, 197.8; LC/MS (+ESI): $m/z = 413.2$ [MH^+]; $R_t = 4.67$ ($\geq 98\%$).

3,5-di(naphthalen-2-yl)-5-oxopentanoic acid, (6S):

Synthesized according to Method N **4S** (0.25 g, 0.61 mmol); pale beige solid; yield: 0.17 g (76 %); mp 151-153 °C;

^1H -NMR (500 MHz, CDCl_3): δ (ppm) = 2.86 (dd, $J = 7.9, 16.1$ Hz, 1H), 2.99 (dd, $J = 6.9, 16.1$ Hz, 1H), 3.53-3.63 (m, 2H), 4.08-4.13 (m, 1H), 7.39-7.46 (m, 3H), 7.53 (dt, $J = 0.9, 8.2$ Hz, 1H), 7.59 (dt, $J = 1.3, 8.4$ Hz, 1H), 7.74 (ds, $J = 1.3$ Hz, 1H), 7.76-7.79 (m, 3H), 7.84 (d, $J = 8.8$ Hz, 2H), 7.91 (d, $J = 8.2$ Hz, 1H), 7.96 (dd, $J = 1.9, 8.8$ Hz, 1H), 8.43 (s, 1H). ^{13}C -NMR (125 MHz, CDCl_3): δ (ppm) = 37.4, 40.2, 44.6, 123.8, 125.6, 125.7, 125.9, 126.1, 126.7, 126.8, 127.6, 127.73, 127.75, 128.45, 128.48, 129.6, 129.8, 132.4, 132.5, 133.5, 134.1, 135.6, 140.5, 176.8, 198.0; LC/MS (+ESI): $m/z = 369.2$ [MH^+]; $R_t = 5.20$ ($\geq 95\%$).

2-(3-(1H-Indol-3-yl)-3-oxo-1-phenylpropyl)malonic acid, (4T):

(E)-1-(1H-Indol-3-yl)-3-phenylprop-2-en-1-one, (1T):

Synthesized according to Method A using benzaldehyde (1.59 mL, 15.7 mmol) and 3-acetylindole (2.5 g, 15.7 mmol); gold-colored solid; yield: 2.40 g (62 %);

^1H -NMR (500 MHz, $(\text{CD}_3)_2\text{SO}$): δ (ppm) = 7.21-7.27 (m, 2H), 7.40-7.44 (m, 3H), 7.48 (d, $J = 7.6$, 1H), 7.64 (d, $J = 15.8$, 1H), 7.83-7.86 (m, 3H), 7.83-7.84 (m, 1H), 8.74 (s, 1H), 12.1 (s, NH). ^{13}C -NMR (125 MHz, $(\text{CD}_3)_2\text{SO}$): δ (ppm) = 112.1, 117.7, 121.6, 121.7, 121.8, 123.1, 124.6, 125.9, 128.3, 128.8, 129.7, 135.2, 136.8, 139.5, 183.5.

Dimethyl 2-(3-(1H-indol-3-yl)-3-oxo-1-phenylpropyl)malonate, (2T):

Synthesized according to Method J using **1T** (0.70 g, 2.83 mmol), diethyl malonate (0.48 mL, 2.83 mmol) and sodium hydride (cat.); pale yellow solid; yield: 0.60 g (56 %);

^1H -NMR (500 MHz, $(\text{CD}_3)_2\text{SO}$): δ (ppm) = 3.10 (dd, $J = 3.9, 15.7$ Hz, 1H), 3.37 (s, 3H), 3.30 (dd, $J = 10.1, 15.7$ Hz, 1H), 3.67 (s, 3H), 3.96 (d, $J = 10.4$ Hz, 1H), 3.99 (dt, $J = 3.7, 10.1$ Hz, 1H), 7.10-7.13 (m, 2H), 7.18 (dd, $J = 1.2, 6.9$ Hz, 1H), 7.20 (t, $J = 7.6$ Hz, 2H), 7.31 (d, $J = 8.5$ Hz, 2H), 7.42 (d, $J = 7.9$ Hz, 1H), 8.07 (d, $J = 7.9$ Hz, 1H), 8.25 (d, $J = 3.1$ Hz,

1H), 11.9 (s, NH). ¹³C-NMR (125 MHz, (CD₃)₂SO): δ (ppm) = 46.3, 47.7, 57.2, 57.7, 62.2, 117.2, 121.8, 126.5, 126.9, 128.0, 130.4, 131.9, 133.2, 133.5, 139.0, 141.7, 145.9, 173.0, 173.5, 197.5.

2-(3-(1H-Indol-3-yl)-3-oxo-1-phenylpropyl)malonic acid, (4T):

Synthesized according to Method L using **2T** (0.44 g, 1.16 mmol) and NaOH_{aq} (2 mL, 5.80 mmol); pale yellow solid; yield: 0.29 g (71 %); mp 169-171 °C;

¹H-NMR (500 MHz, (CD₃)₂SO): δ (ppm) = 3.05 (dd, *J* = 3.5, 15.8 Hz, 1H), 3.47 (dd, *J* = 10.7 Hz, 1H), 3.71 (d, *J* = 10.7 Hz, 1H), 3.94 (dt, *J* = 3.5, 10.7 Hz, 1H), 7.07 (t, *J* = 7.6 Hz, 1H), 7.08-7.12 (m, 4H), 7.30 (d, *J* = 7.7 Hz, 2H), 7.39 (d, *J* = 8.2 Hz, 1H), 8.06 (d, *J* = 7.9 Hz, 1H), 8.23 (d, *J* = 2.8 Hz, 1H), 11.84 (s, NH), 12.51 (s, OH), 12.88 (s, OH). ¹³C-NMR (125 MHz, (CD₃)₂SO): δ (ppm) = 46.3, 47.7, 57.2, 57.7, 62.2, 117.2, 121.8, 126.5, 126.9, 128.0, 130.4, 131.9, 133.2, 133.5, 139.0, 141.7, 145.9, 173.0, 173.5, 197.5; LC/MS (+ESI): *m/z* = 352.2 [MH⁺]; *R_t* = 3.23 (≥ 95 %).

2-(3-Oxo-3-(phenanthren-2-yl)-1-phenylpropyl)malonic acid, (4U):

(E)-1-(Phenanthren-2-yl)-3-phenylprop-2-en-1-one, (1U):

Synthesized according to Method A using benzaldehyde (0.46 mL, 4.54 mmol) and 2-acetylphenanthrene (1.0 g, 4.54 mmol); pale yellow solid; yield: 1.20 g (86 %);

¹H-NMR (500 MHz, CDCl₃): δ (ppm) = 7.41-7.48 (m, 3H), 7.66-7.74 (m, 5H), 7.84 (q, *J* = 8.8 Hz, 2H), 7.89-7.93 (m, 2H), 8.29 (dd, *J* = 1.89, 8.5 Hz, 1H), 8.57 (d, *J* = 1.89 Hz, 1H), 8.73 (d, *J* = 7.9 Hz, 1H), 8.78 (d, *J* = 8.8 Hz, 1H). ¹³C-NMR (125 MHz, CDCl₃): δ (ppm) = 122.1, 123.2, 123.3, 125.6, 127.0, 127.3, 127.7, 127.9, 128.5, 128.7, 129.0, 129.7, 130.6, 131.5, 133.0, 133.3, 135.0, 136.0, 144.9, 190.1.

Diethyl 2-(3-oxo-3-(phenanthren-2-yl)-1-phenylpropyl)malonate, (2U):

Synthesized according to Method H using **1U** (1.0g, 3.24 mmol) and diethyl malonate (0.49 mL, 3.24 mmol) and magnesium oxide (0.324 g) ; white solid; yield: 1.20 g (79 %);

¹H-NMR (500 MHz, CDCl₃): δ (ppm) = 1.02 (t, *J* = 7.2 Hz, 3H), 1.27 (t, *J* = 7.2 Hz, 3H), 3.62 (dd, *J* = 9.1, 9.1 Hz, 1H), 3.71 (dd, *J* = 4.4, 4.4 Hz, 1H), 3.89 (d, *J* = 9.4 Hz, 1H), 3.97 (q, *J* = 7.2 Hz, 2H), 4.18-4.30 (m, 3H), 7.17 (tt, *J* = 1.4, 7.6 Hz, 1H), 7.25 (t, *J* = 7.9 Hz, 2H), 7.31 (dd, *J* = 1.2, 8.2 Hz, 2H), 7.64-7.70 (m, 2H), 7.78 (q, *J* = 8.8 Hz, 2H), 7.91 (dd, *J* = 1.9,

7.2 Hz, 1H), 8.14 (dd, $J = 1.9, 8.8$ Hz, 1H), 8.45 (d, $J = 1.9$ Hz, 1H), 8.68-8.71 (m, 2H). ^{13}C -NMR (125 MHz, CDCl_3): δ (ppm) = 13.8, 14.0, 41.0, 42.8, 57.6, 61.3, 61.7, 123.1, 123.3, 125.1, 127.0, 127.1, 127.4, 127.7, 127.8, 128.3, 128.4, 128.7, 129.5, 129.7, 131.4, 133.0, 133.4, 134.6, 140.5, 167.8, 168.4, 197.4.

2-(3-Oxo-3-(phenanthren-2-yl)-1-phenylpropyl)malonic acid, (4U):

Synthesized according to Method L using **2U** (0.6 g, 1.28 mmol) and 10M NaOH_{aq} (5 mL); white solid; yield: 0.45 g (85 %); mp 170-171 °C;

^1H -NMR (500 MHz, $(\text{CD}_3)_2\text{SO}$): δ (ppm) = 3.49 (dd, $J = 3.5, 10.9$ Hz, 1H), 3.77-3.82 (m, 2H), 3.98 (dt, $J = 3.5, 10.9$ Hz, 1H), 7.11 (t, $J = 7.2$ Hz, 1H), 7.21 (t, $J = 7.6$ Hz, 2H), 7.33 (d, $J = 7.2$ Hz, 2H), 7.70-7.76 (m, 2H), 7.95 (q, $J = 8.8$ Hz, 2H), 8.02-8.39 (m, 1H), 8.07 (dd, $J = 1.9, 8.8$ Hz, 1H), 8.59 (d, $J = 1.9$ Hz, 1H), 8.86-8.90 (m, 2H). ^{13}C -NMR (125 MHz, $(\text{CD}_3)_2\text{SO}$): δ (ppm) = 40.7, 42.6, 57.5, 123.4, 123.6, 124.8, 126.5, 127.2, 127.7, 127.8, 127.9, 128.0, 128.5, 128.6, 129.6, 131.0, 132.1, 132.5, 132.6, 134.5, 141.3, 169.0, 169.8, 197.7; LC/MS (+ESI): $m/z = 413.2$ [MH^+]; $R_t = 4.78$ (≥ 98 %).

5-Oxo-5-(phenanthren-2-yl)-3-phenylpentanoic, (6U):

Synthesized according to Method M using **4U** (0.15 g, 0.36 mmol); white solid; yield: 0.105 g (79 %); mp 199-201 °C;

^1H -NMR (500 MHz, $(\text{CD}_3)_2\text{SO}$): δ (ppm) = 2.62 (dd, $J = 8.5$ Hz, 1H), 2.76 (dd, $J = 6.6$ Hz, 1H), 3.58 (dd, $J = 6.6$ Hz, 1H), 3.64 (dd, $J = 7.6$ Hz, 1H), 3.73-3.79 (m, 1H), 7.15 (t, $J = 7.6$ Hz, 1H), 7.26 (t, $J = 7.9$ Hz, 2H), 7.35 (d, $J = 8.2$ Hz, 2H), 7.71-7.76 (m, 2H), 7.96 (q, $J = 8.8$ Hz, 2H), 8.01-8.04 (m, 1H), 8.13 (dd, $J = 1.9, 8.8$ Hz, 1H), 8.66 (ds, $J = 1.9$ Hz, 1H), 8.87 (d, $J = 9.1$ Hz, 1H), 8.90 (d, $J = 8.8$ Hz, 1H), 12.15 (s, OH). ^{13}C -NMR (125 MHz, $(\text{CD}_3)_2\text{SO}$): δ (ppm) = 37.2, 40.4, 44.1, 116.2, 123.3, 123.5, 124.8, 126.1, 127.1, 127.2, 127.5, 127.6, 127.9, 128.1, 128.5, 129.0, 129.4, 131.0, 132.4, 132.6, 134.5, 143.9, 198.2; LC/MS (+ESI): $m/z = 369.2$ [MH^+]; $R_t = 5.35$ (≥ 95 %).

2-(3-(9H-Carbazol-2-yl)-3-oxo-1-phenylpropyl)malonic acid, (4V):

(E)-1-(9H-Carbazol-2-yl)-3-phenylprop-2-en-1-one, (1V):

Synthesized according to Method A using benzaldehyde (0.51 g, 4.78 mmol) and 2-acetylcarbazole (1.0 g, 4.78 mmol); yellow solid; yield: 0.75 g (53 %);

$^1\text{H-NMR}$ (500 MHz, CDCl_3): δ (ppm) = 7.22 (t, J = 7.9 Hz, 1H), 7.45-7.51 (m, 4H), 7.58 (d, J = 8.2 Hz, 1H), 7.78 (d, J = 15.6 Hz, 1H), 7.91-7.93 (m, 2H), 8.01 (dd, J = 1.6, 8.2 Hz, 1H), 8.06 (d, J = 15.6 Hz, 1H), 8.23 (d, J = 7.9 Hz, 1H), 8.27-8.30 (m, 2H), 11.55 (s, NH). $^{13}\text{C-NMR}$ (125 MHz, CDCl_3): δ (ppm) = 111.3, 111.6, 119.1, 120.11, 120.13, 121.1, 121.5, 122.6, 126.2, 127.0, 128.7, 128.9, 130.4, 134.7, 134.8, 139.2, 141.3, 143.3, 189.1.

Dimethyl 2-(3-(9H-carbazol-2-yl)-3-oxo-1-phenylpropyl)malonate, (2V):

Synthesized according to Method H using **1V** (0.5 g, 1.68 mmol) and diethyl malonate (0.28 mL, 1.85 mmol) and magnesium oxide (0.17 g); white solid; yield: 0.43 g (60 %);

$^1\text{H-NMR}$ (500 MHz, $(\text{CD}_3)_2\text{SO}$): δ (ppm) = 3.37 (s, 3H), 3.46 (dd, J = 3.6, 17.1 Hz, 1H), 3.69 (s, 3H), 3.77 (dd, J = 9.1, 9.1 Hz, 1H), 4.00-4.08 (m, 2H), 7.13 (t, J = 7.3 Hz, 1H), 7.19-7.24 (m, 3H), 7.32 (d, J = 7.3 Hz, 2H), 7.46 (d, J = 8.2 Hz, 1H), 7.54 (d, J = 8.2 Hz, 1H), 7.72 (dd, J = 1.5, 8.2 Hz, 1H), 8.90 (s, 1H), 8.19 (t, J = 7.9 Hz, 2H), 11.5 (s, NH). $^{13}\text{C-NMR}$ (125 MHz, $(\text{CD}_3)_2\text{SO}$): δ (ppm) = 41.1, 42.6, 52.4, 52.6, 57.4, 110.9, 111.0, 119.5, 119.9, 120.0, 121.1, 122.4, 127.2, 127.3, 128.1, 128.5, 134.2, 139.0, 140.4, 141.0, 168.2, 168.8, 197.6.

2-(3-(9H-Carbazol-2-yl)-3-oxo-1-phenylpropyl)malonic acid, (4V):

Synthesized according to Method L using **2V** (0.30 g, 0.78 mmol) and 10M NaOH_{aq} (0.9 mL, 2.31 mL); white solid; yield: 0.15 g (48 %); mp 181-182 °C;

$^1\text{H-NMR}$ (500 MHz, $(\text{CD}_3)_2\text{SO}$): δ (ppm) = 3.40 (dd, J = 3.3, 16.75 Hz, 1H), 3.74 (dd, J = 10.3, 16.75 Hz, 1H), 3.81 (d, J = 10.3 Hz, 1H), 3.96 (dt, J = 3.0, 10.7 Hz, 1H), 7.11 (t, J = 7.3 Hz, 1H), 7.19-7.22 (m, 3H), 7.32 (d, J = 7.3 Hz, 2H), 7.46 (d, J = 7.9 Hz, 1H), 7.53 (d, J = 7.9 Hz, 1H), 7.71 (dd, J = 1.2, 7.9 Hz, 1H), 7.99 (ds, J = 0.6 Hz, 1H), 8.17-8.20 (m, 2H), 11.5 (s, NH), 12.71 (s, 2OH). $^{13}\text{C-NMR}$ (125 MHz, $(\text{CD}_3)_2\text{SO}$): δ (ppm) = 40.6, 42.5, 57.4, 110.8, 111.2, 118.2, 119.0, 119.9, 121.0, 121.4, 126.0, 126.3, 126.9, 127.8, 128.4, 133.7, 139.0, 141.2, 141.3, 169.0, 169.7, 197.6; LC/MS (+ESI): m/z = 402.2 [MH^+]; R_t = 4.30 (\geq 96 %).

6.1.3.3. Compounds described in Chapter 3.3.

5-(4-Chlorophenyl)-3-(naphthalen-2-yl)pent-2-enoic acids, (26E & 26Z):

(E)-1-(4-Chlorophenyl)-3-(naphthalen-2-yl)prop-2-en-1-one, (26c):

Synthesized according to Method A using 4-chlorobenzaldehyde (5.0 g, 35.57 mmol) and 2-acetylnaphthalene (6.05 g, 35.57 mmol); pale yellow solid; yield: 9.32 g (90 %);

$^1\text{H-NMR}$ (500 MHz, CDCl_3): δ (ppm) = 7.41 (d, J = 8.2 Hz, 2H), 7.56-7.63 (m, 4H), 7.67 (d, J = 15.8 Hz, 1H), 7.82 (d, J = 15.8 Hz, 1H), 7.90 (d, J = 8.2 Hz, 1H), 7.94 (d, J = 9.8 Hz, 1H), 8.00 (d, J = 8.2 Hz, 1H), 8.10 (d, J = 8.5 Hz, 1H), 8.53 (s, 1H). $^{13}\text{C-NMR}$ (125 MHz, CDCl_3): δ (ppm) = 122.5, 124.4, 126.8, 127.8, 128.5, 128.6, 129.2, 129.5, 129.6, 129.9, 132.5, 133.5, 135.4, 135.5, 136.4, 143.2, 189.9.

1-(4-Chlorophenyl)-3-(naphthalen-2-yl)propan-1-one, (26b):

Synthesized according to Method B using **26c** (1.0 g, 3.41 mmol), HEH (1.30 g, 5.12 mmol) and silica gel (6.82 g); colourless oil; yield: 0.87 g (87 %);

$^1\text{H-NMR}$ (500 MHz, CDCl_3): δ (ppm) = 3.11 (t, J = 7.9 Hz, 2H), 3.42 (t, J = 7.9 Hz, 2H), 7.22 (d, J = 8.5 Hz, 2H), 7.27 (d, J = 8.5 Hz, 2H), 7.55 (t, J = 7.5 Hz, 1H), 7.59 (t, J = 7.5 Hz, 1H), 7.89 (t, J = 8.8 Hz, 2H), 7.94 (d, J = 8.2 Hz, 1H), 8.01 (dd, J = 1.8, 8.5 Hz, 1H), 8.53 (s, 1H). $^{13}\text{C-NMR}$ (125 MHz, CDCl_3): δ (ppm) = 29.5, 40.2, 117.4, 123.8, 127.8, 128.4, 128.5, 128.6, 129.5, 129.6, 129.8, 131.9, 132.5, 134.1, 135.6, 139.8, 198.7.

Ethyl 5-(4-chlorophenyl)-3-(naphthalen-2-yl)pent-2-enoate, (26a):

Synthesized according to Method C using **26b** (0.75 g, 2.54 mmol), NaH (0.31 g, 7.63 mmol) and triethyl phosphonoacetate (1.58 mL, 7.87 mmol);

26Ea: colourless oil; yield: 0.55 g (59 %); $^1\text{H-NMR}$ (500 MHz, CDCl_3): δ (ppm) = 1.33 (t, J = 7.2 Hz, 3H), 2.74-2.77 (m, 2H), 3.48-3.52 (m, 2H), 4.22 (q, J = 7.2 Hz, 2H), 6.20 (s, 1H), 7.15 (d, J = 8.5 Hz, 2H), 7.22 (d, J = 8.2 Hz, 2H), 7.51-7.54 (m, 2H), 7.56 (dd, J = 1.9, 8.5 Hz, 1H), 7.84-7.88 (m, 3H), 7.90 (d, J = 1.6 Hz, 1H). $^{13}\text{C-NMR}$ (125 MHz, CDCl_3): δ (ppm) = 14.3, 32.8, 34.5, 60.0, 118.4, 124.3, 126.2, 126.6, 126.8, 127.6, 128.3, 128.4, 128.5, 129.9, 131.7, 133.2, 133.5, 138.1, 139.9, 158.9, 166.3.

26Za: colourless oil; yield: 0.38 g (41 %); $^1\text{H-NMR}$ (500 MHz, CDCl_3): δ (ppm) = 1.00 (t, J = 7.2 Hz, 3H), 2.68-2.71 (m, 2H), 2.82-2.86 (m, 2H), 3.97 (q, J = 7.2 Hz, 2H), 5.97 (s, 1H), 7.05 (d, J = 8.5 Hz, 2H), 7.23 (d, J = 8.5 Hz, 2H), 7.30 (dd, J = 1.9, 8.5 Hz, 1H), 7.47-7.51

(m, 2H), 7.64 (d, $J = 1.6$ Hz, 1H), 7.82-7.86 (m, 3H). $^{13}\text{C-NMR}$ (125 MHz, CDCl_3): δ (ppm) = 13.9, 32.2, 41.9, 59.9, 118.4, 125.9, 126.0, 126.1, 126.2, 127.5, 127.7, 128.1, 128.5, 129.7, 131.9, 132.9, 133.0, 137.1, 139.2, 157.7, 165.8.

(E)-5-(4-Chlorophenyl)-3-(naphthalen-2-yl)pent-2-enoic acid, (26E):

Synthesized according to Method D using **26Ea** (0.4 g, 1.09 mmol) and NaOH_{aq} (1.10 mL, 3.29 mmol); white solid; yield: 0.20 g (54 %);

$^1\text{H-NMR}$ (500 MHz, CDCl_3): δ (ppm) = 2.77-2.80 (m, 2H), 3.51-3.54 (m, 2H), 6.27 (s, 1H), 7.15 (d, $J = 8.5$ Hz, 2H), 7.23 (d, $J = 8.5$ Hz, 2H), 7.53-7.56 (m, 2H), 7.58 (dd, $J = 1.9, 8.5$ Hz, 1H), 7.86-7.91 (m, 3H), 7.94 (d, $J = 1.6$ Hz, 1H). $^{13}\text{C-NMR}$ (125 MHz, CDCl_3): δ (ppm) = 33.1, 34.6, 117.1, 117.2, 117.5, 124.2, 126.5, 126.7, 127.0, 127.6, 128.4, 128.5, 129.8, 131.8, 133.1, 133.7, 137.9, 139.7, 162.0.

(Z)-5-(4-Chlorophenyl)-3-(naphthalen-2-yl)pent-2-enoic acid, (26Z):

Synthesized according to Method D using **26Za** (0.3 g, 0.82 mmol) and NaOH_{aq} (1.40 mL, 4.11 mmol); white solid; yield: 0.22 g (80 %);

$^1\text{H-NMR}$ (500 MHz, CDCl_3): δ (ppm) = 2.65-2.68 (m, 2H), 2.82-2.85 (m, 2H), 5.92 (s, 1H), 7.02 (d, $J = 8.2$ Hz, 2H), 7.22 (d, $J = 8.2$ Hz, 2H), 7.42-7.45 (m, 2H), 7.52 (dd, $J = 1.9, 8.5$ Hz, 1H), 7.62 (s, 1H), 7.76-7.78 (m, 3H). $^{13}\text{C-NMR}$ (125 MHz, CDCl_3): δ (ppm) = 33.1, 34.6, 117.1, 117.2, 124.3, 125.9, 126.1, 126.3, 126.4, 127.7, 128.1, 128.6, 129.6, 129.8, 132.0, 133.0, 136.4, 138.9, 160.5.

5-(4-Chlorophenyl)-3-(naphthalen-1-yl)pent-2-enoic acids, (27E & 27Z):

(E)-3-(4-Chlorophenyl)-1-(naphthalen-1-yl)prop-2-en-1-one, (27c):

Synthesized according to Method A using 4-chlorobenzaldehyde (5.0 g, 35.57 mmol) and 1-acetylnaphthalene (5.40 mL, 35.57 mmol); yellow solid; yield: 7.10 g (68 %);

$^1\text{H-NMR}$ (500 MHz, CDCl_3): δ (ppm) = 7.35 (d, $J = 16.1$ Hz, 1H), 7.44 (d, $J = 7.9$ Hz, 2H), 7.57 (d, $J = 7.9$ Hz, 2H), 7.59-7.67 (m, 4H), 7.85 (d, $J = 7.2$ Hz, 1H), 7.99 (d, $J = 7.9$ Hz, 1H), 8.08 (d, $J = 8.2$ Hz, 1H), 8.41 (d, $J = 8.2$ Hz, 1H). $^{13}\text{C-NMR}$ (125 MHz, CDCl_3): δ (ppm) = 124.4, 125.6, 126.5, 127.2, 127.4, 127.7, 128.4, 129.2, 129.6, 130.4, 131.8, 133.1, 133.8, 136.6, 136.8, 144.2, 195.2.

3-(4-Chlorophenyl)-1-(naphthalen-1-yl)propan-1-one, (27b):

Synthesized according to Method B using **27c** (1.0 g, 3.41 mmol), HEH (1.30 g, 5.12 mmol) and silica gel (6.82 g); colourless oil; yield: 0.57 g (57 %);

¹H-NMR (500 MHz, CDCl₃): δ (ppm) = 3.07 (t, *J* = 7.2 Hz, 2H), 3.32 (t, *J* = 7.2 Hz, 2H), 7.15 (d, *J* = 7.9 Hz, 2H), 7.22 (d, *J* = 8.2 Hz, 2H), 7.34 (d, *J* = 8.5 Hz, 1H), 7.46-7.53 (m, 2H), 7.77 (dd, *J* = 1.3, 7.2 Hz, 1H), 7.84 (d, *J* = 7.9 Hz, 1H), 7.94 (d, *J* = 8.2 Hz, 1H), 8.50 (dd, *J* = 8.8 Hz, 1H).

Ethyl 5-(4-chlorophenyl)-3-(naphthalen-1-yl)pent-2-enoate, (27a):

Synthesized according to Method C using **27b** (0.58 g, 1.97 mmol), NaH (0.29 g, 5.91 mmol) and triethyl phosphonoacetate (1.20 mL, 6.11 mmol);

27Ea: colourless oil; yield: 0.30 g (42 %); ¹H-NMR (500 MHz, CDCl₃): δ (ppm) = 0.78 (t, *J* = 7.2 Hz, 3H), 2.69-2.85 (m, 4H), 3.81 (q, *J* = 7.2 Hz, 2H), 6.21 (s, 1H), 7.05 (d, *J* = 8.5 Hz, 2H), 7.18-7.23 (m, 3H), 7.39-7.49 (m, 3H), 7.72 (d, *J* = 8.2 Hz, 1H), 7.81 (d, *J* = 8.2 Hz, 1H), 7.86 (d, *J* = 8.8 Hz, 1H). ¹³C-NMR (125 MHz, CDCl₃): δ (ppm) = 13.5, 33.1, 42.0, 59.7, 120.3, 123.7, 124.8, 125.0, 125.7, 126.0, 127.6, 128.2, 128.5, 129.6, 130.5, 131.8, 133.4, 138.2, 139.2, 156.8, 165.3.

27Za: colourless oil; yield: 0.32 g (44 %); ¹H-NMR (500 MHz, CDCl₃): δ (ppm) = 1.36 (t, *J* = 7.2 Hz, 3H), 2.68-2.71 (m, 2H), 3.40-3.42 (m, 2H), 4.27 (q, *J* = 7.2 Hz, 2H), 5.97 (s, 1H), 7.07 (d, *J* = 8.5 Hz, 2H), 7.17 (d, *J* = 8.5 Hz, 2H), 7.23-7.49 (m, 1H), 7.37-7.53 (m, 3H), 7.80-7.90 (m, 3H). ¹³C-NMR (125 MHz, CDCl₃): δ (ppm) = 14.3, 33.9, 36.0, 60.1, 121.2, 124.8, 125.2, 125.3, 128.3, 128.4, 128.5, 129.8, 130.6, 131.6, 133.7, 134.5, 140.2, 159.9, 166.3.

(E)-5-(4-Chlorophenyl)-3-(naphthalen-1-yl)pent-2-enoic acid, (27E):

Synthesized according to Method D using (*E*)-ethyl 5-(4-chlorophenyl)-3-(naphthalen-1-yl)pent-2-enoate (0.3 g, 1.09 mmol) and NaOH_{aq} (0.82 mL, 2.47 mmol); white solid; yield: 0.15 g (54 %);

¹H-NMR (500 MHz, CDCl₃): δ (ppm) = 2.81-2.84 (m, 2H), 3.58-3.60 (m, 2H), 6.15 (s, 1H), 7.02 (d, *J* = 8.5 Hz, 2H), 7.20 (d, *J* = 8.5 Hz, 2H), 7.42-7.49 (m, 3H), 7.66 (d, *J* = 8.5 Hz, 1H), 7.80 (d, *J* = 8.2 Hz, 1H), 7.85 (d, *J* = 7.6 Hz, 2H). ¹³C-NMR (125 MHz, CDCl₃): δ (ppm) = 33.1, 42.2, 117.3, 119.2, 123.9, 124.6, 125.0, 125.9, 126.2, 126.3, 127.7, 127.9, 129.6, 131.9, 133.4, 137.4, 138.9, 159.7, 168.4.

(Z)-5-(4-Chlorophenyl)-3-(naphthalen-1-yl)pent-2-enoic acid, (27Z):

Synthesized according to Method D using (Z)-ethyl 5-(4-chlorophenyl)-3-(naphthalen-1-yl)pent-2-enoate (0.32 g, 0.87 mmol) and NaOH_{aq} (0.90 mL, 2.61 mmol); white solid; yield: 0.20 g (68 %);

¹H-NMR (500 MHz, CDCl₃): δ (ppm) = 2.72-2.74 (m, 2H), 3.42-3.45 (m, 2H), 6.05 (s, 1H), 7.06 (d, *J* = 8.5 Hz, 2H), 7.17 (d, *J* = 8.5 Hz, 2H), 7.24-7.31 (m, 2H), 7.51-7.64 (m, 3H), 7.83-7.93 (m, 2H). ¹³C-NMR (125 MHz, CDCl₃): δ (ppm) = 34.0, 36.3, 120.2, 124.7, 125.1, 125.2, 126.1, 126.5, 128.4, 128.5, 128.6, 128.8, 129.8, 133.7, 134.8, 137.0, 139.6, 163.2, 170.2.

5-(4-Chlorophenyl)-3-(4-methoxyphenyl)pent-2-enoic acids, (28Z & 28Z):**(E)-3-(4-Chlorophenyl)-1-(4-methoxyphenyl)prop-2-en-1-one, (28c):**

Synthesized according to Method A using 4-chlorobenzaldehyde (5.0 g, 35.57 mmol) and 4'-methoxyacetophenone (5.34 mL, 35.57 mmol); yellow solid; yield: 8.46 g (87 %);

¹H-NMR (500 MHz, CDCl₃): δ (ppm) = 3.87 (s, 3H), 6.96 (d, *J* = 8.5 Hz, 2H), 7.36 (d, *J* = 8.5 Hz, 2H), 7.50 (d, *J* = 15.4 Hz, 1H), 7.54 (d, *J* = 8.2 Hz, 2H), 7.72 (d, *J* = 15.8 Hz, 1H), 8.01 (d, *J* = 8.8 Hz, 2H). ¹³C-NMR (125 MHz, CDCl₃): δ (ppm) = 55.5, 113.9, 122.3, 129.2, 129.5, 130.8, 130.9, 133.6, 136.2, 142.4, 163.5, 188.4.

3-(4-Chlorophenyl)-1-(4-methoxyphenyl)propan-1-one, (28b):

Synthesized according to Method B using **27c** (1.0 g, 3.67 mmol), HEH (1.39 g, 5.50 mmol) and silica gel (7.34 g); colourless oil; yield: 0.84 g (84 %);

¹H-NMR (500 MHz, CDCl₃): δ (ppm) = 3.04 (t, *J* = 7.2 Hz, 2H), 3.22 (t, *J* = 7.2 Hz, 2H), 3.86 (s, 3H), 6.92 (d, *J* = 8.8 Hz, 2H), 7.17 (d, *J* = 8.8 Hz, 2H), 7.25 (d, *J* = 8.2 Hz, 2H), 7.93 (d, *J* = 8.8 Hz, 2H). ¹³C-NMR (125 MHz, CDCl₃): δ (ppm) = 29.6, 39.8, 55.5, 113.8, 128.6, 129.8, 129.9, 130.3, 131.8, 139.9, 163.5, 197.4.

Ethyl 5-(4-chlorophenyl)-3-(4-methoxyphenyl)pent-2-enoate, (28a):

Synthesized according to Method C using 3-(4-chlorophenyl)-1-(4-methoxyphenyl)propan-1-one (0.80 g, 2.91 mmol), NaH (0.35 g, 8.73 mmol) and triethyl phosphonoacetate (1.80 mL, 9.0 mmol);

27Ea: colourless oil; yield: 0.48 g (48 %); $^1\text{H-NMR}$ (500 MHz, CDCl_3): δ (ppm) = 1.30 (t, J = 7.2 Hz, 3H), 2.69-2.72 (m, 2H), 3.34-3.57 (m, 2H), 3.85 (s, 3H), 4.19 (q, J = 7.2 Hz, 2H), 6.04 (s, 1H), 6.91 (d, J = 9.1 Hz, 2H), 7.15 (d, J = 8.5 Hz, 2H), 7.22 (d, J = 8.5 Hz, 2H), 7.41 (d, J = 9.1 Hz, 2H). $^{13}\text{C-NMR}$ (125 MHz, CDCl_3): δ (ppm) = 14.3, 32.6, 34.6, 55.3, 59.8, 114.0, 116.2, 128.0, 128.3, 129.9, 131.6, 132.9, 140.0, 158.4, 160.5, 166.5.

27Za: colourless oil; yield: 0.49 g (49 %); $^1\text{H-NMR}$ (500 MHz, CDCl_3): δ (ppm) = 1.15 (t, J = 7.2 Hz, 3H), 2.63-2.66 (m, 2H), 2.70-2.74 (m, 2H), 3.83 (s, 3H), 4.02 (q, J = 7.2 Hz, 2H), 5.82 (s, 1H), 6.89 (d, J = 8.8 Hz, 2H), 7.04 (d, J = 8.5 Hz, 2H), 7.14 (d, J = 8.5 Hz, 2H), 7.23 (d, J = 9.1 Hz, 2H). $^{13}\text{C-NMR}$ (125 MHz, CDCl_3): δ (ppm) = 14.0, 33.3, 41.8, 55.2, 59.8, 113.4, 117.4, 128.5, 128.8, 129.6, 131.3, 131.8, 139.3, 157.5, 159.4, 166.0.

(E)-5-(4-Chlorophenyl)-3-(4-methoxyphenyl)pent-2-enoic acid, (28E):

Synthesized according to Method D using **28Ea** (0.35 g, 1.01 mmol) and NaOH_{aq} (1.70 mL, 5.07 mmol); pale beige solid; yield: 0.20 g (62 %);

$^1\text{H-NMR}$ (500 MHz, CDCl_3): δ (ppm) = 2.72-2.75 (m, 2H), 3.36-3.39 (m, 2H), 3.86 (s, 3H), 6.10 (s, 1H), 6.94 (d, J = 8.8 Hz, 2H), 7.14 (d, J = 8.2 Hz, 2H), 7.23 (d, J = 8.5 Hz, 2H), 7.45 (d, J = 9.1 Hz, 2H). $^{13}\text{C-NMR}$ (125 MHz, CDCl_3): δ (ppm) = 32.9, 34.7, 55.4, 114.1, 114.5, 128.2, 128.4, 129.8, 131.7, 139.9, 156.5, 160.9, 161.5, 170.7.

(Z)-5-(4-Chlorophenyl)-3-(4-methoxyphenyl)pent-2-enoic acid, (28Z):

Synthesized according to Method D using **28Za** (0.38 g, 1.10 mmol) and NaOH_{aq} (1.85 mL, 5.51 mmol); pale beige solid; yield: 0.20 g (57 %);

$^1\text{H-NMR}$ (500 MHz, CDCl_3): δ (ppm) = 2.63-2.66 (m, 2H), 3.33-3.36 (m, 2H), 3.85 (s, 3H), 6.10 (s, 1H), 6.91 (d, J = 8.8 Hz, 2H), 7.14 (d, J = 8.5 Hz, 2H), 7.22 (d, J = 8.5 Hz, 2H), 7.44 (d, J = 8.8 Hz, 2H). $^{13}\text{C-NMR}$ (125 MHz, CDCl_3): δ (ppm) = 32.9, 34.7, 55.3, 113.5, 114.8, 128.2, 128.5, 128.9, 129.7, 129.8, 130.9, 139.1, 160.2, 170.6.

3-(biphenyl-4-yl)-5-(4-chlorophenyl)pent-2-enoic acids, (29E & 29Z):

(E)-1-(Biphenyl-4-yl)-3-(4-chlorophenyl)prop-2-en-1-one, (29c):

Synthesized according to Method A using 4-chlorobenzaldehyde (3.58 g, 25.48 mmol) and 1-(biphenyl-4-yl)ethanone (5.00 g, 25.48 mmol); pale yellow solid; yield: 7.74 g (95 %);

$^1\text{H-NMR}$ (500 MHz, CDCl_3): δ (ppm) = 7.41 (t, J = 8.2 Hz, 3H), 7.49 (t, J = 7.9 Hz, 2H), 7.56 (d, J = 15.5 Hz, 1H), 7.60 (d, J = 8.8 Hz, 2H), 7.66 (d, J = 8.2 Hz, 2H), 7.74 (d, J = 8.5

Hz, 2H), 7.80 (d, $J = 15.5$ Hz, 1H), 7.81 (d, $J = 8.5$ Hz, 2H). ^{13}C -NMR (125 MHz, CDCl_3): δ (ppm) = 122.4, 127.3, 127.31, 128.2, 129.0, 129.1, 129.2, 129.6, 133.4, 136.4, 136.7, 139.9, 143.2, 145.7, 189.6.

1-(Biphenyl-4-yl)-3-(4-chlorophenyl)propan-1-one, (29b):

Synthesized according to Method B using **29c** (2.0 g, 6.27 mmol), HEH (2.38 g, 9.41 mmol) and silica gel (12.54 g); colourless oil; yield: 1.80 g (90 %);

^1H -NMR (500 MHz, CDCl_3): δ (ppm) = 3.07 (t, $J = 7.4$ Hz, 2H), 3.31 (t, $J = 7.4$ Hz, 2H), 7.20 (d, $J = 8.5$ Hz, 2H), 7.27 (d, $J = 8.5$ Hz, 2H), 7.40 (t, $J = 7.6$ Hz, 1H), 7.47 (t, $J = 6.9$ Hz, 2H), 7.62 (t, $J = 6.9$ Hz, 2H), 7.68 (d, $J = 8.5$ Hz, 2H), 8.02 (d, $J = 8.5$ Hz, 2H). ^{13}C -NMR (125 MHz, CDCl_3): δ (ppm) = 29.4, 40.2, 127.2, 127.3, 128.2, 128.6, 128.9, 129.8, 131.9, 135.4, 139.7, 139.8, 145.8, 198.4.

Ethyl 3-(biphenyl-4-yl)-5-(4-chlorophenyl)pent-2-enoate, (29a):

Synthesized according to Method C using **29b** (1.5 g, 4.67 mmol), NaH (0.56 g, 14.00 mmol) and triethyl phosphonoacetate (2.89 mL, 14.47 mmol);

29Ea: colourless oil; yield: 0.85 g (47 %); ^1H -NMR (500 MHz, CDCl_3): δ (ppm) = 1.32 (t, $J = 7.3$ Hz, 3H), 2.74-2.77 (m, 2H), 3.41-3.44 (m, 2H), 4.21 (q, $J = 7.0$ Hz, 2H), 6.14 (s, 1H), 7.17 (d, $J = 8.5$ Hz, 2H), 7.24 (d, $J = 8.5$ Hz, 2H), 7.38 (t, $J = 7.3$ Hz, 1H), 7.47 (d, $J = 7.3$ Hz, 2H), 7.53 (d, $J = 8.2$ Hz, 2H), 7.63 (d, $J = 7.9$ Hz, 4H). ^{13}C -NMR (125 MHz, CDCl_3): δ (ppm) = 14.3, 32.7, 34.5, 59.9, 117.8, 127.0, 127.2, 127.3, 127.7, 128.3, 128.9, 129.9, 131.6, 139.6, 139.9, 140.2, 141.9, 146.7, 158.4, 166.3.

29Za: colourless oil; yield: 0.89 g (49 %); ^1H -NMR (500 MHz, CDCl_3): δ (ppm) = 1.09 (t, $J = 7.1$ Hz, 3H), 2.69-2.73 (m, 2H), 2.77-2.86 (m, 2H), 4.02 (q, $J = 7.1$ Hz, 2H), 5.91 (s, 1H), 7.26 (d, $J = 8.2$ Hz, 4H), 7.36 (t, $J = 7.3$ Hz, 2H), 7.46 (t, $J = 1.9, 8.5$ Hz, 1H), 7.61 (d, $J = 8.2$ Hz, 2H), 7.64 (d, $J = 7.3$ Hz, 2H). ^{13}C -NMR (125 MHz, CDCl_3): δ (ppm) = 13.9, 33.2, 41.8, 59.9, 118.0, 126.6, 127.0, 127.3, 127.8, 128.5, 128.7, 129.7, 131.8, 138.4, 139.2, 140.6, 157.5, 165.9.

(E)-3-(Biphenyl-4-yl)-5-(4-chlorophenyl)pent-2-enoic acid, (29E):

Synthesized according to Method D using **29Ea** (0.6 g, 1.53 mmol) and NaOH_{aq} (1.50 mL, 4.60 mmol); white solid; yield: 0.45 g (81 %);

^1H -NMR (500 MHz, CDCl_3): δ (ppm) = 2.77-2.81 (m, 2H), 3.43-3.46 (m, 2H), 6.21 (s, 1H), 7.16 (d, $J = 8.2$ Hz, 2H), 7.25 (d, $J = 8.5$ Hz, 2H), 7.39 (t, $J = 7.2$ Hz, 1H), 7.48 (t, $J = 7.2$ Hz,

1H), 7.56 (d, $J = 8.2$ Hz, 2H), 7.65 (d, $J = 8.2$ Hz, 4H). ^{13}C -NMR (125 MHz, CDCl_3): δ (ppm) = 33.1, 34.6, 116.7, 127.1, 127.2, 127.4, 127.8, 128.5, 128.9, 131.8, 139.4, 139.7, 140.1, 142.4, 161.6, 171.2.

(Z)-3-(biphenyl-4-yl)-5-(4-chlorophenyl)pent-2-enoic acid, (29Z):

Synthesized according to Method D using **29Za** (0.6 g, 1.53 mmol) and NaOH_{aq} (1.50 mL, 4.60 mmol); white solid; yield: 0.40 g (72 %);

^1H -NMR (500 MHz, CDCl_3): δ (ppm) = 2.67-2.70 (m, 2H), 2.77-2.80 (m, 2H), 5.88 (s, 1H), 7.05 (d, $J = 8.8$ Hz, 2H), 7.24 (d, $J = 8.5$ Hz, 2H), 7.25 (d, $J = 8.2$ Hz, 2H), 7.35 (d, $J = 7.9$ Hz, 2H), 7.44 (t, $J = 7.9$ Hz, 2H), 7.58 (d, $J = 7.58$ Hz, 2H), 7.61 (t, $J = 7.9$ Hz, 2H). ^{13}C -NMR (125 MHz, CDCl_3): δ (ppm) = 33.2, 42.1, 126.8, 127.1, 127.5, 127.8, 128.6, 128.7, 129.7, 132.0, 137.7, 138.9, 139.0, 141.4, 161.0, 166.5.

3,5-Di(naphthalen-2-yl)pent-2-enoic acids, (30Z & 30E):

(E)-1,3-Di(naphthalen-2-yl)prop-2-en-1-one, (30c):

Synthesized according to Method A using 2-naphthaldehyde (10.9 g, 64.03 mmol) and 1-(naphthalen-2-yl)ethanone (11.9 g, 64.03 mmol); yellow solid; yield: 18.8 g (95 %);

^1H -NMR (500 MHz, CDCl_3): δ (ppm) = 7.52-7.55 (m, 2H), 7.56-7.65 (m, 2H), 7.82 (d, $J = 15.8$ Hz, 1H), 7.86-7.92 (m, 5H), 7.97 (d, $J = 8.8$ Hz, 1H), 8.02-8.07 (m, 2H), 8.08 (s, 1H), 8.14 (dd, $J = 1.6, 8.5$ Hz, 1H), 8.59 (s, 1H). ^{13}C -NMR (125 MHz, CDCl_3): δ (ppm) = 117.7, 122.2, 123.7, 124.5, 126.8, 127.4, 127.81, 127.84, 128.4, 128.6, 128.7, 128.8, 129.5, 129.9, 130.7, 132.5, 132.6, 133.4, 134.4, 35.5, 135.7, 144.9, 190.2.

1,3-Di(naphthalen-2-yl)propan-1-one, (30b):

Synthesized according to Method B using **30c** (2.0 g, 6.48 mmol), HEH (2.46 g, 9.73 mmol) and silica gel (12.96 g); colourless oil; yield: 1.25 g (62 %);

^1H -NMR (500 MHz, CDCl_3): δ (ppm) = 3.30 (t, $J = 7.6$ Hz, 2H), 3.54 (t, $J = 7.6$ Hz, 2H), 7.41-7.48 (m, 3H), 7.54 (t, $J = 6.9$ Hz, 1H), 7.60 (t, $J = 7.9$ Hz, 1H), 7.74 (s, 1H), 7.79-7.83 (m, 3H), 7.87-7.91 (m, 2H), 7.94 (d, $J = 8.2$ Hz, 1H), 8.06 (dd, $J = 1.9, 8.8$ Hz, 1H), 8.48 (s, 1H), ^{13}C NMR (CDCl_3 , 125 MHz): δ (ppm) = 30.4, 40.5, 123.8, 125.3, 126.0, 126.5, 126.8, 127.2, 127.22, 127.4, 127.8, 128.2, 128.4, 128.5, 129.5, 129.7, 132.1, 132.5, 134.2, 135.6, 138.8, 146.7, 199.1.

Ethyl 3,5-di(naphthalen-2-yl)pent-2-enoate, (30a):

Synthesized according to Method C using **30b** (1.0 g, 3.22 mmol), NaH (0.39 g, 9.66 mmol) and triethyl phosphonoacetate (2.00 mL, 9.98 mmol);

30Ea: colourless oil; yield: 0.56 g (46 %); ¹H-NMR (500 MHz, CDCl₃): δ (ppm) = 1.32 (t, *J* = 7.3 Hz, 3H), 2.98-3.01 (m, 2H), 3.64-3.66 (m, 2H), 4.25 (q, *J* = 6.9 Hz, 2H), 7.59-7.61 (m, 3H), 7.50-7.54 (m, 2H), 7.59 (dd, *J* = 1.9, 8.2 Hz, 1H), 7.65 (s, 1H), 7.75-7.80 (m, 3H), 7.84-7.87 (m, 3H), 7.95 (ds, *J* = 1.9, 1H). ¹³C NMR (CDCl₃, 125 MHz): δ (ppm) = 14.3, 33.0, 35.4, 59.9, 118.6, 124.5, 125.1, 125.8, 126.3, 126.5, 126.6, 126.7, 127.4, 127.5, 127.6, 127.6, 127.9, 128.3, 128.5, 132.3, 133.4, 133.7, 133.8, 138.6, 139.2, 159.0, 166.3.

30Za: colourless oil; yield: 0.61 g (50 %); ¹H-NMR (500 MHz, CDCl₃): δ (ppm) = 0.99 (t, *J* = 7.3 Hz, 3H), 2.91-2.94 (m, 2H), 2.96-2.99 (m, 2H), 3.96 (q, *J* = 7.3 Hz, 2H), 7.27 (dd, *J* = 1.9, 8.2 Hz, 1H), 7.35 (dd, *J* = 1.6, 8.2 Hz, 1H), 7.40-7.46 (m, 2H), 7.46-7.50 (m, 2H), 7.56 (s, 1H), 7.68 (s, 1H), 7.73-7.76 (m, 2H), 7.79 (d, *J* = 9.2 Hz, 1H), 7.81-7.86 (m, 3H). ¹³C NMR (CDCl₃, 125 MHz): δ (ppm) = 13.9, 34.3, 41.9, 59.8, 118.6, 125.3, 126.0, 126.02, 126.1, 126.2, 126.22, 126.6, 127.0, 127.5, 127.5, 127.7, 127.8, 128.1, 128.2, 132.4, 133.1, 133.3, 133.8, 137.6, 138.5, 157.8, 165.9.

(E)- 3,5-Di(naphthalen-2-yl)pent-2-enoic acid, (30E):

Synthesized according to Method D using **30Ea** (0.50 g, 1.31 mmol) and NaOH_{aq} (1.32 mL, 3.94 mmol); white solid; yield: 0.20 g (43 %);

¹H-NMR (500 MHz, CDCl₃): δ (ppm) = 2.98 -3.01 (m, 2H), 3.63-3.67 (m, 2H), 6.30 (s, 1H), 7.40-7.45 (m, 3H), 7.53-7.57 (m, 2H), 7.63 (dd, *J* = 1.9, 8.2 Hz, 2H), 7.75-7.79 (m, 3H), 7.87-7.91 (m, 3H), 7.99 (ds, *J* = 1.3 Hz, 1H). ¹³C NMR (CDCl₃, 125 MHz): δ (ppm) = 33.3, 35.5, 117.3, 124.4, 125.2, 125.9, 126.5, 126.6, 126.6, 126.9, 127.3, 127.5, 127.6, 128.0, 128.5, 128.6, 133.2, 133.6, 138.1, 138.9, 162.4, 171.0, 178.9.

(Z)- 3,5-Di(naphthalen-2-yl)pent-2-enoic acid, (30Z):

Synthesized according to Method D using **30Za** (0.55 g, 1.44 mmol) and NaOH_{aq} (1.44 mL, 4.32 mmol); white solid; yield: 0.22 g (51 %);

¹H-NMR (500 MHz, CDCl₃): δ (ppm) = 2.86-2.89 (m, 2H), 2.95-2.98 (m, 2H), 6.00 (s, 1H), 7.25 (dd, *J* = 1.5, 8.5 Hz, 1H), 7.32 (dd, *J* = 1.6, 8.5 Hz, 1H), 7.41-7.46 (m, 3H), 7.47-7.50 (m, 1H), 7.53 (s, 1H), 7.58 (dd, *J* = 1.3, 8.8 Hz, 1H), 7.70 (s, 1H), 7.76 (d, *J* = 8.8 Hz, 1H), 7.78-7.85 (m, 4H). ¹³C NMR (CDCl₃, 125 MHz): δ (ppm) = 34.0, 35.7, 117.1, 124.4, 124.7, 125.4, 125.8, 126.3, 126.9, 127.2, 127.7, 128.1, 128.2, 131.7, 132.2, 133.4, 133.5, 133.7, 136.7, 137.4, 138.0, 138.8, 161.3, 169.8, 176.5.

5-(4-phenoxyphenyl)-3-phenylpent-2-enoic acids, (31E & 31Z):**(E)-3-(4-Phenoxyphenyl)-1-phenylprop-2-en-1-one, (31c):**

Synthesized according to Method A using 4-phenoxybenzaldehyde (3.0 g, 15.1 mmol) and 1-(naphthalen-2-yl)ethanone (2.58 g, 15.1 mmol); pale yellow solid; yield: 4.70 g (89 %);

¹H-NMR (CDCl₃, 500 MHz): δ (ppm) = 7.05 (d, J = 7.6 Hz, 2H), 7.08 (d, J = 7.6 Hz, 2H), 7.19 (t, J = 7.3 Hz, 1H), 7.40 (t, J = 7.6 Hz, 2H), 7.63-7.55 (m, 3H), 7.67 (d, J = 8.8 Hz, 2H), 7.87 (t, J = 15.5 Hz, 1H), 7.90 (d, J = 8.5 Hz, 1H), 7.94 (d, J = 8.5 Hz, 1H), 8.00 (d, J = 7.9 Hz, 1H), 8.11 (dd, J = 1.5, 8.8 Hz, 1H), 8.54 (s, 1H). ¹³C NMR (CDCl₃, 125 MHz): δ (ppm) = 118.4, 119.7, 120.8, 124.2, 124.5, 126.7, 127.8, 128.3, 128.5, 129.5, 129.7, 129.8, 129.9, 130.2, 132.5, 135.4, 135.6, 144.1, 156.0, 159.8, 190.1.

3-(4-Phenoxyphenyl)-1-phenylpropan-1-one, (31b):

Synthesized according to Method B using **31c** (2.0 g, 5.70 mmol), HEH (2.20 g, 8.56 mmol) and silica gel (11.40 g); colourless oil; yield: 1.54 g (77 %);

¹H-NMR (CDCl₃, 500 MHz): δ (ppm) = 3.13 (t, J = 7.4 Hz, 2H), 3.44 (t, J = 7.4 Hz, 2H), 6.86 (d, J = 8.5 Hz, 2H), 6.99 (d, J = 8.8 Hz, 2H), 7.08 (t, J = 7.3 Hz, 1H), 7.25 (d, J = 8.5 Hz, 2H), 7.32 (t, J = 8.5 Hz, 2H), 7.56 (dt, J = 1.3, 8.2 Hz, 1H), 7.61 (dt, J = 6.9, 8.1 Hz, 1H), 7.89 (t, J = 8.5 Hz, 2H), 7.95 (d, J = 7.9 Hz, 1H), 8.05 (dd, J = 1.6, 8.8 Hz, 1H), 8.47 (s, 1H). ¹³C NMR (CDCl₃, 125 MHz): δ (ppm) = 29.6, 40.6, 118.6, 119.2, 123.0, 123.8, 126.8, 127.8, 128.4, 128.5, 129.5, 129.6, 129.71, 129.77, 132.5, 134.2, 135.6, 136.3, 155.5, 157.5, 199.2.

Ethyl 5-(4-phenoxyphenyl)-3-phenylpent-2-enoate, (31a):

Synthesized according to Method C using 3-(4-phenoxyphenyl)-1-phenylpropan-1-one (1.40 g, 3.97 mmol), NaH (0.48 g, 12.31 mmol) and triethyl phosphonoacetate (2.46 mL, 12.31 mmol);

31Ea: colourless oil; yield: 0.78 g (52 %); ¹H NMR (CDCl₃, 500 MHz): δ (ppm) = 1.34 (t, J = 6.7 Hz, 3H), 2.78-2.81 (m, 2H), 3.52-3.55 (m, 2H), 4.25 (q, J = 6.7 Hz, 2H), 6.23 (s, 1H), 6.93 (d, J = 7.9 Hz, 2H), 6.96 (d, J = 8.2 Hz, 2H), 7.08 (t, J = 7.3 Hz, 1H), 7.21 (d, J = 7.9 Hz, 2H), 7.31 (t, J = 7.6, 2H), 7.55-7.51 (m, 2H), 7.58 (d, J = 8.5 Hz, 1H), 7.89-7.86 (m, 3H), 7.93 (s, 1H). ¹³C NMR (CDCl₃, 125 MHz): δ (ppm) = 14.4, 33.1, 34.6, 59.9, 118.3, 118.4, 119.0, 122.8, 124.4, 126.3, 126.5, 126.7, 127.6, 128.3, 128.4, 129.6, 129.7, 133.2, 133.5, 136.6, 138.3, 155.2, 157.7, 159.2, 166.3.

31Za: colourless oil; yield: 0.69 g (47 %); ^1H NMR (CDCl_3 , 500 MHz): δ (ppm) = 1.02 (t, J = 7.3 Hz, 3H), 2.72-2.75 (m, 2H), 2.86-2.89 (m, 2H), 4.03 (q, J = 7.3 Hz, 2H), 6.00 (s, 1H), 6.94 (d, J = 8.5 Hz, 2H), 6.99 (d, J = 8.8 Hz, 2H), 7.07-11 (m, 3H), 7.30-7.35 (m, 3H), 7.47-7.51 (m, 2H), 7.67 (ds, J = 1.5 Hz, 1H), 7.87-7.83 (m, 3H). ^{13}C NMR (CDCl_3 , 125 MHz): δ (ppm) = 13.9, 33.2, 42.2, 59.8, 118.2, 118.6, 119.0, 119.2, 123.0, 126.0, 126.1, 126.1, 127.4, 127.4, 127.7, 128.1, 129.5, 129.7, 133.0, 135.7, 137.3, 139.2, 155.4, 157.5, 158.1, 166.9.

(E)-5-(4-phenoxyphenyl)-3-phenylpent-2-enoic acid, (31E):

Synthesized according to Method D using **31Ea** (0.60 g, 1.42 mmol) and NaOH_{aq} (1.6 mL, 4.83 mmol); white solid; yield: 0.40 g (71 %);

^1H -NMR (CDCl_3 , 500 MHz): δ (ppm) = 2.79-2.83 (m, 2H), 3.53-3.56 (m, 2H), 6.27 (s, 1H), 6.91 (d, J = 8.5 Hz, 2H), 6.94 (d, J = 8.5 Hz, 2H), 7.06 (tt, J = 1.3, 7.3 Hz, 1H), 7.18 (d, J = 8.8 Hz, 2H), 7.27-7.32 (m, 2H), 7.52-7.56 (m, 2H), 7.59 (dd, J = 1.2, 8.5 Hz, 1H), 7.86-7.90 (m, 3H), 7.95 (ds, J = 1.6 Hz, 1H). ^{13}C NMR (CDCl_3 , 500 MHz): δ (ppm) = 33.4, 34.6, 117.1, 118.5, 119.0, 122.9, 124.3, 126.5, 126.7, 127.2, 126.9, 127.6, 128.4, 128.6, 129.6, 129.7, 133.2, 133.7, 136.3, 138.1, 155.3, 157.6, 162.4.

(Z)-5-(4-phenoxyphenyl)-3-phenylpent-2-enoic acid, (31Z):

Synthesized according to Method D using (*Z*)-ethyl 5-(4-phenoxyphenyl)-3-phenylpent-2-enoate (0.50 g, 1.18 mmol) and NaOH_{aq} (1.8 mL, 5.37 mmol); white solid; yield: 0.41 g (88 %);

^1H -NMR (CDCl_3 , 500 MHz): δ (ppm) = 2.67-2.70 (m, 2H), 2.84-2.87 (m, 2H), 5.92 (s, 1H), 6.90 (d, J = 8.5 Hz, 2H), 6.98-6.95 (m, 2H), 7.05-7.09 (m, 3H), 7.27-7.33 (m, 3H), 7.46-7.51 (m, 2H), 7.64 (ds, J = 1.6 Hz, 1H), 7.78-7.85 (m, 3H). ^{13}C NMR (CDCl_3 , 500 MHz): δ (ppm) = 33.1, 42.6, 117.1, 118.6, 119.0, 123.0, 125.7, 126.1, 126.2, 126.3, 127.6, 127.7, 128.2, 129.5, 129.7, 132.9, 133.0, 135.5, 136.6, 155.4, 157.5, 160.8, 169.8.

3-(Naphthalen-2-yl)-5-(quinolin-2-yl)pent-2-enoic acids, (32E & 32Z):

(E)-1-(Naphthalen-2-yl)-3-(quinolin-2-yl)prop-2-en-1-one, (32c):

Synthesized according to Method A using quinoline-2-carbaldehyde (3.0 g, 19.09 mmol) and 1-(naphthalen-2-yl)ethanone (3.25 g, 19.09 mmol); yellow solid; yield: 4.95 g (84 %);

1-(Naphthalen-2-yl)-3-(quinolin-2-yl)propan-1-one, (32b):

Synthesized according to Method B using **32c** (1.50 g, 4.85 mmol), HEH (1.71 g, 7.27 mmol) and silica gel (9.70 g); colourless oil; yield: 0.95 g (63 %);

¹H-NMR (500 MHz, CDCl₃): δ (ppm) = 3.51 (t, *J* = 7.3 Hz, 2H), 3.77 (t, *J* = 7.3 Hz, 2H), 7.43 (d, *J* = 8.5 Hz, 1H), 7.48 (t, *J* = 7.9 Hz, 1H), 7.54 (t, *J* = 7.9 Hz, 1H), 7.58 (t, *J* = 8.2 Hz, 1H), 7.66 (t, *J* = 8.5 Hz, 1H), 7.78 (d, *J* = 9.1 Hz, 1H), 7.87-7.91 (m, 2H), 7.97 (t, *J* = 9.1 Hz, 2H), 8.07-8.10 (m, 2H), 8.57 (s, 1H). ¹³C NMR (CDCl₃, 125 MHz): δ (ppm) = 32.9, 37.5, 121.9, 124.0, 125.8, 126.7, 126.9, 127.5, 127.7, 128.3, 128.4, 128.8, 129.3, 129.6, 129.7, 132.6, 134.4, 135.6, 136.2, 147.9, 161.2, 199.3.

Ethyl 3-(naphthalen-2-yl)-5-(quinolin-2-yl)pent-2-enoate, (32a):

Synthesized according to Method C using **32b** (0.90 g, 2.89 mmol), NaH (0.35 g, 8.67 mmol) and triethyl phosphonoacetate (1.79 mL, 8.96 mmol);

32Ea: yellow oil; yield: 0.53 g (48 %); ¹H-NMR (500 MHz, CDCl₃): δ (ppm) = 1.32 (t, *J* = 6.9 Hz, 3H), 3.18-3.21 (m, 2H), 3.72-3.75 (m, 2H), 4.23 (t, *J* = 6.9 Hz, 2H), 6.25 (s, 1H), 7.42 (d, *J* = 8.5 Hz, 1H), 7.45-7.51 (m, 3H), 7.62 (dd, *J* = 1.9, 8.5 Hz, 1H), 7.66 (dt, *J* = 1.6, 8.5 Hz, 1H), 7.74 (dd, *J* = 1.3, 8.2 Hz, 1H), 7.81-7.83 (m, 3H), 7.97 (ds, *J* = 1.9 Hz, 1H), 8.01-8.04 (m, 2H). ¹³C NMR (CDCl₃, 125 MHz): δ (ppm) = 14.3, 31.2, 38.5, 60.0, 118.3, 121.6, 124.4, 125.7, 126.4, 126.5, 126.6, 126.8, 127.4, 127.5, 128.3, 128.4, 128.9, 129.2, 133.2, 133.5, 136.1, 138.2, 147.9, 159.4, 161, 7, 166.4.

32Za: yellow oil; yield: 0.49 g (44 %); ¹H-NMR (500 MHz, CDCl₃): δ (ppm) = 0.99 (t, *J* = 7.0 Hz, 3H), 3.10-3.17 (m, 4H), 3.95 (t, *J* = 7.0 Hz, 2H), 6.06 (s, 1H), 7.19 (d, *J* = 8.5 Hz, 1H), 7.35 (d, *J* = 8.5 Hz, 1H), 7.36-7.50 (m, 3H), 7.67-7.70 (m, 2H), 7.75 (d, *J* = 8.5 Hz, 1H), 7.79-7.85 (m, 3H), 8.01-8.04 (m, 2H). ¹³C NMR (CDCl₃, 125 MHz): δ (ppm) = 13.9, 36.9, 39.8, 59.8, 118.2, 121.3, 124.5, 125.9, 126.0, 126.1, 126.11, 126.9, 127.0, 127.4, 127.5, 127.7, 128.1, 128.9, 129.4, 133.0, 136.3, 137.4, 148.0, 158.2, 160.8, 165.9.

(E)-3-(Naphthalen-2-yl)-5-(quinolin-2-yl)pent-2-enoic acid, (32E):

Synthesized according to Method D using **32Ea** (0.45 g, 1.18 mmol) and NaOH_{aq} (1.20 mL, 3.53 mmol); white solid; yield: 0.20 g (48 %);

¹H-NMR (500 MHz, (CD₃)₂SO): δ (ppm) = 3.03-3.06 (m, 2H), 3.67-3.71 (m, 2H), 6.22 (s, 1H), 7.42 (d, *J* = 8.5 Hz, 1H), 7.51-7.56 (m, 3H), 7.69-7.23 (m, 2H), 7.89 (dd, *J* = 1.3, 8.2 Hz, 1H), 7.91-7.98 (m, 4H), 8.14 (ds, *J* = 1.6 Hz, 1H), 8.23 (d, *J* = 8.2 Hz, 1H).

^{13}C NMR (125 MHz, $(\text{CD}_3)_2\text{SO}$): δ (ppm) = 29.4, 37.4, 121.3, 124.3, 125.6, 126.0, 126.3, 126.6, 127.3, 127.6, 128.1, 128.2, 128.3, 129.2, 132.7, 132.9, 136.0, 137.6, 141.2, 147.1, 161.1, 167.1, 170.1.

(Z)-3-(Naphthalen-2-yl)-5-(quinolin-2-yl)pent-2-enoic acid, (32Z):

Synthesized according to Method D using **32Za** (0.40 g, 1.05 mmol) and NaOH_{aq} (1.00 mL, 3.16 mmol); white solid; yield: 0.15 g (36 %);

^1H -NMR (500 MHz, $(\text{CD}_3)_2\text{SO}$): δ (ppm) = 2.99-3.03 (m, 2H), 3.03-3.08 (m, 2H), 6.00 (s, 1H), 7.38 (dd, $J = 1.6, 8.5$ Hz, 1H), 7.41 (d, $J = 8.5$ Hz, 1H), 7.50-7.55 (m, 3H), 7.71 (dt, $J = 1.6, 8.2$ Hz, 1H), 7.78 (s, 1H), 7.88 (d, $J = 8.2$ Hz, 1H), 7.89-7.94 (m, 4H), 8.24 (d, $J = 8.2$ Hz, 1H).

5-(Biphenyl-4-yl)-3-(naphthalen-2-yl)pent-2-enoic acids, (33Z & 33Z):

(E)- 3-(Biphenyl-4-yl)-1-(naphthalen-2-yl)prop-2-en-1-one, (33c):

Synthesized according to Method A using biphenyl-4-carbaldehyde (5.0 g, 29.3 mmol) and 1-(naphthalen-2-yl)ethanone (5.35 g, 29.3 mmol); yellow solid; yield: 7.80 g (79 %);

^1H -NMR (500 MHz, CDCl_3): δ (ppm) = 7.40 (t, $J = 7.6$ Hz, 1H), 7.48 (t, $J = 7.9$ Hz, 2H), 7.52-7.55 (m, 2H), 7.57-7.66 (m, 3H), 7.68 (d, $J = 8.2$ Hz, 2H), 7.73 (d, $J = 15.7$ Hz, 1H), 7.76 (t, $J = 8.2$ Hz, 2H), 7.93 (q, $J = 9.1$ Hz, 2H), 8.02 (d, $J = 7.9$ Hz, 1H), 8.13 (d, $J = 8.5$ Hz, 1H), 8.57 (s, 1H).

3-(Biphenyl-4-yl)-1-(naphthalen-2-yl)propan-1-one, (33b):

Synthesized according to Method B using **33c** (2.0 g, 5.98 mmol), HEH (2.27 g, 8.97 mmol) and silica gel (11.96 g); colourless oil; yield: 1.74 g (86 %);

^1H NMR (CDCl_3 , 500 MHz): δ (ppm) = 8.49 (s, 1H), 8.07 (dd, 1H), 7.95 (d, $J = 8.2$ Hz, 1H), 7.90 (t, 2H), 7.62-7.54 (m, 6H), 7.44 (t, $J = 7.3$ Hz, 2H), 7.38 (d, $J = 8.5$ Hz, 2H), 7.34 (tt, $J = 7.3$ Hz, 1H), 3.49 (t, $J = 7.3$ Hz, 2H), 3.19 (t, $J = 7.9$ Hz, 2H). ^{13}C NMR (CDCl_3 , 125 MHz): δ (ppm) = 199.1, 180.0, 141.0, 140.4, 139.2, 135.6, 134.2, 132.5, 129.7, 129.5, 128.9, 128.7, 128.5, 128.4, 127.8, 127.3, 127.1, 127.0, 126.8, 126.8, 40.5, 29.9.

Ethyl 5-(biphenyl-4-yl)-3-(naphthalen-2-yl)pent-2-enoate, (33a):

Synthesized according to Method C using **33b** (1.5 g, 4.46 mmol), NaH (0.54 g, 12.93 mmol) and triethyl phosphonoacetate (2.68 mL, 13.4 mmol);

33Ea: colourless oil; yield: 0.85 g (47 %); $^1\text{H NMR}$ (CDCl_3 , 500 MHz): δ (ppm) = 1.35 (t, J = 7.3 Hz, 5H), 2.82-2.86 (m, 2H), 3.54-3.58 (m, 2H), 4.24 (q, J = 7.3 Hz, 2H), 7.31-7.34 (m, 3H), 7.42 (t, J = 7.9 Hz, 2H), 7.49-7.53 (m, 4H), 7.56 (dd, J = 1.9, 8.8 Hz, 2H), 7.60 (dd, J = 1.9, 8.8 Hz, 2H), 7.83-7.89 (m, 3H), 7.94 (ds, J = 1.6 Hz, 1H). $^{13}\text{C NMR}$ (CDCl_3 , 125 MHz): δ (ppm) = 14.4, 33.1, 35.0, 60.0, 118.3, 122.9, 123.4, 124.0, 124.4, 126.3, 126.5, 126.7, 127.0, 127.02, 127.6, 128.3, 128.5, 128.7, 128.9, 133.1, 133.2, 133.5, 139.0, 140.7, 141.2, 149.6, 153.5.

33Za: colourless oil; yield: 0.83 g (46 %); $^1\text{H NMR}$ (CDCl_3 , 500 MHz): δ (ppm) = 1.01 (t, J = 7.3 Hz, 3H), 2.77-2.80 (m, 2H), 2.89-2.93 (m, 2H), 3.97 (q, J = 7.3 Hz, 2H), 6.03 (s, 1H), 7.21 (d, J = 8.2 Hz, 2H), 7.32-7.36 (m, 2H), 7.41 (t, J = 7.9 Hz, 2H), 7.48-7.52 (m, 4H), 7.57 (t, J = 7.9 Hz, 2H), 7.68 (s, 1H), 7.87-7.83 (m, 3H). $^{13}\text{C NMR}$ (CDCl_3 , 125 MHz): δ (ppm) = 13.9, 33.6, 42.1, 59.9, 126.0, 126.1, 126.12, 127.0, 127.1, 127.2, 127.4, 127.7, 128.1, 128.7, 128.7, 132.9, 133.0, 137.3, 139.0, 139.9, 140.9, 158.2, 166.0.

(E)-5-(Biphenyl-4-yl)-3-(naphthalen-2-yl)pent-2-enoic acid, (33E):

Synthesized according to Method D using **33Ea** (0.60 g, 1.47 mmol) and NaOH_{aq} (1.5 mL, 4.41 mmol); white solid; yield: 0.37 g (63 %);

$^1\text{H NMR}$ (CDCl_3 , 500 MHz): δ (ppm) = 2.87-2.90 (m, 2H), 3.57-3.61 (m, 2H), 6.30 (s, 1H), 7.32 (t, J = 8.2 Hz, 3H), 7.40 (t, J = 7.9 Hz, 2H), 7.52 (t, J = 8.2 Hz, 2H), 7.53-7.57 (m, 4H), 7.63 (dd, J = 1.6, 8.5 Hz, 1H), 7.88-7.91 (m, 3H), 7.99 (s, 1H).

(Z)-5-(Biphenyl-4-yl)-3-(naphthalen-2-yl)pent-2-enoic acid, (33Z):

Synthesized according to Method D using **33Za** (0.60 g, 1.47 mmol) and NaOH_{aq} (1.5 mL, 4.41 mmol); white solid; yield: 0.42 g (72 %);

$^1\text{H NMR}$ (CDCl_3 , 500 MHz): δ (ppm) = 2.73-2.76 (m, 2H), 2.89-2.91 (m, 2H), 5.98 (s, 1H), 7.18 (d, J = 8.2 Hz, 2H), 7.30-7.34 (m, 2H), 7.42 (t, J = 7.3 Hz, 2H), 7.47-7.51 (m, 4H), 7.55 (dd, J = 0.9, 8.23 Hz, 2H), 7.66 (s, 1H), 7.80-7.85 (m, 3H).

5-(6-Hydroxynaphthalen-2-yl)-3-(naphthalen-2-yl)pent-2-enoic acid, (34Z & 34E):**6-(Methoxymethoxy)-2-naphthaldehyde, (34e):**

Synthesized according to Method G using bromomethyl-methylether (1.50mL, 18.3 mmol), 6-hydroxy-2-naphthaldehyde (2.1 g, 12.2 mmol) and sodium hydride (0.73 g, 18.3 mmol); yellow solid; yield: 2.64 g (91%);

¹H-NMR (500 MHz, CDCl₃): δ (ppm) = 3.53 (s, 3H), 5.33 (s, 2H), 7.31 (d, *J* = 8.8 Hz, 1H), 7.44 (s, 1H), 7.73-7.82 (m, 1H), 7.91 (ds., *J* = 1.9 Hz, 2H), 8.26 (s, 1H), 10.10 (s, 1H). ¹³C-NMR (125 MHz, CDCl₃): δ (ppm) = 56.3, 94.4, 110.0, 120.1, 123.5, 128.1, 128.4, 131.2, 132.7, 134.2, 138.0, 157.6, 192.0.

(E)- 3-(6-(Methoxymethoxy)naphthalen-2-yl)-1-(naphthalen-2-yl)prop-2-en-1-one, (34c):

Synthesized according to Method A using **34e** (2.0 g, 9.25 mmol) and 1-(naphthalen-2-yl)ethanone (1.57 g, 9.25 mmol); yellow solid; yield: 1.90 g (56 %);

¹H-NMR (500 MHz, CD₃Cl): δ (ppm) = 3.54 (s, 3H), 5.32 (s, 2H), 7.27 (dd, *J* = 1.9, 8.8 Hz, 1H), 7.42 (ds, *J* = 2.2 Hz, 1H), 7.56-7.63 (m, 2H), 7.76-7.84 (m, 4H), 7.91 (d, *J* = 7.9 Hz, 1H), 7.95 (d, *J* = 8.8 Hz, 1H), 8.04-8.01 (m, 3H), 8.14 (dd, *J* = 1.6, 8.2 Hz, 1H), 8.58 (s, 1H). ¹³C NMR (125 MHz, CDCl₃): δ (ppm) = 56.2, 94.5, 110.0, 119.7, 121.4, 124.4, 124.6, 126.7, 127.8, 127.8, 128.3, 128.5, 129.3, 129.5, 129.8, 130.3, 130.5, 130.8, 132.6, 135.7, 135.7, 135.8, 145.0, 156.4, 190.2.

3-(6-(Methoxymethoxy)naphthalen-2-yl)-1-(naphthalen-2-yl)propan-1-one, (34b):

Synthesized according to Method B using **34c** (1.5 g, 4.07 mmol), HEH (1.44 g, 6.11 mmol) and silica gel (8.14 g); colourless oil; yield: 1.10 g (73 %);

¹H-NMR (500 MHz, CD₃Cl): δ (ppm) = 3.26 (t, *J* = 7.9 Hz, 2H), 3.51 (t, *J* = 7.9 Hz, 2H) 3.53 (s, 3H), 5.29 (s, 2H), 7.21 (dd, *J* = 2.4, 8.8 Hz, 1H), 7.38-7.41 (m, 2H), 7.54 (t, *J* = 7.9 Hz, 1H), 7.59 (d, *J* = 8.2 Hz, 1H), 7.67 (s, 1H), 7.70-7.73 (m, 2H), 7.89 (t, *J* = 7.9 Hz, 2H), 7.94 (d, *J* = 8.8 Hz, 1H), 8.06 (dd, *J* = 1.5, 8.2 Hz, 1H), 8.48 (s, 1H). ¹³C NMR (125 MHz, CDCl₃): δ (ppm) = 30.3, 40.5, 56.0, 94.6, 109.9, 123.8, 126.3, 126.7, 127.3, 127.7, 127.8, 128.4, 128.5, 129.0, 129.5, 129.7, 132.5, 133.0, 134.2, 135.6, 136.9, 154.7, 199.1.

Ethyl 5-(6-(methoxymethoxy)naphthalen-2-yl)-3-(naphthalen-2-yl)pent-2-enoate, (34a₁):

Synthesized according to Method C using **34b** (0.8 g, 2.16 mmol), NaH (0.25 g, 6.26 mmol) and triethyl phosphonoacetate (1.30 mL, 6.26 mmol);

34Ea₁: colourless oil; yield: 0.45 g (47 %); ¹H-NMR (500 MHz, CD₃Cl): δ (ppm) = 1.30 (t, *J* = 7.0 Hz, 3H), 2.90-2.93 (m, 2H), 3.53 (s, 3H), 3.58-3.61 (m, 2H), 4.22 (q, *J* = 7.0 Hz, 2H), 5.29 (s, 2H), 6.21 (s, 1H), 7.18 (dd, *J* = 2.5, 8.8 Hz, 1H), 7.35-7.38 (m, 2H), 7.51-7.54 (m, 2H), 7.56 (s, 1H), 7.60 (dd, *J* = 2.5, 8.5 Hz, 1H), 7.65- 7.69 (m, 2H), 7.84-7.88 (m, 3H), 7.93 (ds, *J* = 1.6 Hz, 1H). ¹³C NMR (CDCl₃, 125 MHz): δ (ppm) = 14.3, 33.0, 35.2, 56.0, 59.9, 94.6, 109.9, 116.8, 188.3, 118.8, 124.4, 126.3, 126.5, 126.7, 127.0, 127.6, 127.9, 128.3, 128.5, 129.0, 129.6, 133.2, 137.2, 138.4, 154.6, 159.2, 166.4.

34Za₁: colourless oil; yield: 0.46 g (48 %); ¹H-NMR (500 MHz, CD₃Cl): δ (ppm) = 1.01 (t, *J* = 7.2 Hz, 3H), 2.85-2.89 (m, 2H), 2.92-2.96 (m, 2H), 3.52 (s, 3H), 3.96 (q, *J* = 7.2 Hz, 2H), 5.29 (s, 2H), 6.01 (s, 1H), 7.19 (dd, *J* = 2.5, 8.8 Hz, 1H), 7.20 (dd, *J* = 2.5, 8.5 Hz, 1H), 7.33-7.36 (m, 2H), 7.47-7.50 (m, 3H), 7.65-7.68 (m, 3H), 7.82- 7.86 (m, 3H). ¹³C NMR (CDCl₃, 125 MHz): δ (ppm) = 13.9, 33.9, 42.1, 56.0, 59.8, 94.6, 109.9, 118.2, 119.0, 125.9, 126.0, 126.1, 126.3, 127.2, 127.4, 127.5, 127.7, 128.1, 129.6, 132.9, 133.0, 133.02, 136.4, 137.3, 154.7, 158.3, 165.9.

(E)-Ethyl 5-(6-hydroxynaphthalen-2-yl)-3-(naphthalen-2-yl)pent-2-enoate, (34Ea₂):

Synthesized according to Method K using **34Ea₁** (0.25 g, 0.57 mmol) and 2 mL 10 % HCl; yellow oil; yield: 0.095 g (quant, without further purification);

¹H-NMR (500 MHz, CD₃Cl): δ (ppm) = 1.31 (t, *J* = 7.0 Hz, 3H), 2.89-2.93 (m, 2H), 3.58-3.621 (m, 2H), 4.23 (q, *J* = 7.0 Hz, 2H), 5.15 (s, OH), 6.21 (s, 1H), 7.06 (dd, *J* = 2.5, 8.5 Hz, 1H), 7.10 (ds, *J* = 1.6 Hz, 1H), 7.35 (dd, *J* = 1.6, 8.2 Hz, 1H), 7.52- 7.61 (m, 5H), 7.63 (d, *J* = 8.8 Hz, 1H), 7.85-7.88 (m, 3H), 7.94 (ds, *J* = 1.6 Hz, 1H).

(Z)-Ethyl 5-(6-hydroxynaphthalen-2-yl)-3-(naphthalen-2-yl)pent-2-enoate, (34Za₂):

Synthesized according to Method K using **34Ea₂** (0.35 g, 0.80 mmol) and 2 mL 10 % HCl; yellow oil; yield: 0.32 g (quant, without further purification);

¹H-NMR (500 MHz, CD₃Cl): δ (ppm) = 1.01 (t, *J* = 7.0 Hz, 3H), 2.83-2.86 (m, 2H), 2.92-2.96 (m, 2H), 4.11 (q, *J* = 7.0 Hz, 2H), 6.02 (s, 1H), 7.04 (dd, *J* = 2.4, 8.8 Hz, 1H), 7.08 (ds, *J* = 2.4 Hz, 1H), 7.21 (dd, *J* = 1.9, 8.2 Hz, 1H), 7.32- 7.35 (m, 1H), 7.47-7.50 (m, 3H), 7.58 (d, *J* = 8.5 Hz, 1H), 7.63 (d, *J* = 8.8 Hz, 1H), 7.68 (s, 1H), 7.82-7.86 (m, 3H).

(E)- 5-(6-Hydroxynaphthalen-2-yl)-3-(naphthalen-2-yl)pent-2-enoic acid, (34E):

Synthesized according to Method D using **34Ea₂** (0.07 g, 0.18 mmol) and NaOH_{aq} (0.2 mL, 0.53 mmol); white solid; yield: 0.55 g (83 %);

¹H-NMR (500 MHz, (CD₃)₂SO): δ (ppm) = 2.75-2.77 (m, 2H), 3.48-3.52 (m, 2H), 6.17 (s, 1H), 6.21 (s, 1H), 6.99 (dd, *J* = 2.4, 8.5 Hz, 1H), 7.02 (ds, *J* = 2.1 Hz, 1H), 7.28 (dd, *J* = 1.5, 8.5 Hz, 1H), 7.52- 7.57 (m, 4H), 7.62 (d, *J* = 8.8 Hz, 1H), 7.69 (dd, *J* = 1.5, 8.2 Hz, 1H), 7.91-7.95 (m, 2H), 7.98-8.00 (m, 1H), 8.13 (s, 1H), 9.57 (s, OH).

(Z)- 5-(6-Hydroxynaphthalen-2-yl)-3-(naphthalen-2-yl)pent-2-enoic acid, (34Z):

Synthesized according to Method D using **34Za₂** (0.30 g, 0.76 mmol) and NaOH_{aq} (1.30 mL, 3.78 mmol); white solid; yield: 0.16 g (57 %);

¹H-NMR (500 MHz, (CD₃)₂SO): δ (ppm) = 2.72-2.75 (m, 2H), 2.90-2.93 (m, 2H), 5.97 (s, 1H), 7.02-7.09 (m, 2H), 7.24 (dd, *J* = 1.5, 8.2 Hz, 1H), 7.37 (dd, *J* = 1.9, 8.5 Hz, 1H), 7.51-7.53 (m, 3H), 7.58 (d, *J* = 8.5 Hz, 1H), 7.65 (d, *J* = 8.8 Hz, 1H), 7.78 (s, 1H), 7.88-7.93 (m, 3H), 9.59 (s, OH), 11.94 (s, OH).

6.2. Biological Section

6.2.1. Material and reagents

6.2.1.1. Apparatus

EP-Motion 5070 Pipetting workstation (Eppendorf)

Typhoon Phosphoimager (GE Healthcare); Fla9000 Starion (Fujifilm)

VP-ITC titration calorimetric system (MicroCal Inc, MA)

Origin7 Software

Cell culture incubator Biosafe (Revco)

Cell counter (Casy)

Centrifuge universal 30 RF (Hettich GmbH)

Table centrifuge Micro (Hettich GmbH)

Ultracentrifuge 2330 Ultraspinn 55 Hitachi (Pharmacia)

Sonicator Sonopuls HD60 (Bandelin)

HPLC system Agilent

LC-MS/MS: TSQ quantum (Thermo Electron Corporation) instrument equipped with an ESI source and a triple quadrupole mass detector (Thermo Finnigan)

PolarStar plate reader (BMG Labtech)

6.2.1.2. Materials for kinase activity assays

96 well plate (V-bottom; Greiner)

DMSO > 99,8 % (Roth)

MgCl₂ (Sigma)

ATP (Sigma)

Tris-HCl (Sigma)

β-mercaptoethanol (Sigma)

Albumin from bovine serum (Sigma)

Brij (Sigma)

Phosphoric acid (Sigma)

[γ-³²P]ATP (GE Amersham Pharmacia)

T308tide (KTFCGTPEZLAPEVRR)
PIFtide (REPRILSEEEQEMFRDFDYIADWC)
Crosstide (GRPRTSSFAEG)
P81 3MM paper (Whatman)

6.2.1.3. Materials for ITC

PDK1₅₀₋₃₅₉[Tyr228Gly-Gln2922Ala]
TrisHCl (Sigma)
NaCl (Sigma)
DTT (Sigma)

6.2.1.4. Materials for Cell assays

Petri dishes (Greiner)
Falcon tubes (Greiner)
Cell culture flasks (Greiner)
DMEM (Gibco)
RPMI-1640
FBS (Sigma)
Trypsin (Sigma)
PenStrep (Invitrogen)
PBS (Sigma)
HCl (Sigma)
Ethyl acetate (Sigma)
Methanol (Sigma)
Trifluoroacetic acid (Sigma)
Reporter gene plasmid (pGL4.32[luc2P/NF- κ B-RE/Hygro] (Promega)
Fu Gene HD (Roche Diagnostics)
TNF α (Sigma)
Luciferase detection reagent (Bright-Glo, Promega)

6.2.2. Protein kinases assays

To test the effect of the compounds on the activity of the AGC protein kinases, radioactivity kinase assays were performed.^{11, 26, 30, 74, 167} The corresponding kinase were incubated with the radiolabeled phosphate from [γ 32 P]ATP in the presence of the appropriate substrate and the compounds. The amount of the radioactivity incorporated into the substrate was measured. The assays were performed in a 96-well formate, at least in duplicates and with less than 10 % difference between the duplicates. The total volume of each reaction was 20 μ L.

- 1) A reaction mixture I was prepared on ice using the enzyme, the corresponding substrate, 50 mM Tris-HCl (pH 7.5), dilution buffer containing 0.05 mg/ml of BSA, 0.1 % β -mercaptoethanol and 0.003% of Brij.
- 2) For each test-compound, appropriate dilution of the stock solution was prepared with DMSO.
- 3) The enzyme mixture was preincubated with the compound for 20 min at room temperature.
- 4) The reaction was started by addition of mixture II containing the [γ 32 P]ATP (5–50 c.p.m./pmol), 10 mM MgCl₂ and ATP. The reaction time was 30 min.
- 5) The enzymatic reaction was quenched by the addition of 0.01 % phosphoric acid.
- 6) 4 μ L aliquots were spotted on P81 phosphocellulose paper using the pipetting workstation ep motion 5070 (Eppendorf).
- 7) The P81 paper was washed 4 x 15 min in 0.01 % phosphoric acid in order to remove the [γ 32 P]ATP not bound to the peptide substrate and dried.
- 8) The incorporated radioactivity into the appropriate substrate was quantified in a PhosphoImager.

Wild type and mutant protein kinases were expressed in HEK293 cells after transient transfection as GST fusion proteins and purified using glutathione sepharose. Determination of the cell-free protein kinase activity of the wild-type and mutants of PDK1 was performed using T308tide (KTFCGTPEYLAPEVRR) as substrate peptide.²⁶ The activity of PKC ζ and PKC ι was measured using myelin basic protein (MBP, Millipore) as substrate.^{Fröhner11} For activity assays of classical PKCs, the enzymes PKC α (Millipore) and PKC β (ProQinase) were used and for the novel PKCs, PKC θ (ProQinase) and PKC δ (ProQinase). For both families Histone H1 (Millipore) served as substrate.¹⁵⁴ In order to measure the activity of the

compounds toward S6K and SGK the method was performed as described previously using S6K1-T2[T412E] and SGK1-ΔN[S422D] and Crosstide (GRPRTSSFAEG).^{11, 74}

6.2.3. Isothermal titration calorimetry^{20, 74}

Isothermal titration calorimetry was performed using the high precision VP-ITC titration calorimetric system (MicroCal Inc, MA) to determine binding energetics of the 3,5-diarylpent-2-enoic acid series. We followed the protocol previously described by Schaeffer *et al.*¹⁶⁹

- 1) PDK1₅₀₋₃₅₉[Tyr228Gly-Gln2922Ala] was dissolved in the buffer containing 50 mM TrisHCl (pH 7.5), 200 mM NaCl and 1 mM DTT.
- 2) The ligand solutions were also prepared with the buffer containing 50 mM TrisHCl (pH 7.5), 200 mM NaCl and 1 mM DTT.
- 3) Both solutions were degased by generating of vacuum for 3 min.
- 4) Setting of the apparatus temperature (3-4 °C below the experimental run temperature) and of the experimental parameters:

Cell:	20 μM PDK1
Syringe:	450 μM ligand
Buffer:	TrisHCl (pH 7.5), 200 mM NaCl and 1 mM DTT
- 5) Loading of the reference cell with degased water.
- 6) Rinsing of the sample cell with buffer (2x) and loading with the protein solution.
- 7) Loading of the ITC syringe with the ligand solution.
- 8) The pipette was inserted into the sample cell and the ITC run was started.
- 9) Each experiment was performed at 20°C by one injection of 2 μl followed by 29 injections of 10 μl with 210 seconds between injections using a 290 rpm rotating syringe.
- 10) Heat signals were corrected for the heats of dilution and normalized to the amount of compound injected. Normalization and deconvolution of the binding isotherms was carried out using Origin7¹⁷⁰ provided by the manufacturer.

6.2.4. HPLC-MS/MS detection of hydrolysis of the prodrugs in L6 cells

L6 cells were seeded in 10 cm petri dishes at the density of 10⁶/mL in DMEM, supplemented with penicillin and streptomycin and 10% FBS. To induce differentiation to

myocytes, the cells were allowed to reach confluence for two days after plating, and the medium was changed to medium containing 2 % of FBS for four days, with medium change after 2nd day. After the 4th day the L6 cells were washed with PBS, the medium was replaced to DMEM without FBS and the cells were treated with the compounds at appropriate time intervals (5-90 min). At the end of the incubation the supernatant was removed and the cells were washed three times with phosphate-buffered saline (PBS). The cells were harvested and the cell suspensions transferred to a flask and counted. At that point, carbamazepine was added to the suspension as an internal standard to determine the recovery rate. 1 mL 0.6N HCl in water was added and the dicarboxylic acids were extracted using 3 mL of ethyl acetate shaking the samples for 20 min. The samples were centrifuged and 1 mL aliquots of the ethyl acetate supernatant were taken and evaporated to dryness. The samples were resuspended in 500 μ l of methanol and analyzed using HPLC-ESI-MS/MS, and the amount of the compounds was calculated using a standard calibration curve. DMSO-treated cells were processed in parallel and analyzed as a control. The disappearance of the ester and the appearance of the correspondic dicarboxylic acid were additionally confirmed by UV peak quantifications and spiking of the samples with the purified compounds. Mobile phase A was water containing 0.5 % trifluoroacetic acid and mobile phase B was methanol containing 0.5 % trifluoroacetic acid. The following elution profile was used: 0-8 min, 100 % B. The gradient of B from 70 to 100 % was applied, followed by 100 % B until end; sample volume was 25 μ L, the flow rate 0.5 mL/min, and the column temperature 40 °C.

6.2.5. Reporter Gene Assay¹⁶⁷

U937 cells were cultured in RPMI-1640 containing 10% FCS and penicillin/streptomycin. Transfection was performed in 6-well plates at a density of 106 cells/ml (2 ml per well) in the same medium without antibiotics. The transfection complex was prepared by mixing the reporter gene plasmid (pGL4.32[luc2P/NF- κ B-RE/Hygro], with FuGene HD transfection reagent at a ratio of 1:6 (Ng DNA : NI transfection reagent) in RPMI-1640 medium according to the manufacturer's instructions. The transfection mixture was added dropwise to the wells while gently shaking, and the plates were incubated at 37°C/5% CO₂ for 6h. Medium was then exchanged to serum-free RPMI-1640/ penicillin/ streptomycin without phenol red and the cells starved overnight. The next day, test compounds dissolved in DMSO were pipetted into white 96-well plates (0.2 NI), followed by 100 NI of the transfected cells per well. After 3h at 37°C/5% CO₂, the NF- κ B pathway was induced by addition of 50 ng/NI TNF α to the

wells (except uninduced controls). The cells were incubated at 37°C/5% CO₂ for 2.5 h, then the luciferase detection reagent was added (100nI per well) and the luminescence measured after 5min. at RT in a PolarStar plate reader.

7 References

1. Pearce, L. R.; Komander, D.; Alessi, D. R., The nuts and bolts of AGC protein kinases. *Nat Rev Mol Cell Biol* **2010**, 11, (1), 9-22.
2. Fischer, P. M., The design of drug candidate molecules as selective inhibitors of therapeutically relevant protein kinases. *Curr Med Chem* **2004**, 11, (12), 1563-83.
3. Manning, G.; Whyte, D. B.; Martinez, R.; Hunter, T.; Sudarsanam, S., The protein kinase complement of the human genome. *Science* **2002**, 298, (5600), 1912-34.
4. Hanks, S. K.; Hunter, T., Protein kinases 6. The eukaryotic protein kinase superfamily: kinase (catalytic) domain structure and classification. In *Faseb J*, 1995; Vol. 9, pp 576-96.
5. Cohen, P., Protein kinases-the major drug targets of the twenty-first century? *Nat Rev Drug Discov* **2002**, 1, 309-315.
6. Zhang, J.; Yang, P. L.; Geay, N. S., Targeting cancer with small molecule kinase inhibitors. *Nat Rev Cancer* **2009**, 9, 28-39.
7. Kiselyov, A.; Balakin, K. V.; Tkachenko, S. E.; Savchuk, N. P., Recent progress in development of non-ATP competitive small-molecule inhibitors of protein kinases. *Mini Rev Med Chem* **2006**, 6, (6), 711-7.
8. Wikipedia, Tyrosinkinase-Inhibitor. In.
9. Cantley, L. C., The phosphoinositide 3-kinase pathway. *Science* **2002**, 31, 1655-7.
10. Maehama, T.; Taylor, G. S.; Dixon, J. E., PTEN and myotubularin: novel phosphoinositide phosphatases. *Annu Rev Biochem* **2001**, 70, 247-79.
11. Biondi, R. M.; Kieloch, A.; Currie, R. A.; Deak, M.; Alessi, D. R., The PIF-binding pocket in PDK1 is essential for activation of S6K and SGK, but not PKB. *Embo J* **2001**, 20, (16), 4380-90.
12. Biondi, R. M., Phosphoinositide-dependent protein kinase 1, a sensor of protein conformation. *Trends Biochem Sci* **2004**, 29, (3), 136-42.
13. Bayascas, J. R., Dissecting the role of the 3-phosphoinositide-dependent protein kinase-1 (PDK1) signalling pathways. *Cell Cycle* **2008**, 7, (19), 2978-82.
14. Frias, M. A.; Thoreen, C. C.; Jaffe, J. D.; Schroder, W.; Sculley, T.; Carr, S. A.; Sabatini, D. M., mSin1 is necessary for Akt/PKB phosphorylation, and its isoforms define three distinct mTORC2s. *Curr Biol* **2006**, 16, (18), 1865-70.
15. Wullschleger, S.; Loewith, R.; Hall, M. N., TOR signaling in growth and metabolism. *Cell* **2006**, 124, (3), 471-84.

16. Feldman, R. I.; Wu, J. M.; Polokoff, M. A.; Kochanny, M. J.; Dinter, H.; Zhu, D.; Biroc, S. L.; Aliche, B.; Bryant, J.; Yuan, S.; Buckman, B. O.; Lentz, D.; Ferrer, M.; Whitlow, M.; Adler, M.; Finster, S.; Chang, Z.; Arnaiz, D. O., Novel small molecule inhibitors of 3-phosphoinositide-dependent kinase-1. *J Biol Chem* **2005**, 280, (20), 19867-74.
17. Biondi, R. M.; Komander, D.; Thomas, C. C.; Lizcano, J. M.; Deak, M.; Alessi, D. R.; van Aalten, D. M., High resolution crystal structure of the human PDK1 catalytic domain defines the regulatory phosphopeptide docking site. *Embo J* **2002**, 21, (16), 4219-28.
18. Mora, A.; Komander, D.; van Aalten, D. M.; Alessi, D. R., PDK1, the master regulator of AGC kinase signal transduction. *Semin Cell Dev Biol* **2004**, 15, (2), 161-70.
19. Bayascas, J. R.; Leslie, N. R.; Parsons, R.; Fleming, S.; Alessi, D. R., Hypomorphic mutation of PDK1 suppresses tumorigenesis in PTEN(+/-) mice. *Curr Biol* **2005**, 15, (20), 1839-46.
20. Stroba, A.; Schaeffer, F.; Hindie, V.; Lopez-Garcia, L.; Adrian, I.; Frohner, W.; Hartmann, R. W.; Biondi, R. M.; Engel, M., 3,5-Diphenylpent-2-enoic acids as allosteric activators of the protein kinase PDK1: structure-activity relationships and thermodynamic characterization of binding as paradigms for PIF-binding pocket-targeting compounds. *J Med Chem* **2009**, 52, (15), 4683-93.
21. Manning, B. D., Balancing Akt with S6K: implications for both metabolic diseases and tumorigenesis. *J Cell Biol* **2004**, 167, (3), 399-403.
22. Um, S. H. F., F.; Watanabe, M.; Picard, F.; Joaquin, M.; Sticker, M.; Fumagalli, S.; Allegrini, P.R.; Kozma, S.C.; Auwerx J.; Thomas, G., Absence of S6K protects against age- and diet-induced obesity while enhancing insulin sensitivity. *Nature* **2004**, 31, 200-205.
23. Casamayor, A.; Morrice, N. A.; Alessi, D. R., Phosphorylation of Ser-241 is essential for the activity of 3-phosphoinositide-dependent protein kinase-1: identification of five sites of phosphorylation in vivo. *Biochem J* **1999**, 342 (Pt 2), 287-92.
24. Park, P., Hill, M.M.; Hess, D.; Brazil, D.P.; Hofsteenge J.; Hemmings B., Identification of Tyrosine Phosphorylation Sites on 3-Phosphoinositide-dependent Protein Kinase-1 and Their Role in Regulating Kinase Activity. *The Journal of Biological Chemistry* **2001**, 276, 37459-37471.
25. Scheid, M. P. P., M.; Woodgett J.R., Phosphoinositide-Dependent Phosphorylation of PDK1 Regulates Nuclear Translocation *Molecular and Cellular Biology* **2005**, 25, 2347-2363.
26. Biondi, R. M. C., P.C.F.; Casamayor, A.; Deak, M.; Currie, R.A.; Alessi, D.R., identification of a pocket in the PDK1 kinase domain that interacts with PIF and the C-terminal residues of PKA. *The EMBO J* **2000**, 19, 979-988.
27. Komander, D.; Kular, G. S.; Schuttelkopf, A. W.; Deak, M.; Prakash, K. R.; Bain, J.; Elliott, M.; Garrido-Franco, M.; Kozikowski, A. P.; Alessi, D. R.; van Aalten, D. M., Interactions of LY333531 and other bisindolyl maleimide inhibitors with PDK1. *Structure* **2004**, 12, (2), 215-26.

28. CURRIE, R. A. W., K.S.; GRAY, A.; DEAK, M.; CASAMAYOR, A.; DOWNES, C.P.; COHEN, P.; ALESSI, D.R.; LUCOCQ, J., Role of phosphatidylinositol 3,4,5-trisphosphate in regulating the activity and localization of 3-phosphoinositide-dependent protein kinase-1. *Biochem J* **1999**, 337, 575-583.
29. Stephens, L. A., K.; Stokoe, D.; Erdjument-Bromage, H.; Painter, G.F.; Holmes, A.B.; Gaffney, P.R.; Reese, C.B.; McCormic, F.; Tempst, P.; Coadwell, J.; Hawkins, P.T., Protein Kinase B kinases that mediate phosphatidylinositol 3, 4,5-triphosphate-dependent activation of protein kinase B. *Science* **1998**, 279, 710-714.
30. Balendran, A.; Biondi, R. M.; Cheung, P. C.; Casamayor, A.; Deak, M.; Alessi, D. R., A 3-phosphoinositide-dependent protein kinase-1 (PDK1) docking site is required for the phosphorylation of protein kinase C ζ (PKC ζ) and PKC-related kinase 2 by PDK1. *J Biol Chem* **2000**, 275, (27), 20806-13.
31. Frodin, M.; Jensen, C. J.; Merienne, K.; Gammeltoft, S., A phosphoserine-regulated docking site in the protein kinase RSK2 that recruits and activates PDK1. *Embo J* **2000**, 19, (12), 2924-34.
32. Collins, B. J.; Deak, M.; Arthur, J. S.; Armit, L. J.; Alessi, D. R., In vivo role of the PIF-binding docking site of PDK1 defined by knock-in mutation. *Embo J* **2003**, 22, (16), 4202-11.
33. Collins, B. J.; Deak, M.; Murray-Tait, V.; Storey, K. G.; Alessi, D. R., In vivo role of the phosphate groove of PDK1 defined by knockin mutation. *J Cell Sci* **2005**, 118, (Pt 21), 5023-34.
34. Alessi, D. R.; James, S. R.; Downes, C. P.; Holmes, A. B.; Gaffney, P. R.; Reese, C. B.; Cohen, P., Characterization of a 3-phosphoinositide-dependent protein kinase which phosphorylates and activates protein kinase B α . *Curr Biol* **1997**, 7, (4), 261-9.
35. Peifer, C.; Alessi, D. R., Small-molecule inhibitors of PDK1. *ChemMedChem* **2008**, 3, (12), 1810-38.
36. Maurer, M.; Su, T.; Saal, L. H.; Koujak, S.; Hopkins, B. D.; Barkley, C. R.; Wu, J.; Nandula, S.; Dutta, B.; Xie, Y.; Chin, Y. R.; Kim, D. I.; Ferris, J. S.; Gruvberger-Saal, S. K.; Laakso, M.; Wang, X.; Memeo, L.; Rojzman, A.; Matos, T.; Yu, J. S.; Cordon-Cardo, C.; Isola, J.; Terry, M. B.; Toker, A.; Mills, G. B.; Zhao, J. J.; Murty, V. V.; Hibshoosh, H.; Parsons, R., 3-Phosphoinositide-dependent kinase 1 potentiates upstream lesions on the phosphatidylinositol 3-kinase pathway in breast carcinoma. *Cancer Res* **2009**, 69, (15), 6299-306.
37. Maira, S. M.; Stauffer, F.; Schnell, C.; Garcia-Echeverria, C., PI3K inhibitors for cancer treatment: where do we stand? *Biochem Soc Trans* **2009**, 37, (Pt 1), 265-72.
38. Islam, I.; Bryant, J.; Chou, Y. L.; Kochanny, M. J.; Lee, W.; Phillips, G. B.; Yu, H.; Adler, M.; Whitlow, M.; Ho, E.; Lentz, D.; Polokoff, M. A.; Subramanyam, B.; Wu, J. M.; Zhu, D.; Feldman, R. I.; Arnaiz, D. O., Indolinone based phosphoinositide-dependent kinase-1 (PDK1) inhibitors. Part 1: design, synthesis and biological activity. *Bioorg Med Chem Lett* **2007**, 17, (14), 3814-8.

39. Islam, I.; Brown, G.; Bryant, J.; Hrvatin, P.; Kochanny, M. J.; Phillips, G. B.; Yuan, S.; Adler, M.; Whitlow, M.; Lentz, D.; Polokoff, M. A.; Wu, J.; Shen, J.; Walters, J.; Ho, E.; Subramanyam, B.; Zhu, D.; Feldman, R. I.; Arnaiz, D. O., Indolinone based phosphoinositide-dependent kinase-1 (PDK1) inhibitors. Part 2: optimization of BX-517. *Bioorg Med Chem Lett* **2007**, *17*, (14), 3819-25.
40. Schering AG; Arnaiz, D. B., Y.; Chou, Y.L.; Feldmann, R.; Hrvatin, P.; Islam, I.; Kochanny, M.J.; Lee, W.; Polokoff, M.; Yu, S.; Yuan, S., *US 07105563* **2006**.
41. Sato, S.; Fujita, N.; Tsuruo, T., Interference with PDK1-Akt survival signaling pathway by UCN-01 (7-hydroxystaurosporine). *Oncogene* **2002**, *21*, (11), 1727-38.
42. Stauffer, F.; Maira, S. M.; Furet, P.; Garcia-Echeverria, C., Imidazo[4,5-c]quinolines as inhibitors of the PI3K/PKB-pathway. *Bioorg Med Chem Lett* **2008**, *18*, (3), 1027-30.
43. Hill, M. M.; Andjelkovic, M.; Brazil, D. P.; Ferrari, S.; Fabbro, D.; Hemmings, B. A., Insulin-stimulated protein kinase B phosphorylation on Ser-473 is independent of its activity and occurs through a staurosporine-insensitive kinase. *J Biol Chem* **2001**, *276*, (28), 25643-6.
44. Sausville, E. A.; Arbuck, S. G.; Messmann, R.; Headlee, D.; Bauer, K. S.; Lush, R. M.; Murgo, A.; Figg, W. D.; Lahusen, T.; Jaken, S.; Jing, X.; Roberge, M.; Fuse, E.; Kuwabara, T.; Senderowicz, A. M., Phase I trial of 72-hour continuous infusion UCN-01 in patients with refractory neoplasms. *J Clin Oncol* **2001**, *19*, (8), 2319-33.
45. Welch, S.; Hirte, H. W.; Carey, M. S.; Hotte, S. J.; Tsao, M. S.; Brown, S.; Pond, G. R.; Dancey, J. E.; Oza, A. M., UCN-01 in combination with topotecan in patients with advanced recurrent ovarian cancer: a study of the Princess Margaret Hospital Phase II consortium. *Gynecol Oncol* **2007**, *106*, (2), 305-10.
46. Edelman, M. J.; Bauer, K. S., Jr.; Wu, S.; Smith, R.; Bisaccia, S.; Dancey, J., Phase I and pharmacokinetic study of 7-hydroxystaurosporine and carboplatin in advanced solid tumors. *Clin Cancer Res* **2007**, *13*, (9), 2667-74.
47. Kortmansky, J.; Shah, M. A.; Kaubisch, A.; Weyerbacher, A.; Yi, S.; Tong, W.; Sowers, R.; Gonen, M.; O'Reilly, E.; Kemeny, N.; Ilson, D. I.; Saltz, L. B.; Maki, R. G.; Kelsen, D. P.; Schwartz, G. K., Phase I trial of the cyclin-dependent kinase inhibitor and protein kinase C inhibitor 7-hydroxystaurosporine in combination with Fluorouracil in patients with advanced solid tumors. *J Clin Oncol* **2005**, *23*, (9), 1875-84.
48. Komander, D.; Kular, G. S.; Bain, J.; Elliott, M.; Alessi, D. R.; Van Aalten, D. M., Structural basis for UCN-01 (7-hydroxystaurosporine) specificity and PDK1 (3-phosphoinositide-dependent protein kinase-1) inhibition. *Biochem J* **2003**, *375*, (Pt 2), 255-62.
49. Zhao, B.; Bower, M. J.; McDevitt, P. J.; Zhao, H.; Davis, S. T.; Johanson, K. O.; Green, S. M.; Concha, N. O.; Zhou, B. B., Structural basis for Chk1 inhibition by UCN-01. *J Biol Chem* **2002**, *277*, (48), 46609-15.

50. Davies, S. P.; Reddy, H.; Caivano, M.; Cohen, P., Specificity and mechanism of action of some commonly used protein kinase inhibitors. *Biochem J* **2000**, 351, (Pt 1), 95-105.
51. Davis, P. D.; Elliott, L. H.; Harris, W.; Hill, C. H.; Hurst, S. A.; Keech, E.; Kumar, M. K.; Lawton, G.; Nixon, J. S.; Wilkinson, S. E., Inhibitors of protein kinase C. 2. Substituted bisindolylmaleimides with improved potency and selectivity. *J Med Chem* **1992**, 35, (6), 994-1001.
52. Lim, J. T.; Piazza, G. A.; Han, E. K.; Delohery, T. M.; Li, H.; Finn, T. S.; Buttyan, R.; Yamamoto, H.; Sperl, G. J.; Brendel, K.; Gross, P. H.; Pamukcu, R.; Weinstein, I. B., Sulindac derivatives inhibit growth and induce apoptosis in human prostate cancer cell lines. *Biochem Pharmacol* **1999**, 58, (7), 1097-107.
53. Piazza, G. A.; Rahm, A. K.; Finn, T. S.; Fryer, B. H.; Li, H.; Stoumen, A. L.; Pamukcu, R.; Ahnen, D. J., Apoptosis primarily accounts for the growth-inhibitory properties of sulindac metabolites and involves a mechanism that is independent of cyclooxygenase inhibition, cell cycle arrest, and p53 induction. *Cancer Res* **1997**, 57, (12), 2452-9.
54. Arico, S.; Pattingre, S.; Bauvy, C.; Gane, P.; Barbat, A.; Codogno, P.; Ogier-Denis, E., Celecoxib induces apoptosis by inhibiting 3-phosphoinositide-dependent protein kinase-1 activity in the human colon cancer HT-29 cell line. *J Biol Chem* **2002**, 277, (31), 27613-21.
55. Kulp, S. K.; Yang, Y. T.; Hung, C. C.; Chen, K. F.; Lai, J. P.; Tseng, P. H.; Fowble, J. W.; Ward, P. J.; Chen, C. S., 3-phosphoinositide-dependent protein kinase-1/Akt signaling represents a major cyclooxygenase-2-independent target for celecoxib in prostate cancer cells. *Cancer Res* **2004**, 64, (4), 1444-51.
56. Zhu, J.; Huang, J. W.; Tseng, P. H.; Yang, Y. T.; Fowble, J.; Shiau, C. W.; Shaw, Y. J.; Kulp, S. K.; Chen, C. S., From the cyclooxygenase-2 inhibitor celecoxib to a novel class of 3-phosphoinositide-dependent protein kinase-1 inhibitors. *Cancer Res* **2004**, 64, (12), 4309-18.
57. Zhang, S.; Suvannasankha, A.; Crean, C. D.; White, V. L.; Johnson, A.; Chen, C. S.; Farag, S. S., OSU-03012, a novel celecoxib derivative, is cytotoxic to myeloma cells and acts through multiple mechanisms. *Clin Cancer Res* **2007**, 13, (16), 4750-8.
58. Gopalsamy, A.; Shi, M.; Boschelli, D. H.; Williamson, R.; Olland, A.; Hu, Y.; Krishnamurthy, G.; Han, X.; Arndt, K.; Guo, B., Discovery of dibenzo[c,f][2,7]naphthyridines as potent and selective 3-phosphoinositide-dependent kinase-1 inhibitors. *J Med Chem* **2007**, 50, (23), 5547-9.
59. Vernalis R & D Limited; Walmsley, D. L. D., M. J.; Northfield, C. J.; Fromont, Pyrazole-substituted benzimidazole derivatives for use in the treatment of cancer and autoimmune disorders. *WO 2006134318* **2006**.
60. Vertex Pharmaceuticals Incorporated; Binch, H. M., M.; Robinson, D.; Stamons, D.; Everitt, S., Benzimidazoles useful as inhibitors of protein kinases. *WO 2007015923* **2007**.

61. Hubbard, R. E., Fragment approaches in structure-based drug discovery. *J Synchrotron Radiat* **2008**, 15, (Pt 3), 227-30.
62. Facchinetti, M. M.; De Siervi, A.; Toskos, D.; Senderowicz, A. M., UCN-01-induced cell cycle arrest requires the transcriptional induction of p21(waf1/cip1) by activation of mitogen-activated protein/extracellular signal-regulated kinase kinase/extracellular signal-regulated kinase pathway. *Cancer Res* **2004**, 64, (10), 3629-37.
63. Bain, J.; McLauchlan, H.; Elliott, M.; Cohen, P., The specificities of protein kinase inhibitors: an update. *Biochem J* **2003**, 371, (Pt 1), 199-204.
64. Morphy, R., Selectively nonselective kinase inhibition: striking the right balance. *J Med Chem* **53**, (4), 1413-37.
65. Harrison, S.; Das, K.; Karim, F.; Maclean, D.; Mendel, D., Non-ATP-competitive kinase inhibitors - enhancing selectivity through new inhibition strategies. *Expert Opin Drug Discov* **2008**, 3, 761-774.
66. Lewis, J. A.; Lebois, E. P.; Lindsley, C. W., Allosteric modulation of kinases and GPCRs: design principles and structural diversity. *Curr Opin Chem Biol* **2008**, 12, (3), 269-80.
67. May, L. T.; Leach, K.; Sexton, P. M.; Christopoulos, A., Allosteric modulation of G protein-coupled receptors. *Annu Rev Pharmacol Toxicol* **2007**, 47, 1-51.
68. Urwyler, S., Allosteric modulation of family C G-protein-coupled receptors: from molecular insights to therapeutic perspectives. *Pharmacol Rev* **63**, (1), 59-126.
69. Han, S.; Zhou, V.; Pan, S.; Liu, Y.; Hornsby, M.; McMullan, D.; Klock, H. E.; Haugen, J.; Lesley, S. A.; Gray, N.; Caldwell, J.; Gu, X. J., Identification of coumarin derivatives as a novel class of allosteric MEK1 inhibitors. *Bioorg Med Chem Lett* **2005**, 15, (24), 5467-73.
70. Bogoyevitch, M. A.; Fairlie, D. P., A new paradigm for protein kinase inhibition: blocking phosphorylation without directly targeting ATP binding. *Drug Discov Today* **2007**, 12, (15-16), 622-33.
71. Barnett, S. F.; Defeo-Jones, D.; Fu, S.; Hancock, P. J.; Haskell, K. M.; Jones, R. E.; Kahana, J. A.; Kral, A. M.; Leander, K.; Lee, L. L.; Malinowski, J.; McAvoy, E. M.; Nahas, D. D.; Robinson, R. G.; Huber, H. E., Identification and characterization of pleckstrin-homology-domain-dependent and isoenzyme-specific Akt inhibitors. *Biochem J* **2005**, 385, (Pt 2), 399-408.
72. Lindsley, C. W.; Barnett, S. F.; Yaroschak, M.; Bilodeau, M. T.; Layton, M. E., Recent progress in the development of ATP-competitive and allosteric Akt kinase inhibitors. *Curr Top Med Chem* **2007**, 7, (14), 1349-63.
73. Harrison, M.; Swanton, C., Epothilones and new analogues of the microtubule modulators in taxane-resistant disease. *Expert Opin Investig Drugs* **2008**, 17, 523-546.
74. Engel, M.; Hindie, V.; Lopez-Garcia, L. A.; Stroba, A.; Schaeffer, F.; Adrian, I.; Imig, J.; Idrissova, L.; Nastainczyk, W.; Zeuzem, S.; Alzari, P. M.; Hartmann, R. W.; Piiper,

- A.; Biondi, R. M., Allosteric activation of the protein kinase PDK1 with low molecular weight compounds. *Embo J* **2006**, 25, (23), 5469-80.
75. Stroba, A., Synthese und Struktur-Wirkungs-Beziehungen allosterischer Modulatoren der Phosphoinositol-abhängigen Kinase (PDK1). In *Pharmaceutical and Medicinal Chemistry*, Saarland University: 2005.
76. Stockman, B. J. K., M.; Kohls, D.; Weibley, L.; Connolly, B.J.; Sheils, A.L.; Cao, Q.; Cheng, A.C.; Yang, L.; Kamath, A.V.; Ding, Y.H.; Charlton, M.E., Identification of allosteric PIF-pocket ligands for PDK1 using NMR-based fragment screening and 1H-15N TROSY experiments. *Chem Biol Drug Des* **2009**, 73, 179-188.
77. Bobkova, E. V.; Weber, M. J.; Xu, Z.; Zhang, Y. L.; Jung, J.; Blume-Jensen, P.; Northrup, A.; Kunapuli, P.; Andersen, J. N.; Kariv, I., Discovery of PDK1 kinase inhibitors with a novel mechanism of action by ultrahigh throughput screening. *J Biol Chem* **285**, (24), 18838-46.
78. Hirai, T.; Chida, K., Protein kinase C ζ (PKC ζ): activation mechanisms and cellular functions. *J Biochem* **2003**, 133, (1), 1-7.
79. Bell, R. M.; Burns, D. J., Lipid activation of protein kinase C. *J Biol Chem* **1991**, 266, (8), 4661-4.
80. Newton, A. C., Protein kinase C: structural and spatial regulation by phosphorylation, cofactors, and macromolecular interactions. *Chem Rev* **2001**, 101, (8), 2353-64.
81. Steinberg, S. F., Structural basis of protein kinase C isoform function. *Physiol Rev* **2008**, 88, (4), 1341-78.
82. Nishizuka, Y., Protein kinase C and lipid signaling for sustained cellular responses. *Faseb J* **1995**, 9, (7), 484-96.
83. Whitson, E. L.; Bugni, T. S.; Chockalingam, P. S.; Concepcion, G. P.; Harper, M. K.; He, M.; Hooper, J. N.; Mangalindan, G. C.; Ritacco, F.; Ireland, C. M., Sphecioesterol sulfates, PKC ζ inhibitors from a philippine sponge *Spheciospongia* sp. *J Nat Prod* **2008**, 71, (7), 1213-7.
84. Bandyopadhyay, G.; Standaert, M. L.; Sajan, M. P.; Kanoh, Y.; Miura, A.; Braun, U.; Kruse, F.; Leitges, M.; Farese, R. V., Protein kinase C-lambda knockout in embryonic stem cells and adipocytes impairs insulin-stimulated glucose transport. *Mol Endocrinol* **2004**, 18, (2), 373-83.
85. Fields, A. P.; Regala, R. P., Protein kinase C iota: human oncogene, prognostic marker and therapeutic target. *Pharmacol Res* **2007**, 55, (6), 487-97.
86. Soloff, R. S.; Katayama, C.; Lin, M. Y.; Feramisco, J. R.; Hedrick, S. M., Targeted deletion of protein kinase C lambda reveals a distribution of functions between the two atypical protein kinase C isoforms. *J Immunol* **2004**, 173, (5), 3250-60.
87. Duran, A.; Diaz-Meco, M. T.; Moscat, J., Essential role of RelA Ser311 phosphorylation by zetaPKC in NF-kappaB transcriptional activation. *Embo J* **2003**, 22, (15), 3910-8.

88. Levy, D.; Kuo, A. J.; Chang, Y.; Schaefer, U.; Kitson, C.; Cheung, P.; Espejo, A.; Zee, B. M.; Liu, C. L.; Tangsombatvisit, S.; Tennen, R. I.; Kuo, A. Y.; Tanjing, S.; Cheung, R.; Chua, K. F.; Utz, P. J.; Shi, X.; Prinjha, R. K.; Lee, K.; Garcia, B. A.; Bedford, M. T.; Tarakhovsky, A.; Cheng, X.; Gozani, O., Lysine methylation of the NF-kappaB subunit RelA by SETD6 couples activity of the histone methyltransferase GLP at chromatin to tonic repression of NF-kappaB signaling. *Nat Immunol* **12**, (1), 29-36.
89. Yang, X. D.; Chen, L. F., Talking to histone: methylated RelA serves as a messenger. *Cell Res* **21**, (4), 561-3.
90. Leitges, M.; Sanz, L.; Martin, P.; Duran, A.; Braun, U.; Garcia, J. F.; Camacho, F.; Diaz-Meco, M. T.; Rennert, P. D.; Moscat, J., Targeted disruption of the zetaPKC gene results in the impairment of the NF-kappaB pathway. *Mol Cell* **2001**, *8*, (4), 771-80.
91. Martin, P.; Duran, A.; Minguet, S.; Gaspar, M. L.; Diaz-Meco, M. T.; Rennert, P.; Leitges, M.; Moscat, J., Role of zeta PKC in B-cell signaling and function. *Embo J* **2002**, *21*, (15), 4049-57.
92. Martin, P.; Villares, R.; Rodriguez-Mascarenhas, S.; Zaballos, A.; Leitges, M.; Kovac, J.; Sizing, I.; Rennert, P.; Marquez, G.; Martinez, A. C.; Diaz-Meco, M. T.; Moscat, J., Control of T helper 2 cell function and allergic airway inflammation by PKCzeta. *Proc Natl Acad Sci U S A* **2005**, *102*, (28), 9866-71.
93. Gruber, T.; Fresser, F.; Jenny, M.; Uberall, F.; Leitges, M.; Baier, G., PKCtheta cooperates with atypical PKCzeta and PKCdelta in NF-kappaB transactivation of T lymphocytes. *Mol Immunol* **2008**, *45*, (1), 117-26.
94. San-Antonio, B.; Iniguez, M. A.; Fresno, M., Protein kinase Czeta phosphorylates nuclear factor of activated T cells and regulates its transactivating activity. *J Biol Chem* **2002**, *277*, (30), 27073-80.
95. Ghosh, S.; May, M. J.; Kopp, E. B., NF-kappa B and Rel proteins: evolutionarily conserved mediators of immune responses. *Annu Rev Immunol* **1998**, *16*, 225-60.
96. Bonizzi, G.; Karin, M., The two NF-kappaB activation pathways and their role in innate and adaptive immunity. *Trends Immunol* **2004**, *25*, (6), 280-8.
97. Karin, M., How NF-kappaB is activated: the role of the IkappaB kinase (IKK) complex. *Oncogene* **1999**, *18*, (49), 6867-74.
98. Tergaonkar, V., NFkappaB pathway: a good signaling paradigm and therapeutic target. *Int J Biochem Cell Biol* **2006**, *38*, (10), 1647-53.
99. Gilmore, T. D., Introduction to NF-kappaB: players, pathways, perspectives. *Oncogene* **2006**, *25*, (51), 6680-4.
100. Scheidereit, C., IkappaB kinase complexes: gateways to NF-kappaB activation and transcription. *Oncogene* **2006**, *25*, (51), 6685-705.
101. Moynagh, P. N., The NF-kappaB pathway. *J Cell Sci* **2005**, *118*, (Pt 20), 4589-92.

102. Hoffmann, A.; Natoli, G.; Ghosh, G., Transcriptional regulation via the NF-kappaB signaling module. *Oncogene* **2006**, 25, (51), 6706-16.
103. Rayet, B.; Gelinias, C., Aberrant rel/nfkb genes and activity in human cancer. *Oncogene* **1999**, 18, (49), 6938-47.
104. Beg, A. A.; Baltimore, D., An essential role for NF-kappaB in preventing TNF-alpha-induced cell death. *Science* **1996**, 274, (5288), 782-4.
105. Beg, A. A.; Sha, W. C.; Bronson, R. T.; Ghosh, S.; Baltimore, D., Embryonic lethality and liver degeneration in mice lacking the RelA component of NF-kappa B. *Nature* **1995**, 376, (6536), 167-70.
106. Muller, G.; Ayoub, M.; Storz, P.; Rennecke, J.; Fabbro, D.; Pfizenmaier, K., PKC zeta is a molecular switch in signal transduction of TNF-alpha, bifunctionally regulated by ceramide and arachidonic acid. *Embo J* **1995**, 14, (9), 1961-9.
107. Filomeno, R.; Poirson-Bichat, F.; Billerey, C.; Belon, J. P.; Garrido, C.; Solary, E.; Bettaieb, A., Atypical protein kinase C zeta as a target for chemosensitization of tumor cells. *Cancer Res* **2002**, 62, 1815-21.
108. de Thonel, A.; Bettaieb, A.; Jean, C.; Laurent, G.; Quillet-Mary, A., Role of protein kinase C zeta isoform in Fas resistance of immature myeloid KG1a leukemic cells. *Blood* **2001**, 98, (13), 3770-7.
109. Bezombes, C.; de Thonel, A.; Apostolou, A.; Louat, T.; Jaffrezou, J. P.; Laurent, G.; Quillet-Mary, A., Overexpression of protein kinase Czeta confers protection against antileukemic drugs by inhibiting the redox-dependent sphingomyelinase activation. *Mol Pharmacol* **2002**, 62, (6), 1446-55.
110. Standaert, M. L.; Galloway, L.; Karnam, P.; Bandyopadhyay, G.; Moscat, J.; Farese, R. V., Protein kinase C-zeta as a downstream effector of phosphatidylinositol 3-kinase during insulin stimulation in rat adipocytes. Potential role in glucose transport. *J Biol Chem* **1997**, 272, (48), 30075-82.
111. Zhang, J. F.; Yang, J. P.; Wang, G. H.; Xia, Z.; Duan, S. Z.; Wu, Y., Role of PKCzeta translocation in the development of type 2 diabetes in rats following continuous glucose infusion. *Diabetes Metab Res Rev* 26, (1), 59-70.
112. Lee, S. J.; Kim, J. Y.; Nogueiras, R.; Linares, J. F.; Perez-Tilve, D.; Jung, D. Y.; Ko, H. J.; Hofmann, S. M.; Drew, A.; Leitges, M.; Kim, J. K.; Tschop, M. H.; Diaz-Meco, M. T.; Moscat, J., PKCzeta-regulated inflammation in the nonhematopoietic compartment is critical for obesity-induced glucose intolerance. *Cell Metab* 12, (1), 65-77.
113. Podar, K.; Raab, M. S.; Zhang, J.; McMillin, D.; Breitkreutz, I.; Tai, Y. T.; Lin, B. K.; Munshi, N.; Hideshima, T.; Chauhan, D.; Anderson, K. C., Targeting PKC in multiple myeloma: in vitro and in vivo effects of the novel, orally available small-molecule inhibitor enzastaurin (LY317615.HCl). *Blood* **2007**, 109, (4), 1669-77.
114. Podar, K.; Raab, M. S.; Chauhan, D.; Anderson, K. C., The therapeutic role of targeting protein kinase C in solid and hematologic malignancies. *Expert Opin Investig Drugs* **2007**, 16, (10), 1693-707.

115. Gonelli, A.; Mischiati, C.; Guerrini, R.; Voltan, R.; Salvadori, S.; Zauli, G., Perspectives of protein kinase C (PKC) inhibitors as anti-cancer agents. *Mini Rev Med Chem* **2009**, *9*, (4), 498-509.
116. Martiny-Baron, G.; Fabbro, D., Classical PKC isoforms in cancer. *Pharmacol Res* **2007**, *55*, (6), 477-86.
117. Omura, S.; Iwai, Y.; Hirano, A.; Nakagawa, A.; Awaya, J.; Tsuchya, H.; Takahashi, Y.; Masuma, R., A new alkaloid AM-2282 OF *Streptomyces* origin. Taxonomy, fermentation, isolation and preliminary characterization. *J Antibiot (Tokyo)* **1977**, *30*, (4), 275-82.
118. Baltuch, G. H.; Dooley, N. P.; Couldwell, W. T.; Yong, V. W., Staurosporine differentially inhibits glioma versus non-glioma cell lines. *J Neurooncol* **1993**, *16*, (2), 141-7.
119. de Vries, D. J.; Herald, C. L.; Pettit, G. R.; Blumberg, P. M., Demonstration of sub-nanomolar affinity of bryostatin 1 for the phorbol ester receptor in rat brain. *Biochem Pharmacol* **1988**, *37*, (21), 4069-73.
120. Isakov, N.; Galron, D.; Mustelin, T.; Pettit, G. R.; Altman, A., Inhibition of phorbol ester-induced T cell proliferation by bryostatin is associated with rapid degradation of protein kinase C. *J Immunol* **1993**, *150*, (4), 1195-204.
121. Hennings, H.; Blumberg, P. M.; Pettit, G. R.; Herald, C. L.; Shores, R.; Yuspa, S. H., Bryostatin 1, an activator of protein kinase C, inhibits tumor promotion by phorbol esters in SENCAR mouse skin. *Carcinogenesis* **1987**, *8*, (9), 1343-6.
122. Wu, J.; Zhang, B.; Wu, M.; Li, H.; Niu, R.; Ying, G.; Zhang, N., Screening of a PKC zeta-specific kinase inhibitor PKCzI257.3 which inhibits EGF-induced breast cancer cell chemotaxis. *Invest New Drugs* *28*, (3), 268-75.
123. Yuan, L.; Seo, J. S.; Kang, N. S.; Keinan, S.; Steele, S. E.; Michelotti, G. A.; Wetsel, W. C.; Beratan, D. N.; Gong, Y. D.; Lee, T. H.; Hong, J., Identification of 3-hydroxy-2-(3-hydroxyphenyl)-4H-1-benzopyran-4-ones as isoform-selective PKC-zeta inhibitors and potential therapeutics for psychostimulant abuse. *Mol Biosyst* **2009**, *5*, (9), 927-30.
124. Trujillo, J. I.; Kiefer, J. R.; Huang, W.; Thorarensen, A.; Xing, L.; Caspers, N. L.; Day, J. E.; Mathis, K. J.; Kretzmer, K. K.; Reitz, B. A.; Weinberg, R. A.; Stegeman, R. A.; Wrightstone, A.; Christine, L.; Compton, R.; Li, X., 2-(6-Phenyl-1H-indazol-3-yl)-1H-benzo[d]imidazoles: design and synthesis of a potent and isoform selective PKC-zeta inhibitor. *Bioorg Med Chem Lett* **2009**, *19*, (3), 908-11.
125. Noble, M. E.; Endicott, J. A.; Johnson, L. N., Protein kinase inhibitors: insights into drug design from structure. *Science* **2004**, *303*, (5665), 1800-5.
126. Hindie, V.; Stroba, A.; Zhang, H.; Lopez-Garcia, L. A.; Idrissova, L.; Zeuzem, S.; Hirschberg, D.; Schaeffer, F.; Jorgensen, T. J.; Engel, M.; Alzari, P. M.; Biondi, R. M., Structure and allosteric effects of low-molecular-weight activators on the protein kinase PDK1. *Nat Chem Biol* **2009**, *5*, (10), 758-64.

127. Yasui, S.; Fujii, M.; Ohno, A., NAD(P)⁺-NAD(P)H Models. 64. The Quantitative Elucidation of the Mechanistic Aspects in the Silica Gel-Catalyzed Reduction of α,β -Unsaturated Carbonyl Compounds by a Model of NAD(P)H. *Bull. Chem. Soc. Jpn.* **1987**, 60, (11), 4019-4026.
128. Anniyappan, M.; Muralidharan, D.; Perumal, P. T., Synthesis of Hantzsch 1,4-Dihydropyridines Under Microwave Irradiation. *Synthetic Communications* **2002**, 32, 659-663.
129. Yoshizawa, K.; Toyota, S.; Toda, F.; Csöreg, I., Preparative and mechanistic studies of solvent-free Rap-Stoermer reactions *Green Chemistry* **2003**, 5, 353-356.
130. Beck, J., Direct synthesis of benzo[b]thiophene-2-carboxylate esters involving nitro displacement. **1972**, (37), 3224-3226.
131. Ladbury, J. E., Isothermal titration calorimetry: Application to the structure-based drug design. *Thermochimica Acta* **2001**, 209-215.
132. Velazquez-Campoy, A., The application of thermodynamic methods in drug design. *Thermochimica Acta* **2001**, 380, 217-227.
133. Nezami, A.; Luque, I.; Kimura, T.; Kiso, Y.; Freire, E., Identification and characterization of allophenylnorstatine-based inhibitors of plasmepsin II, an antimalarial target. *Biochemistry* **2002**, 41, (7), 2273-80.
134. Laatikainen, R.; Ratilainen, J.; Sebastian, R.; Santa, H., NMR Study of Aromatic-Aromatic Interactions for Benzene and Some Other Fundamental Aromatic Systems Using Alignment of Aromatics in Strong Magnetic Field. *J. Am. Chem. Soc.* **1996**, 117, 11006-11010.
135. Bissantz, C.; Kuhn, B.; Stahl, M., A medicinal chemist's guide to molecular interactions. *J. Med. Chem.* **2010**, 53, 5061-84.
136. Grover, J. R.; Walters, E. A.; Hui, E. T., Dissociation energies of the benzene dimer and dimer cation. *J. Phys. Chem.* **1987**, 91, 3233-3237.
137. Sinnokrot, M. O.; Sherrill, C. D., Substituent effects in pi-pi interactions: sandwich and T-shaped configurations. *J Am Chem Soc* **2004**, 126, (24), 7690-7.
138. Nishio, M.; Umezawa, Y.; Hirota, M.; Takeuchi, Y., The CH/ π interaction: significance in molecular recognition. *Tetrahedron* **1995**, 51, 8665-8701.
139. Gilli, P.; Ferretti, V.; Gilli, G.; Borea, P. A., Enthalpy-entropy compensation in drug-receptor binding. *J. Phys. Chem.* **1994**, 98, 1515-1518.
140. Grunwald, E.; Steel, C., Solvent Reorganization and Thermodynamic Enthalpy-Entropy Compensation. *J. Phys. Chem.* **1995**, 117, 5687-5692.
141. Grunwald, E., *Thermodynamics of Molecular Species*. Wiley & Sons: New York, 1997.

142. Velazquez-Campoy, A.; Luque, I.; Todd, M. J.; Milutinovich, M.; Kiso, Y.; Freire, E., Thermodynamic dissection of the binding energetics of KNI-272, a potent HIV-1 protease inhibitor. *Protein Sci* **2000**, *9*, 1801-1809.
143. Dunitz, J. D., Win some, lose some: enthalpy-entropy compensation in weak intermolecular interactions. *Chem Biol* **1995**, *2*, (11), 709-12.
144. Lafont, V.; Armstrong, A. A.; Ohtaka, H.; Kiso, Y.; Mario Amzel, L.; Freire, E., Compensating enthalpic and entropic changes hinder binding affinity optimization. *Chem Biol Drug Des* **2007**, *69*, (6), 413-22.
145. Anderka, O.; Loenze, P.; Klabunde, T.; Dreyer, M. K.; Defossa, E.; Wendt, K. U.; Schmoll, D., Thermodynamic characterization of allosteric glycogen phosphorylase inhibitors. *Biochemistry* **2008**, *47*, (16), 4683-91.
146. Ruben, A. J.; Kiso, Y.; Freire, E., Overcoming roadblocks in lead optimization: a thermodynamic perspective. *Chem Biol Drug Des* **2006**, *67*, (1), 2-4.
147. Xu, C.; Bartley, J. K.; Enache, D. I.; Knight, D. W.; Hutschings, G. J., High Surface Area MgO as a Highly Effective Heterogeneous Base Catalyst for Michael Addition and Knoevenagel Condensation Reactions. *Synthesis* **2005**, *19*, 3468-3476.
148. Ma, S.; Yu, S.; Yin, S., Studies on K₂CO₃-catalyzed 1,4-addition of 1,2-allenic ketones with diethyl malonate: controlled selective synthesis of beta,gamma-unsaturated enones and alpha-pyrones. *J Org Chem* **2003**, *68*, (23), 8996-9002.
149. Ma, S.; Yin, S.; Li, L.; Tao, F., K₂CO₃-catalyzed Michael addition-lactonization reaction of 1,2-allenyl ketones with electron-withdrawing group substituted acetates. An efficient synthesis of alpha-pyrone derivatives. *Org Lett* **2002**, *4*, (4), 505-7.
150. March, J., The Decarboxylation of Organic Acids. *Journal of Chemical Education* **1963**, *40*, 212-213.
151. Ni, J.; Auston, D. A.; Freilich, D. A.; Muralidharan, S.; Sobie, E. A.; Kao, J. P., Photochemical gating of intracellular Ca²⁺ release channels. *J Am Chem Soc* **2007**, *129*, (17), 5316-7.
152. Mai, A.; Cheng, D.; Bedford, M. T.; Valente, S.; Nebbioso, A.; Perrone, A.; Brosch, G.; Sbardella, G.; De Bellis, F.; Miceli, M.; Altucci, L., epigenetic multiple ligands: mixed histone/protein methyltransferase, acetyltransferase, and class III deacetylase (sirtuin) inhibitors. *J Med Chem* **2008**, *51*, (7), 2279-90.
153. Bundgaard, H.; Nielsen, N. M., Esters of N,N-disubstituted 2-hydroxyacetamides as a novel highly biolabile prodrug type for carboxylic acid agents. *J Med Chem* **1987**, *30*, (3), 451-4.
154. Lopez-Garcia, L. A. Allosteric modulation of the AGC kinases PDK1 and PKCzeta by small compounds. Saarland University 2010.
155. Feng, Y.; Coward, J. K., Prodrug forms of N-[(4-deoxy-4-amino-10-methyl)pteroyl]glutamate-gamma-[psiP(O)(OH)]-glutar ate, a potent inhibitor of folylpoly-gamma-glutamate synthetase: synthesis and hydrolytic stability. *J Med Chem* **2006**, *49*, (2), 770-88.

156. Klip, A.; Ramlal, T.; Cragoe, E. J., Jr., Insulin-induced cytoplasmic alkalinization and glucose transport in muscle cells. *Am J Physiol* **1986**, 250, (5 Pt 1), C720-8.
157. Ferres, H., Pro-Drugs of β -Lactam Antibiotics. *Drugs of Today* **1983**, 19, 499-538.
158. Jansen, A. B.; Russell, T. J., Some Novel Penicillin Derivatives. *J Chem Soc* **1965**, 65, 2127-32.
159. Niimi, T.; Orita, M.; Okazawa-Igarashi, M.; Sakashita, H.; Kikuchi, K.; Ball, E.; Ichikawa, A.; Yamagiwa, Y.; Sakamoto, S.; Tanaka, A.; Tsukamoto, S.; Fujita, S.; Tatsuta, K.; Maeda, Y.; Chikauchi, K., Design and synthesis of non-peptidic inhibitors for the Syk C-terminal SH2 domain based on structure-based in-silico screening. *J Med Chem* **2001**, 44, (26), 4737-40.
160. Gao, Y.; Luo, J.; Yao, Z. J.; Guo, R.; Zou, H.; Kelley, J.; Voigt, J. H.; Yang, D.; Burke, T. R., Jr., Inhibition of Grb2 SH2 domain binding by non-phosphate-containing ligands. 2. 4-(2-Malonyl)phenylalanine as a potent phosphotyrosyl mimetic. *J Med Chem* **2000**, 43, (5), 911-20.
161. Auffinger, P.; Hays, F. A.; Westhof, E.; Ho, P. S., Halogen bonds in biological molecules. *Proc Natl Acad Sci U S A* **2004**, 101, (48), 16789-94.
162. Lu, Y.; Shi, T.; Wang, Y.; Yang, H.; Yan, X.; Luo, X.; Jiang, H.; Zhu, W., Halogen bonding--a novel interaction for rational drug design? *J Med Chem* **2009**, 52, (9), 2854-62.
163. Daehne, W.; Frederiksen, E.; Gundersen, E.; Lund, F.; Morch, P.; Petersen, H. J.; Roholt, K.; Tybring, L.; Godtfredsen, W. O., Acyloxymethyl esters of ampicillin. *J Med Chem* **1970**, 13, (4), 607-12.
164. Chanteux, H.; Van Bambeke, F.; Mingeot-Leclercq, M. P.; Tulkens, P. M., Accumulation and oriented transport of ampicillin in Caco-2 cells from its pivaloyloxymethylester prodrug, pivampicillin. *Antimicrob Agents Chemother* **2005**, 49, (4), 1279-88.
165. Bundgaard, H.; Klixbüll, U., Hydrolysis of pivampicillin in buffer and plasma solutions. Formation of a 4-imidazo- lidinone from ampicillin and formaldehyde. *International Journal of Pharmaceutics* **1985**, 27, 175-183.
166. Folguiera, L.; McElhinny, J. A.; Bren, G. D.; MacMorran, W. S.; Diaz-Meco, M. T.; Moscat, J.; Paya, C. V., Protein kinase C-zeta mediates NF-kappa B activation in human immunodeficiency virus-infected monocytes. *J. Virol.* **1996**, 70, 223-231.
167. Frohner, W.; Lopez-Garcia, L. A.; Neimanis, S.; Weber, N.; Navratil, J.; Maurer, F.; Stroba, A.; Zhang, H.; Biondi, R. M.; Engel, M., 4-benzimidazolyl-3-phenylbutanoic acids as novel PIF-pocket-targeting allosteric inhibitors of protein kinase PKCzeta. *J Med Chem* 54, (19), 6714-23.
168. Godl, K.; Wissing, J.; Kurtenbach, A.; Habenberger, P.; Blencke, S.; Gutbrod, H.; Salassidis, K.; Stein-Gerlach, M.; Missio, A.; Cotten, M.; Daub, H., An efficient proteomics method to identify the cellular targets of protein kinase inhibitors. *Proc Natl Acad Sci U S A* **2003**, 100, (26), 15434-9.

169. Schaeffer, F.; Matuschek, M.; Guglielmi, G.; Miras, I.; Alzari, P. M.; Beguin, P., Duplicated dockerin subdomains of *Clostridium thermocellum* endoglucanase CelD bind to a cohesin domain of the scaffolding protein CipA with distinct thermodynamic parameters and a negative cooperativity. *Biochemistry* **2002**, 41, (7), 2106-14.
170. Wiseman, T.; Williston, S.; Brandts, J. F.; Lin, L. N., Rapid measurement of binding constants and heats of binding using a new titration calorimeter. *Anal Biochem* **1989**, 179, (1), 131-7.